THE JOURNAL
OF
CHEMICAL PHYSICS

VOLUME 8 JANUARY, 1940 NUMBER 1

The Reaction of Atomic Hydrogen and Azomethane*

H. HENKIN AND H. AUSTIN TAYLOR
Department of Chemistry, New York University, New York, New York

(Received October 25, 1939)

At 27°C the only reaction between atomic hydrogen and azomethane is an addition to the nitrogen double bond to produce *s*-dimethylhydrazine by a mechanism with a maximum activation energy of 3–4 kcal. At 110°C there is in addition to this a rupture of the C—N bond in azomethane and the N—N bond in the hydrazine producing methane and methylamine, respectively. The energy of activation of each rupture appears to be about 8 kcal. At 195°C an additional reaction is evident involving association of methyl radicals with azomethane.

THE decomposition of azomethane, by both pyrolysis and photolysis, has recently been shown[1] to involve an initial production of methyl radicals, their addition to azomethane and the subsequent decomposition of the tetramethylhydrazine. In view of this it was considered interesting to determine the results of other methods of attack on the azomethane molecule. Emmett and Harkness,[2] for example, studied the catalytic decomposition using an iron synthetic ammonia catalyst. The course of the reaction is quite different from that occurring in homogeneous systems apparently involving the production of methylamine as an intermediate and yielding ammonia, hydrogen and carbon as the principal end products. The similarity of these results to those found by them for the catalyzed decomposition of symmetrical dimethylhydrazine would suggest that the latter might be a possible intermediate, previous to methylamine, in azomethane decomposition. The reaction of atomic hydrogen with azomethane was thus investigated.

The possibility of this reaction has already been pointed out by Patat,[3] who investigated the photolysis of azomethane at 265°C in presence of parahydrogen. From the effect of temperature on the over-all reaction he concludes that hydrogen atoms produced by the reaction:

$$CH_3+H_2\rightarrow CH_4+H$$

may react with azomethane with an energy of activation of 5.1 kcal. as follows:

$$H+CH_3N=NCH_3\rightarrow CH_4+N_2+CH_3.$$

No analyses were reported to show that methane and nitrogen were the sole products.

EXPERIMENTAL

Azomethane was prepared by Jahn's method[4] from dimethylhydrazine dihydrochloride and purified by repeated fractionation from solid carbon dioxide to liquid nitrogen. The product

* Abstract from a thesis presented in partial fulfillment of the requirements for the degree of Doctor of Philosophy at New York University, 1939.

[1] H. A. Taylor and F. P. Jahn, J. Chem. Phys. **7**, 470 (1939). References to earlier work are given here.

[2] P. H. Emmett and R. W. Harkness, J. Am. Chem. Soc. **54**, 538 (1932).

[3] F. Patat, Nachr. Ges. Wiss. Göttingen, Math.-physik. Klasse, Fachgruppe II. (N.F.) **2**, 77 (1936).

[4] F. P. Jahn, J. Am. Chem. Soc. **59**, 1761 (1937).

had a vapor pressure of 7.2 mm at −78°C and 751 mm at 0°C.

The hydrogen used was taken from a tank of electrolytic hydrogen. No attempt was made to remove the small amount of oxygen which may have been present since small quantities of oxygen have been found to aid the proper working of a Wood's discharge tube. The flow of hydrogen was regulated by a needle valve, several stopcocks and a capillary tube of small bore about 60 cm in length and was measured by a double McLeod gauge serving as a flowmeter.

The Wood's discharge tube was about 135 cm long and 1.3 cm in diameter. The hydrogen inlet was near one electrode, the outlet being in the center of the tube. The electrodes were hollow aluminum cylinders about 10 cm in length, 1 cm in diameter and 1 mm in thickness. They were spot-welded to tungsten leads. The walls of the tube were poisoned against recombination of hydrogen atoms by allowing the system to stand under vacuum in presence of 100 percent sulphuric acid.

The reaction vessel was a 500-cc bulb with two inlets, one for each reactant, and an outlet tube leading to the pumping system, consisting of a mercury diffusion pump backed by a Hyvac oil pump. The inlet tubes faced each other diametrically in the bulb to cause the incoming gas streams to mix in the center of the vessel. The tubes were tapered at the ends to reduce back diffusion of the gases. For the lower temperature experiments a water thermostat was used. At the higher temperatures an electrically heated furnace surrounded the reaction vessel.

From the discharge tube the hydrogen passed directly to the reaction system where it mixed with the azomethane stream coming from a storage reservoir kept in solid carbon dioxide; the rate of flow of the azomethane was measured by a capillary flowmeter similar to that used for the hydrogen. The exit gases from the reaction system were drawn first through a trap in liquid nitrogen and then over silica gel also in liquid nitrogen; the latter serves to separate nitrogen as well as hydrogen from the hydrocarbons. The condensation traps were connected to a Toepler pump of one liter capacity from which the reaction products could be sent to a Fisher gas analyzer.

TABLE I.

RUN	1	2	3	4	5	6	7
T°C	27.0	27.0	27.0	26.8	27.0	27.0	27.2
I amp.	0.0	7.0	6.8	0.0	7.8	7.4	7.4
V_{Az} cc	73.6	99.0	70.0	85.6	112.0	119.0	60.4
P_{Az} mm	0.42	0.63	0.40	0.58	0.73	0.75	0.33
V_{H_2} cc	160.2	192.4	170.0	186.6	204.2	208.7	191.4
P_{H_2} mm	0.68	0.76	0.65	0.70	0.76	0.75	0.72
P_H mm	0.00	0.14	0.13	0.00	0.19	0.17	0.15
V_{H_2}/V_{Az}	2.18	1.95	2.57	2.18	1.82	1.75	3.18
V_L cc	73.2	1.8	1.5	86.1	1.8	—	1.2
V_s cc	0.3	0.6	0.5	0.4	0.7	0.7	0.6

The atomic hydrogen gauge, based on that suggested by Poole,[5] consisted of a silver tube 7 mm in diameter and 0.75 mm thick cemented coaxially in a glass tube 40 cm long and 2.5 cm wide, the ends being tapered to 7 mm. The hydrogen stream enters in the middle of the glass tube and is pumped out at one end; the other end carried a McLeod gauge. The atomic hydrogen recombines on the outside of the silver tube and the heat of reaction is thus communicated through the silver to a stream of water flowing through it at a fixed rate. The increase in temperature of the water was measured by two thermometers, which could be read to 0.002°, located in the silver tube and therefore in the water stream. Twisted strands of copper wire placed in the silver tube caused thorough mixing of the water. The heat loss due to the hydrogen stream itself was determined by passing water which was several degrees below room temperature through the calorimeter and observing the temperature change for various pressures of hydrogen. Throughout the entire work the rate of flow of the water stream was maintained at 100 cc per 15 min. The heat loss correction was found to lie between six and eight percent.

Initially the Wood's tube was operated for twenty-four hours at a high current (9–10 amp.) to burn out any active spots. Before each run, the evacuated tube having stood over night in contact with sulphuric acid, was operated for thirty minutes to attain a steady state. Normal operating conditions corresponded to 350–400 milliamp. at about 3000 volts. Azomethane was then run in and the reaction allowed to proceed for forty-five minutes. Just before the azomethane was admitted and immediately after it was

[5] H. G. Poole, Proc. Roy. Soc. **A163**, 404 (1937).

shut off, readings were taken on the atomic hydrogen gauge to determine the hydrogen atom concentration. The gauge was situated at exactly the same distance from the outlet of the Wood's tube as was the reaction vessel and was connected to it by tubing of the same bore and having the same number of bends. No change was observed either in the pressure or in the rate of flow when the hydrogen stream was diverted from one path to the other. It is logical to assume therefore that the calorimeter actually measures the hydrogen atom concentration entering the reaction vessel. The only effect of the azomethane stream on the hydrogen flow was a momentary one; the flow quickly readjusted itself to the previous value as did also the arc current.

Results and Discussion

The experimental results and their interpretation can best be studied by examining the data at each temperature separately and then contrasting the observations. Data were obtained at 27°C, 110°C and 195°C.

Experiments at 27°C

Table I presents the data obtained for seven runs at 27°C. Each run covered a period of forty-five minutes.

In the table I represents the primary current in the transformer; the arc current is one-twentieth of this value. V_{Az} is the total volume of azomethane at a pressure P_{Az} mm which entered the reaction system during the run. Similarly V_{H_2} is the total volume of hydrogen (molecular plus atomic) flowing at a combined pressure P_{H_2}. P_H is the atomic hydrogen pressure entering the reaction vessel as calculated from the gauge readings. V_L represents the volume of product which could be drawn from the first condensing trap at −78°C using a Toepler pump. V_s is the volume of product condensed in the silica gel trap at liquid nitrogen temperature. All volumes were measured under laboratory conditions, approximately 25°C and one atmosphere pressure.

The first run was made with molecular hydrogen alone to test for its possible reaction with azomethane and also to check on the adsorbability for hydrogen of the silica gel. It will be seen that the latter is less than 0.2 percent. The volume of product in the first trap agrees almost exactly with the original azomethane and it was found to be completely soluble in dilute sulphuric acid. Since experiments 2 and 3 gave evidence of the formation of dimethylhydrazine, run 1 was duplicated in 4 and the sulphuric acid solution of the products was tested for secondary hydrazines by addition of cupric chloride. No characteristic red precipitate was found.

Table II.

	Picrate		Oxalate	
	M.P.	% N_2	M.P.	% N_2
Observed	144	23.98 24.04	130	18.54 18.66
Theoretical	147	24.14	132	18.67

In all the other experiments the arc was operated yielding approximately 0.15 mm atomic hydrogen. The most striking result is the almost complete absence of gaseous product. Only a very small amount of the product collected in the first trap at the temperature of liquid nitrogen was volatile at −78°C. This product was a colorless liquid, definitely basic since it reacted vigorously and exothermally with hydrochloric acid. It was a good reducing agent precipitating silver from Tollen's reagent but giving a positive test with Fehling's solution only upon heating. A test with buffered cupric chloride solution gave the characteristic azo-cuprous chloride complex indicating the compound to be secondary hydrazine, probably symmetrical dimethylhydrazine.

The small amount, V_L, volatile at −78°C is probably some unchanged azomethane or due to a small vapor pressure of the hydrazine. That it is not methylamine was shown in experiment 6 where the whole sample from the first trap was removed and tested for primary amine by the Rimini test with negative results.

The volumes, V_s, collected from the silica gel trap show the absence of ethane or methane. The volumes of the last three runs amounting to 2 cc were accumulated and passed over hot copper oxide. 0.4 cc remained unreacted showing that the majority of the gas was hydrogen and that only minute traces of hydrocarbon could possibly be present.

The sole product appears therefore to be dimethylhydrazine. The identity was definitely confirmed by a microanalysis of the picrate of the compound produced in run 6 and of the oxalate of the product from run 7. The compounds were recrystallized from alcohol. Melting points were taken and the percentage nitrogen was determined by micro-Dumas analysis. Table II gives the results found as compared with the values quoted in Beilstein. The absence of hydrocarbons among the products definitely indicates that no rupture of the azomethane molecule has occurred. It is known that the C−N bond is weaker than the C−C bond in ethane yet rupture of the latter is possible by atomic hydrogen at room temperature.[6] It can only be concluded that the addition reaction of hydrogen to azomethane requires a smaller energy of activation. This is strengthened by the observation that practically all the azomethane has reacted. Even if the small amount of product volatile at −78°C is all azomethane, the total reaction would correspond at least to 97–98 percent of the azomethane.

Since the ratio of atomic hydrogen to azomethane was in every case much less than unity and since two hydrogen atoms are required to saturate the azomethane molecule it is evident that some of the hydrogenation must have involved molecular hydrogen, for example:

$$CH_3N{=}NCH_3{+}H{\rightarrow}CH_3NH{-}NCH_3, \quad (1)$$

$$CH_3NH{-}NCH_3{+}H_2 \rightarrow CH_3NH{-}NHCH_3{+}H. \quad (2)$$

Although there are no data available[7] for the

TABLE III.

RUN	9	10	11	12	13	14	15	16
T°C	110	110	108	109	110	110	110	109
I amp.	6.4	7.2	7.2	7.4	7.0	7.6	7.0	7.2
V_{Az} cc	84.2	66.0	92.0	81.6	73.3	69.6	91.2	74.1
P_{Az} mm	0.53	0.32	0.64	0.51	0.42	0.34	0.64	0.50
V_{H_2} cc	198.2	164.0	191.3	212.0	198.4	213.0	218.0	222.4
P_{H_2} mm	0.76	0.73	0.78	0.80	0.76	0.77	0.81	0.84
P_H mm	0.19	0.19	0.21	0.22	0.19	0.20	0.23	0.22
V_{H_2}/V_{Az}	2.35	2.79	2.09	2.60	2.74	3.20	2.39	3.00
V_L cc	19.0	14.4	16.7	17.0	15.8	16.0	19.0	16.9
V_{CH_4} cc	20.8	20.0	18.2	22.7	21.7	22.3	25.6	23.0
$V_{C_2H_6}$ cc	2.3	1.6	3.4	2.0	2.0	1.6	2.7	2.0

[6] Trenner, Morikawa and Taylor, J. Chem. Phys. **5**, 203 (1937).

[7] Imanishi, Sci. Papers, Inst. Phys. Chem. (Tokyo) **15**, 166 (1931) says the continuum in hydrazine begins at 2200A. This would give 128 kcal. as a maximum N−H bond strength.

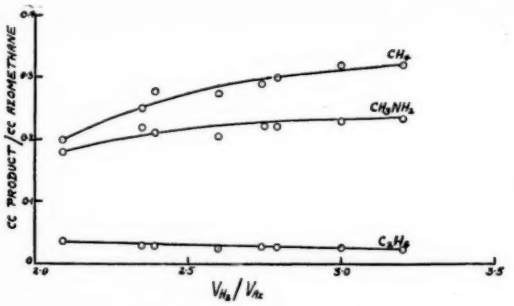

FIG. 1. Reaction products at 110°C.

N−H bond strength in the hydrazines, reaction (2) as a rapid reaction at room temperature does not seem probable when it is realized that the similar reaction between methyl radicals and molecular hydrogen only proceeds at higher temperatures. A possible mechanism presents itself, however, in this particular case, reminiscent of a recently suggested scheme for the Walden inversion.[8] The presence of the hydrogen atom in the radical produced in reaction (1) may have so modified the N−N bond that a hydrogen molecule could add on, simultaneously with the ejection of the hydrogen atom. Such a scheme would require a considerably smaller energy of activation than that involved in the rupture of a hydrogen molecule and production of an N−H bond.

The rapidity of this hydrogenation reaction at room temperature indicates that the energy of activation cannot be much greater than about 3–4 kcal. It is reasonable to assume that step (1) requires no activation and that the 3–4 kcal. is to be associated with step (2). This may be contrasted with the addition of methyl radicals to azomethane as postulated by Burton, Davis and Taylor.[9] Methyl addition was first observable at a temperature around 150°. This is in qualitative agreement with the relative strengths of the N−H and N−C bonds formed.

Finally, that the sole product found here is dimethylhydrazine may be contrasted with the work of Dixon[10] on the reaction of atomic hydrogen with hydrazine. He found up to 80 percent

[8] F. O. Rice and E. Teller, J. Chem. Phys. **6**, 489 (1938).

[9] Burton, Davis and Taylor, J. Am. Chem. Soc. **59**, 1989 (1937).

[10] J. K. Dixon, J. Am. Chem. Soc. **54**, 4262 (1932).

of the hydrazine decomposed to give ammonia at room temperature; methylamine, which would be the corresponding product here, was not found. It is true that the conditions during Dixon's experiments were quite different from those in this work, inasmuch as he had a higher proportion of hydrogen atoms and was using moist hydrogen. Furthermore Steiner[11] has shown that atomic hydrogen up to ten percent has no effect on the hydrazine yield from N and H_2, meaning that hydrogen atoms do not attack hydrazine except at high concentrations. It seems certain therefore that the absence of reaction in the present study is a pure concentration effect.

Experiments at 110°C

Table III summarizes the results obtained.

The symbols in Table III have already been explained save the last two, V_{CH_4}, and, $V_{C_2H_6}$, which denote the volumes of methane and ethane isolated from the silica gel trap, and analyzed by the usual combustion method. In calculating these, an allowance was made for 0.4 cc hydrogen which the previous results had shown was adsorbed during a run. Tests for unsaturated hydrocarbons gave negative results.

The first feature of difference in the above from the results at 27°C is the presence of the methane and ethane in the approximate ratio of ten to one. The second, is in the content of the first trap. At 27°C the product was almost entirely dimethylhydrazine which was involatile at −78°C. In the present case a considerable amount of the product was volatile at −78°C. Combustion of this gas gave carbon dioxide and nitrogen and from these and the oxygen consumed, a formula CH_5N was deduced. Actually the carbon was 2–3 percent too low and the hydrogen a trifle high. The gas was readily soluble in dilute acid and gave a test for primary amines. It is probably, therefore, methylamine. The residual liquid in the first trap, analyzed in the manner previously indicated proved to be solely dimethylhydrazine.

Figure 1 shows the results obtained in all the runs, plotted as cc product per cc azomethane against V_{H_2}/V_{Az}. The methane and methylamine yields are seen to increase with increase in the reactant ratio. The ethane is roughly constant but appears to decrease slightly with increase in the ratio.

The most reasonable mechanism which can explain these results is the following:

$$H+CH_3N=NCH_3\rightarrow CH_4+CH_3N=N, \quad (3)$$

$$CH_3N=N\rightarrow CH_3+N_2, \quad (4)$$

$$CH_3+CH_3\rightarrow C_2H_6, \quad (5)$$

$$2CH_3+H_2\rightarrow 2CH_4, \quad (6)$$

in addition to reactions (1) and (2) postulated previously. Reaction (5) probably occurs as a three-body process or heterogeneously and reaction (6) possibly as two successive bimolecular steps.[12]

If the above mechanism is accepted then the amount of azomethane decomposing in this manner is given by the sum of the ethane and one-half of the methane. Using the relation $v=sZe^{-E/RT}$ where, v, is the reaction rate, s, is the steric factor and, Z, is the collision frequency it is possible to calculate, E, the energy of activation of reaction (3). Taking the data of experiment 15 as typical, the concentration of H atoms is 5.65×10^{-9} mole/cc; of azomethane is 2.38×10^{-8} mole/cc and the reaction rate is 2.74×10^{-10} cc/mole/sec. Assuming a collision diameter for H of 2.14A and for azomethane, 4.54A,[13] with a steric factor of 0.1 as has been used in other reactions involving atomic hydrogen, a value of 8 kcal. is obtained for E. Patat[3] has reported a value of 5.1 kcal. for this reaction based on the para-orthohydrogen conversion. Since Patat did not consider the possibility of a

TABLE IV.

Run	8	17	18	19	20	21	22	23
T°C	193	195	195	194	195	195	195	193
I amp.	7.0	0.0	7.2	7.8	7.8	7.6	7.4	7.2
V_{Az} cc	80.2	67.0	76.3	73.0	87.0	71.3	84.0	92.0
P_{Az} mm	0.51	0.34	0.49	0.43	0.61	0.39	0.55	0.67
V_{H_2} cc	189.0	183.6	197.0	191.2	210.4	206.0	191.7	221.7
P_{H_2} mm	0.75	0.72	0.78	0.75	0.80	0.78	0.74	0.81
P_H mm	0.19	0.00	0.20	0.19	0.22	0.21	0.19	0.22
V_{H_2}/V_{Az}	2.36	2.74	2.58	2.62	2.42	2.63	2.28	2.41
V_L cc	35.6	67.6	33.1	31.8	37.6	29.0	36.0	38.6
V_{CH_4} cc	25.7	0.0	24.0	23.2	28.0	23.8	27.2	29.2
$V_{C_2H_6}$ cc	0.5	0.0	0.3	0.3	0.3	0.4	0.6	0.4

[11] W. Steiner, Zeits. f. Electrochem. **36**, 807 (1930).

[12] H. A. Taylor and M. Burton, J. Chem. Phys. **7**, 679 (1939).

[13] H. Henkin and H. A. Taylor, J. Chem. Phys. **7**, 829 (1939).

hydrogenation reaction proceeding simultaneously and gave no gas analyses to substantiate his proposed mechanism it is quite likely that his value of 5.1 is an average of the 3–4 kcal. for the hydrogenation and the 8 kcal. for the rupture.

The source of the methylamine seems most likely to be the dimethylhydrazine. In the corresponding case of hydrazine Wiig and Kistiakowsky, and Wiig[14] have postulated the following reactions to account for ammonia photolysis, especially at higher temperatures:

$$N_2H_4+H\rightarrow NH_3+NH_2$$
$$NH_2+H\rightarrow NH_3.$$

The absence here of dimethylamine makes other possibilities unlikely and thus the probable reactions are:

$$CH_3NH-NHCH_3+H \rightarrow CH_3NH_2+CH_3NH, \quad (7)$$

$$CH_3NH+H\rightarrow CH_3NH_2. \quad (8)$$

The relative weakness of the N–N bond as compared with the N–C and N–H bonds makes the scheme likely. The presence of traces of ammonia (not more than 2–3 percent) in the methylamine may result as a side reaction from the radicals in (7). If however it is formed as the result of a rupture of a C–N bond in the dimethylhydrazine the value of E for reaction (3) previously calculated would be a minimum value.

According to the above scheme one molecule of the hydrazine gives two of methylamine. If it is assumed, in the absence of more definite information, that the hydrazine concentration is 0.85 of the original azomethane concentration an estimate of the energy of activation of reaction (7) can be made. Taking the same value for the diameter of the hydrazine as for azomethane a value of 8 kcal. is again found. In view of the arbitrary assumptions made the reliability of this figure is by no means as great as that for reaction (3). That each gives the same value, however, may be significant.

Experiments at 195°C

The experimental results at this temperature are given in Table IV.

[14] E. O. Wiig and G. B. Kistiakowsky, J. Am. Chem. Soc. **54**, 1806 (1932); E. O. Wiig, *ibid.* **59**, 827 (1937).

The most striking difference between the results in Tables III and IV is in the value, V_L, which has almost doubled. Analysis showed that the gas was still practically pure methylamine. At the same time the ethane has decreased almost to the limit of the analytical experimental error, while the methane is only some 15–20 percent greater. Analysis of the fraction which is not volatile at −78°C showed also a change; neither the melting point of the derivative nor the nitrogen determination agreed with the theoretical for dimethylhydrazine. The oxalate derivative melted over a range of five degrees around 120°C; that of the hydrazine oxalate is 132°C. Three micro-Dumas determinations of the nitrogen content were all low as may be seen from the following:

Dimethylhydrazine		18.67 percent	N_2
Micro-Dumas	(1)	18.03 "	"
" "	(2)	17.87 "	"
" "	(3)	18.07 "	".

The difference cannot be attributed to experimental error (at most 0.2 percent) and must therefore be due to the presence of a compound other than dimethylhydrazine possessing a lower percentage nitrogen.

In order to test whether molecular hydrogen was reacting with azomethane at this temperature experiment 17 was performed. No hydrocarbons were formed and the volume of "product" as a gas was the same as the original azomethane. No reaction was occurring.

From the increase in temperature it was to be expected that the yield of products should increase. This is true for the methylamine suggesting that its source is similar to that already described at 110°C. The absence of larger amounts of ammonia would preclude the possibility of reaction between atomic hydrogen and methylamine under the experimental conditions.

The increase in yield of methylamine is not, however, paralleled by the ethane and methane. The former is actually reduced, the latter only slightly increased. Since the source of these hydrocarbons is presumably methyl radicals and since with an increased production of methylamine there should also be an increased production of methyls, the conclusion is inescapable that some other reaction which removes methyl

radicals has set in. Evidence has already been presented that methyl radicals may add on to azomethane[9] with the ultimate production of tetramethylhydrazine or in presence of hydrogen atoms, trimethylhydrazine:

$$CH_3N=NCH_3+CH_3\rightarrow(CH_3)_2N-NCH_3,$$
$$(CH_3)_2N-NCH_3+CH_3\rightarrow(CH_3)_2N-N(CH_3)_2$$

or $$(CH_3)_2N-NCH_3+H\rightarrow(CH_3)_2NNHCH_3.$$

The presence of such compounds in the dimethylhydrazine residue would give the observed result of a lowered nitrogen content.

Calculations based on the nitrogen percentages of various hydrazines and on the Dumas determinations show that if the mixture contained only di- and trimethylhydrazine, the amount of the trimethylhydrazine would have to be about $\frac{3}{8}$ of the total liquid fraction corresponding roughly to 20–25 cc of gas, that is, approximately equal to the methane yield. If it were all di- and tetramethylhydrazine then only $\frac{1}{5}$ of the liquid need be the tetra compound to give the observed nitrogen percentage. This would correspond to about 10 cc of gas, that is about $\frac{1}{2}-\frac{1}{3}$ the methane yield. If, since the methylamine yield is doubled in the temperature range 110–195°, it is assumed that the methane would also have doubled had there been no other methyl removing reaction, it would seem that the bulk of the association reaction must have resulted in trimethylhydrazine.

In conclusion it may be observed that with increasing temperature the stability of methane in presence of hydrogen atoms is reduced by the reaction

$$CH_4+H\rightarrow CH_3+H_2.$$

This would increase the methyl concentration and thus favor the association reaction with azomethane.

JANUARY, 1940 JOURNAL OF CHEMICAL PHYSICS VOLUME 8

High Velocity Atomic Beams*

I. Amdur and H. Pearlman
Research Laboratory of Physical Chemistry, Massachusetts Institute of Technology, Cambridge, Massachusetts
(Received September 27, 1939)

A general method has been developed for the production and intensity measurement of high velocity atomic beams. The method has been applied to beams of hydrogen atoms with energies equivalent to 200–800-volt electrons. Measurement of the collision cross section of these atoms when scattered by molecular hydrogen confirms the prediction that such scattering is predominantly due to repulsive forces between the beam and scattering particles.

THE scattering of molecular or atomic beams by gases provides an experimental method for evaluation of the interaction potential between the beam particles and the scattering particles. When the beam particles have ordinary thermal velocities, analysis of the angular scattering distribution can be used to estimate the attractive part of the potential; when the beam particles have extremely high velocities, repulsive forces cause most of the scattering. For example, the effect of the attractive part of the potential is undetectable in the scattering, beyond about one degree, of 200 equivalent volt helium atoms scattered by helium at ordinary temperatures.

As the first step in a program for evaluating the repulsive part of the interaction potential, the authors have sought to develop the necessary experimental methods for the production and quantitative intensity measurement of particle beams having high, controllable velocities. The present experiments are concerned with the production and characteristics of beams of hydrogen atoms having energies equivalent to 200–800-volt electrons and with the measurement of the

* Contribution from the Research Laboratory of Physical Chemistry, Massachusetts Institute of Technology, No. 429. Presented before the Division of Physical and Inorganic Chemistry of the American Chemical Society at the Baltimore meeting, April 5, 1939.

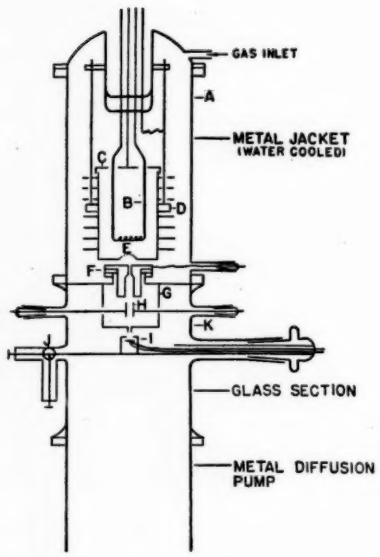

FIG. 1. Diagram of apparatus.

axis intensities of such beams both in vacuum and after scattering in molecular hydrogen. A combination of these intensity measurements directly yields values for the total collision cross section of fast hydrogen atoms in molecular hydrogen at ordinary temperatures.

In 1934 Lamar and Luhr[1] published details of a proton source which could produce, after proper seasoning, beams of ions containing over 98 percent protons. This proton source was the basis of the present apparatus in which beams of fast atoms were produced by proper neutralization of accelerated atomic ions.

The operation of the fast atom source, using atomic hydrogen beam production as an example, is conveniently explained with the aid of the accompanying diagram (Fig. 1).

Molecular hydrogen is admitted to the upper metal section *A* at a pressure of 0.3–0.4 mm of Hg. A low voltage arc (50 to 75 volts, 1.0 to 1.5 amperes) is struck between the filament *B* and the anode *C*. Positive ions are drawn to the cathode *D* (provided with radiation disks for cooling) which is kept at 160 volts negative and collects currents of 0.25–0.35 ampere. Some of these positive ions are pulled through the hemispherical grid *E* by the atom gun *F* which is at a negative potential of 200–800 volts. Depending upon the filament position and the atom gun voltage, these positive ions, which tend to focus due to the curvature of the grid, produce currents of 1–50 milliamperes on the atom gun surface. A small fraction of the ions pulled through the gauze grid pass through the channel (0.5 mm in diameter and 2 mm long) of the atom gun and, during their passage through this channel, some of the ions are neutralized without appreciable loss of kinetic energy. It is these atoms which form the high velocity beam which issues into the glass section *K* where the pressure can be kept at 5×10^{-5} mm of Hg by means of a very fast diffusion pump.[2] The internal diameter of this glass section, 3 inches, is sufficiently large that there is insignificant pressure gradient in this region even with scattering pressures as high as 0.1 mm. The absence of gradient insures uniform pressure along the path of the beam. Ions which remain charged after passage through the atom gun channel are swept out of the beam by a potential of 1500 volts across the condenser plates *H*. The intensity of the beam is measured by a specially constructed thermopile *I*[3] which is aligned in the axis of the beam by three bellows *J*. Thermopile e.m.f.'s are measured with a potentiometric galvanometer arrangement.[4] *G* is a radiation shield to protect the thermopile from radiation from the hot atom gun.

RESULTS

Characteristics of the source

Experiments were performed with the atom source, using hydrogen, to check its reproducibility of operation, to identify the beam particles and to determine the effect of arc characteristics upon beam intensity.

It was found that upon insertion of a new filament it was necessary to run the arc for about 10 hours to season properly the metal surfaces. After this period the arc became red, showing the presence of atomic hydrogen and the characteristics attained their steady-state values in agreement with the findings of Lamar and Luhr. After this initial seasoning, a shorter seasoning period of 1 to 2 hours is required each time the

[1] Lamar and Luhr, Phys. Rev. **46**, 87 (1934).

[2] Amdur, Rev. Sci. Inst. **7**, 395 (1936).
[3] Amdur and Pearlman, Rev. Sci. Inst. **10**, 174 (1939).
[4] Amdur and Pearlman, Rev. Sci. Inst. **9**, 194 (1938).

arc is started. Once the arc has been seasoned the characteristics are reproducible and steady.

Using ordinary Wood's tube atomic hydrogen, various oxides including CuO, WO_3, MoO_3 and all oxides of lead were tested to find the best chemical indicator for atomic hydrogen. It was decided to use MoO_3. This oxide, smoked onto microscope cover slips, was used to examine the fast beam. After the arc had been seasoned and the characteristics had reached their steady-state values, a blue circular spot, 1 mm in diameter, resulting from reduction of the oxide by atomic hydrogen, appeared on the indicator in less than 30 seconds after application of the atom gun voltage. It was not possible to obtain this coloration when the atom gun voltage was not applied. The size of the spot showed that the beam was well defined, being no greater than 1 mm in diameter at the point where the thermopile detector was placed (8.57 cm from the center of the atom gun channel). If the pressure in the arc was lowered to less than 0.2 mm of Hg and the atom gun voltage applied, the blue coloration on the indicator was considerably less intense for the same time of exposure to the beam. This agrees with the findings of Lamar and Luhr that, at the proper arc characteristics, high arc pressures favored the formation of pure proton beams (in the present case, pure atom beams) whereas low pressures introduced large percentages of molecular ions (in the present case, molecular beam particles). The chemical tests showed that the same arc conditions which were necessary for producing pure proton beams were required for producing atomic beams.

A quantitative study of the arc characteristics further confirmed the expectation that the production of fast hydrogen atoms would be in strict analog to the production of accelerated protons in the same type of apparatus. Lamar and Luhr, for example, found that, at a given voltage, the number of protons issuing from the ion gun channel was a constant fraction of the number of ions striking the ion gun surface. In the present case, a proportionality between atom gun current and the number of neutrals issuing from the atom gun channel at constant voltage, should result in proportionality between the e.m.f. recorded by the thermopile and the atom gun current, the voltage being constant. This follows from the fact that the thermopile measures the energy of the neutral beam, that is, the product of the number of beam particles and the average energy of each particle. This average energy is, of course, constant at a given atom gun voltage. The expected result implies a relation between thermopile e.m.f. and atom gun current of the form

$$\frac{\text{thermopile e.m.f.}}{\text{atom gun current}} = f(\text{atom gun voltage}).$$

Figure 2A shows how well the above prediction is verified. The equation of the curve is of the form

$$\frac{\text{thermopile e.m.f.}}{\text{atom gun current}} = a + b \times \text{atom gun voltage}.$$

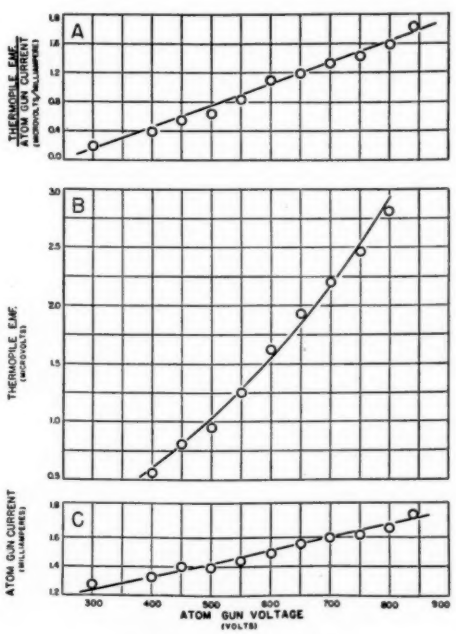

FIG. 2. Arc characteristics.

For constant atom gun voltage, therefore, we have the anticipated relation

$$\text{thermopile e.m.f.} = c \times \text{atom gun current}.$$

When the atom gun current is permitted to vary with the voltage, the thermopile e.m.f. is quadratic in the voltage as shown in Fig. 2B. This implies a linear variation of atom gun current

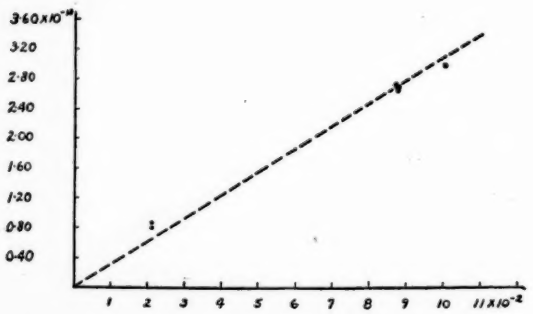

FIG. 3. Applicability of equation for collision cross section: $7.608\times10^{-18}\log_{10} I_{P_2}/I_{P_1}$ *versus* $(P_1/T_1-P_2/T_2)$. Here I_1 is the beam intensity for a scattering gas pressure of P_1 mm at T_1°K, and I_2 is a similar quantity. The experimental points (499-volt atoms) should lie on the straight line:

$$7.608\times10^{-18}\log_{10}(I_{P_2}/I_{P_1}) = (\text{collision cross section})(P_1/T_1-P_2/T_2).$$

The dashed line in the plot is this line, the collision cross section being found by the method of least squares to be 3.10×10^{-17} cm².

with atom gun voltage as verified by the experimental points shown in Fig. 2C.

The magnitude of the e.m.f.'s developed by the thermopile show clearly that the beam particles have extremely high velocities, since the effective temperature of the particles of a thermal beam would have to be about 150,000°K to reproduce the observed e.m.f.'s at 500 volts. The estimate assumes that the intensity of such a thermal beam is that given by the formulas applicable to a theoretically perfect thermal beam system. Since the present apparatus does not fall into this class, the effective temperature for the present case should be probably many times greater than that given above. In short, the experimental evidence is in complete accord with the assumption that the beam particles are hydrogen atoms having velocities corresponding to the voltages applied to the atom gun. These results also agree with the findings of Oliphant[5] who reported little loss of kinetic energy in neutralizing accelerated helium ions.

Measurement of collision cross sections

Since it had been shown that the apparatus produced beams of fast hydrogen atoms and that the operation was reproducible and steady, measurements were made of the absorption, which is due to scattering, of fast hydrogen atoms in molecular hydrogen at ordinary temperatures. The beam atoms had velocities corresponding to 200–800 volts and were scattered in hydrogen at 10^{-4} to 10^{-1} mm of Hg.

At a given voltage, several independent measurements of the beam intensity were usually made at each of three scattering pressures, the first and third being as near alike as possible. Two thermopile readings were needed for a single intensity determination. The first or blank reading was taken without voltage applied to the atom gun and recorded energy effects due to arc radiation or thermal beam particles. The potentiometric method of measuring thermopile e.m.f.'s permitted the balancing out of these minor energy effects prior to the second reading which gave directly, therefore, the e.m.f. due to the high velocity beam. It was found that conditions were sufficiently steady to make unnecessary the final check set of measurements so that these were often omitted, especially in the later experiments. In most cases, an entire run for a given voltage was repeated over a different pressure range. For example, at 500 volts, four check runs were made during a period of more than three weeks. Two observers were used throughout so that experimental conditions, such as arc pressure, arc currents and arc potentials, could be kept constant.

At any pressure, the beam intensity was obtained by multiplying the observed thermopile e.m.f. by the previously determined sensitivity of the thermopile at that pressure. Pressures were read on a McLeod gage having a large bore capillary, care being taken to prevent sticking of the mercury. Gas temperatures were measured with a copper-constantan thermocouple placed in the scattering gas, near the thermopile.

From the means of the three groups of data at a given voltage, two values of L_v, the mean free path at 1 mm of Hg and 0°C, were computed. The relation used was

$$\frac{I_{P_1}}{I_{P_2}} = e^{-(273x/L_v)(P_1/T_1-P_2/T_2)},$$

where I_{P_1} and I_{P_2} are the intensities at pressures P_1 and P_2; T_1 and T_2, the absolute temperature of the scattering gas at these pressures; and x, the distance through which scattering occurred—

[5] Oliphant, Proc. Roy. Soc. **A124**, 228 (1929).

that is, the distance from atom gun to thermopile (8.57 cm). When three groups of data were available, the second value of the mean free path was obtained by replacing I_{P1}, P_1 and T_1 by I_{P3}, P_3 and T_3. The validity of the equation is subject to the condition that a beam particle should be lost to the detector after its first collision. In cases where intensities were measured at a sufficient number of different pressures in the course of the check runs, a plot of $\log_{10} I_{P2}/I_{P1}$ against $(P_1/T_1 - P_2/T_2)$ gave, within the experimental error, a straight line passing through the origin (see Fig. 3). The present experimental conditions, therefore, justified the use of the equation for the evaluation of L_v.

The total collision cross section, S_v, is computed from the mean free path by using the relation

$$S_v = \frac{1}{nL_v}$$

where n is the number of molecules of scattering gas per cc at 1 mm of Hg and 0°C. This equation is applicable to the special case of a beam of molecules, homogeneous in velocity, absorbed by a gas whose molecules are at rest in comparison with the motion of the beam molecules. In the present case, the average velocity of the scattering molecules is less than one percent of the beam atom velocity as computed from the atom gun voltage.

Table I summarizes the present results on the scattering of high velocity hydrogen atoms in hydrogen gas. In all, 166 independent intensity measurements were made. These fell into 50 groups, from which were computed 32 individual mean free paths. The values recorded in the table are means, obtained by the method of least squares from the several individual values

TABLE I.

VOLTAGE	L_v CM	S_v (10^{-16}CM^2)	PERCENT ERROR (±)	r_v (10^{-8}CM)
196	0.181	1.567	3.5	0.706
306	0.473	0.599	5.7	0.437
398	0.685	0.413	2.4	0.363
499	0.912	0.310	1.8	0.314
552	0.812	0.349	1.1	0.333
592	0.915	0.309	1.9	0.314
695	1.122	0.252	2.1	0.283
810	1.240	0.228	4.2	0.270

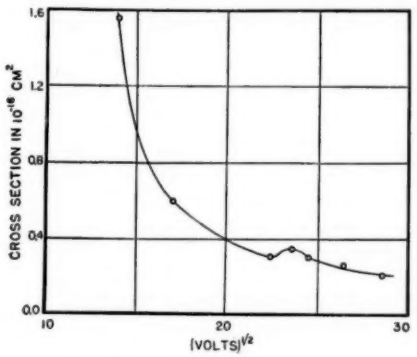

FIG. 4. Classical collision cross sections.

at each of the eight voltages. The voltages are also mean values. It was found more feasible to permit the voltage to vary slightly (about 2 percent) in repeat runs, and take cognizance of the variation by computing a mean, than to control the voltage accurately to a fixed value. The collision radius, r_v, is computed from the relation $r_v = (S_v/\pi)^{\frac{1}{2}}$. The percent error is the probable percentage error of the mean L_v and S_v values.

The average error for all L_v and S_v values is 2.8 percent. This figure represents the reproducibility of the shape of the plot in Fig. 4 of collision cross section against the square root of the atom gun voltage.

DISCUSSION

The relative maximum at 550 volts in Fig. 4 is particularly interesting. It is not likely that it is due to diffraction since the de Broglie wave-length at this voltage is not at all comparable to the collision radius of the system, the values being 0.02×10^{-8} and 0.33×10^{-8} cm, respectively. At 500–600 volts most of the scattering would be quite classical with little expectation of diffraction effects. It is therefore highly probable that the relative maximum is due to the presence of inelastic collisions and may be due to dissociation of the scattering gas or to excitation or ionization of either the beam or scattering particles. Such processes would require electrons of 11–50 volts and protons or fast hydrogen atoms of very much greater energy. The fact that such inelastic collisions would have to exhibit, in the present case, a maximum efficiency at 550 volts has its analog in the fact that ionization and excitation probabilities for

electrons show fairly sharp maxima at energies several volts above the critical potentials. To specify uniquely the nature of the inelastic process occurring at 500–600 volts would require experiments to detect the presence of dissociated particles (comparatively slow hydrogen atoms), excited neutrals, or ions resulting from collisions of 500–600-volt hydrogen atoms with low velocity hydrogen molecules.

The radii listed in Table I are so-called classical radii. As explained by Mott and Massey,[6] this is due to the fact that the average angular aperture of the present detecting system (2.25° with respect to the beam axis, 3.37° in the relative coordinates used by Mott and Massey) was too large to permit the detection of particles lost to the beam by diffraction. The value 2.25° was obtained by averaging, over the entire scattering distance, the maximum angle (referred to the beam axis) through which a beam atom could be deflected and still strike the thermopile receiver. This average included angles ranging from 0.55° for a particle scattered at the beam source to 90° for a particle scattered at the thermopile detector. It was found that the 1-mm alignment nozzle in the radiation shield rather than the 1.6-mm opening above the thermopile receiver, determined the aperture geometry. For the purpose of these calculations the beam was considered as originating in the center of the atom gun channel. Had the average angular aperture of the detecting system been vanishingly small, the experimental cross sections would be expected to be about twice as large as those listed in Table I, giving collision radii whose values would be about $\sqrt{2}$ times the present values. The larger cross sections and radii are referred to as wave-mechanical cross sections and radii since their enhanced values are due to diffraction effects which cannot be present according to classical concepts. For the present system, the relative angular aperture required to detect the first effects due to diffraction lies between 1.15° and 1.72°, depending upon the voltage, as compared with the 3.37° aperture of the present apparatus.

The potential energy curve for the system, $H-H_2$, is not known at the small distances of separation which are of interest in the scattering of high velocity particles. From the information that is available with respect to the potential at larger distances, however, it is practically certain that the radii of Table I, even if multiplied by $\sqrt{2}$ to take into account wave mechanical effects, would fall on the highly repulsive part of such a curve, in confirmation of the prediction that the elastic scattering of particles with velocities as high as those involved in these experiments is due to repulsive forces of interaction.

Since the present experiments have indicated the feasibility of producing high velocity beams and of quantitatively measuring the intensity of such beams, work is being continued to permit the measurement, as a function of angle, of the scattering of fast helium atoms by helium at ordinary temperatures. Such measurements at 200 to 1000 volts should give information concerning the repulsive potential of the He−He system at distances of about 0.5 to 2A. The estimation of interaction potentials from viscosity and equation of state data gives no clue as to the form of the potential at these distances.

[6] Mott and Massey, Proc. Roy. Soc. **A141**, 434 (1933); **A144**, 188 (1934).

The Beta′-Beta Transformation in Lithium-Lead Alloys*

THOMAS C. WILSON**
Yale University, New Haven, Connecticut
(Received August 7, 1939)

Measurements made by Grube and Klaiber in 1934 on the alloys of lithium and lead indicate that a transformation of peculiar character occurs in the beta-phase of these alloys. The behavior of this transformation under high hydrostatic pressure has been investigated by measurements of the electrical resistance. The results, together with those from rough thermal expansion measurements, indicate that the transition takes place gradually on heating from a phase of abnormally high energy and entropy content to a phase of more normal character. X-ray analyses suggest that the transition is accompanied by movements of the lithium atoms in the lattice to more orderly positions.

INTRODUCTION

GRUBE and Klaiber,[1] while making thermal analysis and resistance measurements upon the alloys formed by lithium and lead, found that a transformation of peculiar character took place in solid alloys of composition near the equiatomic ratio of these two metals. This present report describes several measurements made as a supplement to those of the earlier investigators to determine more exactly the nature of this transformation.

The phase diagram for the complete series of alloys, as determined by Grube and Klaiber from their two methods of investigation, is reproduced in Fig. 1. As the diagram indicates, alloys near the equiatomic ratio form a stable compound LiPb, having a melting point of 482°C as compared with that of 327°C for lead, and 178°C for lithium. This so-called beta-phase is homogeneous over a range of about three atomic percent of the constituents. Grube and Klaiber observed that the electrical resistance of alloys in this beta-field is characterized by a negative temperature coefficient at low temperatures (50°C to about 200°C) and a normal positive coefficient at higher temperatures. Their resistance-temperature curves show the transition from an abnormal to a normal behavior occurring abruptly, and at temperatures ranging from 186°C to 214°C depending on the composition of the alloy. These abrupt breaks are assumed to indicate a phase change which is entered upon Fig. 1 as the beta′-beta transformation. It should be noted that the points shown on this phase diagram are taken only from the resistance measurements; cooling curves did not show breaks indicative of an evolution or absorption of latent heat at coincident temperatures.

Grube and Klaiber made and tested two speculations regarding the nature of the beta′-beta transition. Although the resistivity of LiPb is distinctly metallic in magnitude, the peculiar decrease of resistance of the beta′-phase with temperature was first compared to the similar behavior of many semi-conductors. It is known, for example, that small grained specimens of silicon are characterized by a negative temperature coefficient of resistance, whereas single crystals of silicon have a positive coefficient. With the thought, therefore, that grain size might have an effect upon the electrical behavior of LiPb, several large grain specimens were prepared. No significant differences were found between these and the earlier samples examined.

They next compared the decrease in resistance of LiPb as it approaches the critical point on heating to the decrease observable in a quenched alloy of CuAu or Cu_3Au as it is changed by annealing from a metastable (disordered) to an equilibrium (ordered) condition. Because their observations were made on well-annealed specimens, this possibility was dismissed.

Grube and Klaiber concluded that the com-

* Part of a dissertation presented to the Faculty of the Graduate School of Yale University in candidacy for the degree of Doctor of Philosophy.

** Now with New Jersey Zinc Company, Palmerton, Pennsylvania.

[1] G. Grube and H. Klaiber, Zeits. f. Elektrochemie **40**, 745 (1934).

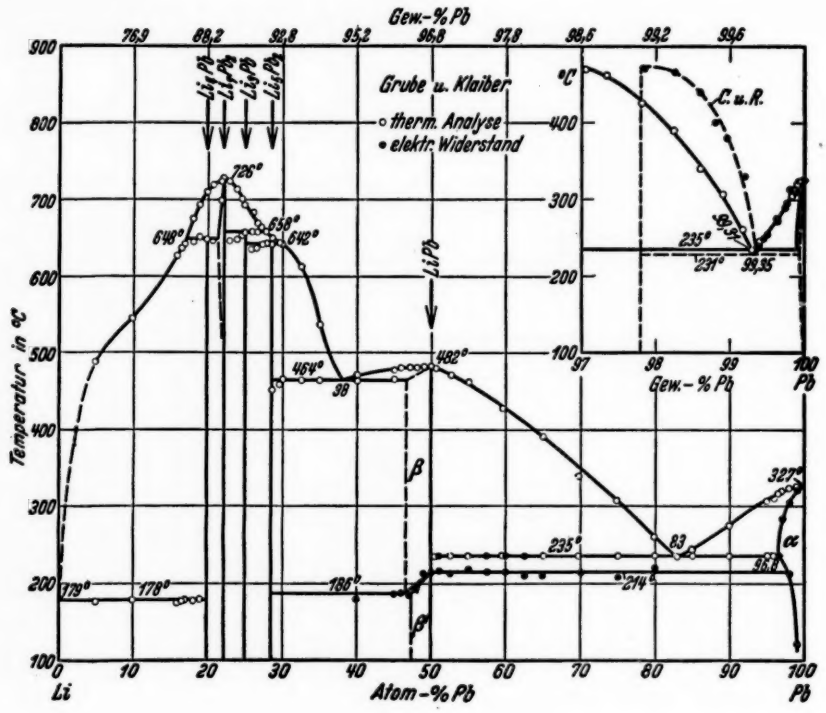

FIG. 1.

pound LiPb can exist in two different forms, the high temperature form beta having a positive temperature coefficient of electrical resistance, the low temperature form beta′ a negative coefficient.

GENERAL

Several anomalous transitions such as that just described have been shown in recent years to be order-disorder transformations. There are in fact three points of similarity observable from the phase diagram between the transition in LiPb and the order-disorder transformation in other alloys. (1) It appears at or near a stoichiometric ratio of the components, occurring over a fairly wide composition range. (2) It occurs in a temperature range near the melting point of one component, as in the case of beta-brass. (3) The transition temperature reaches its maximum at the equiatomic ratio, falling to lower values for alloys on the lithium rich side of this point. Such behavior is characteristic of all order-disorder transformations.

Because of these facts, it was thought of interest to include the alloy LiPb in a general investigation (reported elsewhere[2]) on the effect of high hydrostatic pressure on the order-disorder transformation. Measurements of the electrical resistance of the alloy under pressure are here reported,* as well as several observations of a rough character made to explain in part the electrical behavior.

PREPARATION OF SPECIMENS

Since lithium reacts with glass, quartz and most common crucible materials, the alloys were made, following Grube and Klaiber, in a soft steel crucible. Desired amounts of lithium (Kahlbaum) were weighed in a beaker of mineral oil after the usual oxide coating on the sticks had been scraped off under petroleum ether. The weighed quantities were rinsed off in the scraping dish and quickly inserted into the crucible, likewise filled with petroleum ether. The lead (labeled Test Lead—Silver Free) was added, and the crucible closed with a screw plug. The plug was pierced in such a way that it made a tight

[2] T. C. Wilson, Phys. Rev. **56**, 598 (1939).
* The technique used is described in reference 2.

seal when screwed down, but if left slightly loose permitted the crucible to be evacuated through an attached tube. The plug was sealed around the threads with Apiezon putty, the crucible evacuated and then sealed by tightening the plug. After heating to about 550°C, the crucible was removed from the furnace and shaken vigorously as it cooled. This proved necessary to prevent separation of the liquid metals and so obtain a homogeneous alloy. The fact that both ends of the crucible were closed with screw plugs facilitated the removal of the ingot.

Resistance specimens were cast by thrusting a steel mold into a second crucible in which the alloy was later melted. The surface of the metal, although protected to some degree by a stream of illuminating gas, invariably was covered with various compounds (lithium forms oxides, nitrides, and hydrides) after this process, and from 3 to 5 percent lithium was lost. These factors were not considered serious, however, since the mold was thrust so far into the body of the melt that surface impurities did not become part of the castings, and since allowance could be made for lithium loss when weighing out the components of the alloy.

This method of casting resistance specimens is due to Grube and Klaiber. They, however, used open crucibles in a purified argon atmosphere for both preparing their alloys and casting their specimens.

Results and Conclusions

Alloys of several compositions were prepared. All of those examined showed the peculiar behavior of the electrical resistance described above. Fig. 2 for example, shows the observed course of the resistivity-temperature curve for the alloy prepared with the highest lithium content (55.6 atomic percent—calculated from x-ray measurements of the lattice constant and from density). Over the temperature range used by the other investigators, 50°C and above, the shape of the curve is quite similar to that they gave for about the same composition. The critical temperature, however, is about 14°C lower and the resistivity slightly lower (67. (10)$^{-6}$ ohm·cm at 50°C as against Grube and Klaiber's value of about 70. (10)$^{-6}$ ohm·cm). The latter difference may be explained by dimensional errors since alloys of this composition are so brittle that it is very difficult to get large specimens out of the mold and relatively small fragments must be used for resistance measurements.

From Fig. 2 it may be noticed that the low temperature modification of LiPb (beta') has a negative temperature coefficient of resistance only over the restricted temperature range used by the earlier investigators. For low temperatures its resistance behavior is purely metallic in character. The shape of the curve also suggests that whatever transition is occurring between the beta'- and the beta-phase has already progressed considerably at temperatures as low as 50°C. Measurements made upon the alloy between this temperature and the critical point may therefore only be indicative of the state of the alloy in the latter stages of the transformation.

The dotted lines in Fig. 2 show the resistivity changes of the same alloy when under pressures

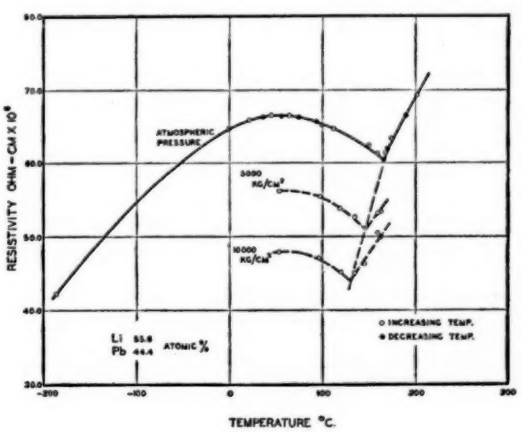

Fig. 2.

of 5000 kg/cm² and 10,000 kg/cm². The points on these dotted curves are derived from the resistance-pressure runs made at the constant temperatures shown in Figs. 3 and 4. The average pressure coefficients up to 10,000 kg/cm² (Table I) were applied to the values of the resistivity obtained on the run at atmospheric pressure (full line) to derive the lower curves. This indirect procedure was made necessary by

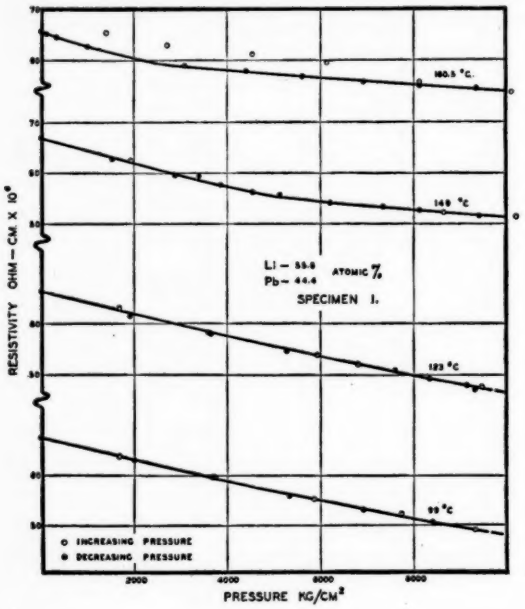

FIG. 3.

the slight permanent changes in resistance which took place in the specimen, due, no doubt to the shifting of the solder under pressure. (See for example the curve for 160.5°C, Fig. 3.)

The instantaneous rates of change of the resistivity with pressure are given in Table II; these quantities are also derived from the curves of Figs. 3 and 4.

There are three general statements justified by the behavior of this alloy under pressure. These are: (1) The values of the quantities listed in Tables I and II are of relatively large magnitude for the low temperature or beta′-phase. The high temperature or beta-phase, however, has a comparatively normal behavior. (The average pressure coefficient of resistance of lead is about 12 $(10)^{-6}$ cm²/kg.) (2) The pressure coefficients increase but slightly as the temperature of the transition is approached on heating. (3) The transition point is lowered by pressure.

In order to determine whether the latter fact could be attributed to a contraction of the alloy as it is heated through the critical point, thermal expansion measurements were made by placing a rod of the alloy (it was necessary to use an alloy of about 47 percent lithium consisting of alpha and beta mixed crystals to obtain the required mechanical strength) in a dilatometer of the type described by Bridgman[3] for his compressibility measurements. The whole assembly was heated in a mineral oil bath to prevent oxidation of the specimen. The results may be listed as a further statement. (4) There is no contraction in length as the alloy is heated, but instead a steady expansion at rates given roughly by

$$\frac{1}{L}\left(\frac{\Delta L}{\Delta T}\right)_{\beta'} = 4(10)^{-5}\ °C^{-1},$$

$$\frac{1}{L}\left(\frac{\Delta L}{\Delta T}\right)_{\beta} = 2(10)^{-5}\ °C^{-1}.$$

These four facts should be explained by any proposal concerning the nature of the beta′-beta transformation. On thermodynamic considerations, Maxwell's fourth relation

$$\left(\frac{\partial V}{\partial T}\right)_p = -\left(\frac{\partial \phi}{\partial p}\right)_T$$

provides a connection between (1) and (4), in that (4) shows the left-hand side of the equation to be positive for both phases and about twice as great in magnitude for the beta′ as for the beta-phase. It therefore can be asserted that a decrease of the entropy ϕ occurs under pressure, and at a rate approximately twice as great in the beta′-phase as in the beta-phase. This is reflected in the behavior of the resistance under pressure as stated in (1) and as shown in a more quantitative way in Table II.

TABLE I. LiPb. *Average pressure coefficients of resistance.*

°C TEMP.	SPECIMEN	$-\frac{1}{R}\frac{\Delta R}{\Delta p}\times 10^6$ CM²/KG				
		2000 KG/CM²	4000 KG/CM²	6000 KG/CM²	8000 KG/CM²	10,000 KG/CM²
54	II	33.3	32.3	30.5	28.7	27.6
97.6	II	31.8	31.0	30.7	29.6	28.6
99	I	32.4	31.6	30.8	29.8	29.5
119	II	33.7	33.7	32.5	31.1	30.1
123	I	33.9	33.1	32.1	31.3	30.0
135	II	36.9	35.1	33.1	31.3	29.2
147	II	37.7	37.0	35.6	29.7	26.0
149	I	36.6	35.2	31.0	26.3	23.3
160.5	I	38.4	28.5	22.8	19.6	17.6
164	II	36.1	25.1	21.5	19.3	17.6

[3] P. W. Bridgman, *Physics of High Pressure* (Macmillan, 1931).

The total entropy ϕ may be considered as a sum of two terms, ϕ_V the entropy of the thermal vibrations of the atoms, and ϕ_c the configurational entropy depending upon the orderliness of their arrangement in the lattice. With a pure metal, the total entropy consists of only ϕ_V and the effect of pressure is in general to decrease this quantity. With order-disorder alloys, such as CuAu and Cu_3Au, the entropy of a partially or wholly disordered alloy consists of contributions from both terms. As has been shown in reference (2), pressure upon such an alloy decreases both types of entropy, but that the rate of decrease of the configurational entropy with pressure, $-(\partial\phi/\partial p)_c$, changes from a low value at low temperatures to a high value at temperatures at and slightly above the critical point, and thereafter falls again to a negligibly small amount.

TABLE II. LiPb. *Instantaneous slopes* $d\rho/dp$ *ohm·cm³* $kg^{-1}\times 10^4$.

°C Temp.	Specimen	2000 kg/cm²	4000 kg/cm²	6000 kg/cm²	8000 kg/cm²
54	II	19.9	18.0	15.6	14.4
97.6	II	19.1	18.6	17.6	16.4
99	I	20.9	20.0	18.6	17.9
119	II	20.7	20.1	17.8	16.3
123	I	21.7	20.7	19.5	18.2
135	II	21.7	19.3	17.5	14.3
147	II	23.2	21.9	13.6	7.1
149	I	23.4	22.5	9.0	7.8
160.5	I	21.4	7.2	7.0	7.0
164	II	9.0	8.6	7.7	6.6

In the case of LiPb, there are two possible postulates; (A) that the entropy content is made up of both configurational and vibrational parts. (B) that the entropy is wholly of the vibrational type.

Assuming the validity of postulate A, the behavior described under statement (1) is consistent with the view that the beta′-phase consists of a disordered arrangement of the constituent atoms and that the effect of pressure is to promote a more orderly array. With this view, the comparatively normal behavior of the beta-phase would indicate that here the alloy is in a completely disordered state and at a temperature too high to permit the arrangement to be affected by the pressures used, or that in the beta-phase the atoms are already in a uniform distribution and that pressure cannot therefore promote a further ordering.

Postulate B rules out such an explanation in terms of degree of order but requires that some change takes place in the magnitude of the forces holding the atoms to their unchanging positions of equilibrium and that the amplitude and frequency of their vibrations are thereby affected as the alloy passes from the beta′- to the beta-phase.

Statement (2) seems to point only to the fact that the transition which occurs takes place very gradually in the range of temperatures 50°C to the critical point, a possibility already suggested by the shape of the resistivity-temperature curve. Such behavior is not typical of the order-disorder alloys CuAu and Cu_3Au.

Statement (3) describes a shift in the critical point with pressure that is opposite in direction to that occurring with the alloys CuAu and Cu_3Au. This effect also shows that the transformation is somehow different from the usual order-disorder transition. Because of this negative shift, it is possible to transform the beta′-

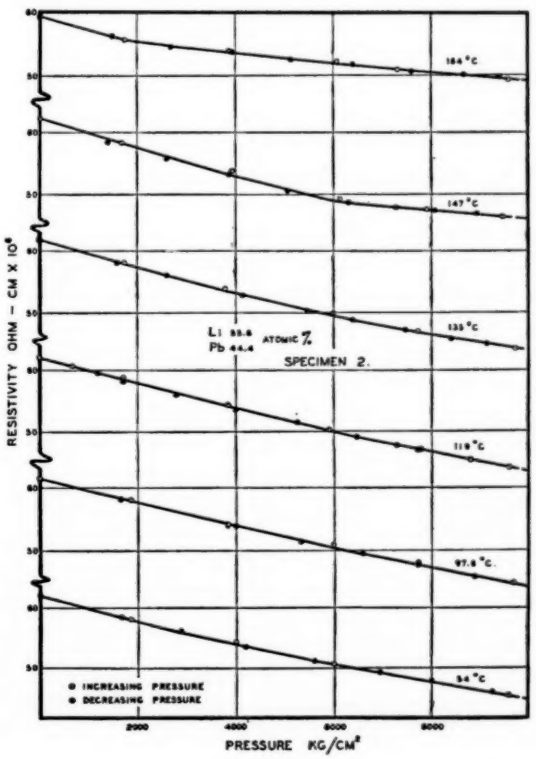

FIG. 4.

phase into the beta-phase by pressure alone. Since, however, pressure decreases the entropy, it is evident that at constant temperature the beta-phase is of lower entropy content than the beta′-phase, and inferentially that the rate of increase of entropy with temperature in passing from the beta′ to the beta-phase at constant pressure is less than a normal value.

In view of the fact that Grube and Klaiber's observations indicate that this transition involves no latent heat at the critical point, Clapeyron's equation does not apply to the change of the critical point with pressure. If the assumption is made, however, that the transformation is one of the second kind (Ehrenfest's terminology), then Ehrenfest's equation

$$\frac{dT_c}{dp} = T\frac{\Delta(\partial V/\partial T)_p}{\Delta C_p} \qquad (1)$$

may be applied to the observed shift. Inserting experimental values for the known quantities, the equation predicts that the specific heat of the alloy should rise, as it passes through the critical point on heating, by about 0.03 cal. g^{-1} $°C^{-1}$. There have been theoretical objections to Ehrenfest's equation* and questions may be justifiably raised regarding the magnitude of this quantitative prediction on the specific heat. There seems, however, little reason to doubt the sign of the predicted change.

That an increase in the rate of absorption of energy should occur as the alloy is transformed by heating to the beta-phase, implies (in view of the relative entropy content of the two phases) that the beta-phase is one of more normal energy content. The transition between the two phases on heating would, in such a case, be accompanied by a gradual release of the excess energy of the beta′-phase. This process would be evidenced by an abnormally low value of the specific heat in the latter stages of the transition, and a rise in the specific heat to a normal value as the transition point was crossed. (A normal value of the specific heat of LiPb, calculated from the specific heats of Li and Pb assuming a pure mixture would be about 0.07 cal. g^{-1} $°C^{-1}$.)

A further argument regarding the behavior of the energy may be based upon the shape of the resistivity-temperature curve. In most metals and even in the order-disorder alloys the resistance and the energy are dependent upon the same factors and in a roughly similar way. The energy-temperature curves and resistance-temperature curves have therefore similar shapes. The resistivity-temperature curve of LiPb seems to indicate that there is a contribution to the resistance in the beta′-phase which gradually vanishes as the transition point is approached. It might be inferred that this is also true of the energy of the alloy. The analogy cannot be carried too far, however, as it seems fundamental that the energy-temperature curve have a positive slope at all times.

An attempt was made to test directly the conclusions above regarding the energy by measuring the specific heat. The method used was that of Sykes,[4] modified by substituting a light copper calorimeter containing fragments of the alloy for a massive specimen of the alloy itself. Due to oxidation of the alloy during the measurements, and due to the small quantity used, (only 6 g compared to 10 g for the calorimeter itself) the results were insufficiently precise to be used in confirmation of these conclusions. The results, however, did confirm Grube and Klaiber's work in that no latent heat could be detected at the critical point.

X-ray analyses of the structure of LiPb are made difficult by the fact that scattering from lithium is so small relative to that from lead that it is not possible to detect the positions of the lithium atoms. Several exposures were made, however, and these showed the lead atoms on a body-centered lattice in both the beta′- and beta-phase.* For the alloy of 55 percent lithium the measured lattice constant was 5.015A at room temperature, the density 6.06 g/cm^3. These figures indicate that there are slightly over two lead atoms to the unit cell and slightly less than three lithium atoms. The exact figures are of little meaning since the density measurements

* See discussion in Epstein's *Thermodynamics*.

[4] C. Sykes, Proc. Roy. Soc. **A148**, 422 (1935).

* These measurements were made by soldering the specimen to a copper rod and recording the diffraction patterns for small glancing angles with the rod at room temperature and with the rod heated electrically to 210°C. The surface of the specimen was protected from oxidation in the first case by a coating of vaseline, in the second by allowing heated mineral oil to drip constantly on the specimen during the exposure.

were made of necessity in kerosene on small fragments and are not therefore precise. It should be noted, however, that this indicated structure requires that the alloy of 60 percent lithium be body-centered in the lead atoms with exactly two atoms per unit cell. The three lithium atoms would in that case be at any of the six equivalent remaining positions at the face centers and at the middle of the cube edges. It would then have to be assumed that with alloys of between 60 percent and 50 percent lithium, the extra lead atoms replace lithium. (This picture seems difficult to reconcile with the phase diagram but no alternative presents itself from the preliminary x-ray analysis.)

Under postulate A, earlier mentioned, the beta′-phase has an abnormally high value of configurational entropy at least in the range of temperatures from room temperature to the transition point, while the beta-phase has a more normal entropy content. This might be explained on the basis of the suggested structure above as follows. At temperatures around 0°C, the lithium atoms are more or less irregularly scattered among the many equivalent positions in the cubic lattice of lead atoms, their irregularity causing the abnormally high entropy content and the high value of the electrical resistance. As room temperatures are approached a slight distortion of the cubic lead lattice takes place, making some of the six equivalent lithium positions more favorable energetically than the others. If the distorted structure is tetragonal the six positions are split two and four, if rhombohedral, three and three. This distortion is accompanied by a rearrangement of the lithium atoms into the more favorable ordered positions. The process of distortion and rearrangement continues as the melting point of pure lithium is approached, culminating in a complete transition to an orderly arrangement at the critical point. The effect of pressure upon the beta′-phase is simply to enhance the distortion and rearrangement process, causing the abnormally high pressure coefficient of resistance earlier mentioned.

Under postulate B, no simple suggestion presents itself regarding the cause of the relative entropy difference between the two phases.

The unusual character of this transformation would seem to warrant a more exhaustive and precise investigation than has been possible in this work, particularly with regard to the x-ray analysis and the behavior of the specific heat.

The writer wishes to acknowledge his indebtedness to Professor L. W. McKeehan under whose guidance this work was carried out. His keen interest and help throughout the entire investigation and throughout many discussions of the problem were invaluable.

Thanks are expressed to Professor P. W. Bridgman of Harvard whose loan to the Sloane Physics Laboratory of part of the pressure equipment simplified the technical difficulties. Acknowledgment should also be made of conversations with Professor J. C. Slater of M.I.T. and Dr. W. Shockley of the Bell Telephone Laboratories which took place subsequent to the experimental work.

Dissociation Treatment of Condensing Systems

III. Properties of Saturated Vapors of H_2O, NH_3, CH_3Cl and CO_2*

T. P. Tseng, S. K. Feng, C. Cheng and W. Band
Yenching University, Peiping, China

(Received October 16, 1939)

It is found that the dissociation treatment previously described gives a satisfactory theory of the saturated vapor pressure curves in temperature ranges not too close to the critical point. Curves are given for PV/NkT and for surface energy in the cases of H_2O, NH_3, CH_3Cl and CO_2. In the case of H_2O there remains an appreciable discrepancy in the energy curves at low values of T/T_c. It is suggested that this may be removed by taking into account the small size of the clusters involved in the equilibrium between vapor and liquid: the surface energy in a cluster may differ from that for the liquid in bulk. A method of estimating mean cluster sizes is suggested, which leads to reasonable results.

Introduction

THE dissociation treatment of condensing systems has been shown to give a perfect gas analog of the equation for the properties of saturated vapors,[1] and to further permit methods of successive approximation towards a more precise equation which takes into account the finite size of the molecules.[2]

This paper presents the results of an application of the simpler equation to the four examples, H_2O, NH_3, CH_3Cl and CO_2.

General Method

The equations to be employed are, from reference 1 Eq. (17):

$$PV=NkT(1+\phi)/(1+\sigma), \tag{1}$$

where

$$\phi=\Sigma_s' s^{3/2}\exp\{-\chi(s,T)/kT\}, \tag{2}$$

$$\sigma=\Sigma_s' s^{5/2}\exp\{-\chi(s,T)/kT\}, \tag{3}$$

and $\chi(s,T)$ is the mean surface energy of a cluster of s molecules. To proceed from this point, some hypothesis as to the form of $\chi(s,T)$ is required. It will be assumed that it is proportional to the number of molecules in the surface of the cluster, the factor of proportionality being a function only of T:

$$\chi(s,T)=A(T)n(s). \tag{4}$$

The number of surface molecules $n(s)$ in a cluster of type s will be assumed equal to

$$n(s)=\alpha(s^{\frac{1}{3}}-1), \tag{5}$$

where α is a constant. Physically there is no very clear definition of what is meant by the number of molecules in the surface of a cluster of molecules, and in Eq. (5) it is quite possible that α should be regarded as a function of T. However, the above vague argument will serve as a partial rationalization of the following mathematical assumption regarding the exact form of $\chi(s,T)$:

$$\chi(s,T)=\alpha A(T)(s^{\frac{1}{3}}-1), \tag{6}$$

where α is a constant.

Write

$$w=\alpha A(T)/kT, \tag{7}$$

then (2), (3) become:

$$\phi=e^w\Sigma_s' s^{3/2}\exp\{-ws^{\frac{1}{3}}\}, \tag{8}$$

$$\sigma=e^w\Sigma_s' s^{5/2}\exp\{-ws^{\frac{1}{3}}\}. \tag{9}$$

These sums will converge rapidly for values of w large enough, and can then be directly tabulated as functions of w. For smaller values of w, the sums are more easily obtained as given approximately by integrals, as follows.

Write

$$x=ws^{\frac{1}{3}},\quad y=w2^{\frac{1}{3}}, \tag{10}$$

then remembering that in transforming the sums, the steps of the infinitesimal ds are unity, a

* Contribution from the Department of Physics, Yenching University.

[1] Part I, W. Band, J. Chem. Phys. **7**, 324 (1939).

[2] Part II, W. Band, J. Chem. Phys. **7**, 927 (1939).

TABLE I. *Values of ϕ, σ from (8) and (9); and from (11) and (12).*

w	y	Integral Method ϕ	Integral Method σ	Integral Method $\frac{(1+\phi)}{(1+\sigma)}$	Summation Method ϕ	Summation Method σ	Summation Method $\frac{(1+\phi)}{(1+\sigma)}$	Accepted $\frac{(1+\phi)}{(1+\sigma)}$
0.5	0.7937	145.2	3311.	0.0441	—	—	—	0.044
1.0	1.5874	16.21	141.2	0.1210	—	—	—	0.117
1.5	2.3811	4.803	26.09	0.2142	—	—	—	0.206
2.0	3.1748	2.024	8.406	0.3215	—	—	—	0.310
2.5	3.9685	1.018	3.558	0.4426	—	—	—	0.427
3.0	4.7622	0.5574	1.757	0.5650	—	—	—	0.545
3.5	5.5559	0.3265	0.9535	0.6791	0.5401	1.351	0.6551	0.655
4.0	6.3496	0.2008	0.5511	0.7742	0.3644	0.8588	0.7340	0.734
4.5	7.1433	0.1263	0.3327	0.8451	—	—	—	0.800
5.0	7.9370	0.08155	0.2074	0.8957	0.1783	0.3913	0.8469	0.847
6.0	9.5244	0.03588	0.08620	0.9537	0.09231	0.1947	0.9143	0.914
7.0	11.1118	0.01683	0.03803	0.9796	0.04924	0.1016	0.9525	0.953
8.0	12.6992	0.008629	0.01740	0.9913	0.02671	0.05443	0.9737	0.974
9.0	14.2866	—	—	—	0.01463	0.02959	0.9855	0.986
10.0	15.8740	—	—	—	0.008058	0.01623	0.9920	0.992
11.0	17.4614	—	—	—	0.004456	0.008949	0.9955	0.996

simple calculation gives the results:

$$\phi = 6\sqrt{2}y^{-3.75}\exp(2^{-\frac{1}{2}}y)\int_y^\infty x^{2.75}e^{-x}dx, \qquad (11)$$

$$\sigma = 12\sqrt{2}y^{-5.25}\exp(2^{-\frac{1}{2}}y)\int_y^\infty x^{4.25}e^{-x}dx. \qquad (12)$$

Therefore, in terms of known integrals:

$$\phi = F(y)\{\Gamma(3.75) - I(y, 2.75)\}, \qquad (13)$$

where

$$\sigma = G(y)\{\Gamma(5.25) - I(y, 4.25)\}, \qquad (14)$$

$$F(y) = 8.4853y^{-3.75}e^{0.62996y}, \qquad (15)$$

$$G(y) = 16.7706y^{-5.25}e^{0.62996y}, \qquad (16)$$

and

$$I(y, n) = \int_0^y x^n e^{-x}dx, \qquad (17)$$

TABLE II. *PV/NkT for* H_2O.

T°K	S DYNES/CM²	$\nu_0 \times 10^{-21}$	$\alpha A(T) \times 10^{+14}$	w	$\frac{(1+\phi)}{(1+\sigma)}$	$\frac{PV}{NkT}$	T/T_c
647	0.0	13.5	0.0	0.0	0.0	0.185	1.0
403	52.84	31.5	25.6	4.64	0.817	0.969	0.623
373	58.85	32.3	28.1	5.50	0.885	0.983	0.577
343	64.42	32.9	30.3	6.45	0.934	0.991	0.530
313	69.56	33.4	32.5	7.56	0.967	0.995	0.484
283	74.22	33.7	34.5	8.88	0.984	0.999	0.437
265	76.96	33.6	35.7	9.84	0.991	0.999	0.410

TABLE III. *PV/NkT for* CH_3Cl.

T°K	S DYNES/CM²	$\nu_0 \times 10^{-21}$	$\alpha A(T) \times 10^{+14}$	w	$\frac{(1+\phi)}{(1+\sigma)}$	$\frac{PV}{NkT}$	T/T_c
416.3	0.0	4.38	0.0	0.0	0.0	0.266	1.00
393.1	2.12	7.77	2.63	0.49	0.044	0.587	0.944
373.1	4.54	8.71	5.20	1.02	0.125	0.690	0.896
353.1	7.22	9.40	7.84	1.62	0.240	0.754	0.848
333.1	10.1	9.99	10.6	2.32	0.400	0.785	0.800
313.1	13.1	10.5	13.2	3.08	0.583	0.866	0.752
293.1	16.3	11.0	16.1	4.01	0.736	0.906	0.704
273.1	19.6	11.5	18.6	4.97	0.844	0.940	0.656
249.1	23.7	12.0	21.9	6.41	0.932	0.969	0.598

TABLE IV. *PV/NkT for* NH_3.

T°K	S DYNES/CM²	$\nu_0 \times 10^{-21}$	$\alpha A(T) \times 10^{+14}$	w	$\frac{(1+\phi)}{(1+\sigma)}$	$\frac{PV}{NkT}$	T/T_c
406	0.0	8.31	0.0	0.0	0.0	0.246	1.000
380	4.8	15.52	3.7	0.71	0.074	0.558	0.936
358	8.2	17.61	5.9	1.20	0.160	0.682	0.882
340	11.5	18.94	7.83	1.68	0.252	0.758	0.837
323	14.8	20.04	9.71	2.19	0.364	0.818	0.796
307	18.1	20.97	11.5	2.73	0.498	0.863	0.756
284	23.4	22.19	14.4	3.70	0.676	0.914	0.700
259	32.8	23.40	19.4	5.47	0.881	0.953	0.638
238	40*	24.35	23.1	7.1	0.955	0.974	0.586
219	46*	25.16	27	9.0	0.986	0.985	0.540
203	51*	25.82	28	9.8	0.987	0.989	0.500

TABLE V. *PV/NkT for* CO_2.

T°K	S DYNES/CM²	$\nu_0 \times 10^{-21}$	$\alpha A(T) \times 10^{+14}$	w	$\frac{(1+\phi)}{(1+\sigma)}$	$\frac{PV}{NkT}$	T/T_c
304.2	0.00	7.17	0.00	0.00	0.0	0.2765	1.000
303.1	0.06	8.24	0.71	0.02	0.002	0.3776	0.996
293.1	1.16	10.64	1.16	0.29	0.026	0.5437	0.964
283.1	2.73	11.85	2.54	0.65	0.055	0.6367	0.931
273.1	4.49	12.75	3.98	1.06	0.128	0.6930	0.898
248.1	9.13	14.51	7.42	2.18	0.357	0.8218	0.816

* Values extrapolated from experimental data.

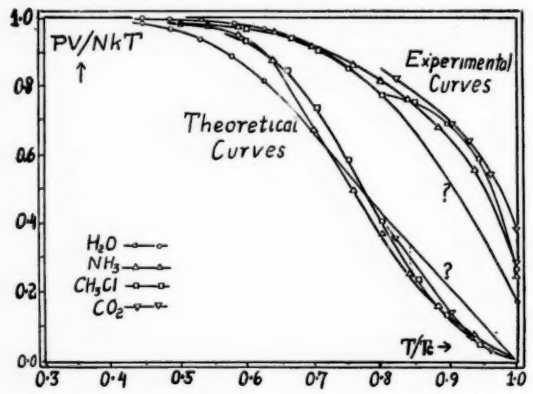

FIG. 1.

is the incomplete gamma-function.[3] Table I gives the sum values from (8) and (9): and also the values of the integrals ϕ and σ derived from (13) and (14).

The integrals are appreciably less than the sums where they have both been obtained; but the agreement between the values of $(1+\phi)/(1+\sigma)$ is good. The sum values of $(1+\phi)/(1+\sigma)$ have been extrapolated to smaller values of w, using the integral results as a guide; they are tabulated in the last column of Table I.

THE SATURATED VAPOR PRESSURE CURVES

Equation (5) gives the total number of molecules in the surface of a cluster of s molecules. Assume that the cluster is roughly spherical in form with radius r; then the volume density of molecules in the cluster is

$$\nu_v = 3s/4\pi r^3 \tag{18}$$

and the surface density, from (5) is roughly

$$\nu_0 = \alpha s^{\frac{1}{3}}/4\pi r^2. \tag{19}$$

Thus

$$\nu_0 = \alpha \nu_v^{\frac{1}{3}}/4.837, \tag{20}$$

and the energy per unit area is therefore

$$E = \nu_0 A(T) = (1/4.837)\nu_v^{\frac{1}{3}}\alpha A(T). \tag{21}$$

Assuming that this is equal to the measured surface tension and that the density of molecules ν_v is the same in clusters as in the liquid, the above equation gives the value of $\alpha A(T)$. These are tabulated in column 4 of Tables II, III, IV and V. Eq. (7) then gives the values of w, and from Table I the corresponding values of $(1+\phi)/(1+\sigma)$ are found. These are compared with the experimental values of PV/NkT, in Tables II, III, IV and V. Fig. 1 also gives the same comparison plotted against the scale of T/T_c. The agreement is excellent for small values of T/T_c; but since in any case the values of $(1+\phi)/(1+\sigma)$ vary very slowly with w in this range, this is hardly a stringent check on the theory.

SURFACE ENERGIES AND MEAN CLUSTER SIZES

A more searching and suggestive test of the theory would seem to be the following. First match the experimental values of PV/NkT with the values of $(1+\phi)/(1+\sigma)$ in Table I, in accordance with Eq. (1), so constructing a table of values of w corresponding to the values of T. From these values of w, and T, Eq. (7) will give values of $\alpha A(T)$; finally Eq. (21) will give the theoretical values of the surface energy E. These results are tabulated in Tables VI, VII, VIII and IX; and shown graphically in Fig. 2.

The values of E per unit area obtained by this approach are consistently higher than the measured surface tension, but the difference decreases at lower values of T/T_c. Considering that

TABLE VI. s *for* H_2O.

T°K	PV/NkT	w	αA(T) ×10⁺¹⁴	ν_v × 10⁻²¹	E DYNES/CM²	S	s	T/Tc
647	0.1847	1.35	11.9	13.5	13.9	0	1.0	1.0
466	0.9143	6.00	38.3	29.3	75.3	37	2.8	0.72
427	0.9525	7.00	41.0	30.7	83.1	47	3.4	0.66
398	0.9737	8.00	43.6	31.6	90.2	53.9	3.9	0.62
367	0.9855	9.00	45.3	32.4	95.1	60.0	4.5	0.57
336	0.9920	10.0	46.1	33.0	98.0	65.7	5.3	0.52
312	0.9955	11.0	47.0	33.4	100.9	69.7	5.8	0.48

TABLE VII. s *for* CH_3Cl.

T°K	PV/NkT	w	αA(T) ×10⁺¹⁴	ν_v ×10⁻²¹	E DYNES/CM²	S	s	T/Tc
415.0	0.3215	2.00	11.4	5.25	7.1	0.06	1.0	1.00
411.8	0.4426	2.50	14.1	6.25	9.9	0.29	1.1	0.99
401.5	0.5650	3.00	16.5	7.23	12.8	1.23	1.2	0.96
381.4	0.6551	3.50	18.3	8.37	15.6	3.50	1.5	0.92
361.9	0.7340	4.00	19.8	9.12	17.9	6.01	1.9	0.87
321.0	0.8469	5.00	22.0	10.3	21.5	1.9	3.4	0.77
289.1	0.9143	6.00	23.8	11.1	24.4	16.9	5.9	0.69
263.4	0.9525	7.00	25.3	11.7	26.9	21.2	10.3	0.63

[3] N. Nielsen, *Handbuch der Theorie der Gamma-funktion* (Leipzig); Jahnke und Emde, *Funktionentafeln* (Leipzig).

there are no variable parameters in the theory, the agreement is really quite good.

Apart from the necessarily approximate nature of the whole method, as emphasized several times already, there is one possible explanation of the discrepancies actually present. Except near the critical point, only small clusters will actually take part in the maintenance of the equilibrium or saturated condition. The mean energies $\chi(s,T)$ will therefore necessarily refer to such small clusters, and the number $n(s)$ in Eq. (4) will be the function of s appropriate for small values. In Eq. (19) the factor $s^{\frac{1}{3}}$ was written for $(s^{\frac{1}{3}}-1)$, to permit the simple relation (20) between ν_0 and ν_v. If the significant values of s are all small, this neglect is not justified. Write, instead, as a second approximation:

$$\nu_0=\alpha s^{\frac{1}{3}}[1-(s)^{-\frac{1}{3}}]/4\pi r^2, \qquad (22)$$

where s is a mean of the significant values of s. Then instead of (20), it now follows that

$$\nu_0=(1/4.837)\alpha\nu_v^{\frac{1}{3}}[1-(s)^{-\frac{1}{3}}]. \qquad (23)$$

The quantity s then becomes a parameter which can be adjusted so as to give an exact agreement between the theoretical E and the surface tension values. Thus, writing S for the observed surface tension values, and E for the uncorrected expression obtained from (21), equating S to the expression derived from (23), it follows that

$$S=E[1-(s)^{-\frac{1}{3}}]$$

or

$$s=[E/(E-S)]^3. \qquad (24)$$

The values of s obtained in this way are also shown in the tables.

TABLE VIII. *s for* NH_3.

T°K	PV/NkT	w	$\alpha A(T)$ $\times10^{+14}$	ν_v $\times10^{-21}$	E DYNES/CM²	S DYNES/CM²	s	T/T_c
406	0.2460	1.65	9.2	8.31	7.8	0.0	1.0	1.00
364	0.6551	3.50	17.5	17.1	24.0	7.2	1.7	0.90
340	0.7340	4.00	18.6	19.0	27.3	12.0	2.4	0.84
313	0.8470	5.00	21.5	20.6	33.4	17.0	3.0	0.77
284	0.9143	6.00	23.4	22.2	38.2	25.0	4.9	0.70
259	0.9525	7.00	24.9	23.4	42.1	33.0	10	0.64
238	0.9737	8.00	26.1	24.5	45.3	40.0	25	0.59
219	0.9855	9.00	27.0	25.2	47.9	46.0	126	0.54

TABLE IX. *s for* CO_2.

T°K	PV/NkT	w	$\alpha A(T)$ $\times10^{+14}$	ν_v $\times10^{-21}$	E DYNES/CM²	S DYNES/CM²	s	T/T_c
304.2	0.2765	1.84	7.67	6.40	5.5	0	1.0	1.00
303.9	0.3398	2.13	8.87	7.59	7.1	0.017	1.0	1.00
299.6	0.4540	2.61	10.72	9.42	9.9	0.40	1.1	0.98
291.4	0.5610	3.07	12.28	10.9	12.4	1.43	1.2	0.96
280.4	0.6551	3.5	13.4	12.1	14.7	3.11	1.4	0.92
263.7	0.7338	4.0	14.5	13.5	16.9	6.04	1.9	0.87
252.3	0.7973	4.5	15.6	14.3	18.9	8.24	2.4	0.83

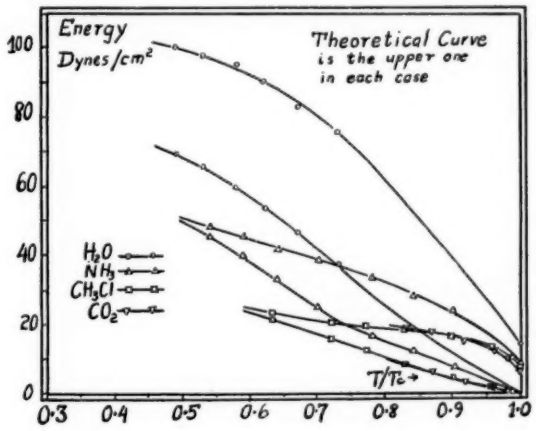

FIG. 2.

At temperatures near the critical point the theory fails for entirely other reasons, but outside this neighborhood these values of s may give some indication as to the size of clusters which take part in the exchange between the liquid and its saturated vapor. Where s is computed as greater than about 30, the result is meaningless because such a value means that the error caused by the small value s is less than 10 percent; and would be masked by other uncertainties.

It is interesting that s decreases with increasing temperature, as is intuitively correct. Near the critical point the formal application of (24) leads to values of s near or even less than 2, whereas intuitively very large clusters are to be expected. However the more accurate theory, applicable near the critical point, will lead to an increase of s close to the critical point.

In conclusion one of us, Tse-Pei Tseng, wishes to thank the Board of Trustees for the Administration of the Indemnity Funds Remitted by the British Government to China, for granting him a Boxer Research Fellowship for 1938–39.

A Study of the Diffraction of Protons of Medium Energy by Vapor Molecules*

H. J. YEARIAN†
Purdue University, Lafayette, Indiana

(Received August 7, 1939)

The diffraction of 15–20 kv protons by carbon tetrachloride vapor has been investigated with a low voltage arc source and electrostatic focusing with photographic registration. The principal difficulties encountered were with space charge dispersion of the beam near the ion source, and with neutralization of the beam as it passed through the vapor. The cross sections for neutralization and re-ionization of protons and hydrogen molecular ions in several gases and vapors were determined. The sensitivity of photographic film was found to diminish as the emulsion was outgassed but to increase fifteen-fold when it was treated with oil. When suitable precautions were taken to minimize the background scattering, diffraction patterns were obtained showing three maxima, the measurements of which are in satisfactory agreement with electron diffraction data.

WORKERS in the field of molecular structure determination by means of electron diffraction have long felt the need of some modification or extension of their methods which would permit investigation of molecules of low scattering power. Since the intensity of scattering of protons by an atom should be approximately 2000-fold greater than that of electrons, it was thought worth while to investigate the diffraction of protons by vapor molecules in the hope that this higher scattering would make it possible to obtain usable patterns from light molecules.

Experiments on the scattering and diffraction of both low and medium energy protons by crystals have been made,[1] but no information is available regarding diffraction by vapors. After some preliminary experiments with 2000-volt particles, the range of 15–20 kv was settled upon as a compromise between the difficulties encountered at the lower voltage and the inconveniently long camera which would be necessary at higher voltages. Throughout these experiments carbon tetrachloride vapor was used almost exclusively as diffraction material.

APPARATUS

The apparatus in its final form is shown schematically with approximate dimensions in Fig. 1. The stainless steel ion source, AS, is of the low voltage capillary arc type.[2] An arc of 0.5 to 2.0 amp. in hydrogen is struck between the oxide-coated filament, OF, and the anode, A, through the 5-mm diameter capillary in the arc body, B. The arc is attached to, but insulated from, the first accelerating electrode by a textalite bolting flange, F, and a rubber gasket. This section is in turn insulated from the remainder of the apparatus by the glass tube, G. Ions from a 0.375-mm opening, S_1, in the center of the capillary are accelerated to approximately 4 kv in the region L, and to the final potential of 15–20 kv in the space L_2. These two cylindrically symmetric accelerating regions act as converging lenses, and, with suitable adjustment of the voltage, focus a nearly parallel beam of ions through the slit S_2.

A magnetic field in the region H serves to resolve the beam into its ionic constituents (approximately 20 percent H_1^+, 50 percent H_2^+, 20 percent H_3^+, remainder heavy ions). By proper adjustment, any one of these beams may pass through the slit S_3 parallel to the camera tube axis. (S_3 is supported on an insulated lead for rough current measurements.) The selected beam is focused onto the fluorescent screen, FS, through slit S_4 by the concentric cylinder lens (*einzellinse*) L_3. The vapor stream is introduced at N through a nozzle of the usual type which is as completely surrounded as possible by a condensing cylinder cooled by the liquid-air trap T.

* Contribution of the Gates and Crellin Chemical Laboratory, No. 716.

† National Research Fellow in Physics, 1936–1938. The work reported was done at California Institute of Technology while on leave from Purdue University.

[1] A. J. Dempster, Phys. Rev. **34**, 1493 (1929) and **35**, 1405 (1930). Y. Sugiura, Inst. Phys. Chem. Research 310, **16**, 29 (1931).

[2] M. A. Tuve, O. Dahl, and R. L. Hafstad, Phys. Rev. **48**, 242 (1935).

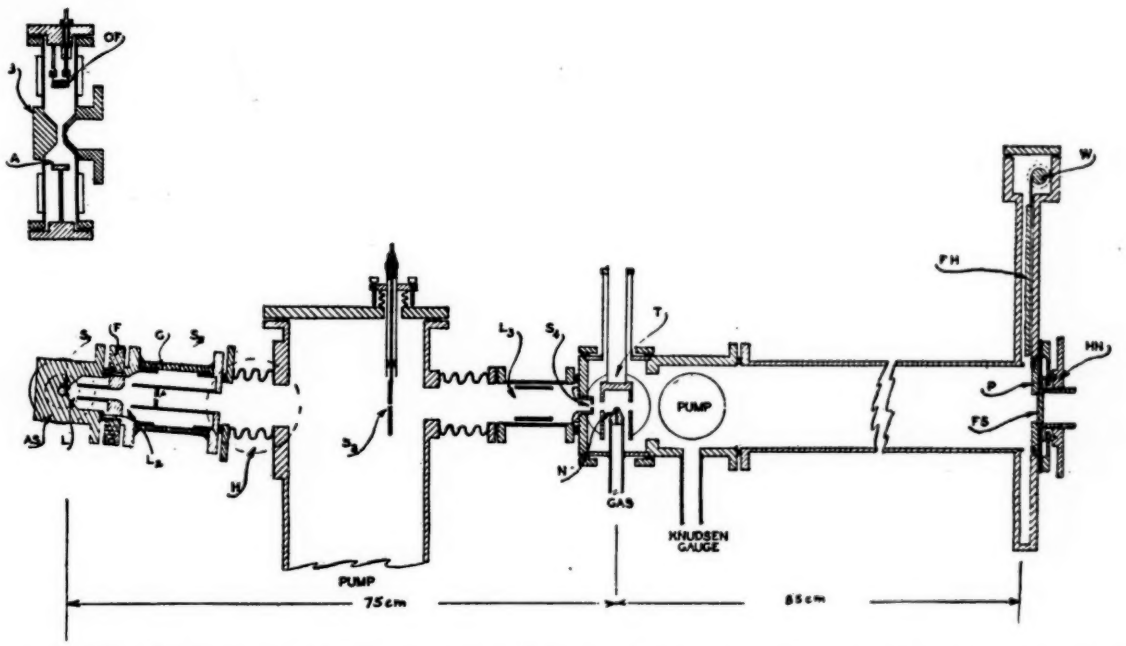

FIG. 1. Diffraction apparatus. *AS*, arc source; *OF*, oxide-coated filament; *B*, arc body; *A*, anode; S_1, S_2, S_3, S_4, slits; *L*, L_2, L_3, electrostatic lenses; *N*, vapor nozzle; *T*, vapor condensing trap; *FS*, fluorescent screen; *FH*, film holder; *P*, plunger to seal film chamber from camera; *HN*, hand nut for control of *P*.

The recording film is carried in the holder *FH*, which may be lowered over the camera end by the windlass *W*. In order that the film may be changed without breaking the vacuum, the plunger *P*, which carries a ring gasket on its face, may be pressed against the camera opening by the hand nut *HN*, thus sealing the film chamber from the camera. A vacuum seal for this plunger, having the necessary 8 mm of motion, is made by a disk of gasket rubber clamped to the plunger at its center and to the chamber wall at its outer edge.

The apparatus is evacuated at the positions shown by double stage oil diffusion pumps by using the continuous distillation principle of Hickman.[3] These are equipped with built-in traps and are backed by a common third diffusion stage and a Megavac. The source pump has a speed for hydrogen of 200 liters/sec., and maintains a pressure of approximately 5×10^{-5} mm Hg with the arc running. The camera pump has a speed for air of 35 liters/sec. and maintains a pressure of 10^{-5} mm Hg as indicated by a Knudsen vacuum gauge.[4] (This figure includes condensable vapors; a McLeod gauge with trap indicates about one-fifth this pressure.)

BEAM PRODUCTION

In forming a small intense beam in television and oscillograph tubes,[5] use is made of the fact that with a given arrangement of object, image, and lens, the magnification is much reduced when the object is a source of electrons of a velocity which is low compared with the final velocity. It was hoped that this could also be done in these experiments by focusing an image of the ion source, S_1, on the film. This proved to be impossible. The image of S_1 (with S_2 removed) was always larger than electron optical calculations would predict.[5] The image size, moreover, increased regularly with the beam current in such a way that the current density in the image was practically constant at a value, under optimum conditions, of approximately 0.02μ amp./mm^2. It was possible, on the other hand, to focus a good image of S_2, of about this same current density, which was only slightly de-

[3] K. C. D. Hickman, J. Frank. Inst. **221**, 215 (1936).
[4] A modification of the design of DuMond and Pickels, J. W. M. DuMond and W. M. Pickels, Jr., Rev. Sci. Inst. **6**, 362 (1935).
[5] See e.g. Maloff and Epstein *Electron Optics in Television* (McGraw-Hill, 1939), p. 98.

pendent upon total ion current.[6] This indicated that the difficulty was due to space charge effects in the low voltage region near the ion source.

The dispersion of a beam of charged particles has been investigated by Watson.[7] He has shown that an initially parallel beam of circular cross section will expand at an increasing rate governed by a scale factor $(\pi i)^{\frac{1}{2}}(2mc/e\varphi^3)^{\frac{1}{4}}$, where e, m, and φ are the charge, mass and volt energy, respectively, of the particles, and i is the current density before expansion. One obtains the maximum current density on a screen at a fixed distance from the origin when i is such that the expansion reaches 2.4 diameters. Because of their large mass this effect should be particularly important for ions.

One might anticipate that this expansion could be nullified by the use of a converging lens, but analysis indicates that this is not true. The theory of Watson has been extended[8] to the case in which a lens is introduced at the point of parallelism. This investigation shows that the action of the lens is not to focus the beam to a focal point, but merely to compress it to a new region of parallelism. Beyond this point the beam expands again at an increased rate corresponding to the increased current density associated with the compression. The amount of compression increases with the power of the lens, but the position of the minimum beam diameter is nearly independent of focal length.[9]

Since the lens action of L and L_2 is seriously modified by such effects, it is not surprising that a good image could not be formed with the low energy ions from S_1. The only alternative was to form an image of S_2 illuminated with high velocity ions. When the image was made sufficiently small for diffraction purposes, the beam available was limited to about 0.002μ amp.

TABLE I. *Cross sections in units of* 10^{-16} *cm*^{2}.

	17.7 kv		27.3 kv	
Protons In	Q_1	Q_2	Q_1	Q_2
H_2	8.03	2.01	6.8	2.9
Air	9.6	6.4	7.02	5.28
CCl_4	15.9	3.5	8.0	4.3
C_2H_5OH	17.6	5.6	11.1	4.4
Molecular Ions in				
H_2	9.76	3.1		
Air	9.1	6.1	8.15	8.15
CCl_4	18.3	4.03	8.85	7.25

[6] Cf. experience of J. Koch and W. Walcher (Zeits. f. Physik **97**, 131 (1935)).
[7] E. E. Watson, Phil. Mag. **3**, 849 (1927).
[8] A detailed account of this treatment will be published in the near future.
[9] Cf. similar results for a wide flat beam and cylindrical lens. A. Bouwers, Physica **2**, 145 (1935).

Neutralization

When CCl_4 vapor was introduced at N, in attempts to produce diffraction, it was found that the beam was very badly neutralized, rather than scattered. That some of the ions of a beam will be neutralized in passing through a gas is a well-known phenomenon.[10] The neutrals continue in a more or less well-defined beam and may subsequently be re-ionized; after traversing a sufficiently large distance, an equilibrium is established between ions and neutrals.

With the notation μ_1 and μ_2 for the coefficients of neutralization and re-ionization, respectively, and assuming a beam of unit number of charged particles per second traveling in the positive x direction, the relations describing these processes are:[10]

Number of neutrals/sec. at distance x in gas at pressure p

$$N(x)=\frac{\mu_1}{\mu_1+\mu_2}[1-e^{-(\mu_1+\mu_2)px}].$$

Total ions/sec. at distance x

$$I(x)=\frac{1}{\mu_1+\mu_2}[\mu_2+\mu_1 e^{-(\mu_1+\mu_2)px}].$$

Since there are few data available on neutralization in the voltage region of these experiments, and none for vapors, a series of measurements of $N(x)$ and $I(x)$ was made with beams of protons and molecular ions in H_2, Air, CCl_4, and C_2H_5OH in the following way.

A long central section of the camera tube was insulated at both ends and a smaller tube attached at one end which extended into the nozzle chamber (with N and T removed) up to a short cylinder of the same diameter attached to S_4. With the surroundings of each end of the insulated section thus made symmetrical, and no axial electric fields present, it was assumed that

[10] See, e.g., E. Rüchardt, Ann. d. Physik **71**, 377 (1923).

the current measured to the cylinder corresponded to the number of neutrals, $N(x)$, formed in this section (no wide angle scattering) and that the current measured to the camera end corresponded to $I(x)$. A magnetic field served to prevent escape of secondaries from the camera end to the insulated section. The field was far enough from the split in the two sections that it did not disturb the symmetry at this point.

The expressions given above for $N(x)$ and $I(x)$ can be considered to be functions of p, so that by measurement of the two currents as functions of the gas pressure, values of the cross sections for neutralization and re-ionization Q_1 and Q_2, respectively, could be obtained. The values found are listed in Table I. The Knudsen gauge used to measure the pressures was carefully calibrated for air and hydrogen against a McLeod gauge, and the scale linearity checked with an ionization gauge. As is well known, the calibration of such a gauge is independent of the kind of gas when the temperature of the heaters is constant. A thermocouple attached to one of the heaters permitted correction of the small change in temperature produced by the different gases.

The results are in satisfactory agreement with the comparable published values, namely Q_1 and Q_2 for protons in air, oxygen, nitrogen and hydrogen.[11] The values of Q_1 agree with the theory of Brinkman and Kramers[12] only in order of magnitude, but the approximation of this theory is not expected to be good at the low velocities of these experiments.

Determination of the ion scattering was attempted by measurement of the current remaining in the beam at distance x. Examination of the processes concerned shows that the beam current involves the scattering coefficient only in an indirect way complicated by neutralization and re-ionization. The measurements were, therefore, very unreliable. One may only say that they indicate a coherent scattering somewhat smaller than that calculated from the Rutherford formula (with a suitable correction for electronic screening).

Recording the Pattern

The sensitivity of film (Eastman Commercial Ortho) for protons and molecular ions was determined by using the end camera section as a Faraday cage. The escape of secondaries was prevented by a transverse magnetic field. By defocusing the beam, spots were obtained on the film which could easily be microphotometered. These were approximately 10 mm in diameter and of sensibly uniform density.

Table II. *Sensitivity of vacuum aged film in units of density/microcoulomb/cm².*

Protons		Molecular ions	
15.2 kv	10.4	15.2 kv	11.0
19.1 kv	14.0	27.2 kv	18.3

It was found that the sensitivity rapidly diminished as the film was aged in the vacuum, probably due to loss of water.[13] The sensitivity of fresh film was impossible to determine because of vacuum requirements, but may be estimated to be five to ten times that of outgassed film, for which typical results are given in Table II.

These values are somewhat lower than might be expected by extrapolation of the data of Kollath[14] for Schumann plates at lower voltages. Sensitization with oil increased the sensitivity remarkably. A fifteen-fold increase was found for 15.2 kv protons, i.e., from 10.4 to 155/microcoulomb/cm².

Many attempts were made to record diffraction patterns from vapors of CCl_4, C_6H_6, C_2H_5OH, CS_2, and As_4O_6. From the point of view of ease of production of a good vapor stream, condensability, and high scattering power, CCl_4 was found most satisfactory and was therefore used in most of the experiments.

In addition to the obvious troubles occasioned by the stringent vacuum requirements and the weak beam available, great difficulty was experienced in reducing the general background to a workable value. Improper focusing of particles due to their passage through lenses as neutrals, scattering due to neutralization, stray scattering from slits, residual gas, and camera walls, multiple scattering, and the increased exposure necessitated by the neutralization, all contribute to produce a heavy background.

[11] E. Rüchardt, Ann. d. Physik **71**, 377 (1923); H. Bartels, *ibid.* **6**, 957 (1930); F. Goldmann, *ibid.* **10**, 460 (1931).
[12] H. C. Brinkman and H. A. Kramers, K. Akad. van Wetenschaffen Amsterdam **33**, 973 (1930).
[13] Stefanie Zila, Akad. Wiss. Wien. Ber. **145**, 503 (1936).
[14] R. Kollath, Ann. d. Physik **26**, 705 (1936).

Various precautions were taken to minimize these effects. Exposure time was reduced as much as possible by use of oiled film and the shortest permissible camera. The pressure of the vapor was adjusted to give optimum single scattering—about 50 percent neutralization. The ions were magnetically separated from the neutrals; this could not, however, remove those particles which were neutralized at an early, and re-ionized at a late stage of passage through the vapor stream. The direct ion beam and the resolved neutrals were screened from the film. And finally, the diffracted beam was deflected in such a way that the pattern was recorded on a region of the film which was shielded from the stray neutrals originating in the diffracting region (from slits and neutralization process) and from light entering the camera through S_4.

With these precautions a few recognizable patterns were obtained from CCl_4 with exposures of from 30 sec. to 2 minutes at a voltage of 17.7 kv. One of these is shown in Fig. 2. On the original photographs three rings are visible, the measurement of which are shown in Table III. Because of the small pattern size the first two maxima are obscured by the shield used to intercept the direct beam.

The error indicated is based entirely on consistency of measurement and does not include any estimate of physiological error due to measurement on a steep background, etc. It is felt that such error, in measurement of patterns as small as this, may easily account for the discrepancy between the experimental and the accepted electron diffraction values of S_k, and that these results satisfactorily demonstrate the existence of diffraction of protons by CCl_4.

Discussion

While these experiments show that diffraction can be observed, the required optimum conditions necessitated wide deviations from the original plan of obtaining usable patterns from light molecules. The weak beam and high neutralization made the use of a small pattern and a good scatterer mandatory.

The principal intrinsic barrier to extension to lighter molecules is that the neutralization is of the same order of magnitude for light as for heavy molecules, whereas coherent scattering diminishes approximately as the square of atomic number. Considerable advantage in this regard may be gained by working at higher voltages, since coherent scattering intensity decreases inversely with voltage while neutralization should diminish somewhat more rapidly (between V^{-1} and V^{-6} according to the Brinkman and Kramers theory[12]). Decreased space charge effects and higher film sensitivity are also to be expected, so that, in spite of the more unwieldy camera that will be necessary, it is planned to extend the experiments to the 80–100 kv range.* Experiments to improve the beam intensity by minimizing the space charge repulsion until considerable acceleration has been accomplished are now in progress.

My thanks are due Professor Linus Pauling and Dr. L. O. Brockway for suggesting the problem, their continued interest during its course, and the provision of facilities which made the experiments possible.

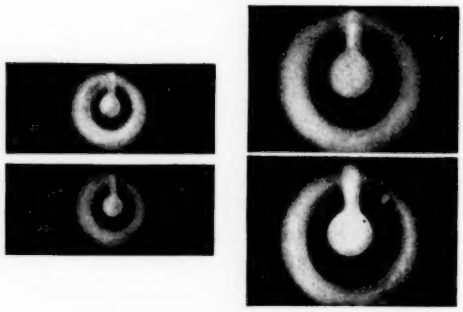

Natural size 2.14-fold enlargement

FIG. 2. Diffraction from CCl_4. $V=17.7$ kv. $\lambda=0.00214$A. Camera length = 86.5 cm. (Printed from the original with a small light source very close to the negative to reduce the steepness of background. This produces a false halo in the outer portions of the reproduction.)

TABLE III. *Comparison of values, $S_k=4\pi(\sin \varphi_k/2)/\lambda 10^{-8}$. A: from original photograph, B: from 2.14 enlargement.*

Maximum no.	Mean diam. in mm		Observed S_k		Electron diffraction* S_k
	$A \pm 0.1$ mm	$B \pm 0.05$ mm	$A \pm 0.17$	$B \pm 0.08$	
$k=3$	4.4	4.29	7.45	7.28	7.13
$k=4$	5.6	5.42	9.49	9.20	9.23
$k=5$	6.8	6.67	11.39	11.33	11.34

* L. Pauling and L. O. Brockway, J. Chem. Phys. 2, 867 (1934).

* The apparatus described has very kindly been made available for continuation of the experiments at Purdue University.

The Diffraction of X-Rays by Liquid and Plastic Sulphur

NEWELL S. GINGRICH
University of Missouri, Columbia, Missouri
(Received September 29, 1939)

X-ray diffraction patterns of plastic sulphur at room temperature and of liquid sulphur at several temperatures ranging from 124°C to 340°C have been obtained. The position of the main peak in terms of $(\sin\theta)/\lambda$ is 0.140 at 124°C, 0.138 at 147°C, 0.138 at 151°C, 0.139 at 157°C, 0.127 at 166°C, 0.127 at 175°C, 0.125 at 225°C, and 0.120 at 340°C. Atomic distribution curves have been obtained in the cases of plastic sulphur, and of liquid sulphur at 124°C, 166°C, 175°C, 225°C, and 340°C. These curves all appear somewhat similar. The nearest neighbors are found at 2.08A for plastic sulphur, and at approximately 2.07A for liquid sulphur at all temperatures. The number of nearest neighbors is 2.0 for plastic sulphur, and it is about 1.7 for liquid sulphur. The possibility of using the present information in explaining certain properties of sulphur is discussed.

INTRODUCTION

A STUDY of the diffraction of x-rays by liquid sulphur at different temperatures is of particular interest because of the large change in the viscosity of liquid sulphur in the region just above 150°C and other properties such as specific gravity, surface tension, thermal expansion and specific heat all show anomalies in this region.[1] In the present work, an effort has been made to determine what information x-ray diffraction methods can supply toward a more complete explanation of these anomalous effects.

Previous work on the diffraction of x-rays by liquid sulphur includes the work of Blatchford,[2] Prins,[3] Das[4] and Das and Das Gupta.[5] Blatchford[2] reported having observed the diffraction pattern of liquid sulphur at temperatures of 130°C, 155°C, 182°C, 221°C, 225°C and 260°C. Considering only the main peak of the diffraction pattern, he calculated a quantity d, defined by the relation $d=\lambda/(2\sin\theta)$, where λ is the wavelength of the x-rays and θ is half the total angle of diffraction. This distance, d, showed an increase at about 220°C, and a correlation of this abrupt change with physical properties was attempted, though 220°C is considerably higher than the usually accepted transition temperature range of roughly 160°C to 190°C. This value, d, varied from 3.68A at 130°C to 4.06A at 260°C. On the other hand, Prins[3] has reported finding no appreciable change in the value of d on raising the temperature from 140°C to 350°C. The value of d reported by him is 3.43A. Das and Das Gupta[5] summarize their results for liquid sulphur at 128°C and for supercooled liquid sulphur at 27°C. They conclude that their best value for d in the 128°C case is 3.76 ± 0.02A and in the 27°C supercooled case it is 3.68 ± 0.02A. The agreement between these reported values of d is not particularly good. Furthermore, it seems that an undue amount of emphasis has been placed upon considerations involving only the position of the main peak, whereas features of other portions of the diffraction pattern have been wholly neglected. Hence, the present investigation has been undertaken in an attempt to obtain as complete a diffraction pattern of liquid sulphur as possible at several temperatures.

EXPERIMENTAL

The experimental apparatus was essentially the same as that used in the study of other liquid elements.[6] X-rays from a molybdenum target tube were monochromatized by reflection from a rocksalt crystal. A cylindrical thin-walled Pyrex tube was evacuated, nearly filled with sulphur and sealed off. The glass wall thickness was made small enough so that diffraction by the glass was negligible. The sample was placed at the center of a cylindrical camera of 8.85 cm radius and

[1] J. W. Mellor, *A Comprehensive Treatise on Inorganic and Theoretical Chemistry* (Longmans, Green and Co., 1930), Vol. X, pp. 53–87.
[2] A. H. Blatchford, Proc. Phys. Soc. London **45**, 493 (1933).
[3] J. A. Prins, Trans. Faraday Soc. **33**, 110 (1937).
[4] S. R. Das, Ind. J. Phys. **12**, 163 (1938).
[5] S. R. Das and K. Das Gupta, Nature **143**, 332 (1939).
[6] F. Trimble and N. S. Gingrich, Phys. Rev. **53**, 278 (1938).

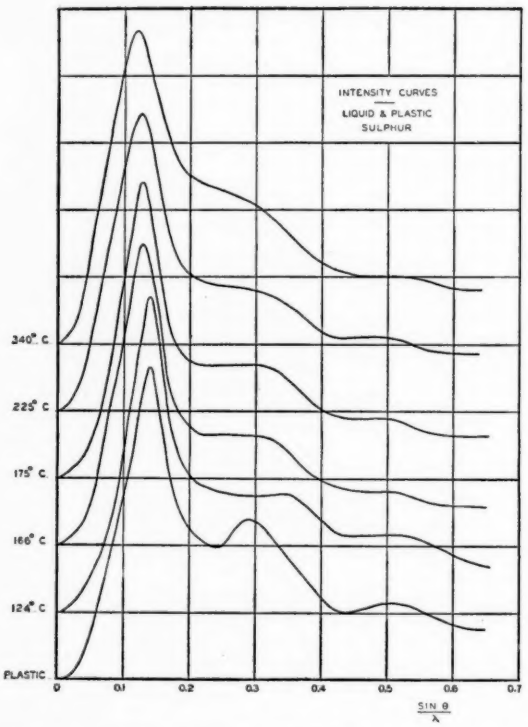

FIG. 1. Intensity as a function of $(\sin\theta)/\lambda$ in the x-ray diffraction patterns of plastic sulphur at room temperature and of liquid sulphur at 124°C, 166°C, 175°C, 225°C and 340°C corrected for absorption, polarization and incoherent radiation.

provision was made to prevent the direct x-ray beam from causing extraneous fogging of the film. Under various conditions of temperature, sample size and lining-up of the camera, exposures of from 40 hr. to 90 hr. were required for suitable diffraction patterns with the x-ray tube operated at about 30 kv and 15 ma. After development of the film under standard conditions, it was microphotometered in the usual manner, and the microphotometer record was converted to relative intensities. Runs of this sort were made at 124°C, 147°C, 151°C, 157°C, 166°C, 175°C, 225°C, and 340°C, and the ones finally used for complete analysis were 124°C, 166°C, 175°C, 225°C, and 340°C in addition to one run using plastic sulphur at room temperature. In this work, the temperature was measured by means of a thermocouple placed near the region of the sample through which the x-rays passed. Since the thermocouple was not in contact with the liquid, it is possible that the actual temperature of the liquid was not quite the same as the measured temperature. This was investigated by means of a mercury-in-glass thermometer which replaced the sulphur sample, and it appeared possible that the temperatures as here reported might be in error by as much as 5°, the reported values being lower than the actual values. The value of $(\sin\theta)/\lambda$ for the main peak was determined from measurement of the distance along the film between the main peak on each side of the direct beam. This distance was between 3 cm and 4 cm, and it is estimated that the error in this determination is no greater than one percent. Different exposures taken at the same temperature, and different microphotometering of the same film were consistent to less than one percent. Perhaps the greatest difficulty was encountered in obtaining completely consistent values for the intensity of the diffraction pattern at large angle. This difficulty is accentuated in the present case because of the diffuse character of the pattern at angles larger than that for the main peak. However, a fairly reliable intensity pattern at large angles was obtained by averaging that obtained on several films.

Plastic sulphur was made by pouring molten sulphur at high temperature into cold water. From the long strings of sulphur so formed, suitable sections were cut into convenient lengths for mounting in the camera. Preliminary diffraction patterns showed that frequently the plastic sulphur became appreciably crystalline within a few hours. Hence it was found necessary to renew the sample every two hours to insure against the possibility of having the sample become crystalline in any appreciable amount.

RESULTS

Figure 1 shows the intensity curves for plastic sulphur at room temperature and for liquid sulphur at 124°C, 166°C, 175°C, 225°C and 340°C. They have been corrected for absorption, for polarization and for incoherent radiation. These corrections have been described elsewhere,[7] and they affect chiefly the intensity at large angle in relation to that at small angle. The positions of the main peaks were not altered appreciably by these corrections. For comparison, the curves are

[7] B. E. Warren and N. S. Gingrich, Phys. Rev. **46**, 368 (1934).

plotted so that the main peaks all have the same maximum value. The intensity curve for plastic sulphur is typical of that for an amorphous substance, and it shows three peaks, each of which can be seen on the original film. The intensity curves for liquid sulphur show a main peak with two plateaus, all of which can be seen on the films, except that at the higher temperatures, some features of the pattern are not easily distinguished. In addition to the obvious washing out of the pattern, there is a shift in the position of the main peak as the temperature of the liquid is raised. The main peak for plastic sulphur at room temperature occurs at $(\sin\theta)/\lambda = 0.140$, the same value, to within experimental error, as that for liquid sulphur at 124°C. From 124°C to 157°C, a slight decrease in the value of $(\sin\theta)/\lambda$ for the peak occurs, from 157°C to 166°C a large change takes place, and from 166°C to 340°C, a gradual decrease is noted. The values of $\sin\theta/\lambda$ for the main peak are as follows: 0.140 at 124°C, 0.138 at 147°C, 0.138 at 151°C, 0.139 at 157°C, 0.127 at 166°C, 0.127 at 175°C, 0.125 at 225°C, and 0.120 at 340°C. These results are shown in Fig. 2. They are not inconsistent with Blatchford's conclusion that there is an abrupt change in $(\sin\theta)/\lambda$ for the peak, but they indicate that this abrupt change occurs at a temperature between 157°C and 166°C rather than at 225°C. It is difficult, however, to reconcile the present work with that of Prins,[3] for in the range from 140°C to 350°C we observe about 15 percent change in $(\sin\theta)/\lambda$ for the main peak whereas he reports no appreciable change. Furthermore, the value of $(\sin\theta)/\lambda$ for the main peak in his work is about 5 percent greater than that obtained in the present work for 124°C, while the corresponding value given by Das and Das Gupta[5] for 128°C is about 6 percent less than our value for 124°C. Because of this discrepancy, our films have been rechecked, and the values here reported are considered to be as reliable as can be obtained from them.

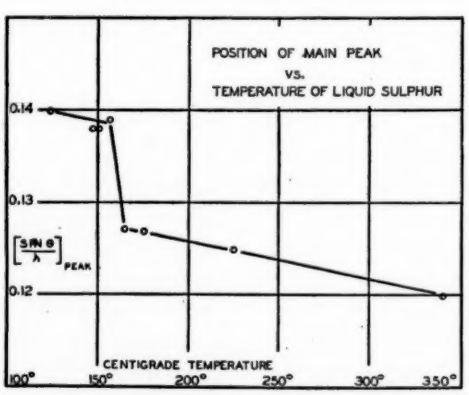

FIG. 2. The position of the main peak of the diffraction patterns of liquid sulphur in terms of $(\sin\theta)/\lambda$ as a function of temperature of the liquid.

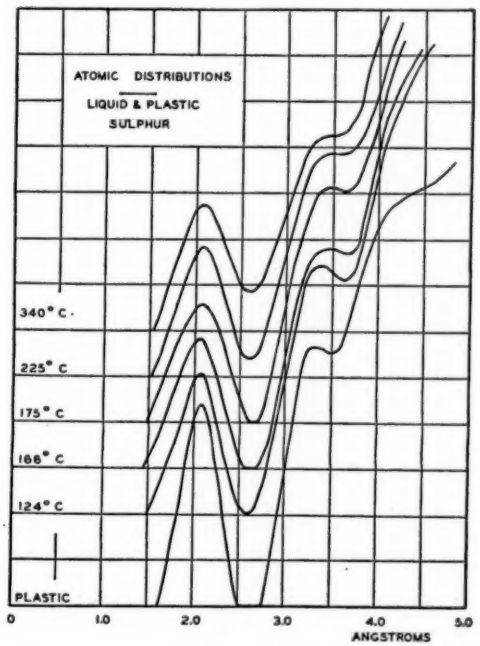

FIG. 3. The atomic distributions in plastic and liquid sulphur at 124°C, 166°C, 175°C, 225°C, and 340°C. $4\pi R^2\rho(R)$ is plotted as a function of R and the origin of ordinates is indicated in each case.

From these intensity curves, it is possible to obtain the atomic distribution of sulphur at each temperature, and the manner of fitting the intensity curves preparatory to an analysis is given elsewhere.[7] One obtains from this analysis, a curve of $4\pi R^2\rho(R)$ *vs.* R so that the area under this curve between two values of R is equal to the number of atoms in that region. These atomic distribution curves for the various cases are shown in Fig. 3.

For plastic sulphur, the first concentration of atoms is at 2.08A, these nearest neighbors are discrete, and the area under this peak is 2.0, indicating that there are two nearest neighbors. This may be compared with the Pauling-Huggins covalent bond radius[8] of 1.04A and with the

[8] L. Pauling and M. Huggins, Zeits. f. Krist. 87, 205 (1934).

structure of rhombic sulphur[9] in which each atom has two nearest neighbors at 2.12A. In rhombic sulphur, the closest distance of approach of atoms in neighboring molecules is about 3.3A, and at approximately this same distance there is a concentration of atoms in the plastic sulphur atomic distribution. The existence of these two distances in both forms of sulphur does not necessarily mean that if the molecule of the crystal has eight atoms in a closed ring, the plastic form also has eight atoms in a closed ring, or indeed that there are true molecules of any sort in plastic sulphur. It is possible that sulphur in this form may consist of long chains of atoms in which each atom is bonded to two nearest neighbors in much the same way as they are in a closed ring and that the second concentration in the atomic distribution curve is due to the next nearest neighbors in the same chain. Simard and Warren[10] have supplied direct evidence for the chain molecule structure of unstretched rubber and from the similarities between the elastic properties of rubber and of plastic sulphur, it appears likely that plastic sulphur also has a chain structure. However, the information supplied by x-ray diffraction alone is apparently not sufficient to distinguish between closed rings of sulphur atoms and long coiled chains of sulphur atoms in plastic sulphur.

The atomic distribution curves for liquid sulphur, shown in Fig. 3, are not alike for all temperatures, but they have certain marked similarities. The first peak occurs at nearly the same value of R for all temperatures. This value of R varies from 2.05A to 2.08A with an average of about 2.07A, and the variations are estimated to be within the experimental error. Hence, it is concluded that there is no measurable alteration of the first interatomic distance in liquid sulphur with temperature in the temperature range here used. The first peak in the distribution curves is discrete in the cases of 124°C, 166°C, and 175°C, but not in the cases of 225°C or 340°C, and the first peak is broader for the liquid at any temperature than for plastic sulphur. The areas under the first peak are between 1.65 and 1.70 for all temperatures, and it is estimated that there is no significance in these differences. The fact that the distribution curves give approximately two nearest neighbors at the covalent bond distance of 2.08A shows that liquid sulphur is not a close-packed liquid such as sodium or mercury, in which there are roughly eight nearest neighbors, but that it is a liquid in which most of the atoms still have two permanent neighbors which are covalently bonded at the same distance as in the S_8 molecule. If liquid sulphur is composed of either closed rings or long coiled chains, each atom should have two nearest neighbors, that is, the area under this peak should be 2.0 as it is for plastic sulphur. In the case of each temperature, two or more complete analyses were made with different intensity curve fittings, and in all cases, the areas under the first peak were approximately the same as here reported. This tends to indicate that the difference between 2.0 and 1.7 in the expected and observed areas is significant. If, on the average, about 30 percent of the atoms have one nearest neighbor, an area of about 1.7 would be anticipated. Physical properties of liquid sulphur seem to preclude the possibility of having an appreciable amount of S_2 at the temperatures here used, and hence, the contribution of atoms with one nearest neighbor from S_2 would be wholly negligible. However, if one postulates that the S_8 ring breaks into an S_8 chain upon melting, then in each chain there will be six atoms with two nearest neighbors, and two atoms with one nearest neighbor. This postulate supplies roughly the right percentage of atoms with one nearest neighbor, and it is suggestive of the mode of polymerization which sets in at about 160°C. Chemical evidence suggests that above 160°C, the molecule is S_{14} to S_{18} or greater. This is probably due to the joining of disrupted rings to form irregular chains which tangle with one another to produce the highly viscous form of sulphur above 160°C.

It is a pleasure to acknowledge that this work has been supported by grants from the Rumford Fund Committee of the American Academy of Arts and Science, the American Association for the Advancement of Science, and the University of Missouri Research Council. Most of the experimental results herein reported were obtained through the able assistance of Mr. Albert Eisenstein.

[9] B. E. Warren and J. T. Burwell, J. Chem. Phys. **3**, 6 (1935).

[10] G. L. Simard and B. E. Warren, J. Am. Chem. Soc. **58**, 507 (1936).

Note on the Continuous Absorptions of N_2O

H. SPONER AND L. G. BONNER
Physics Department, Duke University, Durham, North Carolina
(Received October 10, 1939)

The absorption of N_2O in the long wave-length region of the near ultraviolet has been reinvestigated with an absorption tube 105 feet in length. The well-known absorption in this region has been extended and its resolution into several components is discussed. A few remarks are added about other continuous absorption regions in connection with different dissociation reactions of N_2O.

THE ultraviolet absorption of N_2O has been studied by many investigators. Continuous spectra have been found in the near ultraviolet and in the Schumann region[1–6] and several discrete spectra in the Schumann ultraviolet.[6] The absorption in the near ultraviolet is much weaker than that at shorter wave-lengths. Several attempts have been made to correlate long wave limits of the near ultraviolet absorption with dissociation processes of the N_2O molecule,[1, 3, 4] but it has also been pointed out[6, 7] how fortuitous were most of the agreements obtained. It is, however, theoretically clear that normal N_2O would not separate adiabatically into normal products,[8] since its normal state is a $^1\Sigma$. The potential curves of the triplet states leading to normal dissociation products must therefore cross that of the ground state and absorption to these states should be extremely weak. It seems that none of the observed absorptions can be correlated with these transitions. We concluded that only with very long absorption paths was there a chance for their detection. Since such an apparatus is available here we have investigated once more the absorption of N_2O on the long wave-length side of the near ultraviolet region.

APPARATUS

The absorption tube used in these experiments consisted of a stainless steel pipeline 105 feet long and $1\frac{1}{2}$ inches in diameter inside. The walls were $\frac{1}{8}$ inch thick and the interior of the pipe had a mirror polish. The tube was in five sections of 21 feet each and was held together by means of flat brass flanges soldered to the ends of each section and bolted together. Gum rubber gaskets between the flanges served to make the joints pressure and vacuum tight. A short brass piece inserted between the second and third stainless steel sections carried the pumping lead as well as leads for the manometer and the gas handling system. The tube was evacuated by means of a Cenco Hypervac, separated from the system by an ordinary steam valve of the ball type in which the customary composition valve facing had been replaced by gum rubber. The valve stem and packing gland were, of course, on the pump side of the gate. The entire tube was supported at a convenient distance above the floor at eleven points by means of adjustable brackets attached to rigid uprights and was optically in line.

Windows at the ends of the tube were, for the present work, of fused quartz. For work at pressures below one atmosphere the windows can be simply sealed to brass plates, over holes slightly smaller than the windows, by means of wax, and the plates bolted to the end flanges of the tube. Since, in this work, we contemplated using pressures considerably above atmospheric it was deemed necessary to supplement the above seal with a second similar brass plate outside the window and separated from it by a rubber gasket. The bolts holding the window assemblage to the tube passed through both plates.

In concluding the description of the absorption tube it may be of interest to comment on its vacuum tightness. Using the Hypervac alone we have been able to attain pressures of 10^{-4} mm

[1] A. K. Dutta, Proc. Roy. Soc. London **A138**, 84 (1932).
[2] O. R. Wulf and E. H. Melvin, Phys. Rev. **39**, 180 (1932).
[3] L. Henry, Nature **134**, 498 (1934).
[4] P. K. Sen-Gupta, Nature **136**, 513 (1935).
[5] S. Leifson, Astrophys. J. **63**, 73 (1926).
[6] A. B. F. Duncan, J. Chem. Phys. **4**, 638 (1936).
[7] W. A. Noyes, Jr., J. Chem. Phys. **5**, 807 (1937).
[8] H. Pelzer and E. Wigner, Zeits. f. physik. Chemie **B15**, 445 (1932); G. Herzberg, Zeits. f. physik. Chemie **B17**, 68 (1932).

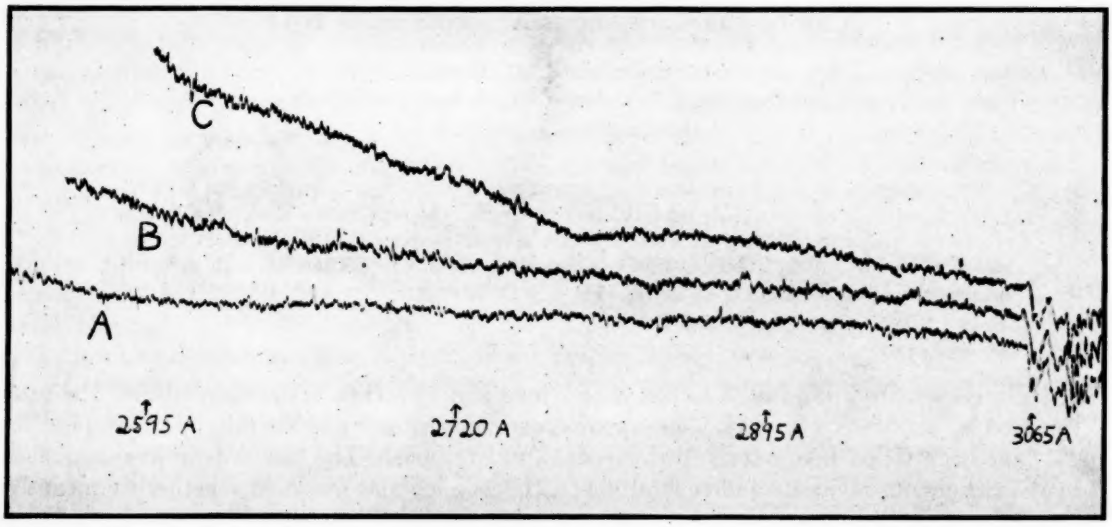

FIG. 1. Microphotometer tracings of absorption of N_2O taken through 33 m path at pressures of (A) vacuum; (B) 1½ atmos.; (C) 5 atmos.

of Hg, and with the pump valve closed, to maintain a pressure of 10^{-3} mm for a period of two weeks.

As light source for the ultraviolet we used a small sealed hydrogen discharge lamp* made entirely of Pyrex, with a bubble window. The lamp operated at 35 ma and emitted a satisfactory continuum down to 2400A.

All the photographs were made with a Hilger E3 instrument.

PROCEDURE

The N_2O used in these experiments was a commercial product supplied in a steel cylinder and used without further purification. The subject of possible impurities is taken up in a later section. For use the absorption tube was evacuated, the pump valve closed, and N_2O passed in from the cylinder until the desired pressure, as indicated on a pressure gauge, had been reached. Photographs were taken with the tube evacuated, filled to 1½ and also to 5 atmosphere pressure of N_2O. Microphotometer tracings of the plates were obtained with a Kipp and Zonen microphotometer.

RESULTS

Spectrograms taken through the tube with pressures up to 5 atmospheres yielded no absorption in the visible region. We then carefully examined the wave-length region from 3000–2400A which contains the well-known near ultraviolet continuum. Dutta places its long wave limit at 2750A when light was transmitted through 1 m of N_2O at atmospheric pressure. We have found that the beginning of this absorption is shifted with increasing pressures. But this shift is apparently not merely an extension of the known absorption as can be seen from the curves *A*, *B* and *C* of Fig. 1, which represents microphotometer tracings of the absorption spectrum for the empty tube, at 1½ and at 5 atmospheres. They indicate the development of an extremely weak absorption on the long wave side of the known absorption. The maximum of this absorption can be roughly placed at about 2900A and the rise of the next absorption at about 2820A. There is perhaps also a slight indication that the rise of this next absorption is not uniform but has a slight break and increases from about 2600A more steeply than before. We have, of course, considered the question of possible impurities which could be responsible for the new weak absorption. As mentioned we have used commercial tank nitrous oxide which has been prepared from NH_4NO_3.* We have looked for NO_2, NO, N_2, O_2 and NH_3 as impurities whose spectra

* We are indebted to Dr. D. G. Sharp of the Duke Hospital for the loan of the discharge lamp.

* Communication from the Matheson Co.; the purity is claimed to be 98 percent, the balance being nitrogen.

are known. We have not been able to detect any of their characteristic absorptions. Hence it is very suggestive to interpret the newly observed weak absorption as being due to N_2O.

Discussion of the Results

Now if this absorption arises from N_2O as it seems to do, then it can be due only to the forbidden intercombination leading to $N_2{}^1\Sigma+O{}^3P$. Of the two states possible (see Table I) the $^3\Pi$ is more likely since the other would be a $^3\Sigma^-$ and hence two selection rules would be violated. The repulsive curve of this triplet state must be very steep because the maximum of this absorption occurs at about 2900A while the underlying dissociation process becomes theoretically possible at 7200A. This value for the maximum is in reasonable agreement with the partial curve drawn by Stearn and Eyring[9] for the repulsive state. If the region from 2820 to 2600A should contain a separate electronic state it might be the repulsive level $^3\Pi$ dissociating into $NO{}^2\Pi+N{}^4S$. The absorption increasing appreciably from 2600A has been investigated in detail before. According to Dutta's observation it is still increasing at 2100A with no indication of a maximum. Now Sen-Gupta[10] reports another absorption at shorter wave-lengths with a long wave limit at 1850A, but Duncan[6] finds that at 7 mm pressure and 2 m path this absorption extends from 1768 to 2068A with a center at 1900A. Possibly at higher pressures Dutta's and Sen-Gupta's absorptions merge into one large continuum. It is almost certain that the long wave part of this absorption is mainly due to a dissociation into $N_2{}^1\Sigma+O{}^1D$, the state probably being a $^1\Pi$ which, in analogy to CO_2, would be the lowest of the three possible singlet states[11] (cf. Table I). The absorption in the short wave-length region with a center at 1900A may contain one of these other singlet states, but it may also include the $^1\Sigma$ resulting from $N_2{}^1\Sigma+O{}^1S$ and one or more singlet states leading to $NO{}^2\Pi+N{}^2D$. It is impossible to make any decision from the continuous spectra alone. But it is interesting to note in these connections that Noyes and collaborators[12] came to the conclusion that with excitation by aluminum spark lines of wave-lengths greater than 1850A (in most runs lines between 1860 and 1990A were used) both primary dissociation processes must occur:

$$N_2O+h\nu\rightarrow N_2+O \quad \text{and} \quad N_2O+h\nu\rightarrow NO+N.$$

The NO must then originate either by process 3

[9] A. E. Stearn and H. Eyring, J. Chem. Phys. **3**, 778 (1935).
[10] P. K. Sen-Gupta, Bull. Acad. Sci. Allahabad **3**, 197 (1934).
[11] R. S. Mulliken, J. Chem. Phys. **3**, 721 (1935).
[12] W. A. Noyes, Jr., J. Chem. Phys. **5**, 807 (1937); F. C. Henriques, Jr., A. B. F. Duncan and W. A. Noyes, Jr., J. Chem. Phys. **6**, 518 (1938).

Table I. *Dissociation processes of* N_2O

No.	Dissociation Products and Possible Electronic States†	Energy Required (Volts)	Observed Absorptions: Maximum (Volts)	Maximum (A)	Long Wave Limit (Volts)	Long Wave Limit (A)
1	$N_2{}^1\Sigma + O{}^3P \leftarrow {}^3\Sigma, {}^3\Pi$	1.71	4.26	2900	4.0	3065[a]
2	$N_2{}^1\Sigma + O{}^1D \leftarrow {}^1\Sigma, {}^1\Pi, {}^1\Delta$	3.68				
3	$NO{}^2\Pi + N{}^4S \leftarrow {}^3\Pi$	3.77	?4.5	2730	?4.4	2820[a]
4	$N_2{}^1\Sigma + O{}^1S \leftarrow {}^1\Sigma$	5.90	6.45	1900	4.7	2600[b]
5	$NO{}^2\Pi + N{}^2D \leftarrow 2\,{}^{1,3}\Sigma, 2\,{}^{1,3}\Pi, {}^{1,3}\Delta$	6.15				
6	$NO{}^2\Pi + N{}^2P \leftarrow 2\,{}^{1,3}\Sigma, {}^{1,3}\Pi, {}^{1,3}\Delta$	7.31	9.6	1280	9.1	1350[c]
7	$N_2{}^3\Sigma + O{}^3P \leftarrow {}^{1,3}\Sigma, {}^{1,3}\Pi$	7.84				
8	$N_2{}^3\Pi + O{}^3P \leftarrow 2\,{}^{1,3}\Sigma, {}^{1,3}\Pi, {}^{1,3}\Delta$	9.0	11.2	1090	10.8	1130[c]
9	$NO{}^2\Sigma + N{}^4S \leftarrow {}^3\Sigma$	9.2				
10	$NO{}^2\Pi^* + N{}^4S \leftarrow {}^3\Pi$	9.4				
11	$NO{}^2\Sigma + N{}^2D \leftarrow {}^{1,3}\Sigma, {}^{1,3}\Pi, {}^{1,3}\Delta$	11.6				
12	$NO{}^2\Pi^* + N{}^2D \leftarrow 2\,{}^{1,3}\Sigma, 2\,{}^{1,3}\Pi, {}^{1,3}\Delta$	11.8				

† Only singlet and triplet states are given. Φ states are completely omitted. It is evident that not all states correspond to repulsive curves.
[a] At 33 m path and 5 atmos. pressure.
[b] Limit for about 1 m path and 1 atmos. pressure. At 0.7 mm and 2 m path absorption from 1770–2070A.
[c] At 2 m path and 0.19 mm pressure.

or process 5 in Table I. Process 5 is possible theoretically only below 2007A and process 3 must occur with a low rate since it results from an intercombination. The latter is quite likely responsible for Wulf and Melvin's[2] observation that the γ-bands of NO occur in absorption upon illumination of N_2O with wave-lengths up to 2300. However, they do not give the short wave-length limit of their observations. We suppose that the appearance of the bands required long exposure times. There is a possibility of formation of NO molecules in secondary reactions after primary process 2 and perhaps 4, but it would occur at a low rate according to Henriques, Duncan and Noyes.[12]

It is still more difficult to correlate definite dissociation processes with the higher continuous regions since the number of possibilities becomes too large. The two continua which Duncan[6] reports with centers at 77,900 cm^{-1} (9.6 volts) and 91,200 cm^{-1} (11.2 volts) may include higher repulsive states of processes 2–5 and lower repulsive states from 6–10. Sen-Gupta has observed the NO β-bands[13] in fluorescence when exciting N_2O vapor with light of a hydrogen discharge lamp with fluorite windows (radiation from 1250A up). This would correspond to Duncan's continuum with center at 77,900 cm^{-1} and also to the short wave-length part of the near ultraviolet absorption. Sen-Gupta concluded that excited NO was produced in the primary process. If this were correct it would happen as a result of process 10 in Table I. Now this possibility is apparently ruled out from intensity considerations because the observed absorption seems much too strong for an intercombination. On the other hand, because of stronger spin orbit interaction and the possible neighborhood of other suitable allowed transitions, the selection rules are likely to break down more easily for higher excited terms, so that the intercombination may occur with some probability and may form part of the continuum with center at 1280A. The other explanation for the occurrence of the β-bands would be that NO was formed in its normal state according to 5 and 6 in Table I and that the bands were emitted after absorption of light of the discharge by normal NO molecules. Sen-Gupta was in favor of a primary photochemical formation of excited NO because he did not observe the β-bands when the fluorite windows were replaced by quartz windows. But this is not necessarily an argument because with the quartz windows all three processes 10, 5 and 6 become impossible and most NO molecules will originate from process 3 and some in secondary reactions after 2 and 4. At the present moment one cannot decide definitely between the two possible interpretations although the dissociation from a triplet state seems a little more plausible. It is also quite possible that both processes occur simultaneously.

A few words should be added about the relative intensities of the different continua. Using Duncan's figure of the lowest pressure at which the different absorptions appear we find a factor 10,000 for the intensity ratio (not taking into account differences in the sensitivity of the plates used) of his near ultraviolet absorption with center at 1900A (7 mm at 2 m path) and our new weak absorption at 5 atmos. and 33 m. This is probably an upper limit. The ratio seems not implausible for $^1\Sigma \rightarrow {}^1\Pi$ and $^1\Sigma \rightarrow {}^3\Pi$ transitions, if for simplicity, we represent the former absorption by one $^1\Pi$ state. Now it is interesting to find that the intensity ratio of the absorption at 1900A and the next absorption with center at 1283A is according to Duncan 1/3000, that is, the latter absorption is 3×10^3 stronger than the first one. This ratio can be understood when we remember from Mulliken's investigation[11] that the analogous transition in CO_2 is $^1\Sigma_g^+ \rightarrow {}^1\Pi_g$ and hence is forbidden.

Although the new weak absorption seems to fit in the level scheme of N_2O rather satisfactorily there is, however, a difficulty arising from the fact that the absorption region seems so limited. Because of the steepness of the upper potential curve one should expect an extended region of absorption. The only possibility we can think of is that the repulsive $^3\Pi$ state is disturbed by the $^3\Pi$ state resulting from 3, so that the potential curve of the former becomes much flatter for nuclear distances above the minimum of the ground state. Another remote possibility is that the new weak absorption leads to the $^1\Delta$ from process 2, which in this case would have an almost horizontal course in this spectral region.

[13] P. K. Sen-Gupta, Proc. Roy. Soc. London **A146**, 824 (1934). The γ-bands were not observed because of the use of glass optics.

The probability of an impurity is not likely, as has been mentioned earlier, but cannot be excluded with definite certainty.

In conclusion, we wish to thank Mr. H. B. Scarborough for his assistance in setting up the long absorption tube and in taking the pictures and Dr. J. S. Kirby-Smith for making several of the microphotometer tracings. We are deeply indebted to the Penrose Fund of the American Philosophical Society and to the National Research Council for grants-in-aid which made this research possible.

JANUARY, 1940 JOURNAL OF CHEMICAL PHYSICS VOLUME 8

The Fluorescence of Diacetyl

G. M. Almy, H. Q. Fuller* and G. D. Kinzer†
Physics Department, University of Illinois, Urbana, Illinois

(Received August 21, 1939)

Diacetyl, in the vapor phase or in water solution, exhibits a bright green fluorescence when excited with light within its absorption band in the violet and near ultraviolet. A detailed measurement of the structure shows that the spectrum is the same as is shown in the fluorescence of acetone vapor when excited with λ3130. The fluorescence spectrum is insensitive to changes in diacetyl pressure (0.1 mm to 50 mm), temperature (10°C to 100°C), exciting wave-length (3650A to 4358A) or amount of added oxygen, which quenches the fluorescence strongly. The intensity of fluorescence, measured with photo-cell and amplifier, is constant in time, with weak excitation. The ratio of intensity of fluorescence to light absorbed is independent of the pressure and the intensity of the fluorescence is linearly proportional to the exciting intensity, at constant pressure. The fluorescence is quenched by oxygen, the intensity falling to one-half at 0.013 mm oxygen. The Stern-Volmer law is followed over a range of oxygen pressures in which the fluorescence drops to 20 percent of the intensity without oxygen; at higher pressures the intensity falls more rapidly than expected. The oxygen is consumed, presumably in the quenching process, and the fluorescence returns to full intensity. From the quenching curve and from an experiment on the diffusion of the excited molecules into shadow the lifetime of the fluorescing molecule is estimated to be about 10^{-5} sec.

These results can be understood on the assumption that the diacetyl molecule emits the fluorescence after excitation and redistribution (spontaneous and through collisions) of the vibrational energy. In the case of acetone the fluorescence builds up gradually from practically zero intensity, as expected if diacetyl is accumulating; it is excited, not by light, but probably by collisions with excited acetone or with combining radicals. The diffusion experiments can scarcely be reconciled with the assumption that the observed emission in pure diacetyl is a recombination spectrum.

Introduction

WHEN diacetyl in water solution (about 1 : 50) is radiated with violet or near ultraviolet light it shows a vivid green fluorescence. The most striking thing about the fluorescence is that it does not appear immediately upon radiation. If a carbon arc is focused in the solution through a violet filter a weak fluorescence occurs, but after a minute or so the brightness suddenly begins to increase rapidly toward a saturation value which persists. The rise in brightness occurs first in the region where the light is most intense and then spreads through the whole region illuminated.

This effect was first noticed by Kalle.[1] His note was called to my attention by Professor Franck who suggested that the delay in the appearance of intense fluorescence might be due to quenching by dissolved oxygen which was in time consumed under the action of light. This was easily shown to be the correct explanation. For if the diacetyl solution is outgassed the fluorescence appears with its final intensity immediately upon radiation. If air or oxygen is bubbled through the solution the delay in fluorescence again occurs. It does not occur if carbon

* Now at Albion College, Albion, Michigan.
† Now at Naval Research Laboratory, Washington, D. C.

[1] Kalle, Naturwiss. **25**, 61 (1937).

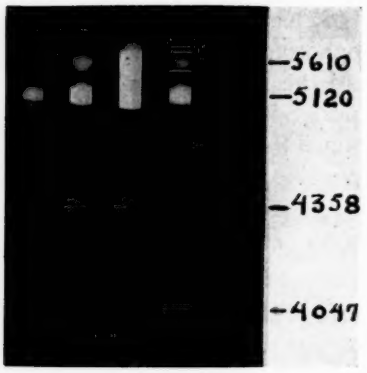

FIG. 1. Photograph of fluorescence of diacetyl, excited (a) mainly by λ4047, (b) by λ4358.

dioxide or nitrogen is introduced. Tank nitrogen contains enough oxygen to delay the fluorescence a short time, but nitrogen prepared by heating sodium azide will not quench the fluorescence.

It was next found that diacetyl vapor fluoresces with the same spectral distribution as the solution. This fluorescence, again, is strongly quenched by oxygen. The green fluorescence which appears when acetone is radiated with λ3130 is also known to be quenched strongly by oxygen. Upon examination it was found that the fluorescence spectrum emitted when acetone is radiated with λ3130 is identical with that appearing when diacetyl is radiated with violet light, say λ4358, even to the detail in the fine structure. This similarity has also been noted by Matheson and Noyes.[2] It seemed of interest to study the properties of diacetyl fluorescence in order to shed light on the questions of what elementary processes occur when this molecule is radiated, what molecule emits the fluorescence and what is the mechanism of the quenching by oxygen. These experiments are the principal subject of this paper. Some study of the absorption of diacetyl vapor while being radiated has also been made with surprising results which will be briefly described.

ABSORPTION OF DIACETYL

The absorption spectrum of diacetyl vapor consists of ultraviolet systems near 2800A and 1950A and a system in the violet and near ultraviolet. In the latter the maximum absorption occurs near λ4150. To longer wave-lengths bands with fairly definite edges appear and the system ends rather abruptly near λ4600. To shorter wave-lengths a continuum extends growing gradually weaker so that the vapor is nearly transparent below λ3600 or λ3500.

Light[3] has studied the spectrum of diacetyl and has arranged the sharper edged bands into several groups. Twenty-two of thirty-four observed edges fit an empirical equation with coefficients indicating vibrational intervals of 1100, 650, and 84 cm^{-1}. The last two intervals stand out conspicuously upon inspection of an absorption plate.

SPECTRUM OF FLUORESCENCE RELATION TO FLUORESCENCE OF ACETONE

Filtered mercury arc radiation provided the excitation of the fluorescence, either from a small 110-volt d.c. quartz arc or from a pair of glass a.c. arcs 150 cm long. The latter arcs were arranged with elliptical mirrors to focus the light in a tube 150 cm long by 3 cm diameter. The tube was surrounded by a jacket closed at the

TABLE I. *Details of fluorescence spectra of radiated acetone and diacetyl.*

Diacetyl		Acetone
	Center of Broad Maxima	
Wave-length	Intensity	Wave-length (Norrish)
5125	strong	5117
5610	medium	5572
6135	weak	6095
	Fine Structure Maxima	
	ν(cm⁻¹ in vac.)	(Padmanabhan)
5014	19939	
5027	19887	
5041	19832	
5060	19757	5058
5071	19715	5070
5083	19668	5081
5099	19606	
5112	19556	
		5140?
		5152 (broad max. near
5170	19337	5171 center of band)
5187	19274	5186
5201	19222	
5221	19148	
5550	18013	5548
5568	17955	5570
5590	17884	5594

[2] Matheson and Noyes, J. Am. Chem. Soc. **60**, 1857 (1938). See also reference 6.

[3] Light, Zeits. f. physik. Chemie **122**, 447 (1926).

ends and held on the fluorescence tube by rubber ring stoppers. Through the jacket water or a filtering solution could be circulated to control the temperature and the exciting wave-length. With water in the jacket and diacetyl in the tube at 20 mm pressure, a good exposure of the green fluorescence was obtained in two seconds with a Steinheil spectrograph with 3 glass prisms and f : 3.5 camera. This arrangement was particularly useful in studying the absorption of diacetyl vapor while it was being radiated. For this experiment a tube with plane Pyrex windows fused to each end was used. For exciting with λ4358 a mixture of cuprammonium and sodium nitrite solutions was circulated through the jacket and copper cooling coils.

The fluorescence consists mainly of three broad bands with maxima of intensity at λλ5125, 5610, 6135. On these is superimposed some finer structure. There is also a weak fluorescence extending from the intense fluorescence toward the region of diacetyl absorption. A reproduction of the spectrum is shown in Fig. 1.

The fluorescence spectrum is identical with that obtained when acetone is radiated with filtered λ3130. This was ascertained by photographing the latter and visually comparing the details of the two spectra. The positions of the finer structure and the general intensity distribution are identical to eye observation. In Table I our measurements of the principal and the finer structure maxima of diacetyl fluorescence are listed and in a parallel column the maxima of acetone fluorescence reported by Norrish, Crone and Saltmarsh,[4] and by Padmanabhan.[5] The identity is clear; every maximum noted with acetone appears with diacetyl. Fainter maxima which appear only in the diacetyl column are simply continuations of the structure. Recent work by Matheson and Zabor[6] shows the similarity of the fluorescence of acetone, diacetyl and other carbonyl compounds.

It should be emphasized that identical fluorescence is obtained when diacetyl is excited with λ4358, which does not excite acetone, and when acetone is excited with λ3130, which does not excite diacetyl. There is, however, an important difference between the intensities in the two cases. When diacetyl is radiated with weak or strong light (λ4358) the fluorescence appears immediately with an intensity which remains constant (or falls slowly as diacetyl is decomposed). With acetone the fluorescence rises gradually from almost zero intensity. In weak light the intensity will increase for hours.[7] These facts can readily be understood if we assume that the fluorescing molecule is diacetyl. It is known[8] that diacetyl if formed in acetone radiated with λ3130, at temperatures less than 60°C. Thus it may be expected that the fluorescence increases in intensity as the amount of diacetyl grows.

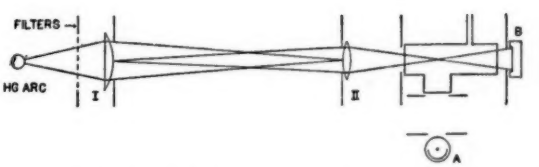

FIG. 2. Experimental arrangement for measurements of intensity. A and B are photo-cells.

The question arises then as to how the diacetyl in acetone is excited when radiated with λ3130 which will not excite appreciable fluorescence in pure diacetyl. It may happen either by a collision of the second kind, diacetyl against excited acetone or as a result of a three-body collision between diacetyl and two combining radicals, in which the energy released in recombination excites the diacetyl molecule.

The absorption spectrum of diacetyl and the fluorescence spectrum have no obvious relation to one another. They are rather definitely separated and the regularities in the vibrational intervals are apparently unrelated in the two spectra. These facts at first sight speak against diacetyl as the fluorescing molecule. In a molecule with many degrees of freedom, however, it is possible that even in the absence of collisions,

[4] Norrish, Crone and Saltmarsh, J. Chem. Soc. 1456 (1934).
[5] Padmanabhan, Proc. Ind. Acad. Sci. **A5**, 594 (1937).
[6] Matheson and Zabor, J. Chem. Phys. **7**, 536 (1939).

[7] Experiments by Mr. Scott Anderson, now in progress, show that this is definitely not the effect of quenching by oxygen. This is shown by condensing acetone in the fluorescence tube. As long as the acetone is rapidly being pumped off the fluorescence is blue and the green fluorescence is practically absent. When the flow is stopped the green fluorescence rises in intensity. Matheson and Noyes (reference 2) also find that the acetone fluorescence is not constant in time and depends upon the past history of the sample.
[8] Barak and Style, Nature **135**, 307 (1935); Spence and Wild, J. Chem. Soc. 352 (1937).

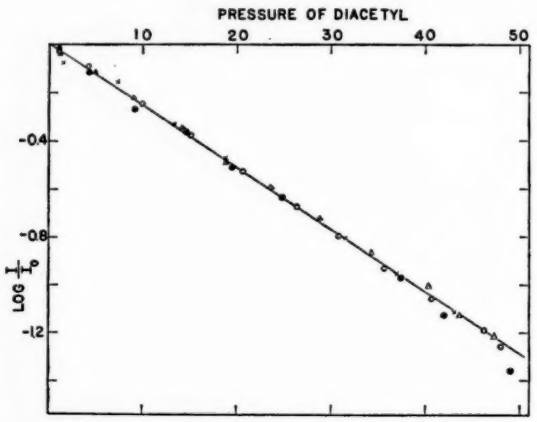

FIG. 3. Data of several runs for determining absorption coefficient of diacetyl for mercury arc lines near λ4358. Pressure in mm mercury.

the vibrational energy, introduced into the molecule on excitation on account of the Franck-Condon principle, is quickly distributed through the molecule and that the more probable distributions of vibrational energy in the excited state do not include that attained on original excitation. That is to say, the excited molecule will return infrequently to the configuration from which emission which is the reverse of the strong absorption could occur. Thus the strong emission may be shifted markedly from the strong absorption and the vibrational structure may be quite different.

The distribution of light in the spectrum is insensitive as judged by eye estimate of photographs to any changes of condition which we have made. The temperature has been varied from 10° to 100°C, the wave-length of the exciting light has been varied by using the groups of Hg lines near 3650A, 4047A and 4358A, and the pressure of diacetyl has been varied from 60 mm Hg to 0.1 mm Hg without affecting the general appearance or the fine detail of the spectrum. Even at 0.1 mm, however, the number of collisions per lifetime is of the order of ten (assuming a collision diameter of 3×10^{-8} cm and a lifetime, as measured below, of 10^{-5} sec.). Hence collisions may play a part in redistribution of vibrational and rotational excitation energy even at the lowest pressures used. Two exposures at 0.025 mm also showed the same broad maxima but the intensity was so little above the background that a change in spectral distribution may have been concealed. At any rate, 6000 collisions produce no effect different from that produced by 10.

In water solution the fluorescence shows the same three broad maxima, but the finer structure is diffused beyond recognition. The presence of 0.2 mm oxygen, which quenches the fluorescence to about two percent of the intensity without oxygen, does not change the spectrum.

The fact that the spectrum does not change when its intensity is 98 percent quenched by oxygen means that in less than 2 percent of its excited life the molecule has gone into the condition from which fluorescence occurs. In this intermediate state the amount of vibrational energy in the important modes of vibration for the fluorescence transition does not depend much upon exciting frequency or pressure. One can understand this by assuming again that the original vibrational excitation is concentrated in a few degrees of freedom, then distributed spontaneously over the thirty degrees of freedom which the molecule possesses in such a way that few quanta are allotted on the time average to the modes important in the fluorescence. Thus the observed vibrational distribution is not very sensitive to the total initial vibrational energy in the excited state nor to the numbers of collisions.

INTENSITY OF FLUORESCENCE

Method

For the investigation of the effect on the fluorescence intensity of diacetyl pressure, intensity of exciting light and pressure of added gases, particularly oxygen, a T-shaped Pyrex fluorescence cell and a photoelectric cell were used. The fluorescence cell was 15 cm long by 5 cm in diameter with three Pyrex windows, each nearly 5 cm in diameter, fused on. For illumination a

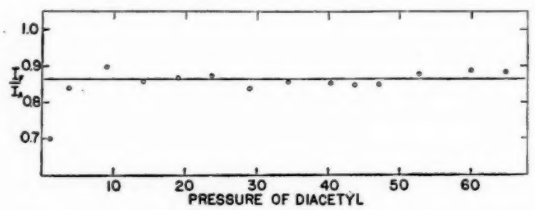

FIG. 4. Ratio of fluorescence intensity to absorbed light as a function of pressure. Ordinate units arbitrary. Pressure in mm mercury. Because of inaccuracy at low pressures, departure of point at 1 mm from line is not significant.

110-volt d.c. quartz arc, supplemented with Corning glass filters or liquid filters, was used. The optical system is shown in Fig. 2.

Only relative intensities have so far been measured. For this purpose the most accurate measurements were made with a caesium oxide vacuum photoelectric cell used in conjunction with a d.c. amplifier employing an electrometer tube in the Barth-Penick circuit. The photo-cell-amplifier system was tested for linear response with a sector disk and green-filtered light from an incandescent lamp. It was found to be nicely linear over a twenty-fold variation of intensity (limits of test) in approximately the intensity range in which the system was used. A slow drift, linear in time, in the zero of the instrument was nearly always present but it could be followed by taking zero readings periodically throughout a run, and the true deflections thereby determined.

For the measurement of the absorption coefficient of diacetyl a photo-cell with linear response used without amplification was placed behind the fluorescence tube and the pressure of diacetyl in the tube of known length was varied. A third cell could be mounted beside lens II where it received a small amount of light from the source and enabled one to make corrections for small variations in incident energy. The whole system except the source was carefully shielded in a black-lined housing so that stray light produced no observable deflections on the glavanometers. It was necessary to make small corrections for light from the source scattered in the fluorescence cell but these could be accurately measured with the fluorescence cell pumped hard or containing air.

Variation of fluorescence intensity with diacetyl pressure

First the absorption coefficient of diacetyl vapor at λ4358, the radiation used in all of the following measurements was determined. The intensity of light (I) transmitted through the cell, which contained a column of vapor of length 12.5 cm, was measured at different pressures of diacetyl. The results of four runs are plotted in Fig. 3 (log I/I_0 against p), from which the absorption coefficient (a) is calculated to be 0.0206 per cm Hg per cm path. If the concentration is expressed in moles per liter, path in cm, the coefficient is 35.1.

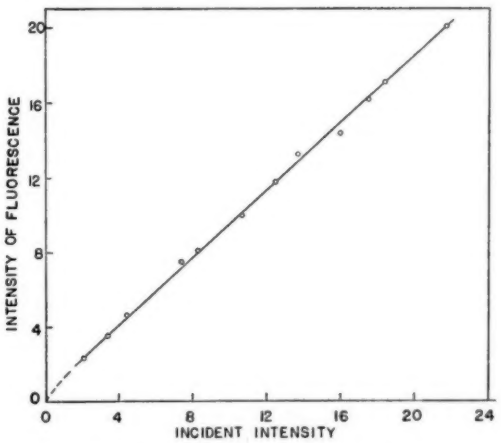

FIG. 5. Fluorescence intensity is proportional to incident intensity, pressure constant. Units arbitrary.

The intensity of the fluorescence (I_F) as a function of diacetyl pressure was then measured. The intensity of the exciting light had to be corrected for absorption between the entrance window and the observing window. The light absorbed in the region seen by the photo-cell was taken to be $I_0(e^{-apx_1} - e^{-apx_2})$ where p is the diacetyl pressure, I_0 is the deflection of a galvanometer on the photo-cell measuring the incident light and x_1 and x_2 are the limits of the fluorescence region available to the photo-cell A, measured from the entrance window.

The ratio of the intensity of the fluorescence to the absorbed light is plotted against pressure in Fig. 4. The ratio remains constant as the pressure rises from 1 to 60 mm. No self-quenching is observed. From the lifetime of excited diacetyl (estimated below to be about 10^{-5} sec.) one can calculate that a hundred or more collisions occur during a lifetime even at 1 mm pressure. At all events tens of thousands of collisions are no more effective than a few hundreds in deactivating excited diacetyl.

Dependence of intensity of fluorescence on incident intensity

Diacetyl was admitted to the cell at a pressure of 42 mm. The fluorescence intensity (I_F) was measured as the incident intensity was varied by introducing combinations of wire screens. The incident intensity was measured with a photo-cell

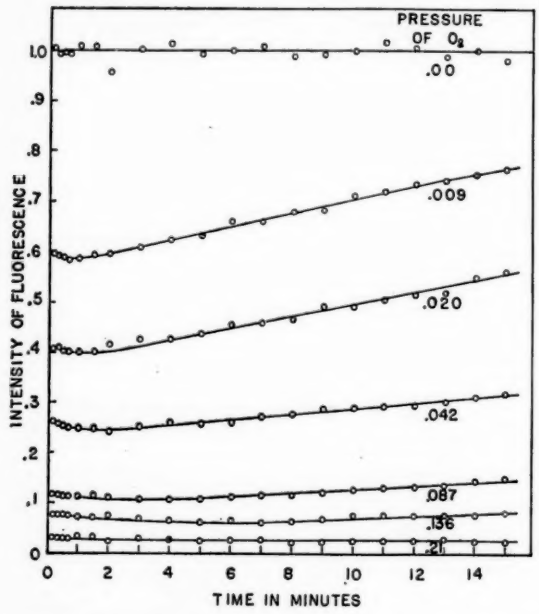

FIG. 6. Typical data on quenching of fluorescence by oxygen. Without oxygen the intensity is constant in time. With increasing pressure of oxygen the fluorescence is strongly quenched. As the exposure increases, with oxygen present, there is at first a decrease in intensity, then a recovery.

with linear response. The results appear in Fig. 5. The fluorescence rises linearly with exciting intensity.

The linear variation is to be expected if a simple process occurs involving one quantum absorbed for each quantum emitted. More complicated processes could, to be sure, give an overall linear variation. This experiment shows merely that it is not necessary to assume a complex process.

Quenching of fluorescence by oxygen

The effect of oxygen on the fluorescence was tested by the use of the T-shaped tube and photo-cell-amplifier system. The procedure was this: the tube was pumped, filled with several mm of oxygen and pumped to the desired pressure, read with a McLeod gauge. Then diacetyl was admitted until the pressure was between 20 and 30 mm. To obtain the lowest oxygen pressures (<0.04 mm) more diacetyl was admitted and after allowing time for mixing the cell was pumped to about 20 mm. The cell was illuminated and the intensity of fluorescence (I_F) observed as soon as a reading could be taken (a few seconds) and at frequent intervals thereafter for 15 minutes.

A typical series of data is shown in Fig. 6. The ratio of fluorescence to absorption is plotted against time. At zero oxygen pressure no change in intensity occurs over fifteen minutes of illumination. With oxygen present the fluorescence is strongly quenched, drops still further during the first moments of illumination, then rises.

If an excited molecule is attacked by a foreign molecule and the emission of light thereby prevented the quenching should follow a hyperbola (Stern-Volmer law); i.e., $I_F/I_A = 1/(1+ap)$ where p is the pressure of the foreign gas. The reciprocal quantity I_A/I_F should rise linearly with the pressure. Both ratios are plotted in Fig. 7. The second can be nicely fitted with a straight line over a range of pressure in which the fluorescence drops to one-fifth of its initial value, but at higher oxygen pressure it rises more steeply. In the latter region the fluorescence is weak and the measured corrections for scattered light become of the same magnitude as the fluorescence. Hence the departure from the Stern-Volmer law at high oxygen pressure cannot be regarded as definitely established.

The drop in intensity during the first moments of illumination when oxygen is present can be explained by the assumption that when an excited molecule is attacked by oxygen a compound molecule (a peroxide ?) is formed which is even more effective than oxygen itself in further quenching of excited diacetyl, and that this compound molecule is reduced in the quenching process to a nonquenching molecule. Hence the fluorescence decreases as the concentration of the intermediate compound is built up but eventually, as both the oxygen and the compound molecule are used up, the fluorescence increases.

Other measurements on the recovery of the fluorescence made with a visual photometer and with stronger illumination showed that the fluorescence does after a time recover to its original intensity, at least to within a few percent Of course, long continued illumination with strong light decomposes the diacetyl to products not condensible with liquid air. As this stage is approached the pressure rises and the fluorescence decays toward zero.

Lifetime of excited molecule

The lifetime of the fluorescing molecule (τ) has been estimated in two ways: (1) from the quenching curve and (2) by observations on the diffusion of the gas into a shadow after excitation. From the quenching curve one finds that the intensity falls to one-half at an oxygen pressure of 0.013 mm. At this pressure the time between quenching collisions with oxygen must equal the mean lifetime of the excited diacetyl molecule. The number of collisions per second which an excited molecule makes with an oxygen molecule is

$$Z = 5.80 \times 10^{21} \sigma^2 p,$$

where p is the oxygen pressure (mm Hg), σ is the distance between centers upon collision. The time between collisions is $1/Z$. If a chemical reaction occurs in the quenching process (oxygen is consumed), the diacetyl molecule probably must be attacked in a definite place and the distance for effective collision must be small. Thus, if σ is taken to be 3×10^{-8} cm (approximately the gas kinetic diameter of O_2), $1/Z$ and hence τ is 1.5×10^{-5} sec.

In the second determination of τ a method described by Heil[9] was used. A series of parallel round bars of different diameters was mounted on the stop at lens I in Fig. 2. Its image was projected by lens II into the tube directly behind the observation window. When the diacetyl pressure is high one sees sharply bounded bands of fluorescence with dark shadows between, where the images of the bars fall. As the pressure is reduced the bright bands diffuse into the shadow, since an excited molecule can then diffuse into the shadow before emitting. The pattern was photographed at various pressures.

Now if a molecule moves at random through a gas of similar molecules for a time τ, its mean squared displacement in a given direction is $\overline{x^2} = 2\tau D$ where D is the coefficient of diffusion. We assume that we can use this expression to calculate the displacement of an excited particle through the gas of similar but unexcited molecules and that $D = \eta/\rho$, where η is the coefficient of viscosity and ρ the density. η has not been measured for diacetyl but for many other light organic molecules it is within 20 percent of 10^{-4} c.g.s. units; for acetone it is about 0.9×10^{-4}. We assume η equal to 10^{-4} and thus can write $\tau = 0.025 \overline{x^2} p$, where x is in cm and p is diacetyl pressure in mm Hg. From a study of the diffuseness of the shadows it is estimated that,

at $p = 1.5$ mm, $\overline{x^2} = 0.0004$ cm², $\overline{x^2} p = 0.0006$:
at $p = 0.5$ mm, $\overline{x^2} = 0.001$ cm², $\overline{x^2} p = 0.0005$.

Hence τ is about 1.4×10^{-5} sec.

If the collision cross section of excited diacetyl against normal diacetyl is so large that the assumptions made do not apply, the lifetime is greater than estimated. Since, however, excited diacetyl is not at all quenched by collisions with normal diacetyl (I_F/I_A independent of pressure, Fig. 4), it is reasonable to suppose that the cross section is not abnormally large.

Neither method of estimating τ is precise and the closeness of the agreement of the two results is accidental. Both, however, should be correct in order of magnitude; we conclude that the lifetime of the fluorescing molecule, in all probability diacetyl, is 10^{-5} sec., or longer.

Remark on hypothesis that fluorescence is due to recombination

These experiments on diffusion also seem to rule out the hypothesis that the emitted light is a luminescence arising from a recombination of radicals formed by light in acetone or diacetyl.[6] The immediate result of the experiment is that

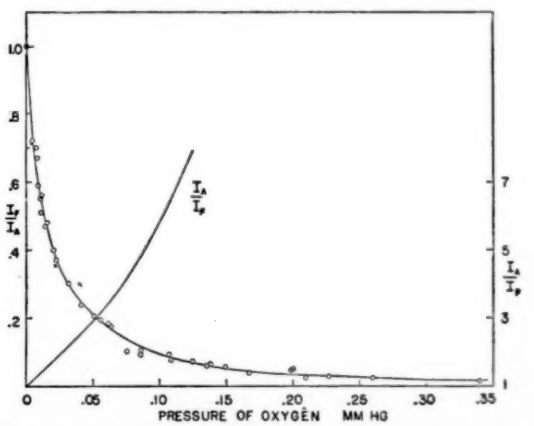

FIG. 7. Quenching of diacetyl fluorescence by oxygen. The ratio of fluorescence to absorbed light follows a Stern-Volmer law during the decrease to 0.2 of the intensity without oxygen. At higher oxygen pressures, where measurements are less reliable, the ratio drops more rapidly than expected.

[9] Heil, Zeits. f. Physik **77**, 563 (1932).

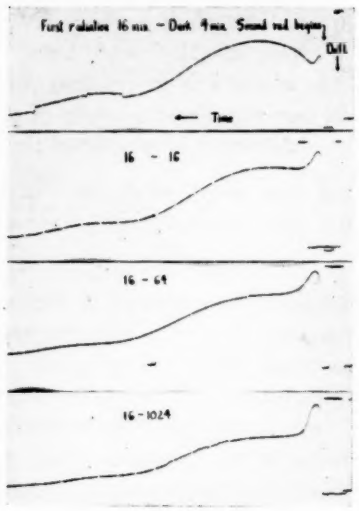

FIG. 8. Typical recording galvanometer traces showing the absorption which sets in when diacetyl vapor is first radiated for 16 minutes, then allowed to remain in the dark for 4, 16, 64 and 1024 minutes, respectively, and then radiated a second time. A fresh supply of diacetyl is used for each run. The breaks in the curves mark 30-second intervals. Zero deflection (at top of each record) and deflection during dark period (same as with unradiated diacetyl) are shown in each record.

the activated particle diffuses for a time of 10^{-5} second before emission, on the assumption that it has a normal gas kinetic cross section against diacetyl molecules. Suppose that the particle is a radical and that it has to encounter a second radical to accomplish the emission. From the diffusion experiment we conclude that it encounters the second particle in 10^{-5} sec.; that is to say, it is making collisions with other radicals at the rate of 10^5 per sec. This requires a partial pressure of radicals of about 10^{-4} atmosphere or about 10^{15} radicals per cc. But if a radical disappears in 10^{-5} second, on the average, their rate of production, to maintain a concentration of 10^{15}, must be $10^{15}/10^{-5}$ or 10^{20} per cc per second. The light absorbed was not measured, but from recent absolute measurements on a similar optical system it must have been less than 10^{20} quanta per cc per sec. by a factor of at least 10^6. The case for recombination is made worse, if one supposes that a third body in the collision is necessary in order to stabilize the molecule before emission, or, alternatively, to take up the energy of recombination and later emit light (chemiluminescence); it is also worse if there are other ways by which the radicals may disappear.

Recombination as essential for emission process is conceivable only if the collision cross sections for radicals in diffusion through diacetyl molecules and for combination with one another are very much greater than the ordinary gas kinetic values, which are assumed in the above calculations of lifetime and recombination.

A further argument against the recombination hypothesis is the slow growth in weak light of the fluorescence in acetone, as contrasted with its immediate appearance with full intensity in diacetyl. It is unlikely that a period of minutes, or even of hours in weak light, should be required to establish equilibrium in a process which is primarily the production and disappearance of radicals. Moreover, if recombination is the essential element in the production of fluorescence in both diacetyl and acetone it is difficult to see how the qualitative difference in the rate of growth of fluorescence in the two compounds can be understood.

ABSORPTION OF DIACETYL WHILE BEING RADIATED

Since the region of intense fluorescence is definitely separated from the region of absorption an attempt was made to examine the absorption spectrum of diacetyl while it was being strongly radiated in order to see if new regions of absorption would appear. The system used was described earlier (150-cm tube radiated by two 150-cm 15-ampere glass Hg arcs). A Pointolite lamp was focused through the tube on the slit of the Steinheil. About 1/25 second exposure with 0.1-mm slit gave an exposure on fast plates. For most of the experiments, however, a photocell was placed behind a slit in the plate holder. The cell was connected to a short period galvanometer whose deflections were recorded photographically.

When the tube was filled with diacetyl vapor[10] (at pressures up to 50 mm) and illuminated with the Hg arc, either unfiltered or filtered to transmit only $\lambda 4358$, no absorption was observed which was not present with unradiated diacetyl in the tube. But if the tube was filled, radiated for a few minutes, then allowed to stand in the

[10] In these experiments diacetyl from two sources, The Lucidol Corporation and Eastman Kodak, were used without further purification. Similar results were obtained in the two cases.

dark for a time (varied from 1 to 1000 minutes) and *then radiated a second time*, strong absorption was observed. It extends continuously through the whole visible region, but is strongest in the region from 4500A to 5500A. It is not distinguished from diacetyl absorption at wave-lengths less than 4500A. It does not show a maximum in the region of fluorescence. During the first radiation and the dark period only diacetyl absorption is observed.

The absorption at all wave-lengths (>4500A) goes through fluctuations in time. A maximum occurs within a few seconds of the beginning of the second radiation, a second about $1\frac{1}{2}$ minutes later, a third after 6 minutes of radiation. These are shown by typical galvanometer traces in Fig. 8 and in a series of spectrum photographs in Fig. 9. Under suitable conditions more than 95 percent of the incident light in the wave-length range under observation was absorbed at the first maximum of absorption.

These observations are being made the subject of a more detailed investigation. The only point that will be made here is that the production of these absorbing substances takes place at the expense of incident energy and must cut down the quantum yield in the over-all process of decomposition of diacetyl into carbon monoxide and hydrocarbons. Several quanta may be necessary to put each molecule through the stages indicated by these new absorption effects.

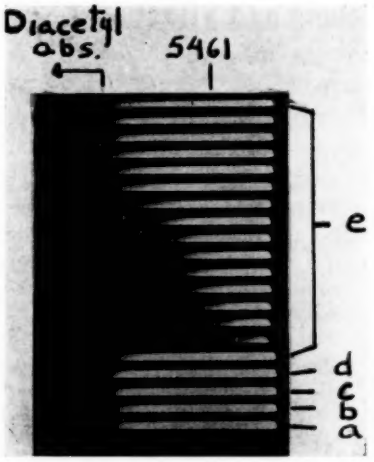

FIG. 9. Spectrographs of absorption of diacetyl when radiated 16 min., allowed to stand in the dark 16 min. and then radiated a second time. The exposures, of one second each, were taken as follows: (a) before first radiation, (b) at start of first radiation, (c) at end of first radiation, (d) at end of dark period, (e) during the second radiation at times after its beginning of 1, 10, 20, 30, 40 sec. 1, 1.5, 2, 2.5, 3, 4, 5, 6, 7, 9, 11 min.

CONCLUSION

The observed properties of the fluorescence of diacetyl and acetone are compatible with the assumption that the fluorescing molecule is, in both cases, diacetyl. Following the excitation of diacetyl there must be a redistribution of vibrational energy in such a way that the amounts allotted to the modes of vibration important in the fluorescence are not very dependent upon the wave-length of exciting light or the numbers of collisions before emission. The lifetime of the excited state is about 10^{-5} sec., as estimated on the assumption that the quenching process with oxygen requires a collision diameter of 3×10^{-8} cm. This is a reasonable figure for a chemical reaction, which, it is inferred, takes place because the oxygen is consumed. A lifetime of the same order of magnitude is obtained in the experiment on the diffusion of the excited molecules into a shadow. This experiment also makes very improbable the hypothesis that the apparent fluorescence of diacetyl and acetone is a recombination spectrum. The apparent fluorescence of acetone is probably light emitted by diacetyl molecules formed from acetyl radicals and excited in collisions with acetone or recombining radicals.*

It is a pleasure to acknowledge that these experiments were begun at the suggestion of Professor James Franck, while one of us (G.M.A.) was spending some months at Johns Hopkins University. We are also indebted to Professor Franck and Dr. F. F. Rieke for discussion of the results.

* *Note added in proof.*—Preliminary direct measurements of the lifetime of the fluorescence with a phosphoroscope, combined with measurements of the quantum yield of the fluorescence, indicate that the lifetime of the excited molecule is, in fact, much longer than 10^{-5} second. This longer lifetime will require only quantitative changes in any of the arguments given in the paper. It may, however, compel a change in our idea of the intermediate state occupied between excitation and emission. Rather than being simply a different vibrational state of the electronic state reached on absorption it may be a different and long-lived electronic state.

The direct determination of the lifetime will make possible a calculation of the efficiency of quenching collisions with oxygen and of cross section of collision of excited against unexcited diacetyl.

Quenching and Vibrational Energy Transfer in the Fluorescence Spectrum of S_2

ERIC DURAND
Johns Hopkins University, Baltimore, Maryland

(Received September 5, 1939)

The ultraviolet fluorescence of S_2 was excited by the strong Mg spark lines λλ2928 and 2937A. A typical Wood resonance progression was observed with pure S_2 only in the vessel, but the addition of a few millimeters of any of the rare gases caused changes in the fluorescence due to quenching and to the transfer of vibrational and rotational energy. The yields per collision for quenching and for vibrational transfer are of the order of magnitude of unity, and both show the same dependence on the atomic weight of the rare gas added, with a minimum in the vicinity of Ar or Kr. Comparisons are made with the results obtained by other methods. Quenching occurs by the addition of two quanta of vibrational energy to the S_2, followed by disruption due to predissociation.

INTRODUCTION

IN recent years four methods for the study of the exchange of vibrational and translational energy between molecules and other particles have been developed. Two are based on studies of molecular dissociation rates[1] and recombination rates,[2] one on the propagation of supersonic waves,[3] and one on the changes produced in fluorescence spectra by the addition of other gases.[4–6]

As yet there is no satisfactory general theory of energy exchange applicable to all types of collisions, so only the case of collisions between diatomic molecules and rare-gas atoms will be considered here.

The vibrational energy transfer yields found with the fluorescence and the recombination methods are much larger than those found with the other two methods—in some instances by a factor of 10^5. Eucken and Franck[7] have attributed this difference to the fact that the molecules studied by the former two methods are in a high vibrational state, so that their electronic configurations should be readily perturbed by collisions, while those studied in the latter two cases possess only one or two quanta of vibrational energy, and so should be more stable. There is, however, considerable uncertainty present in the absolute values of the yields in all of the methods, and the differences may not be as great as the experiments indicate.

The dependence of the yields on the mass of the colliding particle may be determined more accurately, and here, too, the results obtained by the different methods differ. The fluorescence and the recombination methods have been applied only to the heavy halogens I_2 and Br_2, and these show a rising yield with increasing mass of the rare-gas atoms. The dissociation and the acoustical methods, applied to the light molecules Cl_2 and N_2O, have shown the reverse dependence. Rössler,[6] following ideas advanced by Rice[8] and Zener,[9] has attributed this difference to effects depending on the ratio of the period of molecular vibration to the duration of the collision, which should be small with the heavier molecules, and large with the light ones.

The research here presented was in part done to check Rössler's hypothesis, by applying the fluorescence method to a light molecule. Sulfur was selected, since it shows vibrational energy transfer [Heil[4]], and since its band-spectrum is well known. The Mg spark lines λλ2928 and 2937A were used to excite the rotational levels $K'=37$ and $K'=41$ in the vibrational level $V'=8$ of the first excited electronic state [cf.

[1] M. Volmer and M. Bogdan, Zeits. f. physik. Chemie **B21**, 257 (1933).
[2] E. Rabinowitch and W. C. Wood, Trans. Faraday Soc. **32**, 540 (1936); E. Rabinowitch, *ibid.* **33**, 282 (1937); K. Hilferding and W. Steiner, Zeits. f. physik. Chemie **B30**, 399 (1935).
[3] A. Eucken and R. Becker, Zeits. f. physik. Chemie **B27**, 219 (1934).
[4] O. Heil, Zeits. f. Physik **74**, 18 (1932).
[5] B. Rosen, Zeits. f. Physik **43**, 69 (1927).
[6] F. Rössler, Zeits. f. Physik **96**, 251 (1935).
[7] A. Eucken and J. Franck, Zeits. f. physik. Chemie **B20**, 460 (1933).
[8] O. K. Rice, J. Am. Chem. Soc. **54**, 4558 (1932).
[9] C. Zener, Phys. Rev. **37**, 556 (1931); **38**, 588 (1931).

Christy and Naudé[10] and Heil[4]]. The rare gases He, Ne, Ar, Kr, and Xe were used as collision partners.

At low pressures, the molecules, not disturbed by impacts, radiate normally, giving rise to the well-known Wood resonance progression. At high pressure, the more frequent collisions cause considerable energy exchange. Changes in the rotational quantum numbers give rise to whole bands in the places of the small groups of lines forming the original members of the progression, and changes of the vibrational quantum numbers result in bands in new positions. Furthermore, if the molecules are transferred into levels for which $V' \geqslant 10$, disruption occurs, because of predissociation,* and the radiation is quenched. Consequently, quenching, and the occurrence of new bands, both being caused by the transfer of vibrational energy, should show the same dependence on the nature of the collision partner; this was verified experimentally.

Experimental

a. Optical

All optical components were of quartz. To avoid the fluorescence produced by the spark line λ3096A, a monochromator with a large water-filled prism was used. The desired monochromatic spark image was isolated by a slit and brought to a focus within the fluorescence vessel. The fluorescence light was taken off at right angles and focused on the upper half of the slit of a small spectrograph. The intensity and monochromatic purity of the exciting light were determined by intercepting a part of the incident light with a clear polished plate and reflecting it into the lower half of the slit. Exposures from one to three hours were used. Typical spectra are shown in Fig. 2 (p. 48).

For the quenching data, the spectrograph prism was removed and the camera tube swung around colinear with the collimator tube. The slit was opened to 2 mm, so that a 2×6 mm heterochromatic image of the slit was formed on the plates. The monochromator was not used, but a Corning Red-Purple No. 986-A filter was inserted in the path of the comparison beam, to make its color sufficiently similar to that of the fluorescence. 15-second exposures were used.

Density-marks for calibrating the plates were applied by the optical step-wedge method described by Miller,[11] using a mercury arc light-source.

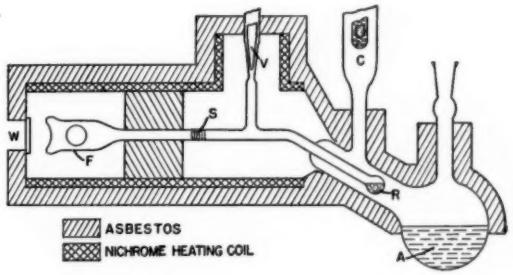

Fig. 1. The gas-system. A, aniline boiler, R, sulfur reservoir, C, refluxing condenser, V, exit valve-seat, S, graded seal, F, fluorescence vessel, W, exit window.

b. The gas-system

The gas-system, shown in Fig. 1, was designed to provide diatomic sulfur at constant pressure. The vapor pressure was determined by the temperature of a reservoir of liquid sulfur, which was kept constant by being bathed in a stream of aniline vapor boiling at atmospheric pressure. A refluxing condenser returned the condensed aniline to the boiler. Variations in barometric pressure were negligible during the ten days of the final run; the vapor pressure of the sulfur was 1.1 mm.

The fluorescence vessel proper was of fused quartz, with windows sucked in at the end and on one side. It was kept at 600°C to insure a high concentration of S_2 relative to the other molecular forms.

A special valve was designed, to seal off the fluorescence vessel. It consisted of a ground tapered rod which could be raised or lowered in a conical seat by a sylphon bellows mechanism. The outlet from the valve connected to a typical high vacuum system. Pressures were measured with a McLeod gauge or a closed-arm ma-

[10] A. Christy and S. M. Naudé, Phys. Rev. **37**, 490, 903 (1931).

* Whether the predissociation is induced or direct [cf. the discussions of Lochte-Holtgreven, Zeits. f. Physik **103**, 395 (1936), and Olsson, Zeits. f. Physik **108**, 40 (1937); **99**, 114 (1936); **100**, 656 (1936)] is not important here in view of the high pressures used.

[11] O. E. Miller, Zeits. f. Wiss. Phot. **31**, 131 (1932).

nometer. The rare gases used were flasks of "Spec-Pure" gas from the Air Reduction Company.

The sulfur had to be very pure and gas-free. It was prepared from crude roll-sulfur by a series of successive distillations, first under a stream of tank He, and then under high vacuum, following the scheme of Farr and McLeod.[12]

The spark electrodes were so shaped that no entrance slit was needed for the monochromator. Power was supplied by a 110/25,000-volt transformer with a primary current of 5 amperes, the secondary being shunted by a 0.01-mf condenser.

Measurements and Computations

a. Intensities

Densities were determined with a recording microphotometer built by Dr. G. H. Dieke. Intensities were determined by reference to a density-intensity curve drawn from the density-mark data in the usual manner.

b. Quenching energy transfer

The usual quenching formula was used:

$$\delta\tau=(1/p)(I_0/I_p-1), \qquad (1)$$

where I_0 and I_p are the intensities, relative to the comparison mark, of the fluorescence under added gas pressure 0 and p mm, respectively, τ is the natural mean lifetime of the excited state, and δ is the quenching probability as defined by Rössler.[6] A correction factor for scattered light was obtained by taking several plates with the aniline boiler cold. The results are shown in Table I.

It will be noted that the values of $\delta\tau$ decrease with increasing pressure. This decrease occurs since, by collisions, lower levels become populated at the expense of the original level. These levels, being farther from the predissociation levels, are less readily quenched. For this reason, only the values obtained at low pressures (italics) were used to determine the final averages (see Table III).

Table I.

Pressure	$\delta\tau$	Pressure	$\delta\tau$	Pressure	$\delta\tau$
5.7 He	*0.086*	6.4 Ne	*0.038*	10.4 Ar	0.021
5.9	*0.078*	7.0	*0.032*	22.9	0.031
8.0	*0.082*	7.1	*0.040*	11.5 Kr	*0.030*
12.0	0.059	11.7	0.032	33.3	0.021
15.5	0.055	22.0	0.025	8.9 Xe	*0.039*
17.2	0.060	6.9 Ar	*0.029*	19.2	0.032
25.9	0.042	8.6	*0.022*	35.2	0.025
45.7	0.027	9.2	0.024	35.2	0.026

[12] C. C. Farr and D. B. McLeod, Proc. Roy. Soc. **A118**, 534 (1928).

c. Band-producing vibrational energy transfer

Figure 2 shows spectra taken with and without added gas. These spectra make clear that the data for the determination of band-producing transfer is limited to the transfer of $\pm1, 3, 5\cdots$ quanta, since the transfer of $\pm2, 4, 6\cdots$ quanta produces bands which coincide with bands of the progression originally excited. Hence Rössler's[6] calculation of the transfer yield between two single levels cannot be applied.

The total probability for transfer of an odd number of quanta may be obtained. Let n_0 and n_p be the numbers of molecules in all of the even-numbered and the odd-numbered levels, respectively, in the steady state. These molecules will give rise to two distinct sets of bands of intensity I_0 and I_p, respectively, these being proportional to n_0 and n_p.

Transfer from either group of levels to the other will be proportional to the number of molecules in the first group, n, to the pressure of added gas, p, and to the transfer yield coefficient, ϵ, which is assumed, for lack of additional data, to be identical for both sets of levels.

The population of the odd-numbered levels will be increased at a rate $n_0\epsilon p$, due to transfer of molecules *from* the even-numbered levels, and it will be decreased at a rate $n_p\epsilon p+n_p/\tau+n_p\delta p$ due to transfer *to* the even levels, to radiation, and to quenching, respectively. In the steady state, these rates are equal, so:

$$n_0\epsilon p=n_p(\epsilon p+1/\tau+\delta p), \qquad (2)$$

and

$$\epsilon\tau=(1/p)\frac{1+\delta p\tau}{I_0/I_p-1}. \qquad (3)$$

The final run consisted of one plate for each gas, the plates having fluorescence spectra at two pressures, and a density-mark. Because of the small dispersion of the spectrograph, it was impossible to measure accurately the areas under

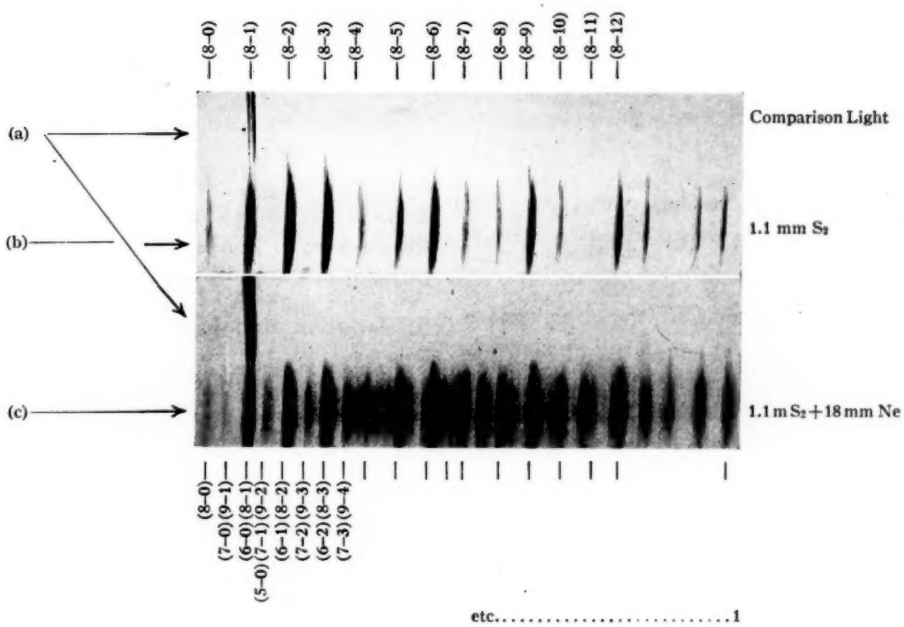

FIG. 2. Fluorescence spectra. (*a*) Comparison mark (present on all plates); (*b*) 1.1 mm pure S_2; (*c*) 1.1 mm S_2, 18 mm neon. Rotational transfer is indicated slightly by the slight winging of the lines on spectrum (*c*) as compared to (*b*). Note also the extreme density of the comparison mark associated with spectrum (*c*). This corresponds to the greatly increased exposure made necessary by the quenching. On spectrum (*c*), each apparent band corresponds in reality to more than one transition. Thus, the band labeled (8–2) in (*b*), contains, in addition, lines of the transitions (6–1) and (4–0), for example. The spectra are 5× as large as the originals.

the peaks, so that actual peak intensities had to be used. Since all bands showed nearly identical rotational structure at a given gas-pressure, this should be satisfactory.

Only the first twelve peaks in each of the two sets of progressions were distinct, and of the odd-numbered progressions, four peaks were too faint to measure. This being so, it was not possible to determine the integrated intensity produced by all of the odd-numbered levels. Therefore, the eight measurable peaks of the odd-numbered progressions were compared in intensity to eight equally representative peaks among the twelve of the even-numbered progressions. The peak 8–1, containing large amounts of scattered exciting light, was omitted. The results are shown in Table II.

To reduce these values to yields per collision, one must divide them by the natural mean life-time, τ, and by Z_v, the number of collisions at unit pressure per second of relative energy greater than the vibrational quantum in the excited state. τ was given the conventional value 10^{-8} sec. since no experimental determination was available. The absolute magnitude of the results is accordingly uncertain. Z_v was calculated from the usual kinetic theory formulae, from data in the *International Critical Tables*. The final results are shown in Table III.

d. Rotational transfer

There was evidence of rotational transfer, since, with no added gas, individual rotational lines were resolved, while with the addition of 5 to 10 mm of rare gas the structure was obliterated, because of the filling in with new lines.

TABLE II.

PRESSURE	I_0/I_p	$\delta p\tau$	$\epsilon\tau$
12.5 He	3.14	1.025	0.755
24.0	2.56	1.97	0.792
6.2 Ne	5.68	0.229	0.423
15.0	4.06	0.555	0.339
16.9 Ar	4.08	0.422	0.273
33.0	3.20	0.825	0.250
21.5 Kr	4.65	0.645	0.209
41.3	3.42	1.24	0.224
23.7 Xe	3.53	0.935	0.321
42.0	3.21	1.64	0.284

TABLE III.

GAS	Z_v	δr	ϵr	δ/Z_v	ϵ/Z_v
He	8.98×10^6	0.082	0.077	0.91±15%	0.86±30%
Ne	4.90	0.037	0.038	0.75±15%	0.77±30%
Ar	4.48	0.025	0.026	0.56±15%	0.58±30%
Kr	3.91	0.030	0.022	0.77±30%	0.56±50%
Xe	3.77	0.039	0.030	1.03±30%	0.80±50%

Since it was impossible to measure the shapes of the bands with any precision, the observations allowed only the conclusion that the probability of rotational transfer is of the same order of magnitude as that of vibrational transfer.

DISCUSSION

a. Order of magnitude

Table III shows that the yields for quenching transfer run, as expected, parallel to the yields for band-producing transfer, and are, moreover, equal to within the experimental error. One would have expected the latter yields to be greater than the former, since band-production occurs by the transfer of $\pm1, -3, \cdots$ quanta, while quenching requires the transfer of at least $+2$ quanta, and since the probability of energy exchange falls off rapidly with the number of quanta transferred. However, this point should not be emphasized too much, since the method of integrating light-intensities described above cannot give accurate results, and since the value of δ used in formula (3) should be some pressure-dependent weighted average of the values for the odd-numbered levels, while the only value obtainable was for the level $V'=8$.

The absolute values of the yields are, as mentioned, much more uncertain than the relative values, due to the uncertainty in τ. Still, it may be worth noting that Rössler's[6] values for (band-producing) vibrational transfer in I_2 are much larger than those found here for S_2. If this difference is real, it may be correlated with the fact that the excited I_2 molecule contained more vibrational energy relative to the dissociation energy of the excited state than did the S_2 molecule. ($\frac{3}{5}$ in the case of I_2; $\frac{1}{4}$ in the case of S_2.) According to the Eucken-Franck hypothesis (cf. p. 46) this difference should make the S_2 molecule less sensitive than the I_2 molecule to disturbances in the shape of the potential curves resulting from the presence of nearby particles, with a correspondingly smaller vibrational transfer yield.

The fact that I_2 also showed a much larger quenching than S_2 is to be expected, since the excitation energy of I_2 was greater than the dissociation energy of the normal state, while in the case of S_2 it was smaller, so that an actual transfer of energy by the collision was necessary.

b. Variation of yield with mass

Table III shows a minimum in the neighborhood of Ar or Kr for both yields, which is surprising, in view of the results of other workers. Rössler[6] has shown that the steady increase with mass found by himself for I_2, and the steady decrease found by Volmer and Bogdan[1] for N_2O, can both be explained in terms of the ratios existing in the two cases between the period of molecular vibration and the duration of the collision. His considerations, as well as considerations of conservation of energy and momentum, both predict a curve with a maximum. A tentative explanation for the minimum found with S_2 is to assume that S_2 lies on the decreasing side of such a curve for all of the rare gases, and that the duration of the collision becomes so great for the heavier atoms that a form of energy-sharing between the sulfur and its collision partner sets in that is independent of further increases.* The subsequent rise in yield is then to be attributed to the higher polarizibility of the heavier rare-gas atoms.

However, in view of the large experimental error for the transfer yields, it is possible that the minimum is not real.

c. Probable error

Several sources of systematic error have already been mentioned, and it is difficult to estimate their probable size. The instrumental errors in photometry should not exceed 5 percent in the case of the quenching plates, nor 15 percent in the case of the transfer plates. Imperfect temperature regulation in the case of the quenching plates would also introduce errors. In the transfer plates, density marks for only a

* The reduced mass in the S_2-Xe collision is not much larger than that in the S_2-Ar collision, so that there is no great difference in the duration of these two types of collision, in any case.

single wave-length were used; the sensitivity and contrast of the plates is not constant with wave-length. The probable errors given in Table III are estimates that apply only to the relative error.

The author wishes to express his indebtedness to the faculty of the Physics Department for assistance in the solution of the problems. He is grateful to Professor James Franck (now at the University of Chicago), for proposing the problem and for guidance; to Professors R. W. Wood and G. H. Dieke, for the loan of equipment and for advice, and to Dr. F. F. Rieke for helpful suggestions.

JANUARY, 1940 JOURNAL OF CHEMICAL PHYSICS VOLUME 8

The Absorption Spectra of Sugars in the Near Infra-Red

E. S. Barr and C. H. Chrisman, Jr.
Department of Physics, Tulane University, New Orleans, Louisiana

(Received September 27, 1939)

The infra-red absorption spectra of aqueous solutions of nine monosaccharides and four disaccharides have been observed in the region between 1.7 and 4.6μ. A special technique of evaporation was used in the preparation of samples, so as to minimize the effect of the solvent upon the transmission curves. It was found that all thirteen materials gave very similar spectra; band locations were very nearly identical, although there was some degree of variation in intensities. Bands not previously reported were found at 2.16 and 2.35μ, and the intense absorption in the region of 3.3μ was partially resolved into component bands.

In order to supplement the small amount of information on the infra-red absorption spectra of sugars which is available in the literature, an investigation of the spectra of thirteen sugars in the near infra-red has been made. The sugars examined were selected so as to be representative of a number of other closely related sugars.

In connection with his work on water of crystallization, Coblentz[1] published transmission curves for six common sugars in the region between 1 and 7μ. Rogers and Williams[2] have given locations of absorption maxima for eight sugars in aqueous solution between 3 and 12μ; relative intensities were not given, although suggested assignments for some of the frequencies were added.

Both of these investigations were carried out with rocksalt prism spectrometers, though different methods were used in the preparation of samples. Coblentz used thin films of solid sugar which had been melted onto rocksalt plates, while Rogers and Williams used cells filled with saturated aqueous solutions in comparison with cells filled with water. This difference in technique may account to some extent for the partial disagreement between the results of Coblentz and those of the later workers, if there is structural modification when a sugar goes into solution.

The thin cells used by Coblentz gave no details in the near infra-red, and Rogers and Williams began their spectral observations at 3μ. For this reason, there seems to be no pertinent infra-red data for comparison with the shorter wave-length portion of the present study.

In connection with Coblentz' curves, it seems desirable to point out that his suggestion that the sucrose curve indicates water of crystallization may be incorrect. The curve shows a small band at 1.5μ, which he takes as indicative of the presence of water. The stronger water band at 2μ is not in evidence, however. It seems more probable that the 1.5μ band is the harmonic of the OH band found at 3μ, since it also appears in the curves for mannite and alcohols. It would seem that the 2μ water band offers a more

---

[1] W. W. Coblentz, "Investigations of Infra-Red Spectra," Pub. No. 65, Carnegie Inst. of Washington, Dec., 1906.

[2] L. H. Rogers and D. Williams, J. Am. Chem. Soc. **60**, 2619 (1938).

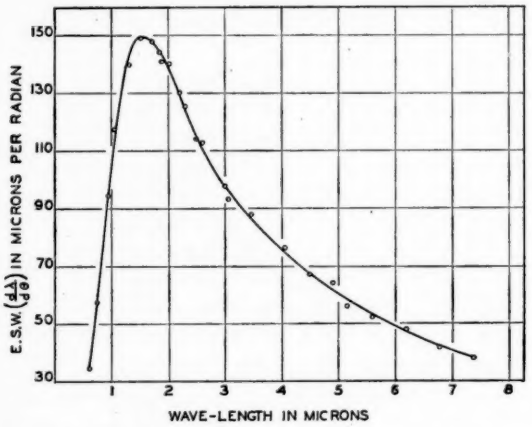

FIG. 1. Effective slit width in microns per radian as a function of wave-length in microns.

satisfactory indication of the presence or absence of water of crystallization.

Raman data on sugars are also incomplete. Polara[3] has made a study of aqueous solutions of sucrose, varying in concentration from 3 to 9 percent, and reported 19 lines, only five of which are above 2100 cm^{-1}. Kutzner[4] studied saturated aqueous solutions of six sugars and found lines at 1180 and 1140 cm^{-1} which he ascribed to the keto and aldehyde forms, respectively. Whiting and Martin[5] found that dextrose gave only a continuous background attributable to decomposition. In general, the agreement between Raman and infra-red data does not seem to be good. This point is not treated here, however, since most of the shifts reported correspond to regions not studied in the present work.

The spectrometer constructed in this laboratory is of conventional design, incorporating a 60° fluorite prism cut from a single crystal of water-white fluorite, and having an aperture of 0.22. The faces of the prism are 45×75 mm. The source of radiation was a Nernst glower, drawing about 0.25 ampere at 110 volts a.c.

The thermocouple, made by Dr. J. D. Hardy, of the Russell Sage Institute of Pathology, New York, was used in an evacuated container. This thermocouple actuated a Leeds & Northrup galvanometer (sensitivity, 0.47 μv/mm; period, 7 sec.), which formed part of a Taylor[6] photoelectric amplifier. The current from the amplifier was measured by use of a second Leeds & Norththrup galvanometer (sensitivity, 0.0004 μa/mm; period, 6.5 sec.). The second galvanometer was about 4 meters from the reading scale.

Because of excess building vibration, both galvanometers were mounted on Julius suspensions (as modified by Brevoort[7]), and all work was done at night.

Prism settings *vs.* wave-lengths tables were calculated from the indices of refraction of fluorite as given by Coblentz.[8] The calibration of the instrument was made by comparison of observed spectra with standard values,[9] after the prism had been set for minimum deviation by use of a jig prism cut for use with sodium light.

For ready determination of the effective slit width, a table of microns-per-radian *vs.* wavelength was computed by use of seven place logarithms from the indices of refraction. From this table the curve shown in Fig. 1 was prepared and is included here for the convenience of other workers using fluorite prisms. The effective slit width for a given exit slit width ds and mirror of focal length r is readily obtained by multiplying the appropriate value given by the curve by ds/r. It is interesting to note that this curve has its maximum near the point of maximum emis-

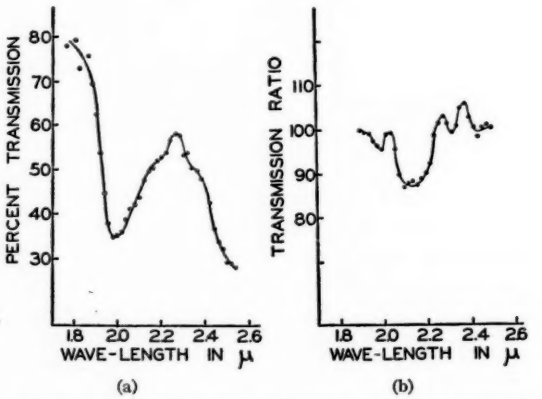

FIG. 2. (a) Transmission of saturated aqueous solution of β-lactose. (b) Transmission of β-lactose solution relative to water.

[3] V. Polara, Accad. Lincei, Atti **14**, 293 (1931).
[4] W. Kutzner, Naturwiss. **20**, 331 (1932).
[5] R. E. Whiting and W. H. Martin, Trans. Roy. Soc. Canada **25**, 87 (1931).
[6] A. H. Taylor, Rev. Sci. Inst. **8**, 124 (1937).
[7] M. J. Brevoort, Rev. Sci. Inst. **2**, 447 (1931).
[8] W. W. Coblentz, J. Opt. Soc. Am. **4**, 432 (1910).
[9] P. E. Shearin and E. K. Plyler, J. Opt. Soc. Am. **28**, 61 (1938).

sion of a Nernst glower under ordinary conditions of use.

The sugars studied were obtained from the Pfanstiehl Chemical Company, and were the purest available from them, being C.P. or better. Those selected were: Monosaccharides—*d*-arabinose, *l*-arabinose, β-glucose, *d*-glucose (dextrose), *d*-mannose, *d*-xylose, *l*-rhamnose, *d*-levulose, and *d*-galactose; Disaccharides—sucrose (cane sugar), maltose, *d*-lactose, and β-lactose. This group thus included both pentoses and hexoses, aldoses and a ketose, the methyl pentose rhamnose, and the β form of two materials.

Preliminary work was done with cells formed from microscope cover glasses (between 1.7 and 2.5μ), varying in thickness from 0.1 to 0.3 mm. Above 2.5μ, fluorite plates held apart by mica washers about 0.03 mm thick were found suitable. The sugars were used in the form of saturated aqueous solutions.

Figure 2(a) shows the transmission for a saturated solution of β-lactose in water. It is seen that, in addition to the strong 2μ water band, additional absorption is present at about 2.2 and 2.35μ. When this curve is compared with a water curve showing approximately the same transmission at 2μ, the curve shown in Fig. 2(b) is obtained. This procedure is equivalent to that used by Rogers and Williams.

Even when there is no interaction with the solvent, accurate results are difficult to obtain, inasmuch as it necessary to use a solvent cell thickness which is in just the same ratio to the solution cell as the volume of the solvent is to the volume of the solution. Obviously there is considerable likelihood that the ratio curve will give a more or less distorted picture of the actual situation, depending upon the degree of incompatibility of the two transmission curves used.

For this reason, the majority of the present transmission curves were obtained by the use of cells prepared in a special manner. It was found that cover glasses smeared with the concentrated solutions could be heated gently over a period of a few hours so as to evaporate almost all of the water, yet without crystallization taking place. As absorption coefficients were not being calculated, the thickness of the film left was of no intrinsic importance. Such cells gave transmission curves showing only a trace of the 2μ water band, and the remaining absorption could be attributed to the solute alone.

It was not possible to treat *d*-arabinose, *d*-lactose, and β-lactose in this manner, as they tended to crystallize, thus producing scattering and resultant low transmission. Accordingly, they were used in the form of saturated solutions, and plotted against water. In these cases, band locations and intensities are less certain.

For samples used above 2.6μ, the evaporated material was pressed out into thin films between two fluorite plates. Thin films were found necessary, due to the intense absorption around 3.3μ. This variation in cell preparation results in a discontinuity at 2.6μ in the transmission curves.

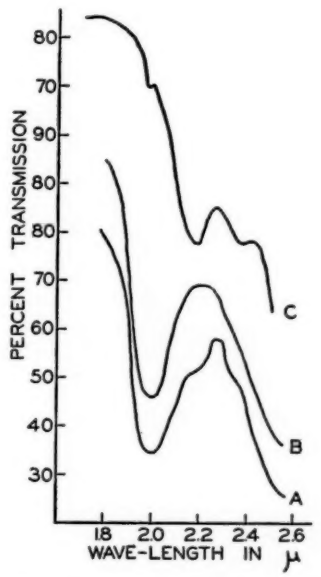

FIG. 3. Comparison of transmissions of (B) water, with that (A) of saturated β-lactose solution, and (C) of evaporated film of levulose.

In the region between 1.7 and 2.7μ, an effective slit width of 0.03μ was used, readings being taken at intervals of 0.02μ. Between 2.5 and 4.6μ, the effective slit width was varied from 0.03 to 0.07μ, with readings taken at intervals from 0.02 to 0.04μ.

Actual points observed have been shown in Fig. 2, so as to give an indication of the precision with which the points fall on a smooth curve. The first few points are somewhat disperse, due to initial instrumental unsteadiness.

In Fig. 3, curve *A*, the transmission of the

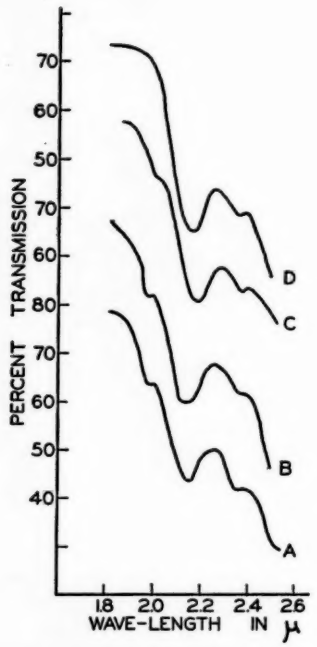

FIG. 4. Transmissions of evaporated films of (A) *l*-rhamnose, (B) β-glucose, (C) *d*-xylose, and (D) *l*-arabinose.

β-lactose solution is shown just below that of water in the same region. It is apparent that the solution absorbs differently from water, but the additional bands are not marked. The advantage gained by evaporation is seen by comparing curve *A* with curve *C*, for an evaporated film of *d*-levulose. In this last sample the almost complete disappearance of the 2μ water band indicates that only a trace is still present. It is now seen that there is a pronounced band at 2.19μ and a somewhat weaker band at about 2.37μ.

In all of the figures containing several curves, the transmission percentage scale is determined by the figures immediately opposite the beginning of the curve.

Figures 4 and 5 give the transmission curves for evaporated samples of eight monosaccharides: *l*-rhamnose, β-glucose, *d*-xylose, *l*-arabinose, *d*-levulose, *d*-mannose, dextrose, and *d*-galactose. It is seen that the spectra are almost identical. In all cases the band at 2.16μ is more intense than the 2.35μ band, although the relative intensities of the two bands vary considerably. For *d*-galactose, the 2.35μ band is very weak, while the two bands are of comparable intensities for *d*-levulose.

As seen from Fig. 6, maltose and sucrose show bands at these same positions. As mentioned above, the other disaccharides had to be studied as solutions. However, their transmissions relative to water indicated bands in the same positions, although no accurate estimate could be made of the relative intensities of the bands. From this, it seems that the observed bands are due to group vibrations unaffected by the combination of the monosaccharide components in the larger molecules, with the accompanying loss of a water molecule.

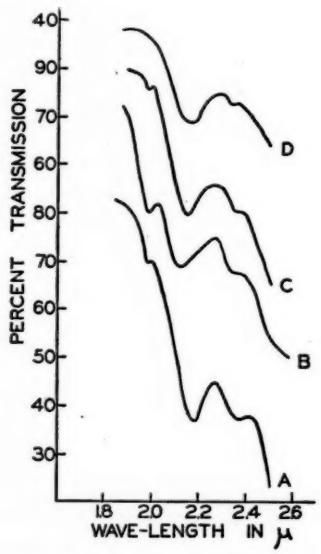

FIG. 5. Transmissions of evaporated films of (A) *d*-levulose, (B) *d*-mannose, (C) *d*-glucose, and (D) *d*-galactose.

Band locations for those materials used in evaporated form are as follows:

l-arabinose	2.16μ	2.36μ
d-galactose	2.17	2.34
d-glucose (dextrose)	2.15	2.35
β-glucose	2.13	2.36
d-levulose	2.19	2.37
maltose (hydrated)	2.14	2.40
d-mannose	2.12	2.35
l-rhamnose (hydrated)	2.15	2.35
sucrose (cane sugar)	2.17	2.38
d-xylose	2.18	2.37

Figures 7 and 8 show the transmissions of a very thin film of water (0.01 mm or less) and eight of the sugars in the region between 2.5 and

4.6μ. It is seen that the region has at least two very strong absorption positions, at about 3μ and 3.45μ, and several weaker bands, the one at about 2.55μ being most distinct. It is probable that the 3μ band is the result of a ν(O−H) vibration, and that the 3.4μ is the ν(C−H) frequency. Due to overlapping, the exact position of these two bands cannot be determined.

The weaker bands between 2 and 3μ seem to be combination bands, involving the δ(C−H) vibration at 6μ and the ν(C−C) vibration at 9.6μ, reported by other workers. The 2.16μ band could arise from the combination of the δ(C−H) and ν(C−H) frequencies, and that at 2.55μ from the ν(C−H) and ν(C−C) frequencies. The band

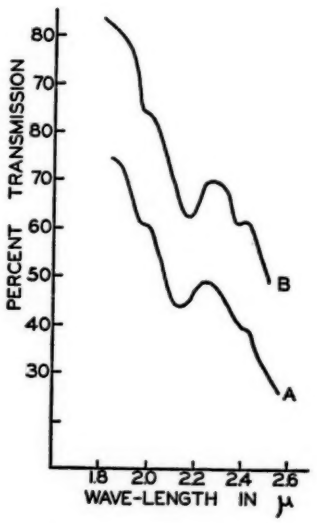

FIG. 6. Transmissions of evaporated films of (A) maltose and (B) sucrose.

at 2.35μ may be the overtone of the band observed at 4.7μ, or the combination of ν(C−C) and ν(O−H) vibrations.

An attempt was made to find spectral differences caused by mutarotation, but in the region investigated no such differences were found. The similarity of the spectra obtained indicates that isomerism plays no part in the determination of band locations found here. It is possible that the relative intensities of the bands in the short

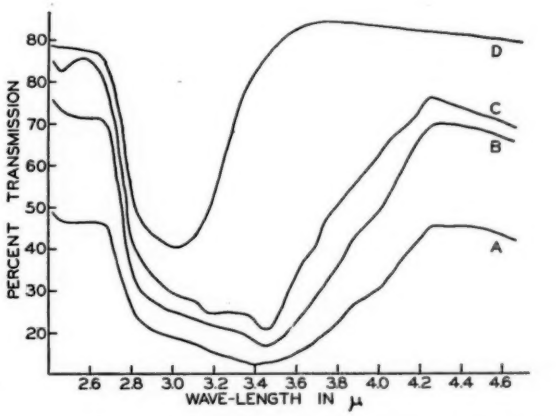

FIG. 7. Transmissions of (D) thin water cell and of evaporated samples of (A) *d*-levulose, (B) β-glucose, and (C) sucrose.

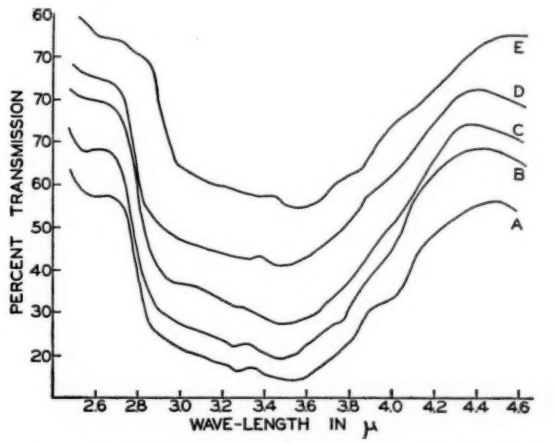

FIG. 8. Transmissions of evaporated samples of (A) *d*-xylose, (B) *l*-galactose, (C) *d*-glucose, (D) *d*-mannose, and (E) *l*-rhamnose.

wave-length region are governed by such structural modifications. This is suggested by a comparison of the curves for *d*-glucose and β-glucose, the 2.16μ band being stronger for β-glucose. A more complete study of relative band intensities, with cell thicknesses accurately controlled should lead to considerable additional information of value. Due to the intense absorption in the 3.4μ region, it is necessary to use film thicknesses too small for good quantitative work. Hence, the weaker bands at shorter wave-lengths seem most suitable for additional work.

Infra-Red and Raman Spectra of Polyatomic Molecules
X. C_2D_2, C_2DH, and C_2H_2

FRED STITT*
Harvard University, Cambridge, Massachusetts
(Received September 9, 1939)

The infra-red spectra of acetylene and its deuterium isotopes have been studied on a prism spectrometer from 450 to 4000 cm^{-1}. All but two of thirty observed bands have been assigned as fundamentals, first and second overtones, and one-one combination or difference bands. Most of the bands of these types which are infra-red active according to the selection rules are either observed or occur in a region where they may be masked by the presence of superimposed bands.

WHEN the deutero-acetylenes became available in the course of the preparation of heavy ethane,[1] it was thought desirable to study their infra-red spectra as these have been only very briefly described.[2]

EXPERIMENTAL

C_2D_2 was prepared by passing (99.5 percent) D_2O vapor over calcium carbide powder which had been dried in vacuum at 500°C. This product is hereafter called *A*.

C_2DH was prepared by passing D_2O vapor over NaC_2H, which in turn was prepared by passing C_2H_2 through a solution of sodium in liquid ammonia.[3] This product will be referred to as *B*.

Prest-o-lite C_2H_2 was used after purification by passage through saturated $NaHSO_3$ solution, 10 percent NaOH solution, $0.2N$ I_2 in KI solution, $\frac{1}{3}N$ $Na_2S_2O_3$ solution, water, calcium chloride, and dehydrite.

I am indebted to Dr. A. O. Nier for determining the composition of the deutero-acetylenes by mass-spectrographic analysis. *A* was found to be 98.5 percent C_2D_2, 1.47 percent C_2DH. *B* was found to be 47.3 percent C_2D_2, 43.0 percent C_2DH, 9.6 percent C_2H_2.

The automatic prism spectrometer described in I[4] of this series was used to study the infra-red absorption spectra from 2 to 22μ. Three different prisms were employed: CaF_2 from 2 to 8.5μ, NaCl from 6 to 13μ, and KBr from 12.5 to 22μ. The spectrometer was calibrated by observing the positions of bands of C_2H_2, C_2H_4, CO_2, C_6H_6, and acetone. The gas was enclosed in either a 20- or a 30-cm long cylindrical cell with windows of either NaCl or KBr. Blanks were recorded over the entire region.

Figure 1 shows the transmission curves obtained. In regions of strong absorption curves at some pressures have been omitted. A comparison of the spectra of the three acetylene samples indicates which bands are due to absorption by each of the three isotopic molecules. The observed positions of the bands are included in Tables IV, V, and VI, as well as an estimated uncertainty arising from the limited dispersion and method of calibration of the spectrometer.

Levin and Meyer[5] studied the infra-red spectrum of C_2H_2 under much higher dispersion than was used in this work. Their positions of the centers of the three strongest C_2H_2 bands in the region studied were among the points used in calibrating the spectrometer. The bands at 1956 and 2213 cm^{-1} have not been reported before.

Randall and Barker made a preliminary report[2] on a study of the absorption spectrum under high dispersion of a sample of deutero-acetylene. They observed[6] $\perp$-type bands at 539.2, 518.9, and 679 cm^{-1} and $\parallel$-type bands at 1043, 1202, and 2585 cm^{-1}. The positions of these bands in the present work agree well with these values except for the band found here at 687 cm^{-1}.

* National Research Fellow in Chemistry, 1937–39. Present address: Chemistry Department, Indiana University.

[1] F. Stitt, J. Chem. Phys. **7**, 297 (1939).

[2] H. M. Randall and E. F. Barker, Phys. Rev. **45**, 124 (1934).

[3] H. Moissan, Comptes rendus **127**, 911 (1898). See also T. H. Vaughan, G. F. Hennon, R. R. Vogt; and J. A. Nieuwland, J. Org. Chem. **2**, 1 (1937).

[4] H. Gershinowitz and E. B. Wilson, Jr., J. Chem. Phys. **6**, 197 (1938).

[5] A. Levin and C. F. Meyer, J. Opt. Soc. Am. **16**, 137 (1928).

[6] See also W. F. Colby, Phys. Rev. **47**, 388 (1935).

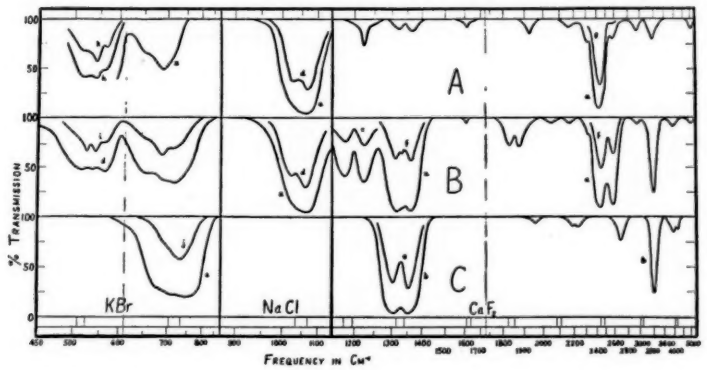

FIG. 1. Infra-red spectra of the acetylenes: *A*. 98.5% C_2D_2, 1.47% C_2DH; *B*. 47.3% C_2D_2, 43.0% C_2DH, 9.6% C_2H_2; *C*. C_2H_2. Effective slit widths are shown at the bottom of the figure. The path length was 30 cm except for *A* and *B* in the CaF_2 region, where it was 20 cm. The gas pressures in mm of Hg: *a*-760; *b*-550; *c*-250; *d*-200; *e*-160; *f*-133; *g*-125; *h*-60; *i*-42; *j*-29; *k*-20.

DISCUSSION

The C_2H_2 and C_2D_2 molecules have point group symmetry $D_{\infty h}$. The normal modes of vibration are of the following types: $2A_{1g}(\nu_1, \nu_2)$, $A_{2u}(\nu_3)$, $E_{1u}(\nu_4)$, $E_{1g}(\nu_5)$. The variation of electric moment is either along the figure axis, giving rise to $\parallel$-type bands (A_{2u}) with a doublet structure and no Q branch, or is normal to the figure axis, giving rise to $\perp$-type bands (E_{1u}) with a Q branch.[7] The transitions allowed by the selection rules to be infra-red active are summarized in Table I, where Δn_i refers to the change of the vibrational quantum number of the ith vibrational mode. For example, if $\Delta n_3=1$, $\Delta n_4=2$, $\Delta n_5=0$ (odd, even, even), the transition is active and gives rise to a $\parallel$-type band.

C_2DH has point group symmetry $C_{\infty v}$ and the normal modes are of only two types: $3A_1(\nu_1, \nu_2, \nu_3)$, $2E_1(\nu_4, \nu_5)$. All vibrational transitions may be infra-red active, giving rise to $\parallel$-bands if of type A_1 and $\perp$-bands if of type E_1.

TABLE I. *Infra-red selection rules for* C_2D_2 *and* C_2H_2. Δn_1, Δn_2 *arbitrary.*

	$\parallel$-bands		$\perp$-bands	
Δn_3	odd	even	even	odd
Δn_4	even	odd	odd	even
Δn_5	even	odd	even	odd

[7] For the contents of this paragraph see D. M. Dennison, Rev. Mod. Phys. **3**, 280 (1931), G. B. B. M. Sutherland, *Infra-Red and Raman Spectra*, or L. Tisza, Zeits. f. Physik 82, 48 (1933). $\parallel$-type bands may have a Q branch if they do not start from the ground state.

Colby[6] calculated the fundamental frequencies of C_2D_2 and of C_2DH on the basis of a simple potential function fitted to the observed values of the C_2H_2 frequencies. He found the calculated values agreed well with the observed ones for the bands measured by Randall and Barker. Subsequent Raman measurements on deuteroacetylenes have furnished more of these fundamental frequencies, and in the present work ν_3 of C_2D_2 has been observed for the first time. Experimental values for the fundamental frequencies of the acetylenes are compared in Table II with those calculated by Colby. The observed values of $\nu_4+\nu_5$ are included because this combination band is very intense in the infra-red spectra of all these acetylenes. The calculated figures are in italics.

The assignments of the observed bands may now be made on the basis of Tables I and II. Except for the infra-red active fundamentals, it is expected that the lowest overtones and the one-one combination bands will appear with the greatest intensity. In order to facilitate the later discussion, there are gathered in Table III values of all $\nu_i+\nu_j$, $2\nu_i$, $3\nu_i$, $\nu_i-\nu_4$, and $\nu_i-\nu_5$ which are allowed by the selection rules to be infra-red active. The difference bands are restricted to those in which the initial state has an appreciable population at room temperature. The assignments of the bands are collected in Tables IV, V, and VI, where the first column lists the frequencies found in this investigation. The frequencies in parentheses are the positions of the centers of $\parallel$-bands calculated from the

TABLE II. *The fundamental frequencies of the acetylenes. (Frequencies calculated by Colby are given in italics.)*

	C_2D_2	C_2DH	C_2H_2
ν_1	1762[a]	1851[a]	1974[c]
	1750	*1840*	*(1974)*
ν_2	2700[a]	3335[a]	3372[c]
	2690	*3335*	*(3372)*
ν_3	2428[f]	2585[b]	3288[d]
	2414	*2560*	*(3288)*
ν_4	539[b]	679[b]	730[d]
	535	*669*	*(730)*
ν_5		519[b]	612[e, e]
	505	*523*	*(605)*
$\nu_4+\nu_5$	1043[b]	1202[b]	1326[d]

[a] G. Glockler and C. E. Morrell, J. Chem. Phys. **4**, 15 (1936).
[b] References 2 and 6.
[c] S. Bhagavantam and A. V. Rao, Proc. Ind. Acad. Sci. **3A**, 135 (1936).
[d] Reference 5.
[e] R. Mecke and R. Ziegler, Zeits. f. Physik **101**, 405 (1936).
[f] This work.

observed frequencies of the P and R branches. Reference to Tables II and III render further discussion of many of these assignments unnecessary, but several require brief comment.

450 to 600 cm^{-1}: In spectrum A the ν_4 band of C_2D_2 is practically free of ν_5 of C_2DH, whereas in B the two are superimposed and the peaks of the Q branches are prominent.

600 to 900 cm^{-1}: In B the superposition of ν_4 of C_2H_2 somewhat changes the appearance of the ν_4-C_2DH band.

900 to 1150 cm^{-1}: $\nu_4+\nu_5$ of C_2D_2 is quite intense in both A and B. It is quite possible that $2\nu_5$ of C_2DH is masked by the high percentage of C_2D_2 in B.

1150 to 1250 cm^{-1}: $\nu_1-\nu_4$ of C_2D_2 is not noticeable in B because of the R branch of $\nu_4+\nu_5$ of C_2DH. Likewise the P branch of the latter probably obscures $\nu_1-\nu_4$ of C_2DH, which is expected at about 1172 cm^{-1}.

1250 to 1500 cm^{-1}: Although $\nu_4+\nu_5$ of C_2H_2 at 1326 cm^{-1} appears with very great intensity, the ||-band in this region of spectrum A is not due to C_2H_2 for two reasons: (1) The percentage of C_2H_2 in A is too low to result in even so weak a band as is observed. (2) The positions of the maxima and the minimum of absorption in A are 1321, 1366, and 1343 cm^{-1}, whereas in C they are 1303, 1352, and 1328. In B the two corresponding absorption peaks are found at 1311 and 1360 cm^{-1} and the intensity seems too great to be due entirely to the 9.6 percent C_2H_2 present. Accordingly it is concluded that the band in A is due to C_2DH, and it is assigned as $2\nu_4$. The small peak in B may be due to the $\perp$-component of $2\nu_4$, but it is more probably $\nu_1-\nu_5$ of C_2DH, a $\perp$-band expected at 1332 cm^{-1}.

It should be mentioned that at $\sim$1245 cm^{-1}, where $\nu_1-\nu_4$ of C_2H_2 is expected to appear, the shape of the $\nu_4+\nu_5$ band envelope of C_2H_2 at 550-mm pressure suggests the presence of a weak band superimposed. This is more noticeable on the large scale plot from which Fig. 1 was made than in the figure itself.

1500 to 2250 cm^{-1}: The weak band at 2045 cm^{-1} in B may be due to either or both of the $\perp$-bands $\nu_3-\nu_5$ and $3\nu_4$, which are expected near 2066 and 2037 cm^{-1}, respectively. The weak band at 1956 cm^{-1} in C is assigned as $\nu_4+2\nu_5$, a $\perp$-band, rather than ν_1 of $C^{12}C^{13}H_2$, the other possible simple assignment, because it is apparently $\perp$-type and is somewhat higher in frequency than is expected for the latter assignment (1939). The assignment of the 2215 cm^{-1} band, which is apparently ||-type, is very uncertain. The only numerically reasonable assignment possible seems to be $3\nu_4$, which however is a $\perp$-type band; also this assignment would mean an anharmonic correction opposite in sign to that expected.

2250 to 2800 cm^{-1}: The band in C at 2690 is

TABLE III. *Calculated positions of some overtones and combination bands of the acetylenes.*

	C_2D_2	C_2DH	C_2H_2
	||-bands		
$\nu_1+\nu_3$	4190	4436	5262
$\nu_2+\nu_3$	5128	5920	6660
$\nu_4+\nu_5$	1044	1198	1342
$\nu_4-\nu_5$	34	160	118
$3\nu_3$	7284	7755	9864
	$\perp$-bands		
$\nu_1+\nu_4$	2301	2530	2704
$\nu_1-\nu_4$	1223	1172	1244
$\nu_2+\nu_4$	3239	4014	4102
$\nu_2-\nu_4$	2161	2656	2642
$\nu_3+\nu_5$	2933	3104	3900
$\nu_3-\nu_5$	1923	2066	2676
$3\nu_4$	1617	2037	2190

Also for C_2DH: $\nu_i\pm\nu_j$: ||-5186; $\perp$-2370, 1332, 3854, 2816, 3264, 1906.
$2\nu_i$: ||-3702, 6670, 5170; $||+\perp(A_1+E_1)$-1358, 1038.
$3\nu_i$: ||-5553, 10005; $\perp$-1557.

TABLE IV. *The infra-red spectrum of* C_2D_2.

Frequency in cm^{-1}	Uncertainty in cm^{-1}	Band type	Assignment	Band type	Calc. or Obs.*
~519 *P br*					
540	±1	⊥	ν_4	⊥	539.2*
560 *R br*					
1026 *P br*					
(1046)	3	∥	$\nu_4+\nu_5$	∥	1043*
1066 *R br*					
1223	1	⊥	$\nu_1-\nu_4$	⊥	1223
1610	3	⊥	$3\nu_4$	⊥	1617
1927	4	⊥	$\nu_3-\nu_5$	⊥	1923
2158	6	⊥?	$\nu_2-\nu_4$	⊥	2161
2312	12		$\nu_1+\nu_4$	⊥	2301
2428	9		ν_3	∥	
2940	18		$\nu_3+\nu_5$	⊥	2933
3280	50		$\nu_2+\nu_4$	⊥	3239
5120	100		$\nu_2+\nu_3$	∥	5128

* References 2 and 6.

TABLE V. *The infra-red spectrum of* C_2DH.

Frequency in cm^{-1}	Uncertainty in cm^{-1}	Band type	Assignment	Band type	Calc. or Obs.
521	±1	⊥	ν_5	⊥	518.9*
687	2	⊥	ν_4	⊥	679*
1179 *P br*					
(1202)	1	∥	$\nu_4+\nu_5$	∥	1202*
1224 *R br*					
1321 *P br*					
(1343)	2	∥	$2\nu_4$	∥+⊥	1358
1366 *R br*					
1330	2	⊥	$\nu_1-\nu_5$	⊥	1332
1829 *P br*					
(1853)	4	∥	ν_1	∥	1851†
1876 *R br*					
2045	5	?	$3\nu_4$, $\nu_3-\nu_5$	⊥, ⊥	2037, 2066
2585	12		ν_3	∥	2585*
3315	30		ν_2	∥	3335†
3950	50		$\nu_2+\nu_5$, $\nu_2+\nu_4$	⊥, ⊥	3854, 4014
5100	100		$2\nu_3$, $\nu_1+\nu_2$	∥, ∥	5170, 5186

* References 2 and 6.
† Reference *a* of Table II.

found under high dispersion to consist of at least four ⊥-bands.[5]

2800 to 5500 cm^{-1}: The two very strong bands in *B* and *C* are at slightly different positions, the former being due to ν_2 of C_2DH and the latter to ν_3 of C_2H_2. Likewise the corresponding band in *A* is of somewhat lower frequency than that in *B*, suggesting that $\nu_2+\nu_4$ of C_2D_2 is responsible for part of the intensity of the former. The positions of the bands above 3600 cm^{-1} are subject to large uncertainties in cm^{-1} units, and the assignments given them in Tables IV, V, and VI are those which are suggested by Table III. The two C_2H_2 bands are resolved into several bands under high dispersion.[5]

TABLE VI. *The infra-red spectrum of* C_2H_2.

Frequency in cm^{-1}	Uncertainty in cm^{-1}	Band type	Assignment	Band type	Calc. or Obs.*
732	±2	⊥	ν_4	⊥	730.3*
1303 *P br*					
(1327)	2	∥	$\nu_4+\nu_5$	∥	1326.3*
1352 *R br*					
1956	4	⊥	$\nu_4+2\nu_5$	⊥	1954
2190 *P br*					
(2215)	6	∥	?		
2240 *R br*					
			$\nu_2-\nu_4$	⊥	2643.2*
2690	15		$\nu_3-\nu_5$	⊥	2669.7*
			$\nu_1+\nu_4$	⊥	2702.2*
3295	30		ν_3	∥	3288*
3935	50		$\nu_3+\nu_5$	⊥	3882.3*
4145	60		$\nu_2+\nu_4$	⊥	4092.0*

* Reference 5.

It has thus been possible to identify all but two of the observed bands as either a fundamental or as one of the simple combination and overtone bands of Table III. Conversely, it is seen that all except $\nu_1+\nu_3$ of the C_2D_2 and C_2H_2 bands of Table III which fall within the region investigated are observed or occur in a region where they may be masked by the presence of other superimposed bands. The same may be said of the analogous bands of C_2DH, and of all but two or three of the other C_2DH bands in the table.

The separations of the *P* and *R* branches expected[7] are 38, 41, and 45 cm^{-1}, respectively, for C_2D_2, C_2DH, and C_2H_2, respectively. The observed separations (see Tables IV, V, and VI) are slightly larger in each case.

I wish to thank Professor E. B. Wilson, Jr. for the use of the automatic recording spectrometer and for his interest in this work.

Infra-Red and Raman Spectra of Polyatomic Molecules

XI. Dimethyl Sulfide $(CH_3)_2S$

R. FONTEYNE*
Mallinckrodt Chemical Laboratory, Harvard University, Cambridge, Massachusetts
(Received October 3, 1939)

The infra-red spectrum of gaseous dimethyl sulfide has been studied from 1.6 to 26μ, as well as the Raman spectrum of the liquid. A tentative vibrational analysis is given.

EXPERIMENTAL

THE material used was obtained from the Eastman Kodak Company. In order to free it from mercaptans and water, the dimethyl sulfide vapor was allowed to bubble through two spiral bubblers containing 30 percent KOH solution, dried over solid KOH and P_2O_5, and fractionated in a one-foot glass spiral packed column. The boiling point of the middle portion was constant: 36.8°C.

INFRA-RED SPECTRUM

The infra-red spectrometer has been previously described;[1] fluorite, rocksalt and KBr prisms were used in the appropriate regions. The spectrometer calibration was checked by observing the position of bands of C_2H_2, C_2H_4 and C_6H_6. The gas was enclosed in a 30 cm long cylindrical vessel with KBr windows at pressures from 10 to 395 mm. Blanks were recorded over the entire region.

The absorption spectrum is shown in Fig. 1; in regions of strong absorption, curves at some pressures have been omitted. The frequencies of the absorption maxima are tabulated in Table I. The extremely weak shoulder at 1390 cm^{-1} is doubtful. No bands appeared in the region between 385 and 690 cm^{-1}. The accuracy of the frequency measurements may be estimated from the slit widths shown near the bottom of Fig. 1.

Several bands are resolved; assuming that the dimethyl sulfide molecule has a C_{2v} symmetry, with the C−S−C angle=105°, C−S distance 1.82A,[2] C−H distance=1.09A and tetrahedral angles in the CH_3 group, a P–R branch separation[3] of 38.5 cm^{-1} was calculated for the parallel type of band, whereas we find spacings of 26, 22, 25 and 24 cm^{-1}. This may indicate that the bands 1024, 1262, 1323 and 1445 cm^{-1} are of the perpendicular type, for which a smaller spacing is expected.

RAMAN EFFECT

The Raman effect of the liquid was also studied, by using a technique previously described.[4] Polarization measurements were made with the Polaroid method.[5] The frequency shifts compared with those of previous investigators[6] are tabulated in Table II. As the dispersion of our apparatus is not very large, some closely spaced lines appear as single broad lines on our records. Though we were not able to find the lines 804 and 2734, listed by Kohlrausch, we did find the 1040 line, listed by Médard, and three broad lines at 480, 920 and 1610 cm^{-1}.

ASSIGNMENTS

Although a quantitative vibrational analysis is not yet possible, certain qualitative conclusions may be pointed out. On the basis of a molecule having a symmetry C_{2v}, the normal coordinate representation, including the two internal rotations, would have the structure: $\Gamma=7A_1+4A_2+4B_1+6B_2$.

The various group frequencies which may be expected are apportioned among the symmetry classes as shown in Table III, where the selection

* C. R. B. Advanced Fellow.
[1] H. Gershinowitz and E. B. Wilson, Jr., J. Chem. Phys. **6**, 197 (1938).
[2] L. Brockway and H. Jenkins, J. Am. Chem. Soc. **58**, 2036 (1936).
[3] S. Gerhard and D. M. Dennison, Phys. Rev. **43**, 197 (1933).
[4] H. Gershinowitz and E. B. Wilson, Jr., J. Chem. Phys. **6**, 27 (1938).
[5] J. T. Edsall and E. B. Wilson, Jr., J. Chem. Phys. **6**, 12 (1938).
[6] C. S. Venkateswaran, Indian J. Phys. **6**, 51 (1931); K. W. Kohlrausch, Monatsh. **68**, 349 (1936); L. Médard and F. Deguillon, Comptes rendus **203**, 1518 (1936).

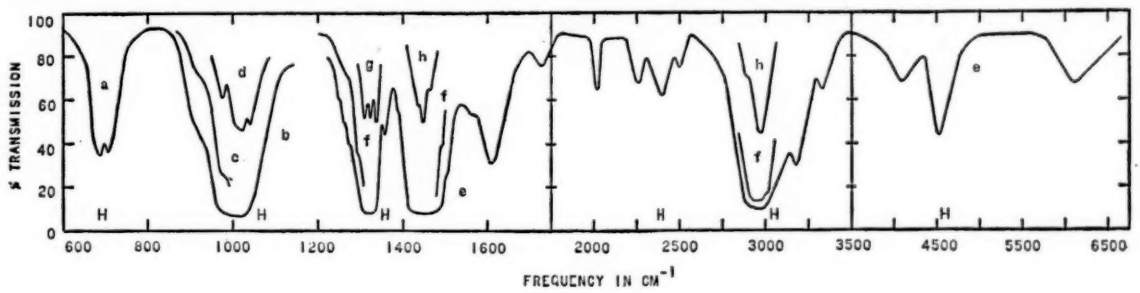

FIG. 1. Infra-red absorption of dimethyl sulfide. Path length, 30 cm. KBr prism: (*a*) 395 mm pressure. Rocksalt prism: (*b*) 395 mm; (*c*) 130 mm; (*d*) 38 mm. Fluorite prism: (*e*) 395 mm; (*f*) 130 mm; (*g*) 38 mm; (*h*) 10 mm. Effective slit-widths are indicated.

TABLE I. *The infra-red spectrum of dimethyl sulfide.*

Observed Frequency and Intensity*	Tentative Assignment and Symmetry	Observed Frequency and Intensity	Tentative Assignment and Symmetry
685 *s*	$\nu_M(\pi)$ A_1	1492 *vw*	
706 *s*	$\nu_M(\sigma)$ B_2	1565 *vw*	285+1265 B_2
905 *w*	220+685 B_1	1605 *s*	285+1323 B_2
975 *m*	285+685 B_2	1724 *vw*	1445+ 285
1024, 1037 *vs*	τ_M B_2	2028 *w*	
1252		2262 *w*	1262+1024
1262, 1274 *w*	τ_M A_1 or B_2	2404 *w*	1024+ 685[2]
1295 *vw*		2500 *vw*	
1310		2900 *vw*	$\nu_H(\pi)$ A_1
1323, 1335 *vs*	$\delta_H\|\|$ B_2 (and A_1?)	2977 *vs*	$\nu_H(\sigma)$ B_1 and B_2
1359 *vw*		3010 *w*	
1390 ?*vw*	685+706 B_2	3174 *vw*	
1435		3322 *w*	
1445, 1459 *vs*	$\delta_H\perp$ A_1 or B_2	4080, 4515, 6130 *w*	various combinations

* *vs* =very strong, *s* =strong, *m* =medium, *w* =weak, *vw* =very weak.

TABLE II. *The Raman spectrum of dimethyl sulfide. Frequencies in* cm^{-1}.*

Venkateswaran	Kohlrausch	Médard	Present Work	Type	Tentative Assignment
284 (1)	283 (6*b*)	278 (*m*)	285 (*s.P*) (*k,i,e*)	δ_M	A_1
			480 (*vw*) (*e*)	2γ	A_1 or A_2 (?)
691 (6)	691 (12)	692 (*s*)	690 (*vs.P*) (*k,i,e*)	$\nu_M(\pi)$	A_1
740 (2)	741 (6)	742 (*m*)	742 (*s.D*) (*k,i,e*)	$\nu_M(\sigma)$	B_2
	804 (0?)				
			919 (*vw.b*) (*e*)		
		1045 (*vw*)	1041 (*vw*) (*k,e*)	τ_M	A_2, B_1 or B_2
	1244 (00)		1224 (*vw*) (*e*)	τ_M	A_1
1335 (0)	1326 (0)	1327 (*w*)	1325 (*w.P*) (*k,e*)	$\delta_H\|\|$	A_1
1424 (6)	1420 (3)	1425 (*m*)	1426 (*m.b.D*) (*k,i,e*)	$\delta_H\perp$	A_2, B_1 or B_2
	1436 (4*b*)	1443 (*m*)		$\delta_H\perp$	A_2, B_1 or B_2
			1609 (*vw*) (*b*) (*e*)		
	2734 (0)			$\nu_H(\sigma)$	A_2 (?)
2844 (6*b*)	2832 (4)	2831 (*w*)	2832 (*w.P*) (*p,k,e*)	$\nu_H(\pi)$	A_1
	2852 (3)	2852 (*w*)			
2914 (8)	2909 (15)	2910 (*vs*)	2911 (*vs.P*) (*p,k,e*)	$\nu_H(\pi)$	A_1
	2952 (5)				
2988 (4*b*)	2979 (8*b*)	2971 (*s.b*)	2980 (*s.b.D*) (*p,k,e*)	$\nu_H(\sigma)$	B_1 and B_2
3010 (2)					

* Intensities are given in parenthesis: *b* =broad; *vs* =very strong; *s* =strong; *m* =medium; *w* =weak; *vw* =very weak; *P* =polarized ($\rho \leqslant 6/7$); *D* =depolarized. ($\rho = 6/7$); *p, k, i, e* =Kohlrausch's notations for exciting lines.

TABLE III. *Types of vibration in dimethyl sulfide.*

DESIGNATION*	SYMMETRY** $A_1(\pi, s)$	$A_2(\sigma, a)$	$B_1(\pi, a)$	$B_2(\sigma, s)$	TOTAL NUMBER	TYPE	APPROXIMATE FREQUENCY TO BE EXPECTED cm^{-1}
γ	0	1	1	0	2	"Internal rotation"	?
ν_H	2	1	1	2	6	C–H stretching	2900
$\delta_H, \perp$	1	1	1	1	4	C–H bending	1450
$\delta_H, \parallel$	1	0	0	1	2	C–H bending	~1400
τ_M	1	1	1	1	4	CH_3 rocking	~900–1200
ν_M	1	0	0	1	2	C–S stretching	~700
δ_M	1	0	0	0	1	C–S–C deformation	~300
Totals	7	4	4	6	21		
Raman-active§	+, *P*	+, *D*	+, *D*	+, *D*			
Infra-red-active§	+, $\perp$	—	+, $\parallel$	+, $\perp$			

* $\parallel$, $\perp$ =parallel and perpendicular, respectively, to the C-S axis of the methyl groups involved.
** π, σ =symmetric and antisymmetric, respectively, to the plane bisecting the C-S-C angle. *s*, *a* =symmetric and antisymmetric, respectively, to plane of the C and S atoms.
§ +, − =active and inactive, *P*, *D* =polarized and depolarized, $\perp$ and $\parallel$ =perpendicular and parallel type of band, respectively.

rules for the fundamentals are also included.

The frequencies to be expected for the several vibrations may be estimated by analogy with other molecules, in particular the methyl halides for the methyl group frequencies and the mercaptans and diethyl sulfide for the C−S frequencies. In agreement with Kohlrausch,[6] we assign the 685 (*P*) and 706 (*D*), gas phase frequencies, to $\nu_M(\pi)$ and $\nu_M(\sigma)$, respectively, and the 285 cm^{-1} (*P*) liquid frequency to δ_M.

The CH_3 rocking frequencies should lie between 900–1200 cm^{-1}. The Raman line 1224 cm^{-1}, being probably polarized, is assigned to the A_1 class. In ethane, the two doubly degenerate assymmetrical rocking frequencies are split apart (827– and 1170 cm^{-1}), by strong interaction between the methyl groups; in dimethyl acetylene, the methyl groups being far apart, those frequencies lie closer together (1050– and 1029 cm^{-1}). In dimethyl sulfide the CH_3 groups being closer than in dimethyl acetylene, we should expect the rocking frequencies to lie further apart. Consequently, the infra-red 1262 cm^{-1} frequency, is believed to be a rocking frequency and may either correspond to the 1244 Raman line and belong to the A_1 class, or it may be distinct and belong to the B_2 class. The 1044 Raman frequency may either be assigned to the A_2 or B_1 class, or correspond to the partially resolved perpendicular band with *Q* branch at 1024 cm^{-1} and belong to the *B* class.

The Raman frequencies 1420 and 1436 cm^{-1} almost certainly are due to $\delta_H\perp$ vibrations, but it is difficult to decide upon their symmetries except to exclude the A_1 class. The corresponding infra-red band may be assigned to either the A_1 or B_2 symmetry classes. It is likely that the four frequencies of this type are close together. The assignment of the $\delta_H\parallel$ frequencies is less ambiguous: the 1325 cm^{-1} Raman line being polarized belongs to the A_1 class, and the infra-red band is to be assigned to the same class unless it is a superposition of the A_1 and B_2 frequencies. The strong polarized Raman line at 2910 cm^{-1} is certainly due to a vibration of the A_1 class, together with one of the 2840 lines. The strong lines at 2929 and 2952 cm^{-1} being infra-red active are supposed to belong to the *B* classes, while the 2734 cm^{-1} vibration (which we do not find) being inactive in the infra-red may be assigned to the A_2 class possibly as a combination.

With regard to the frequency of the torsional vibrations γ, there is the interesting possibility that the Raman line at 480 cm^{-1} is real, and corresponds to $2\gamma(\sigma)$, $2\gamma(\pi)$ or $\gamma(\sigma)+\gamma(\pi)$. Hence the infra-red bands at 905 cm^{-1} and 975 cm^{-1} may be combination tones of the $\gamma(\pi)$ motion (~220 cm^{-1}) with the ν_M vibrations, unless they are related to the rocking frequencies.

Several possible combinations are given in Table I. Reliable information, however, must await the complete vibrational analysis, and accurate thermal data, both of the light and heavy compounds.

In concluding, I wish to express my thanks to Professor E. B. Wilson, Jr., for the use of his laboratory and for many valuable suggestions during this work.

Infra-Red O−H Band and Association

J. Errera, R. Gaspart and H. Sack
University of Brussels, Laboratory of Physical Chemistry, Brussels, Belgium

(Received September 12, 1939)

The vibration of the O−H group in alcohol and HDO has been studied in the 3μ region for solutions and ternary mixtures at different concentrations and temperatures. The experimental results are discussed in terms of association and addition-compound formation.

Introduction

In earlier experiments[1] we studied, by infra-red spectroscopy, especially in the 3μ region, the vibration of the O−H group in different molecules and under different conditions. From this work, as from similar investigations of other workers, it appears that infra-red spectroscopy is able to give important information concerning association phenomena. Finally we pointed out the advantage of working with the fundamental vibrations rather than with harmonics. In this paper we present some new results concerning the O−H bands.

Apparatus and method

In the investigation reported here we used the single-prism quartz-monochromator, described in our last paper.[1g] A very sensitive reception (thermoelement plus galvanometer) and a prism movement of high mechanical precision gives us a relatively high separation power of about $1/1000(\lambda/\Delta\lambda \sim 1000)$. The experimental results are given in the form of curves in which are plotted as ordinates the transmission in percent and as abscissa the wave numbers. The curves are obtained by measuring at different wave numbers the transmission of two measuring cells, one of which is filled with the substance to be studied, the other with the pure solvent, and by dividing the first by the second.

The spectral width of the slit is indicated by "*S*."

All substances were carefully dried and distilled, and special care was taken to prepare the solutions and to fill the cells without introducing the smallest traces of moisture.

Binary Solutions of Alcohols in Inert Solvents

In 1935, we pointed out (for the first time) that the large absorption band at about 3300 cm^{-1} in pure alcohol is not due to the vibration of the O−H group of the isolated molecule (monomolecule) but to the vibration of this group in associated molecules.[1a, 2] In further studies we showed[1d–g] that it is possible to divide the solvents in which the alcohols were dissolved into "inert" solvents (CS_2, CCl_4) and "active" solvents. The molecules of the latter (acetone, dioxan, ether, pyridine) contain an atom of O or N and give rise to addition-compounds with molecules containing an O−H group (alcohols, water) while the inert solvents form no such compounds.[3]

In dilute solutions in inert solvents as well as in the gaseous state at a sufficiently low pressure one observes a narrow band at 3638 cm^{-1} which we have attributed to the O−H group of the isolated molecule. As the concentration of the solution increases the broad O−H band characteristic of associated molecules appears; its intensity increases rapidly and finally masks completely the band of the monomolecules. This result was later confirmed by other workers for the region of the fundamental vibration (3μ) and as well for the region of the harmonics.[4]

[1] (*a*) J. Errera and P. Mollet, Nature **138**, 882 (1936); Comptes rendus **204**, 259 and 1719 (1937); (*b*) G. Bosschieter and J. Errera, J. de phys. et rad. **8**, 229 (1937); Comptes rendus **205**, 560 (1937); (*c*) J. Errera, J. Chim. Phys. **34**, 617 (1937); (*d*) Physica **4**, 1097 (1937); (*e*) Helv. Chim. Acta, **20**, 1373 (1937); (*f*) G. Bosschieter, J. Errera and R. Gaspart, Physica **5**, 115 (1938); (*g*) J. Errera and H. Sack, Trans. Faraday Soc. **34**, 728 (1938).

[2] J. Errera, Trans. Faraday Soc. **33**, 120 (1937).

[3] See also, e.g., (*a*) W. Gordy, J. Am. Chem. Soc. **60**, 605, 1938; (*b*) R. Freymann, J. de phys. et rad. **9**, 517 (1938), **10**, 1 (1939).

[4] (*a*) J. J. Fox and A. E. Martin, Proc. Roy. Soc. **162**, 491 (1937); (*b*) E. L. Kinsey and J. W. Ellis, J. Chem. Phys. **5**, 399 (1937); (*c*) R. M. Badger and S. Bauer, *ibid.* **5**, 938 (1937); (*d*) P. Barchewitz, Comptes rendus **204**, 1184 (1937); R. Freymann, Comptes rendus **204**, 1063 (1937).

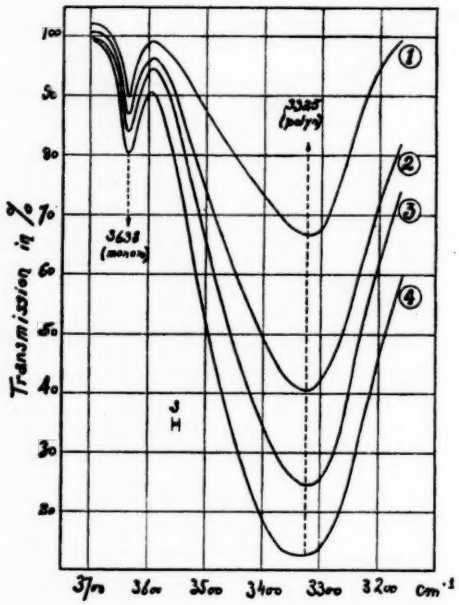

FIG. 1. Ethyl-alcohol in CCl_4; $t = 20°$; layer 0.2 mm; (1) 2%; (2) 4%; (3) 6%; (4) 8%.

The absorption spectra of alcohols are therefore of a special value in the study of the association of these substances.

In the present study we provide some new measurements. Fig. 1 gives the transmission curve of solutions of ethyl alcohol in CCl_4 at 20°C and at volume concentration of 2, 4, 6 and 8 percent. There is evident at 3638 the monomolecular band and at about 3300 a very broad polymolecular band, which increases in intensity very rapidly with the concentration. Fig. 2 shows the same transmission curves at 55°C. As could be foreseen the monomolecular band increases with rising temperature, while the band at 3300 diminishes in intensity because the associated molecules split into monomolecules. But a more detailed study of the curves at 55°C shows that the band at 3300 has not only changed in intensity but also in shape. This appears still more clearly if we divide the transmission curves at 20°C by the corresponding ones at 55° (Fig. 3). A quotient higher than 1, 0 means that the absorption at high temperature is stronger than at low temperature. Thus the increase of the monomolecular band seen in Fig. 1 and 2 finds its equivalent in Fig. 3 in a pronounced maximum at 3638. Besides this first maximum, there is a second maximum at 3523 and a minimum at 3296. This is the consequence of the fact that the absorption band becomes more pronounced at 3500 with increasing temperature and less intense at 3000. This behavior may be interpreted in two different ways: it may be the consequence of a simple shift of the 3300-band towards greater wave numbers but it may also be due to the appearance of a new band at 3523 at the expense of the original polymolecular band. The second interpretation seems the better. One reason for believing this is that when the temperature is raised in steps the maximum and the minimum is always observed at the same wave numbers only their intensities being variable. If it were a question of a simple displacement of the original band it would be difficult to understand why these maximum and minimum should not be gradually shifted. Other arguments in favor of our interpretation will be advanced below.

If our interpretation is correct we must attribute at least three bands to ethyl-alcohol in solution: at 3638, 3523 and about 3300 cm^{-1}. The first one corresponds, as stated above, to the O−H vibration in the monomolecule. We attribute the band at 3520 to the O−H vibration in double molecules. This interpretation is based on experiments in which the alcohol solution in CCl_4 is compared with solutions in active solvents

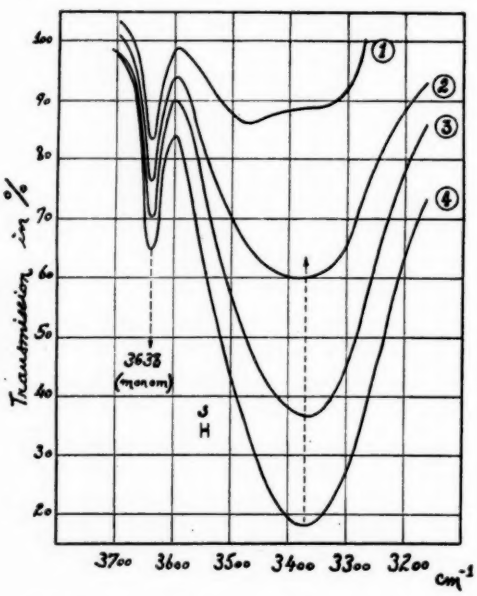

FIG. 2. Ethyl-alcohol in CCl_4; $t = 55°$; layer 0.2 mm; (1) 2%; (2) 4%; (3) 6%; (4) 8%.

containing an atom of O such as acetone (see below). Alcohol in acetone gives a band at about 3500 which is due to an addition-compound of one molecule of alcohol with one molecule of acetone. By analogy it is therefore logical to ascribe the 3520 band in alcohol-CCl_4 solutions also to addition-compounds but now of one alcohol molecule with another alcohol-molecule. The 3300 band must then be due to higher complexes. At ordinary temperature the band of these complexes almost completely masks the band of the double-molecules, but a relatively small increase of temperature (of about 30°) destroys the complexes in favor of the formation of double molecules and monomolecules.

If this interpretation is correct we should find the band of the double molecules even at ordinary temperature if the concentration of the solution is sufficiently diminished. Indeed, the results given in the Fig. 4 confirm this expectation. At the concentration of 1 percent an inflection in the transmission curves appears at 3520, but at 0.125 percent the polymolecular band has disappeared and a feeble but distinct band appears at 3525. The variation with temperature at this small concentration is also in accordance with our interpretation. At relatively great concentrations (Fig. 1 and 2) the 3520 band becomes stronger with increase of temperature because there are more polymolecular complexes decomposed into

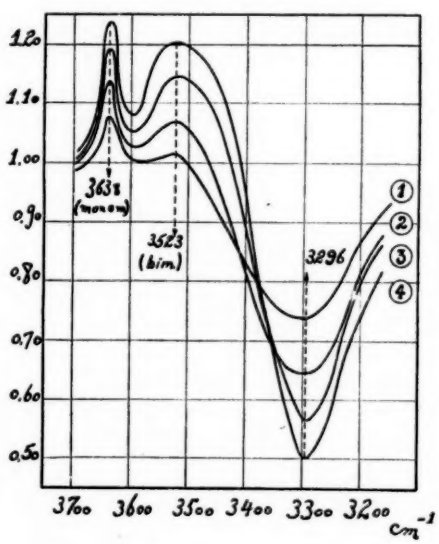

FIG. 3. Ethyl-alcohol in CCl_4; quotient of curves of Fig. 1 by curves of Fig. 2.

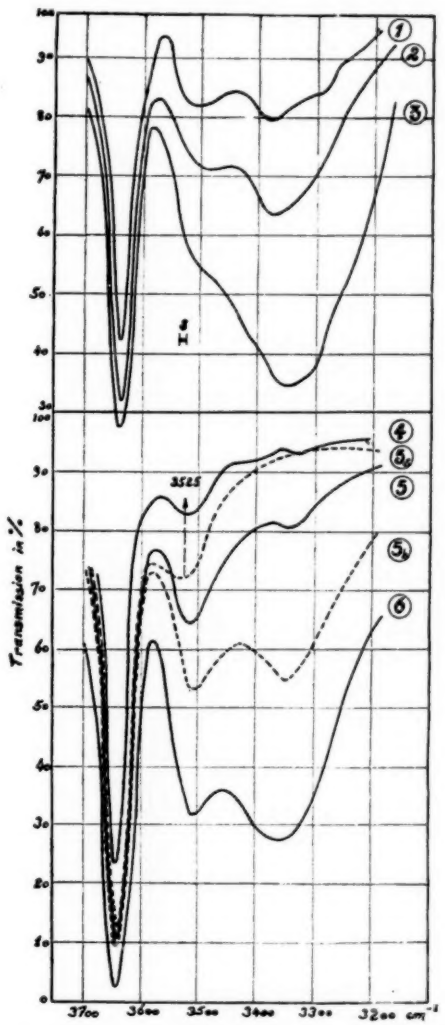

FIG. 4. Ethyl-alcohol in CCl_4; layer 1 mm (1–3) and 5 mm (4–6). (1) 0.5% (20°); (2) 0.75% (20°); (3) 1.0% (20°); (4) 0.125% (20°); (5) 0.25% (20°); (5*a*) 0.25% (55°) (5*b*) 0.25% (5°); (6) 0.5% (20°).

double molecules than double molecules decomposed into monomolecules. At a very low concentration on the contrary, as is to be seen in Fig. 4, the 3520 band decreases with increasing temperature because there are only a very few polymolecules which may be decomposed and the effect of decomposition of double molecules into monomolecules proponderates. On decreasing the temperature below ordinary temperature (5°C) the polymolecular band again appears.*

* In earlier work attention has been drawn on the structure of the association band and the opinion has been advanced that different kinds of complexes exist, e.g. bimolecular and higher complexes (cf. references 1 and 4*a*).

It should be noted that at ordinary temperature it is necessary to go to concentrations smaller than 0.12 percent (=0.02 mole/1) before only monomolecules are found. In the gaseous state at 80°C and at a pressure corresponding also to 0.02 mole/1 distinct bands due to associated molecules[1a] are still observed. Thus we may conclude that the CCl_4 has a higher dissociation power, which is normal and probably due to the higher dielectric constant of CCl_4 compared to that of the gas.

Using CS_2 as solvent we obtained results that are very similar to those obtained with CCl_4. The monomolecular band is somewhat less intense and is located at 3625 instead of 3638. The dissociating power is about the same.

From the quantitative point of view one could try to calculate the concentrations of the different constituents on the bases of the intensities of the different bands. Fox and Martin[4a] have successfully made such a calculation for phenol solutions at ordinary temperature. We repeated this calculation for our data of Fig. 1 and 2. At ordinary temperature our results are very close to those of Fox and Martin. The monomolecular and the polymolecular band (at 20° we neglect the double molecules) obey Beer's law, i.e., log T is proportional to the concentration for all frequencies. Thus we may say that the shape of the curve does not change with concentration. In Table I are given the total concentration, the concentration of the monomolecules, and the concentration of associated molecules (polymolecular band). But these values do not tell us exactly the nature of the reaction that interferes with the association of alcohol. The only thing we may say is that an association of the type

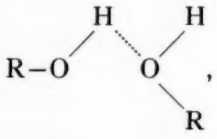

where one O−H group remains "free" is not possible, nor the reaction

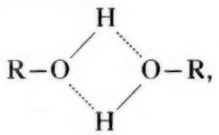

where both O−H groups are involved (these conclusions are reached by calculating from the Table I the constant of the mass action law for the different reactions proposed). This is again in agreement with our interpretation that the broad 3300 band is due to higher molecular complexes.

TABLE I. *Concentrations in volumetric percents.*

C_{total}	0.5	2	4	6	8
C_{monom}	0.4	0.46	0.58	0.73	0.81
C_{assoc}	0.1	1.54	3.42	5.27	7.19

In attempting to apply a similar calculation to the curves obtained at 55°C, one meets the difficulty that the band no longer obeys Beer's law. The shape of the curves changes with concentration, and this is a new argument in favor of our interpretation of Fig. 3. Indeed it is necessary to conclude that at 55° the broad band can no longer be regarded as a single band but rather as a complex band. Unfortunately these curves are so complicated that we have not been able to draw quantitative conclusions concerning the concentration of the different constituents present in the solution.

The phenomena observed in the region of the harmonics are quite similar to those observed in the region of the fundamental, except that the polymolecular band is less pronounced in comparison with the monomolecular band[1g] due to the higher symmetry of the O−H vibration in the associated molecules. Finally it should be noted that our observations are in good agreement with those dealing with other properties of alcohol solutions such as dielectric constant, heat of dissolution, etc. For example, Hoecker[5] observed that for concentrations of the order of 0.00007 to 0.001 molar fraction (=0.0007 to 0.01M/1) the dielectric polarization is independent of the concentration, which means that for these concentrations no association occurred. This is in agreement with our observations at very low concentrations. From an other point of view Wolf and his collaborators[6] were led, in interpreting their experimental results on dielectric constant, heat of dissolution, and other

[5] F. E. Hoecker, J. Chem. Phys. **4**, 431 (1936).

[6] For bibliography, see, e.g., H. Harms, Zeits. f. physik. Chemie **B43**, 257 (1939).

physico-chemical phenomena, to postulate at least two steps of association. At low concentration bimolecular association predominates.

At present there are two different ways by which one attempts to explain the formation of association and addition-compounds in general: the first invokes the hydrogen or hydroxyl bond theory[3, 7] and the second is based on pure electrostatic considerations.[6, 8] Our infra-red measurements do not allow us to decide between these two interpretations.

Ternary Mixtures

It is known that a molecule of alcohol not only forms associated complexes with another molecule of alcohol but also with other molecules containing an atom of O or N (active solvents).[1e, g, 3a] This gives rise in the infra-red to the appearance of new bands which may be called "addition-compound bands," and which are due to the strong interaction between the O−H group of the alcohol and the O or the N of the molecules of the solvent. We have found bands of this type for alcohol in acetone at 3500 and in pyridine at 3350.*

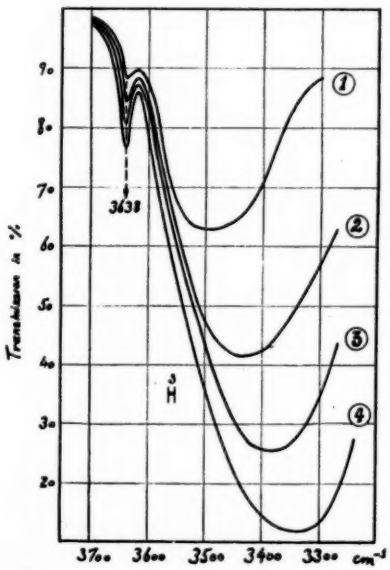

FIG. 5. x% alcohol+(10−x) % acetone+90% CCl_4; $t=20°$; layer 0.2 mm. (1) $x=2$; (2) $x=4$; (3) $x=6$; (4) $x=8$.

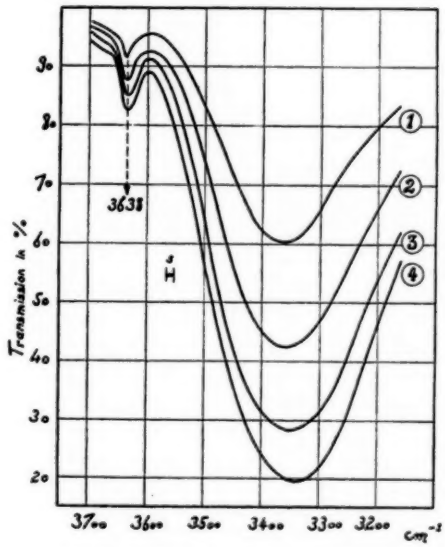

FIG. 6. x% alcohol+(10−x) % pyridine+90% CCl_4; $t=20°$; layer 0.2 mm. (1) $x=2$; (2) $x=3.5$; (3) $x=5$; (4) $x=6.5$.

If well-defined addition-compounds do exist, they must persist to some extent after dissolving the two substances in question (e.g. alcohol and acetone) in an inert solvent such as CCl_4. One would then expect to find side by side the monomolecular, the bimolecular, the polymolecular, and the addition compound O−H bands. Figs. 5 and 6 give two examples of this at ordinary temperature. In these curves the four different bands do not appear clearly because they overlap and mask one another. The facts appear more clearly after dividing the transmission curves of the binary mixtures of the alcohol alone in CCl_4 (Fig. 1) by the transmission curves of the ternary mixtures of the same alcohol concentration. A quotient greater than 1.0 means an increase in the amount of a given complex in the ternary mixtures. Fig. 7 gives an example of such a division for the case of alcohol+acetone+CCl_4. A small minimum appears at about 3640 and another one much more pronounced at about 3300 and a maximum at about 3500, i.e., just at a wave number where the addition-compound band would be expected. We may conclude from these curves that the forma-

[7] J. D. Bernal, Trans. Faraday Soc. **33**, 142, 210 (1937).
[8] M. Magat, Ann. de Physique **6**, 108 (1936); Ed. Bauer and M. Magat, J. de phys. et rad. **9**, 319 (1938).

* For these binary mixtures of alcohol and active solvents there appears only one band, that of the addition-compound, provided the concentrations are not too high. This is understandable since the number of the molecules of the solvent is very great compared to the number of alcohol molecules so that there is almost no possibility for free alcohol molecules to exist.

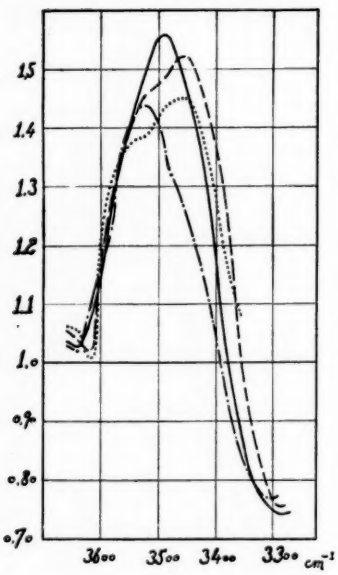

FIG. 7. Quotient of curves of Fig. 1 by curves of Fig. 5.

tion of addition-compounds occurs mainly at the expense of the polymolecules and only very slightly at the expense of monomolecules. The structure shown by the maximum at 3500 is, in our opinion, due to the fact that there must be also a variation, though probably feeble, of the number of double molecules; but since the band of the double molecules almost coincides with the band of the addition compound, the variation of the number of double molecules is revealed by inflections on the pronounced maximum due to the addition compounds.*

At high temperature, 55°C (the curves are not reproduced here), the bands of the spectra of the ternary mixtures are shifted and changed in intensity compared with the curves obtained at 20°C. The division of the curves at 20° by the corresponding ones at 55° discloses further details. As with binary mixtures, the number of polymolecules decreases in favor of monomolecules and of double molecules (and eventually of addition-compounds). The band of the addition compound varies only very little with temperature.

The curves obtained by dividing the transmission curves of the binary mixtures (alcohol+CCl_4) by the corresponding transmission curves of the ternary mixtures obtained at 55°C may be compared with the similar ones obtained at 20°C (Fig. 7). The minimum at 3640 is more pronounced, the one at 3300 is less intense and the maximum is also less intense. This behavior can be explained as follows: the number of polymolecules is very much smaller at 55° than at 20°, and in consequence the addition compounds are formed less at the expense of the polymolecules and more at the expense of the monomolecules and of the double molecules which are now more abundant. It follows, therefore, that the maximum at 3500 is less pronounced because the destruction of double molecules corresponds to a depression of the curve at 3520.

Similar results were found for the ternary mixtures alcohol+pyridine+CCl_4. The only difference is that the addition-compound band is located at another wave number than in the case treated above.

There remains to be discussed the question of the strength of interaction between the molecules forming addition-compounds. The addition-compound band is located at 3500 cm^{-1} for acetone and dioxan and at 3350 cm^{-1} for pyridine. The distance of the addition-compound band from the monomolecular band is therefore much greater for pyridine. From this we may conclude that the interaction between alcohol molecules and pyridine molecules is much stronger than that between alcohol and dioxan (or acetone). The study of a mixture of alcohol+(pyridine+dioxan in equal amounts) e.g., 2 percent alcohol+49

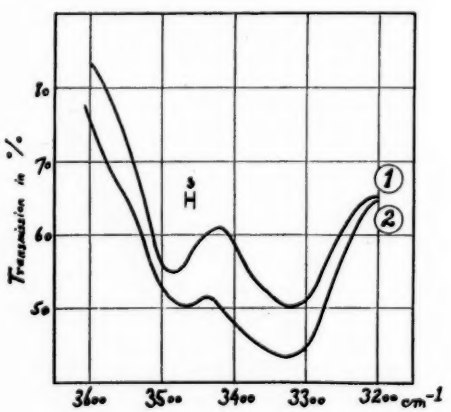

FIG. 8. 2% Ethyl-alcohol+49% dioxan+49% pyridine; $t=20°$; layer 0.2 mm. (1) calculated; (2) observed.

* Acetone solutions of 2 to 8 percent in CCl_4 show a very weak band at 3420 (C=O), which does not influence these results.

percent pyridine+49 percent dioxan, gives further evidence of this fact. Fig. 8 reproduces the transmission curves for this mixture and the band of the two addition-compounds can be seen side by side. It should be possible to calculate the curve of this mixture by adding the experimental curves obtained for the alcohol-dioxan and alcohol-pyridine mixtures separately. Curve 1 gives the result of such a calculation. The agreement is quite good, but in order to obtain it, it was necessary to assume that the probability of the formation of an addition-compound alcohol-dioxan is 2.3 times smaller than the probability of the formation of an addition-compound alcohol-pyridine. Thus the "affinity" of the alcohol for the pyridine is stronger, which is in agreement with the greater displacement of the band.

HDO

The O–H group has also been studied in the HDO molecule. It is rather difficult to study the H_2O absorption in the 3μ region in the liquid state because water absorbs very strongly, which necessitates the use of very thin absorption cells. One finds a very broad band at about 3400 with two feeble inflections at 3500 and 3250.[1e] An attempt has been made to obviate this difficulty and to obtain more precise results by studying a solution of HDO in small concentration in D_2O. As the forces between water molecules and between D_2O molecules are about the same the structure of liquid D_2O will not differ greatly from that of liquid water. From the point of view of infra-red spectroscopy the bands are of course shifted towards smaller wave numbers as a result of the double mass of D as compared to H. If some D atoms are replaced by H atoms one would observe H vibrations in the quasi-crystalline lattice of heavy water. In a first approximation this vibration should be the same as in ordinary water because the structure of the heavy water is so similar to that of ordinary water. But as the number of H atoms is so small the corresponding band will be less intense and therefore more easily observed and eventually a structure should appear.* Fig. 9 shows the

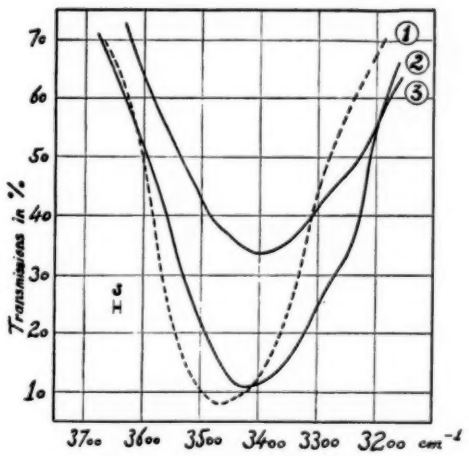

FIG. 9. (1) KI saturated in 99% D_2O+1% H_2O; $t=20°$; layer 0.2 mm (2) 1% H_2O+99% D_2O; $t=20°$; 0.2 mm; (3) H_2O; $t=20°$; layer some μ.

transmission curves of a 2 percent solution of HDO in D_2O.* For purposes of comparison the curve for ordinary water is also reproduced. This curve was obtained[1c] with a measuring cell of a few μ thickness consisting of two cover slides held together by capillary forces. The curves are very similar and we may conclude that there is no fine structure.

The variation of the band with an increase of temperature is also very similar for the HDO solution in D_2O and for ordinary water. Finally the influence of an electrolyte on the absorption curve is also nearly identical for water and HDO solution, as is seen by comparing curves for a saturated solution of KI (Fig. 9) with those for ordinary water published by Ganz.[9] Our investigations thus support the belief that the vibration of the H is very similar in ordinary water and in heavy water where some D is replaced by H.

We also studied the behavior of HDO in the active solvents dioxan, acetone and pyridine. As has been shown earlier[1d, f] ordinary water shows characteristic addition-compound bands similar to those observed in the case of alcohol. In the solvents the molecules of which contain an O, the

* In a calculation of the vibration of liquid water as shown by Magat, reference 8, the mass of the proton does not interfere. The results are thus identical for heavy and ordinary liquid water and for mixtures of these two, provided the distances between the molecules and their special arrangement are not strongly modified.

* Pure D_2O has no band in this spectral region but the smallest traces of moisture (e.g. if the measuring cell is filled without drying the atmosphere) gives rise to a weak HDO band. The D_2O used here had a purity of 99.95 percent (Norsk Hydro-Elektrisk Kvaelstofaktieselskab). The solution of 2 percent HDO was prepared by adding 1 percent ordinary water to the pure D_2O. The exchange reaction is immediate and gives nearly 2 percent HDO.

[9] E. Ganz, Ann. d. Physik. **28**, 445 (1937).

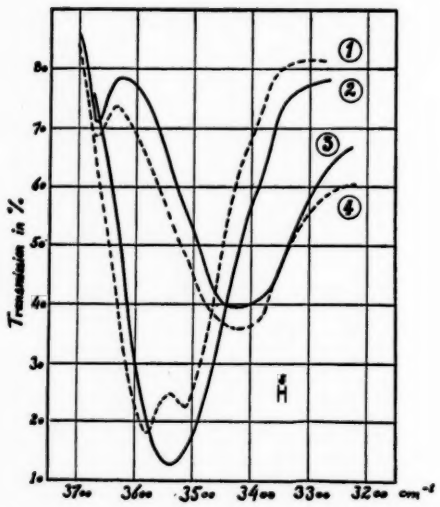

FIG. 10. $t=20°$; layer 0.2 mm (1) 1% H_2O in dioxan; (2) 2% HDO in dioxan; (3) 1% HDO in pyridine; (4) 0.5% H_2O in pyridine.

band is doubled as shown in Fig. 10 for dioxan; in pyridine the band is single but much broader.[10,*] In dissolving HDO in these solvents one finds bands that are very similar to those of H_2O if the solvent is pyridine, but in the case of dioxan and acetone the band is single and not doubled as in the case of water (Fig. 10). Measurements on C_2D_5Br proved that these bands are not due to vibrations of a C−D group which could conceivably be formed by an exchange reaction.†

This behavior of HDO allows us to draw some conclusions concerning the reason for the doubling of the band in the case of H_2O. Let us suppose that H_2O forms with a molecule of the solvent (or with two molecules, but this seems less probable) a rather rigid compound of such kind that the two H are symmetrically bound. The following formula could, for example represent such a compound

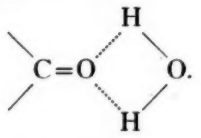

Then there would be a resonance between the vibrations of the two H and as a result of the coupling between the two atoms, there would be a doubling of the vibration band.[11,*] If the symmetry is destroyed by substituting a D for an H, the resonance disappears and with it disappears the doubling of the band; two distinct bands OH and OD would appear.

Anyhow our measurements seem to exclude the formation of compounds in which the two H's of the H_2O molecule would be influenced by the molecule of the solvent in a different way, e.g., as would happen in an arrangement:

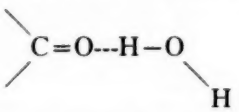

where the second H would be free or bound in a different way with a third molecule. In such a case the doubling must be explained by different forces acting on the two H atoms. But then the doubling should not disappear after substituting an H by a D since it would be at one time the first H and another time the other H that would be substituted so that the two bands corresponding to the two different H atoms would be present, which is not the case.

When pyridine is the solvent the addition-compound band water-pyridine is much broader and not doubled. This must be explained, in our opinion, by the fact that the mutual arrangement of the water and pyridine molecule is not so well defined as in the case of acetone or dioxan, and that therefore the resonance between the two H is not sufficiently pronounced to give a doubling of the band.

CONCLUSIONS

Absorption spectra in the 3μ region, at different concentrations and temperatures, have been

[10] R. Gaspart and L. Gillo, Bull. Soc. Chim. Belg. **47**, 933 (1938); R. Gaspart and G. Serrure, Bull. Soc. Chim. Belg. (in press).

* The relatively great intensity of these addition-compound bands permit their use in a quantitative determination of traces of moisture. A detailed study of this possibility has been undertaken in our laboratory and it has been shown that the limit, of sensitivity is as low as 10^{-6} for water in acetone and $3\cdot10^{-6}$ for water in ether. The precision of this method is thus better than that of the ordinary physico-chemical methods (e.g. ebullioscopic measurements, etc.). Our spectrographic method has been applied in a concrete case where one had to determine the quantity of water produced during the preparation of a solution of colloidal gold in ether.

† We are very much indebted to Professor M. de Hemptinne (University of Louvain) for the sample of this substance prepared by him.

[11] R. Mecke, Zeits. f. Physik **99**, 217 (1936); Also Buswell, Dietz and Rodebush, J. Chem. Phys. **5**, 84, 501 (1937); Bolst, Buswell, and Rodebush, J. Chem. Phys. **6**, 61 (1938).

* Mecke explained in the same manner the appearance of several C−H bands in aliphatic compounds.

studied for alcohol in CCl_4 and CS_2; for ternary mixtures alcohol+pyridine+CCl_4 and alcohol +acetone+CCl_4; and for HDO in D_2O, dioxan and pyridine.

From these measurements it is concluded:

(a) Alcohol (in CCl_4 and CS_2) is only completely dissociated at concentrations smaller than 0.1 percent in volume.

(b) In the mechanism of the association of alcohol at least two steps may be distinguished: formation of double molecules and of polymolecular complexes. The latter are very sensitive to an increase of temperature of the order of 30° to 40°.

(c) Alcohol forms addition-compounds with molecules containing an O or an N and these addition-compounds still exist after diluting them in an inert solvent.

(d) The O−H vibration gives rise to the same band in pure water and in a solution of HDO in D_2O.

(e) For HDO dissolved in a solvent of which the molecule contains an O, the doubling of the band of the addition compound H_2O+solvent disappears.

The authors wish to thank Dr. T. C. Ruch (C.B.R. Fellow) for assisting with the translation and Mr. J. Lazarichvily for his help in the experimental part of the present work. They are also very much indebted to the "Fonds National de la Recherche Scientifique de Belgique" for the fellowship accorded to one of them (R.G.) and for the apparatus put at their disposition.

JANUARY, 1940 JOURNAL OF CHEMICAL PHYSICS VOLUME 8

Coriolis Perturbations in the Spectra of Silane and Germane

GEORGE M. MURPHY
Sterling Chemistry Laboratory, Yale University, New Haven, Connecticut

(Received September 16, 1939)

A Coriolis perturbation on the rotational structure of the fundamental frequency, ν_4 has been computed for silane and germane. Matrix elements of the Coriolis operator, A for the lines $P(9)$, $P(10)$ and $Q(10)$ have also been obtained. The envelope of the resulting absorption curve has been compared with the experimental curve and good agreement found. The most striking difference in the two spectra is that in the case of silane, the Q branch degrades toward lower frequencies and in germane, towards higher frequencies. This is shown to be due to the relative position of the infra-red inactive frequency, ν_2 to which the perturbation is due.

A TETRAHEDRALLY symmetrical molecule like CH_4, SiH_4 or GeH_4 belongs to the symmetry group, $\mathbf{T}_d$ and two triply-degenerate fundamental vibrational frequencies should occur in the infra-red, the symmetry of both corresponding to the irreducible representation of the group, F_2. Since the molecules are spherical tops, the rotational structure of either band should consist of simple P, Q and R branches, resembling the perpendicular bands of a linear molecule. The centers of these two regions of absorption[1] in methane occur at approximately 3014 and 1306 cm^{-1}, respectively, and while the former band is essentially of the theoretical appearance, the latter is considerably more complex than was expected.

The anomalous spacing between rotational lines in bands of this sort is now well understood and is due to a Coriolis interaction between vibration and rotation, the explanation having been given by Teller[2] and further elaborated by Johnston and Dennison.[3] A perturbation of this kind, however, cannot account for the complex structure of the low frequency fundamental, ν_4. A different sort of Coriolis interaction has been

[1] Nielsen and Nielsen, Phys. Rev. **48**, 864 (1935).

[2] Teller, *Hand- und Jahrbuch d. chem. Physik* (1934), Vol. 9, p. 125.

[3] Johnston and Dennison, Phys. Rev. **48**, 868 (1935).

discussed by Wilson[4] which results from the presence of a nearby vibrational state and which causes both a shift and a splitting of the energy levels. Recently the complete theory of this effect has been given and applied to the ν_4 band of methane by Childs and Jahn.[5] The perturbation in this case arises from the infra-red inactive frequency, ν_2 which appears in the Raman effect and which belongs to the doubly degenerate representation, E of $\mathbf{T}_d$. The theory has also been applied to the spectrum of deutero-formaldehyde by Nielsen.[6]

It is the purpose of this paper to make similar calculations for silane and germane and it will be seen that in spite of the approximate character of some of the data, the theoretical spectrum is in good agreement with that observed. The method of calculation is explained in considerable detail by Jahn[7] and by Childs and Jahn.[5] The theory has also been discussed independently by Shaffer, Nielsen and Thomas,[8] who obtain results in agreement with those of Jahn. The procedure of Jahn is as follows. The correct vibrational-rotational wave functions for ν_4 and ν_2 are first found and from these are calculated the matrix elements of the Coriolis operator and the perturbed energy levels. The theoretical intensities of each of the fine structure lines are then calculated and the spectrum plotted. Since the experimental resolving power is insufficient to detect the complicated spectrum which results, an envelope of the structure is drawn which is then compared with the observed data. The calculations on CH_4 have been made to include the lines[9] lying between $R(0)$, $Q(1)$, $P(1)$ and $R(9)$, $Q(9)$ and $P(8)$, presumably because this was the limit of the observed spectrum. The absorption of both silane[10] and germane,[11] however, extends over a somewhat larger region than that of methane and it seemed worth while to extend the calculations to higher values of the rotational quantum number for these cases. The wave functions given by Jahn[7] made it possible to obtain the matrix elements and resulting levels to include $Q(10)$, $P(9)$ and $P(10)$ which gave 25 more lines than those obtained by Childs and Jahn.[5] Extension of the wave functions to still higher quantum numbers would involve a considerable amount of labor and since the observed and calculated spectra are in good agreement, no further wave functions were obtained. A preliminary graph, however, showed that the additional 25 lines changed the appearance of the Q and P branches of silane considerably and as will be shown later, still higher energy levels would be useful in these two cases.

Simple considerations show that the spectrum of both SiH_4 and GeH_4 will be expected to extend over a wider range than that of CH_4 before the intensity reaches a similar value. In CH_4, for example, the weakest lines in the $P(8)$ levels have an intensity of 5, while in SiH_4 the corresponding value is 9 and in $P(10)$ there are lines as strong as 18. In GeH_4, the corresponding figures are 6 and 12. The theoretical intensities depend upon four factors: (1) the transition amplitude; (2) the statistical weight or degeneracy of the rotational level; (3) the nuclear spin degeneracy; (4) the Boltzmann factor. Since the first three of these quantities are the same for CH_4, SiH_4 and GeH_4, any difference in intensity in the three spectra is due to the Boltzmann factor. The latter is $\exp(-Ehc/kT)$ where $E=BJ(J+1)$, approximately and the corresponding values of B are 5.25, 3.10 and 3.95 cm^{-1}, respectively. These differences change the Boltzmann factor correspondingly and hence the total intensity of the rotational line is greater for SiH_4 and GeH_4 than for CH_4. Examination of Table VI in the paper of Childs and Jahn[5] or Table III below shows that the strongest rotational lines are those of symmetry A_1 or A_2. From Table IV, page 490 of reference 7, it is seen, unfortunately that it is just these levels and matrix elements which are most difficult to evaluate. We will therefore only use the information available in the papers of Jahn rather than calculate higher levels.

Matrix Elements of the Coriolis Operator, A

The method of obtaining the matrix elements of the Coriolis operator is given in detail in Jahn's paper and need not be repeated here.

[4] Wilson, J. Chem. Phys. **4**, 313 (1936).
[5] Childs and Jahn, Proc. Roy. Soc. **A169**, 451 (1939).
[6] Nielsen, Phys. Rev. **55**, 289 (1939).
[7] Jahn, Proc. Roy. Soc. **A168**, 469–95; 495–518 (1938)
[8] Shaffer, Nielsen and Thomas, Phys. Rev. **55**, 878; **56**, 895, 1051 (1939).
[9] Following the established nomenclature in the spectra of diatomic molecules, we always write $J=J''$, the rotational quantum number of the lowest level.
[10] Steward and Nielsen, Phys. Rev. **47**, 828 (1935).
[11] Steward and Nielsen, Phys. Rev. **48**, 861 (1935).

TABLE I. *Matrix elements of the Coriolis operator, A.*

$P(9) = A_1 + A_2 + E + 2F_1 + 3F_2$*

A_1: $a_1 = -24\left(\frac{55}{17\cdot 31}\right)^{\frac{1}{2}}$ $\quad E$: $a_1 = -2\left(\frac{130}{17}\right)^{\frac{1}{2}}$

$a_2 = 14\left(\frac{13\cdot 21}{17\cdot 31}\right)^{\frac{1}{2}}$ $\quad a_2 = -4\left(\frac{39\cdot 55}{17\cdot 31}\right)^{\frac{1}{2}}$

A_2: $a_2 = 2(31)^{\frac{1}{2}}$ $\quad a_3 = -2\left(\frac{7}{17\cdot 31}\right)^{\frac{1}{2}}$

$P(10) = A_1 + A_2 + 2E + 2F_1 + 3F_2$

A_1: $a = 36\left(\frac{11}{5\cdot 19}\right)^{\frac{1}{2}}$ $\quad 2F_1$: $a_{14} = -12\left(\frac{42}{5\cdot 19}\right)^{\frac{1}{2}}$

A_2: $a = 12\left(\frac{1}{5}\right)^{\frac{1}{2}}$ $\quad a_{22} = 18\left(\frac{17}{5\cdot 19}\right)^{\frac{1}{2}}$

$2E$: $a_{11} = 36\left(\frac{6}{19\cdot 29}\right)^{\frac{1}{2}}$ $\quad a_{25} = -72\left(\frac{2}{5\cdot 19}\right)^{\frac{1}{2}}$

$a_{13} = 36\left(\frac{13}{19\cdot 29}\right)^{\frac{1}{2}}$ $\quad 3F_2$: $a_{11} = -24\left(\frac{3}{5\cdot 19}\right)^{\frac{1}{2}}$

$a_{21} = -18\left(\frac{3\cdot 13\cdot 17}{5\cdot 19\cdot 29}\right)^{\frac{1}{2}}$ $\quad a_{13} = 9\left(\frac{22}{19}\right)^{\frac{1}{2}}$

$a_{22} = -6\left(\frac{7\cdot 29}{5\cdot 19}\right)^{\frac{1}{2}}$ $\quad a_{14} = -3\left(\frac{13\cdot 14}{5\cdot 19}\right)^{\frac{1}{2}}$

$a_{23} = -6\left(\frac{170}{19\cdot 29}\right)^{\frac{1}{2}}$ $\quad a_{22} = -72\left(\frac{2}{5\cdot 19}\right)^{\frac{1}{2}}$

$2F_1$: $a_{11} = 21\left(\frac{13}{5\cdot 19}\right)^{\frac{1}{2}}$ $\quad a_{24} = 6\left(\frac{5\cdot 7}{19}\right)^{\frac{1}{2}}$

$a_{12} = -3\left(\frac{15}{19}\right)^{\frac{1}{2}}$ $\quad a_{25} = -3\left(\frac{17}{5\cdot 19}\right)^{\frac{1}{2}}$

$a_{35} = 3(3)^{\frac{1}{2}}$

$Q(10) = A_1 + A_2 + 2E + 3F_1 + 2F_2$

A_1: $a_1 = 18\left(\frac{13\cdot 19}{11\cdot 29}\right)^{\frac{1}{2}}$ $\quad 2E$: $a_{21} = 18\left(\frac{17}{5\cdot 29}\right)^{\frac{1}{2}}$

$a_2 = 28\left(\frac{17\cdot 19}{10\cdot 11\cdot 29}\right)^{\frac{1}{2}}$ $\quad a_{22} = 14\left(\frac{17\cdot 19}{29\cdot 55}\right)^{\frac{1}{2}}$

A_2: $a_1 = -10\left(\frac{13}{29}\right)^{\frac{1}{2}}$ $\quad a_{23} = \frac{18}{29}\left(\frac{17\cdot 26}{11}\right)^{\frac{1}{2}}$

$a_2 = 306\left(\frac{2}{5\cdot 17\cdot 29}\right)^{\frac{1}{2}}$ $\quad a_{24} = \frac{14}{29}\left(\frac{5}{11}\right)^{\frac{1}{2}}$

$2E$: $a_{11} = -5\left(\frac{26}{29}\right)^{\frac{1}{2}}$ $\quad 3F_1$: $a_{11} = -7\left(\frac{3\cdot 26}{55}\right)^{\frac{1}{2}}$

$a_{12} = 9\left(\frac{19\cdot 26}{11\cdot 29}\right)^{\frac{1}{2}}$ $\quad a_{13} = 49\left(\frac{2}{55}\right)^{\frac{1}{2}}$

$a_{13} = \frac{4\cdot 127}{29}\left(\frac{5}{11}\right)^{\frac{1}{2}}$ $\quad a_{21} = -6\left(\frac{15}{11}\right)^{\frac{1}{2}}$

$a_{14} = \frac{18}{29}\left(\frac{13\cdot 14}{11}\right)^{\frac{1}{2}}$ $\quad a_{22} = -9\left(\frac{17}{55}\right)^{\frac{1}{2}}$

The results for the Q branch, $J=10$ and the P branch, $J=9$ and 10 are given in Table I, extending Table IV, page 510 of reference 7.

THE PERTURBED ENERGY LEVELS

The wave numbers of the unperturbed lines, but taking into account the Coriolis interaction of Teller, ζ are given by:

$$\begin{aligned} R(J) &= \nu_4 + 2B^*(J+1) \\ Q(J) &= \nu_4 \\ P(J) &= \nu_4 - 2B^*J, \end{aligned} \tag{1}$$

where $B^* = B(1-\zeta)$; $\zeta\hbar$ is the internal angular momentum and ν_4 includes the vibrational frequency as well as an additional term in ζ which is independent of J. The exact form of the latter is given by Johnston and Dennison.[3] We also take $B' = B'' = B$, that is, we neglect any change of the moment of inertia of the molecule as well as any centrifugal distortion, since these terms are probably small. The interaction of ν_4 with ν_2 causes each of the lines of Eq. (1) to split, the perturbation being obtained from the coefficients of the Coriolis operator, A. These perturbations must be further corrected for the R and the P branch as described by Jahn, since the energy difference between the levels of ν_2 and ν_4 varies with J, on account of Teller's coupling term.

The uncorrected perturbations are determined in the following way. Form the Hermitean square, AA' of the matrix of the coupling coefficients, where A' is the transposed of A and the elements of the latter are the a_{ij} of Jahn,

TABLE I.—*Continued.*

$Q(10) = A_1 + A_2 + 2E + 3F_1 + 2F_2$

$a_{24} = \left(\frac{2}{55}\right)^{\frac{1}{2}}$ $\quad 2F_2$: $a_{14} = -6\left(\frac{15}{11}\right)^{\frac{1}{2}}$

$3F_1$: $a_{32} = -3\left(\frac{57}{11}\right)^{\frac{1}{2}}$ $\quad a_{22} = -41\left(\frac{2}{55}\right)^{\frac{1}{2}}$

$a_{35} = -19\left(\frac{10}{11}\right)^{\frac{1}{2}}$ $\quad a_{24} = -9\left(\frac{17}{55}\right)^{\frac{1}{2}}$

$2F_2$: $a_{11} = 31\left(\frac{2}{55}\right)^{\frac{1}{2}}$ $\quad a_{25} = -\left(\frac{57}{11}\right)^{\frac{1}{2}}$

$a_{13} = -7\left(\frac{3\cdot 26}{55}\right)^{\frac{1}{2}}$

* The matrix elements for $2F_1$ and $3F_2$ are given by Jahn (reference 7, Table IV, p. 512).

TABLE II. *Eigenvalues of the Hermitean square matrix of the coupling coefficients.**

P Branch			
$J=9$		$J=10$	
A_1	161.65	A_1	150.06
A_2	124.00	A_2	28.80
E	95.76	E'	25.71
F_1'	30.44	E''	184.98
F_1''	149.33	F_1'	121.99
F_2'	22.18	F_1''	176.24
F_2''	101.36	F_2'	26.69
F_2'''	145.64	F_2''	111.83
		F_2'''	194.77

Q Branch	
$J=10$	
A_1	330.25
A_2	120.80
E'	60.48
E''	335.59
F_1'	41.12
F_1''	185.76
F_1'''	378.85
F_2'	75.58
F_2''	169.30

* Jahn (reference 7, page 516, Table V) designates the levels with the symbols $J'J''$ while we use the notation commonly used in the spectra of diatomic molecules, $J=J''$.

Table IV, page 510 or Table I, above. The matrix AA' has m rows and n columns and any element not given explicitly in the tables is zero. The latent roots or eigenvalues of AA', ϵ_i^2 are simply related to the uncorrected perturbations as shown below and although the results are approximate, they are sufficiently precise for our purpose. They could be improved by direct diagonalization of the original energy matrix. The eigenvalues may be found by applying an iterative method directly to the matrix[12] but we have found it more convenient to expand the secular determinant in powers of λ. The two roots of the quadratic equations were determined in the usual manner and the cubic equations were solved by Graeffe's root-squaring method.[13] Higher equations do not appear until $J=13$, where a biquadratic occurs.

The uncorrected perturbations for the rotational sublevels are then given by $(B^2\zeta_{24}^2\epsilon_i^2)/\Delta$ where $\Delta=\nu_2-\nu_4$; $\zeta_{24}^2=M/(2m_0+M)$; m_0 is the mass of the central atom; m, the mass of the hydrogen atom and $M=m_0+4m$, the total mass of the molecule. In the case of methane, the numerical factor $f=B^2\zeta_{24}^2/\Delta$ is approximately 0.05 cm^{-1} and although Jahn[7] does not give the eigenvalues directly, they may be easily obtained from his uncorrected perturbations (reference 7, Table V, page 516) by multiplying each value by 20. It should be noted that the eigenvalues themselves may be used for any tetrahedrally symmetrical molecule, the uncorrected perturbation for a particular case then being obtained merely by the use of the appropriate numerical factor, f. For this reason, we give in Table II the eigenvalues themselves for the levels $P(9)$, $P(10)$ and $Q(10)$.

[12] Frazer, Duncan and Collar, *Elementary Matrices* (Cambridge Press, 1938).
[13] Scarborough, *Numerical Mathematical Analysis* (The Johns Hopkins Press, 1930).

THE SPECTRUM OF SILANE

The absorption of silane in the 10.5μ region, corresponding to the frequency, ν_4 is shown in

TABLE III. *Rotational sublevels of silane and germane.*

		Silane		Germane	
Level		Intensity	ν, cm^{-1}	Intensity	ν, cm^{-1}
			R Branch		
$J=0$,	A_1	15	913.4	15	938.1
1	F_2	15	916.6	14	942.4
2	E	13	919.8	12	946.8
	F_2	19	919.7	19	946.9
3	F_2	23	922.9	22	951.3
	F_1	23	922.8	22	951.5
	A_1	38	922.5	36	951.8
4	A_1	41	926.2	38	955.7
	F_1	24	926.0	22	956.0
	E	16	925.8	15	956.1
	F_2	24	925.4	22	956.7
5	F_2'	25	929.1	22	960.4
	F_1	25	928.8	22	960.8
	E	17	928.2	15	961.8
	F_2''	25	928.1	22	962.0
6	E	16	932.2	14	965.2
	F_2'	24	932.1	20	965.3
	A_2	40	931.9	34	965.7
	F_2''	24	931.0	20	967.2
	F_1	24	930.7	20	967.5
	A_1	40	930.5	34	967.9
7	F_2'	22	935.3	18	970.0
	F_1'	22	935.1	18	970.2
	A_1	37	934.1	29	972.2
	F_1''	22	933.7	18	972.8
	E	15	933.5	12	973.2
	F_2''	22	933.1	18	973.8
8	A_1	32	938.4	24	974.8
	F_1'	19	938.3	14	975.0
	E'	13	938.3	10	975.1
	F_2'	19	936.8	14	978.0
	F_1''	19	936.2	14	979.0
	E''	13	935.7	10	980.0
	F_2''	19	935.6	14	980.3
9	F_2'	16	941.5	11	979.9
	F_1'	16	941.5	11	980.0
	E	11	939.6	8	983.9
	F_2''	16	939.5	11	984.2
	A_2	27	938.8	19	985.4
	F_2'''	16	938.2	11	986.7
	F_1''	16	938.0	11	987.1
	A_1	27	937.8	19	987.5

TABLE III.—*Continued.*

Level	Silane		Germane		Level	Silane		Germane	
	Intensity	ν, cm^{-1}	Intensity	ν, cm^{-1}		Intensity	ν, cm^{-1}	Intensity	ν, cm^{-1}
		P Branch					*Q* Branch		
$J=1$, F_2	3	906.6	3	929.9	$J=1$, F_1	9	909.9	9	934.1
2 E	5	903.2	5	925.8	2 F_1	14	909.7	13	934.3
F_2	8	902.9	8	926.1	E	9	909.4	9	934.6
3 F_2	12	899.7	12	921.8	3 A_2	29	910.0	28	934.0
F_1	12	899.1	12	922.2	F_2	18	909.2	17	934.8
A_1	21	898.4	20	922.8	F_1	18	908.6	17	935.4
4 A_1	26	896.4	24	917.6	4 F_1	20	909.6	18	934.4
F_1	16	895.8	14	918.0	E	13	908.2	12	935.7
E	10	895.4	10	918.3	F_2	20	907.8	18	936.2
F_2	16	894.2	14	919.1	A_2	33	907.1	31	936.8
5 F_2'	17	892.6	15	913.8	5 F_1'	21	909.3	19	934.7
F_1	17	891.8	15	914.2	E	14	908.9	12	935.1
E	12	890.0	10	915.4	F_2	21	906.7	19	937.2
F_2''	17	889.7	15	915.7	F_1''	21	905.9	19	938.0
6 E	12	888.9	10	909.9	6 A_2	35	909.4	29	934.6
F_2'	18	888.7	15	910.0	F_2	21	908.7	18	935.2
A_2	29	888.0	25	910.4	F_1'	21	908.0	18	936.0
F_2''	18	885.6	15	911.9	A_1	35	905.1	29	938.7
F_1	18	885.0	15	912.2	F_1''	21	904.3	18	939.5
A_1	29	884.5	25	912.6	E	14	904.1	12	939.7
7 F_2'	17	885.2	13	905.9	7 F_1'	19	908.8	16	935.1
F_1'	17	884.8	13	906.1	E	13	907.8	10	936.2
A_1	28	881.8	22	907.8	F_2'	19	907.1	16	936.8
F_1''	17	880.7	13	908.4	A_2	32	905.8	26	938.1
E	11	880.1	9	908.8	F_2''	19	902.3	16	941.5
F_2''	17	879.2	13	909.3	F_1''	19	901.9	16	941.9
8 A_1	26	881.6	19	901.9	8 F_1'	17	908.4	13	935.5
F_1'	15	881.3	11	902.0	E'	12	908.0	9	936.0
E'	10	881.2	8	902.1	F_2'	17	906.3	13	937.6
F_2'	15	876.7	11	904.4	F_1''	17	904.5	13	939.3
F_1''	15	875.1	11	905.2	E''	12	899.6	9	944.1
E''	10	873.6	8	905.9	F_2''	17	899.4	13	944.3
F_2''	15	873.2	11	906.2	A_2	29	899.1	22	944.6
9 F_2'	13	877.7	9	898.0	9 A_2	25	908.4	17	935.6
F_1'	13	877.0	9	898.3	F_2'	15	907.8	10	936.2
E	9	871.6	6	900.8	F_1'	15	907.0	10	936.9
F_2''	13	871.2	9	901.0	A_1	25	905.1	17	938.8
A_2	22	869.3	15	901.9	F_1''	15	903.1	10	940.7
F_2'''	13	867.5	9	902.7	E	10	902.6	7	941.2
F_1''	13	867.2	9	902.8	F_2''	15	896.4	10	947.2
A_1	22	866.2	15	903.3	F_1'''	15	896.2	10	947.4
10 E'	7	873.8	5	894.0	10 F_1'	12	907.9	8	936.1
F_2'	11	873.8	7	894.0	E'	8	906.9	5	937.0
A_2	18	873.6	12	894.1	F_2'	12	906.1	8	937.8
F_2''	11	866.2	7	897.2	A_2	20	903.8	13	940.0
F_1'	11	865.3	7	897.6	F_2''	12	901.3	8	942.5
A_1	18	862.9	12	898.6	F_1''	12	900.4	8	943.3
F_1''	11	860.6	7	899.6	A_1	20	893.0	13	950.5
E''	7	859.8	5	899.9	E''	8	892.7	5	950.8
F_2'''	11	858.9	7	900.3	F_1'''	12	890.4	8	952.9

Fig. 4 of reference 10 and the Raman frequency, ν_2 has been observed in gaseous silane by Stitt and Yost.[14] The numerical values are $\nu_4=910$ cm^{-1}; $\nu_2=978$ cm^{-1}. From Steward and Nielsen,[10] we also take $I_0=8.9\times10^{-40}$ g cm^2 and $B=3.105$ cm^{-1}. Since valency and deformation modes of vibration are good approximations in the case of CH_4, according to Rosenthal,[15] it seems permissible to make the same assumption here, giving $\zeta_4=0.454$ and $\zeta_{24}^2=0.364$. The value of $\Delta=+68.0$ cm^{-1} and the numerical factor $f=0.0516$ cm^{-1}. If Jahn's uncorrected perturbations for CH_4 are applied directly to SiH_4 the error will amount to about 1 cm^{-1} for the largest perturbation. The exact values are obtained by multiplying his values by 1.032 and the numbers in Table II by 0.0516. Approximate values of the position of the *P*, *Q* and *R* branch lines were

[14] Stitt and Yost, J. Chem. Phys. **4**, 82 (1936).
[15] Rosenthal, Phys. Rev. **45**, 538 (1934); cf. also references 7 and 3.

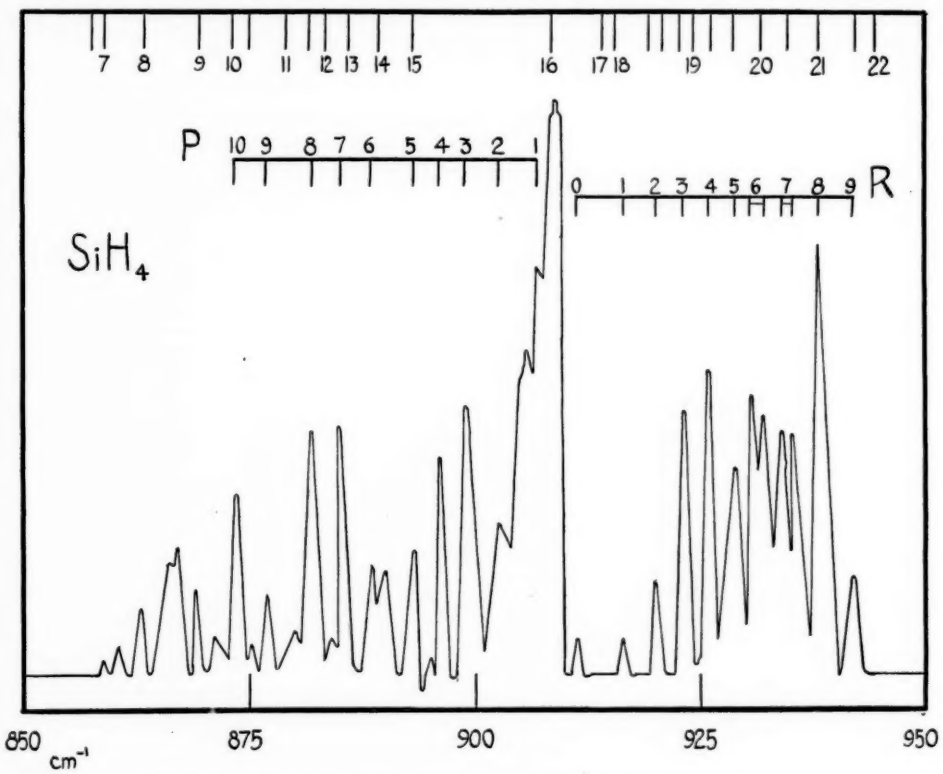

FIG. 1. Theoretical envelope of the 910 cm^{-1} fundamental vibrational band of silane showing fine structure caused by the Coriolis perturbations. The experimentally observed lines of Steward and Nielsen are shown above.

calculated from Eq. (1) and to each was added the appropriate perturbation. The uncorrected values were adjusted as explained above and final correction made to the P and R branches to account for the energy difference between initial and final levels. The resulting calculated values of the wave numbers are given in Table III, where we depart from the nomenclature of Childs and Jahn in designating the doubly and triply degenerate rotational sublevels with one or more primes, instead of using exponents in parentheses. The intensity of each line is obtained as described by Childs and Jahn.[5] We have, however, taken $T=298°K$, giving $hc/kT=4.8188\times10^{-3}$. The resulting intensities are also found in Table III. Each of these lines has then been plotted on a large scale (1 mm = 0.1 cm^{-1}) with an arbitrary scale for intensity (10 mm = intensity 5). According to Steward and Nielsen,[10] the spectrometer slits were 0.7 cm^{-1} and 1.0 cm^{-1} for the high frequency and low frequency sides of the band, respectively, readings being taken along the band at intervals of 0.7 cm^{-1}. We have therefore replaced each line by a triangle with base of 2 cm^{-1} and drawn an envelope of the spectrum, areas of overlapping triangles being added together. In order to make comparison with the observed results, the envelope was then redrawn on a smaller scale in the following way. From the reproduction of Fig. 4 of Steward and Nielsen,[10] we have arbitrarily chosen a base line, corresponding to a galvanometer deflection of about 18 cm. The ratio of the height of the strongest line (No. 16) to the scale of wave numbers was then estimated. Our Fig. 1 was then drawn with the same ratio of ordinate to abscissa. For convenience in comparison, the measured lines of Steward and Nielsen are given on the same figure. Comparison should be made, however, with the published curve of the latter where the numbering of the lines corresponds with that of Fig. 1. It should be noted, however, in the experimental curve that some fairly prominent points, especially on the low fre-

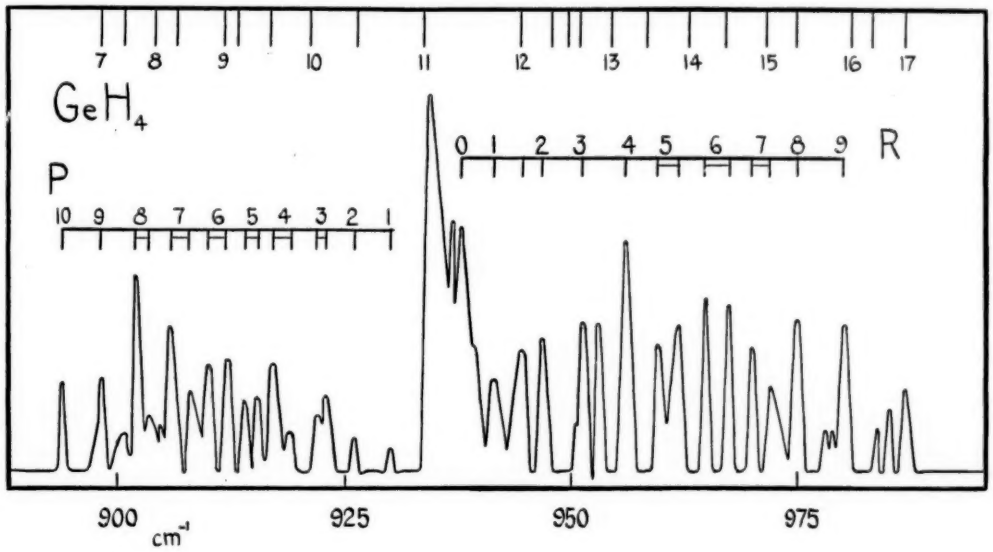

FIG. 2. Theoretical envelope of the 934 cm^{-1} fundamental vibrational band of germane showing fine structure caused by the Coriolis perturbations. The experimentally observed lines of Steward and Nielsen are shown above.

quency side of the Q branch, have not been measured. The theoretical curve indicates that some of them at least are probably significant.

We have also indicated on Fig. 1, as far as possible, the line or group of unresolved lines belonging to the members of the P and R branches. Reference to Table III, shows that this is only an approximation, since there is considerable overlapping of lines with different J values, especially as J becomes larger.

Several interesting agreements between the theoretical and the observed spectra may be noted. The structure of the maximum of the Q branch is very nearly the same in both cases. Weak lines, corresponding with 17 and 18 are seen to be the first two members of the R branch, the intensity building up strongly to a maximum at about line 21. The theoretical curve also predicts a maximum in the R branch at that point, the height being nearly equal to that of line 16 in the Q branch. Somewhat more of the observed band might be calculated if the wave functions and matrix elements were available but we have no explanation to offer for the strong absorption at line 28 although Jahn and Childs[16] suggest that it might be due to activity imparted to the Raman frequency by the perturbation. One further point is of considerable interest. Stitt and Yost[13] propose an alternative assignment of frequencies with $\nu_4=978$ cm^{-1} and ν_2 not yet observed. They believe this to be unlikely and the good agreement of our calculated envelope with the observed spectrum offers further indication that their assignment is correct. It is also interesting to note that if the unobserved Raman frequency were lower than ν_4, the Q branch would overlap the R branch instead of the P branch. It is just such a situation which arises in GeH_4 as previously pointed out by Jahn and Childs[16] and as may be confirmed by examination of Fig. 2 and the discussion below.

[16] Jahn and Childs, Nature **141**, 916 (1938).

THE SPECTRUM OF GERMANE

The 10.7μ band of germane[11] is of the same complexity as that of methane and silane but the resolution is apparently better than in the case of silane. The center of absorption, $\nu_4=934$ cm^{-1} and although the Raman spectrum has not been observed, ν_2 has been estimated as 820 cm^{-1} by Steward and Nielsen.[11] They also get $I_0=7.0\times10^{-40}$ g cm^2, giving $B=3.95$ cm^{-1}. Using valency and deformation modes of vibration, $\zeta_4=0.482$ and $\zeta_{24}^2=0.345$. The value of $\Delta=-114$ cm^{-1} and the numerical factor $f=-0.0472$ cm^{-1}.

As before, the uncorrected perturbations for methane may be used by multiplying them by 0.944. But because of the uncertainty in the value of ν_2, we have taken the uncorrected methane perturbations and used them directly, except for a change in sign. The resulting error is about 1 cm^{-1} in the largest perturbation provided the value of ν_2 is correct. The uncertainty in the latter quantity makes this case less exact than that of methane and silane but the resulting energy levels are probably exact enough, considering the other approximations made in the calculations. The calculations are identical with those in the case of silane, the wave numbers and intensities of the rotational lines being given in Table III. The experimental slit width for germane was 0.6 cm^{-1} and the calculated lines have been plotted as triangles of base corresponding to twice this amount. The resulting envelope is shown in Fig. 2, where as before the resulting large scale plot was redrawn so that the ratio of ordinate to abscissa is proportional to that of Steward and Nielsen's published figure (reference 11, Fig. 3). Comparison with this figure shows gratifying similarity between calculated and observed spectra although the agreement is here perhaps not as good as in the case of methane and germane. The Q branch for example is not as sharply defined on the low frequency side as the theory predicts and the presence of the very strong line 10 is not expected. This and the broad structure of the Q branch on the low frequency side indicate that some lines other than those belonging to the fundamental may be superimposed at this point. Something of this sort has been suspected as due to transitions from higher vibrational levels by both Steward and Nielsen[11] and by Sutherland.[17] An interesting feature is that the Q branch overlaps the R branch, the effect being similar to the degradation of a band from the head which is observed in diatomic molecules. The fact that the Q branch degrades to high frequency here and to low frequency in the case of silane, is due to the fact that in this case, the inactive frequency is lower than ν_4 and vice versa in the case of silane. This changes the sign of the perturbation, since the latter depends on the sign of Δ. The effect was previously predicted by Jahn and Childs.[16] It should prove useful in confirming the assignment of vibrational frequencies in the case of other tetrahedrally symmetrical molecules, since even if the rotational structure is not completely resolved, the unsymmetrical shape of the Q branch might enable a prediction to be made as to whether the Raman frequency is higher or lower than the infra-red frequency.

[17] Sutherland, Proc. Camb. Phil. Soc. **35**, 341 (1939).

Spectroscopic Measurements of Gaseous CN

I. Dissociation in the Electric Discharge

JOHN U. WHITE*
University of California, Berkeley, California
(Received September 18, 1939)

Free CN radicals in the gaseous state are formed in the electric discharge through cyanogen. By the use of a very intense low pressure spark as a background the 0,0 and 1,1 bands of the $^2\Sigma \rightarrow {}^2\Sigma$ transition of CN have been observed in absorption at short intervals of time after the end of this discharge. The intensities of the lines of the bands were measured by means of microphotometer traces of the spectra and of the characteristic curve of the photographic plate. They were corrected for the incomplete resolution of the spectrograph. Relative concentrations of CN were calculated from the sums of the intensities of the lines. The rate of disappearance of CN after the end of the discharge was studied and found to be the same over a large range of pressure and dilution with argon. A mechanism is proposed to account for this. In all cases the disappearance was exponential with a mean half-life of 11 milliseconds. The half-life of the first excited vibration state was 3 milliseconds, during which time about 10,000 collisions occurred. By dilution of the cyanogen in the discharge tube with argon until the CN bands were no longer visible the partial pressure of CN could be calculated on the assumption that near this point all the cyanogen present was observed in the form of CN. The minimum detectable pressure of CN was of the order of 2×10^{-6} mm. The absolute f value of the $^2\Sigma \rightarrow {}^2\Sigma$ transition is 0.026 ($\pm$0.006). By using the corresponding absolute absorption coefficient and the observed temperature distribution in a carbon arc the partial pressure of CN present in an arc is calculated to be of the order of 10 mm.

INTRODUCTION

FROM the known emission spectra of diatomic molecules their energy levels, electron configurations, and relative transition probabilities have been derived. Very little information about their lifetime, properties, or absolute concentrations and absolute transition probabilities has been found. While the properties of the stable molecules are well known, those of most free radicals like CN and NH are not. As shown by Oldenberg,[1] a study of the absorption spectra of the latter constitutes a valuable method for investigating them. The presence in the sun of OH, NH, CN, and CH is indicated by their absorption spectra,[2] but of these only OH has previously been studied carefully in the laboratory at room temperatures.[1] SH has been observed by Lewis and the author,[3] and some of the aluminum halides have been found in absorption by Miescher[4] at slightly higher temperatures. While the strongest absorption of most stable molecules lies in the far ultraviolet, that of most common free radicals occurs in the visible or near ultraviolet. Thus spectroscopic investigation can be used to supplement chemical methods where the latter are weakest.

The violet $^2\Sigma \rightarrow {}^2\Sigma$ system of CN, the 0,0 band of which lies at λ3883, is the resonance system of this molecule, and its absorption should constitute a sensitive test for the presence of free CN. Heretofore this band has been observed in absorption only as a result of thermal dissociation in the sun and stars[2] and in the laboratory.[5] In the present work its lifetime, absorption coefficient, and other properties are studied at room temperature by means of its absorption spectrum. The method of observation is based on that used by Oldenberg in studying the lifetime of OH. The fundamental steps are:

(1) Formation of the radicals by an electric discharge;
(2) Passage of a brief flash of white light through the absorption tube immediately after the discharge;
(3) Dispersion of the white light in a spectrograph of high resolving power;
(4) Measurement of the amount of light absorbed by the lines of the CN band spectrum.

As no source has been found bright enough to allow this measurement to be made with a

* Now with Standard Oil Development Company, Eilzabeth, New Jersey.
[1] O. Oldenberg, J. Chem. Phys. **3**, 266 (1935).
[2] H. N. Russell, Astrophys. J. **79**, 317 (1934).
[3] M. Lewis and J. U. White, Phys. Rev. **55**, 894 (1939).
[4] E. Miescher, Helv. Phys. Acta **9**, 693 (1936).
[5] G. B. Kistiakowsky and H. Gershinowitz, J. Chem. Phys. **1**, 432 (1933).

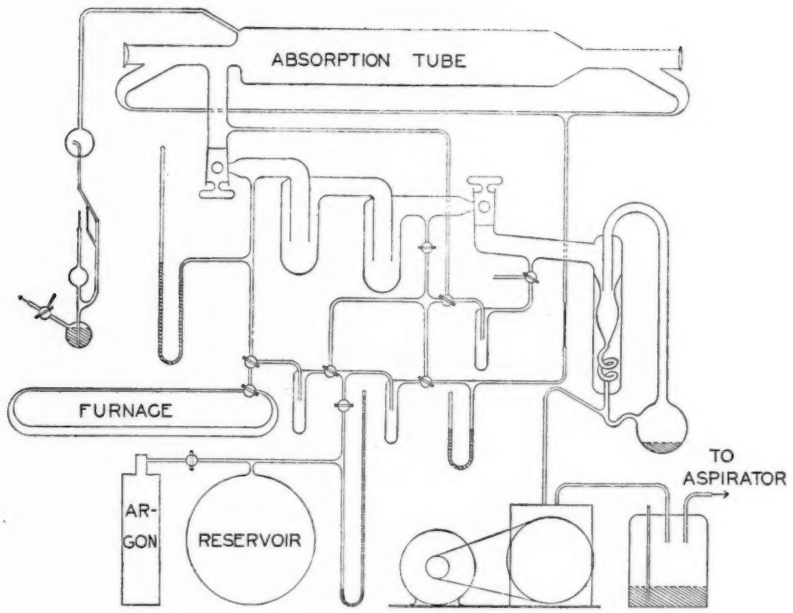

FIG. 1. The vacuum system.

single flash of light, it is necessary to repeat the cycle many times and integrate the spectrum on a photographic plate.

APPARATUS

The apparatus consisted of an absorption tube and vacuum system for flowing C_2N_2 through it continuously, a radiofrequency oscillator fitted with electrodes to pass a discharge through the absorption tube, a source of continuous radiation, a 21-foot concave grating spectrograph, and a synchronous motor driving the switches and an optical shutter.

The cyanogen was prepared in an all-glass system by heating Merck's C.P. grade $Hg(CN)_2$ in an electric furnace to 400°C, after a preliminary baking in vacuum at a lower temperature to drive off water vapor and adsorbed air. The cyanogen generator was specially designed with a movable heating coil and outlets at each end to reduce the losses from the sublimation of the $Hg(CN)_2$. The cyanogen thus made had a vapor pressure of 9.5 mm over dry ice which is so close to the 9.6 mm observed by Perry and Bardwell[6] at this temperature that the gas was used without further purification. The main part of the discharge tube was 70 cm long and 15 cm in diameter. Since cyanogen polymerizes in an electric discharge to dark brown, solid paracyanogen, special precautions had to be taken to keep the windows free of it. They were mounted on smaller tubes sealed on each end of the large one and further protected by a continuous flow of cyanogen from them toward the middle of the tube. The cyanogen was kept in a reservoir of large glass bulbs, from which its flow was regulated by a stopcock, and finally reclaimed over liquid air. As it was desired to flush out the discharge tube completely and remove all products of the preceding discharge between each cycle, a very rapid pumping system was required. A large mercury pump, backed by a Megavac pump, was able to flush out the discharge tube three times between each cycle at the lowest pressures used and 1.2 times at the highest. Pressures were read on a McLeod gauge and rates of flow on a previously calibrated pressure difference gauge across a constriction. By putting a dry-ice bath on a coil of glass tubing the mercury vapor was at first removed from the incoming gas. As it was latter found to have no effect, the coil was removed. After every 1000 cycles the paracyanogen was burned

[6] J. H. Perry and D. C. Bardwell, J. Am. Chem. Soc. **47**, 2629 (1925).

out of the discharge tube by a discharge through oxygen at low pressure. The exhaust from the pumping system was led at a pressure slightly below atmospheric to an aspirator where any cyanogen was washed down the drain with a large amount of water. Fig. 1 shows a diagram of the vacuum system.

The source of the background radiation was the Lyman continuum of a low pressure spark, which gave exposures about three hundred times as fast as the next best alternative, a tungsten strip filament bulb. Its characteristics, amply described in the literature,[7] are ideal for taking a series of rapid snapshots. A 1-μf condenser was charged to 15,000 volts by a Thordarson transformer with a completely insulated secondary and kenotron rectifier tube and discharged through a 2-mm quartz capillary about 3 cm long. Breakdown was regulated by a tickler electrode in an auxiliary spark gap in series with the discharge tube. To make this reproducible the two sides of the auxiliary gap had to be held at equal and opposite potentials relative to the grounded tickler in the center. A high resistance with a grounded center across the condenser accomplished this and, with a milliammeter in series, served as a voltmeter.

The discharge that formed the CN radicals in the absorption tube was made with a radio-frequency oscillator[8] connected by a resonant transmission line to two large iron electrodes on each side of the absorption tube. These were bent around until the discharge appeared uniform throughout the tube. The oscillator was run with 60-cycle a.c. on the plate, and keyed by cutting off the filament power supply during the dead half-cycle. The water cooling leads were arranged so that when the main power supply was cut off the filament became much more positive than the grid. A milliameter in the d.c. power supply gave a ballistic reading of the intensity of each flash of the discharge. While it would not give quantitative relations without further calibration, it would give qualitative indications and show when discharges were of equal intensity.

The oscillator and spark discharge were coordinated accurately to a thousandth of a second by a switching system driven by a synchronous motor. In each circuit there were two switches in series, one on a fast and one on a slow shaft. The oscillator switches were arranged to pass one half-wave of 60-cycle a.c. every twenty seconds. The switches in the other circuit acted through a Ford ignition coil to break down the spark gap a short time later. The time interval between them was varied by adjusting the angle between the switches in the two circuits. An

[7] J. A. Anderson, Astrophys. J. **75**, 394–406 (1932).

[8] D. H. Sloan, R. L. Thornton, and F. A. Jenkins, Rev. Sci. Inst. **6**, 75 (1935).

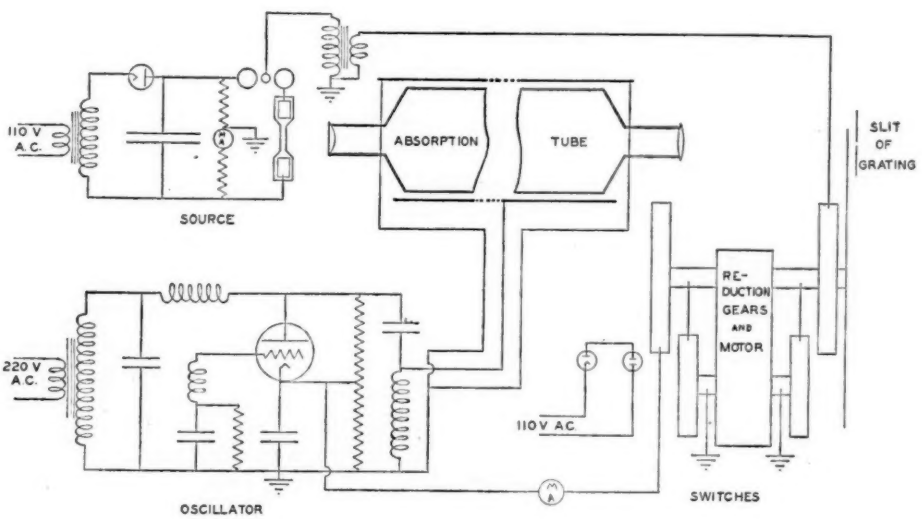

FIG. 2. Wiring diagram.

optical shutter protected the plate from emission during the discharge. As a synchronous motor will run equally well on either sense of the current, a neon bulb was operated on half-wave rectified a.c. near a white mark on the switch to show by the stroboscopic effect in which position the motor was running (see Fig. 2).

As Oldenberg has pointed out,[1] very high resolving power is needed to observe faint, narrow absorption lines like the individual ones in a band. The spectrograph was a 21-foot aluminum concave grating ruled 30,000 lines to the inch and giving a dispersion of 4.4 cm^{-1} per millimeter at λ3883 in the second order. Its theoretical resolving power of 330,000 is about equal to the Doppler half-intensity width of the lines of the violet CN bands under the conditions here used. Actually the observed resolving power was about a third of the theoretical. Under these conditions only the areas of the lines could be measured directly, not the maxima of the absorption coefficients. A cylindrical lens of crystalline quartz placed in front of the plate as recommended by Oldenberg[9] increased the intensity by a factor of fifteen.

All the exposures necessary to determine a rate constant under any set of conditions were put on the same plate. Also on the same plate there was put an exposure through a step weakener transmitting known fractions of the incident light. The step weakener was made of sputtered platinum on quartz and calibrated with a quartz photo-cell and monochromator. The weakener was used directly in front of the plateholder. Eastman 33 plates were used throughout and developed for five minutes in M-Q developer. Microphotometer traces of the spectra and of the calibration marks on each plate were made on a Zeiss recording microphotometer. The amounts of blackening corresponding to the different steps of the step weakener were measured on each plate and plotted against its known transmission intensities to get calibration curves for the different plates. The blackenings of the different lines and corresponding backgrounds were similarly measured and corrected to intensities by the calibration curve for the particular plate. The fraction of the incident light apparently absorbed by each line was obtained by dividing the corrected intensity of the line by that of the background. Several test calibrations that were made on one plate with the spark source at different sparking rates and with a tungsten filament bulb indicated that there was no trouble from the intermittency effect in this experiment. The probable error in the photometric measurements is of the order of ten percent.

[9] O. Oldenberg, J. Opt. Soc. Am. 22, 441 (1932).

Measurements

A preliminary experiment with a d.c. discharge gave strong absorption of the CN band in the first order as explained in a previous communi-

TABLE I. *Half-life of* CN *radicals in milliseconds as a function of pressure and dilution with argon.*

Pressure mm	Dilution with Argon											
	Pure		9 : 1		99 : 1		999 : 1		9999 : 1		99,999 : 1	
0.15	10											
0.475	10, 8		11.5, 7.5						12			
1.5	11		13, 10						12			
4.75					9		15.5					

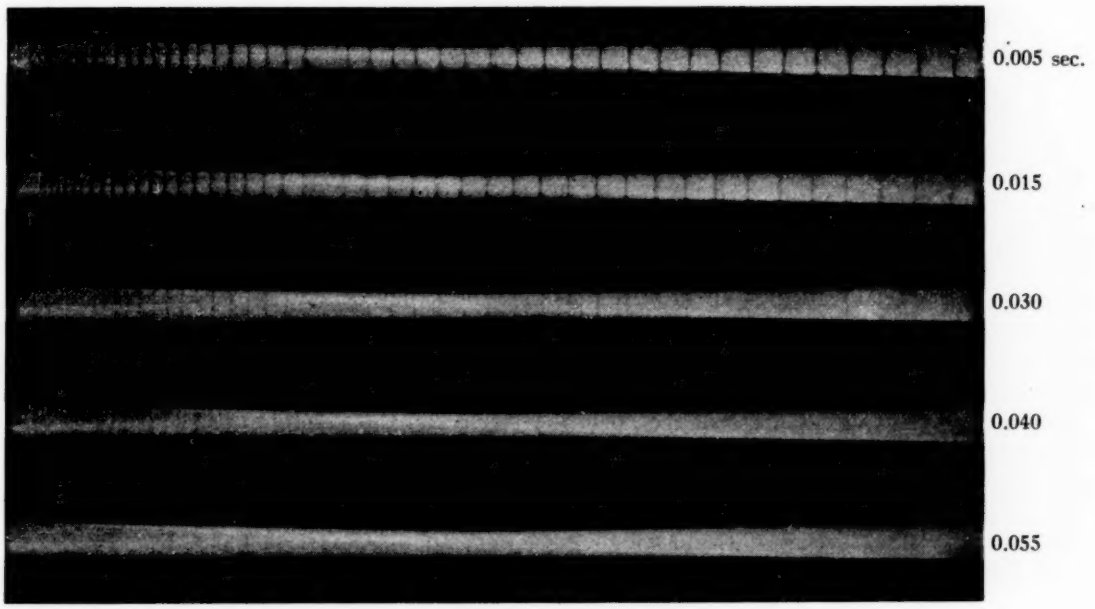

FIG. 3. Successive CN absorption spectra.

cation.[10] It is now clear that the peculiar rate reported there was caused by a very short half-life coupled with the insufficient resolution in the first order of the grating and emphasized by the great intensity of the absorption. In a second preliminary experiment a radiofrequency discharge was used, but the contents of the discharge tube were only changed after every 500 flashes instead of after every flash. Although the correction for poor resolving power, derived later, was not applied, the weaker absorption made it less necessary. The order and rate of the disappearance were calculated approximately and found comparable to the final more accurate results.

On each plate of the final experiment, made with the apparatus described above, there were a number of exposures taken at intervals of 0.005 second after the end of the discharge. They were taken irregularly, rather than in the order of increasing time, to find out whether there was any effect of running the tube after it had been cleaned with oxygen. None was found. On some of the plates exposures were made with two different discharge intensities, and the rates for the two calculated independently. Plates were taken under a large variety of conditions of pressure and dilution where a glow discharge could be maintained and the CN absorption spectrum observed. The intervals of dilution were factors of ten, of pressure the square root of ten. Twenty-two such plates were taken at all combinations of 0.15, 0.475, 1.5 and 4.75 mm total pressure and dilutions of zero, 9 : 1, 99 : 1, 999 : 1, 9999 : 1, and 99,999 : 1 except pure cyanogen at 4.75 mm and the lowest pressure and greatest dilution. All 22 of these showed visible absorption on the first exposure, but only on 16 does it last long enough to permit a measurement of its rate of disappearance. All but these 16 spaces are crossed off in Table I, and in the 9 of the 16 for which the calculations were made there are shown the corresponding half-lives of the CN radicals.

A typical series of exposures, with the times when they were taken, is shown in Fig. 3. As the overlapping of the lines of the P branch near the band head makes accurate measurements of their intensities impossible, only the first 18 lines of the R branch were used in the calculations.

The light source was so much more intense than the discharge that formed the CN radicals

[10] J. U. White, J. Chem. Phys. **6**, 294 (1938).

that their absorption spectrum could be observed at any time during the discharge without appreciable trouble from emission. A few exposures were taken during the discharge, including two at the two lowest partial pressures where absorption was observed. One of them shows that during the discharge there was about four times as much CN present as immediately after it. The lines of the weaker, 1,1 band, which were also observed in absorption on all the plates immediately after the discharge where the 0,0 band was intense, were measured and reduced in the same way as those of the 0,0 band.

The measurement of the areas of the absorption lines needed for the correction for incomplete resolution is the least accurate procedure in the experiment. As it was impractical to do this for every line, the areas and maxima of about 40 representative lines in different parts of the band were measured on large scale microphotometer traces and corrected with the calibration curve of the plate. The graph relating the two is shown in Fig. 4. It was found that for the first 18 lines the spin doublet separation was so much smaller than the effective resolving power that the ratio of area to maximum was constant. Beyond this point it began to increase. This graph was used to convert all the other maxima to areas.

Calculations

Correction for incomplete resolution

In the case of complete resolution of the line form the apparent fraction of light absorbed, which can be measured directly, is the true maximum fraction, for incomplete resolution it is always less than that. However, as the quantity of light absorbed is unaffected by the resolution, it can be measured directly in either case. It is then necessary to calculate the relation between the amount of light absorbed by a line and its true absorption coefficient. The methods of Frost[11] and of van Wijk[12] for measuring relative concentrations cannot be used in the case of CN because they depend on comparing two lines of equal intensities and the same line form. The unresolved spin doubling of CN makes every line different, even though all appear the same. Neglect of this results in serious errors.

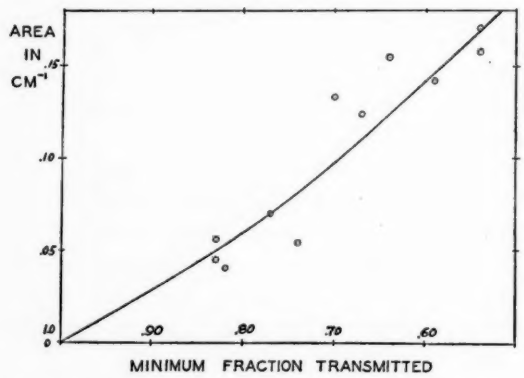

Fig. 4. Relation between area and maximum intensity of the lines.

When light passes through a thin layer of an absorbing mixture, a certain fraction of its intensity, called the absorption coefficient, a, is removed, per unit thickness traversed. If x is the thickness of the absorbing layer, I_0 the initial intensity of the light, and I the intensity at any other point,

$$I = I_0 e^{-ax}.$$

The quantity, a, is a characteristic for any material and proportional to the amount of it present. The total amount of light absorbed, A, is obtained by integration with respect to frequency.

$$A = \int_0^\infty [I_0(\nu) - I(\nu)]d\nu = I_0 \int_0^\infty (1 - e^{-a(\nu)x})d\nu,$$

assuming $I_0(\nu)$ to be constant. While the quantity, A, could be measured directly for the different lines in the band, it is more convenient to measure the maxima of the lines and convert them to areas as explained above. If the true form of the absorption line is known, its maximum can be calculated from A. At pressures below five millimeters and at room temperatures pressure broadening, Stark effect, and natural breadth are all negligible compared to Doppler broadening. The spin doublet separation is theoretically proportional to $K+\frac{1}{2}$. These two facts, together with the theoretical intensity ratios of the doublets, have been assumed to give the true forms of the doublets. The problem then becomes

[11] A. A. Frost, D. W. Mann, and O. Oldenberg, J. Opt. Soc. Am. **27**, 147 (1937).

[12] W. R. van Wijk and A. J. van Koeveringe, Proc. Roy. Soc. **A132**, 98 (1931).

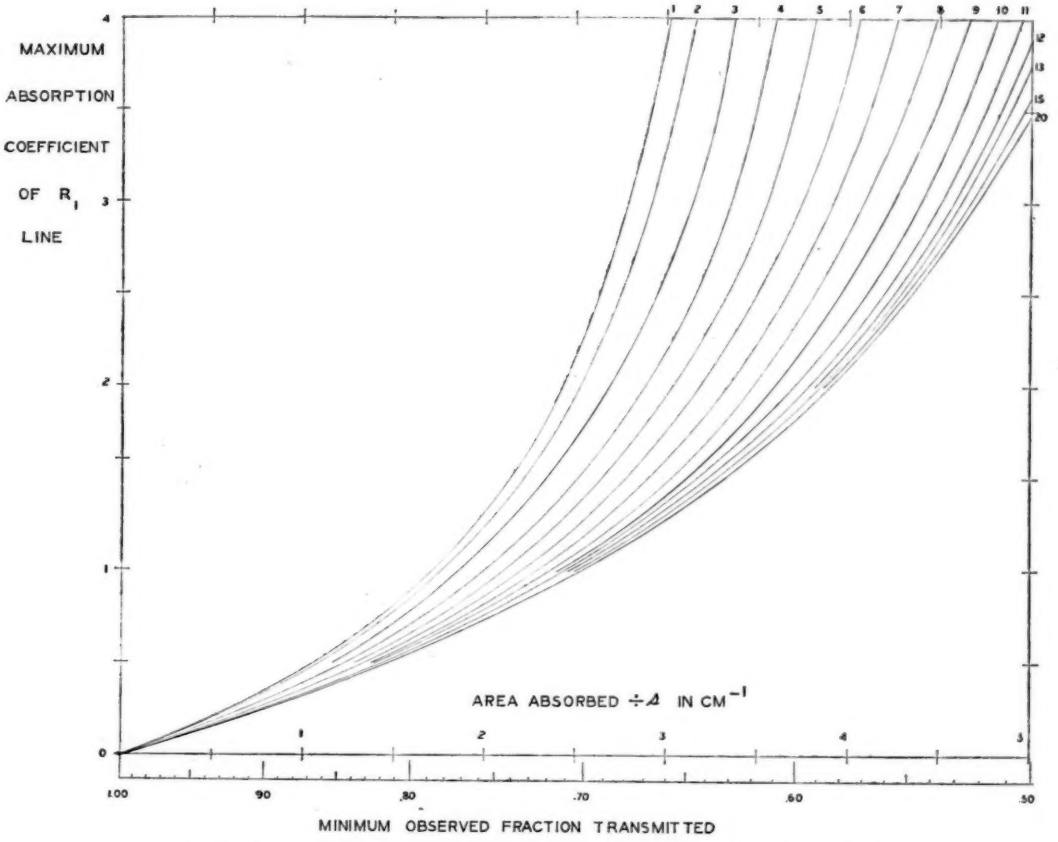

FIG. 5. Relation between absorption coefficient and amount of light absorbed.

one of converting the total amounts of light absorbed to the true absorption coefficients under the above assumptions. If μ=molecular weight, R=gas constant, T=absolute temperature, c=velocity of light, and ν=frequency, the form of a line broadened by the Doppler effect is given by

$$a(\nu)=\exp\left((-\mu/2RT)(c^2/\nu^2)(\nu-\nu_0)^2\right).$$

If b is the relative intensity and $\nu_1-\nu_2$ the separation of a doublet, the form of the absorption coefficient of a double line becomes

$$a(\nu)=a[\exp\left((-\mu c^2/2RT\nu^2)(\nu-\nu_1)^2\right)+b\exp\left((-\mu c^2/2RT\nu^2)(\nu-\nu_2)^2\right)].$$

The total amount of light absorbed by this doublet, in absolute frequency units, is

$$A=I_0\int_0^\infty\left[1-\exp\left(-ax\left\{\exp-\frac{\mu}{2RT}\frac{c^2}{\nu^2}(\nu-\nu_1)^2+b\exp-\frac{\mu}{2RT}\frac{c^2}{\nu^2}(\nu-\nu_2)^2\right\}\right)\right]d\nu.$$

If we set

$$s=(2RT/\mu)^{\frac{1}{2}}\nu_0/c$$

and change variables by

$$\nu=sy+(\nu_1+\nu_2)/2,$$
$$r=(\nu_2-\nu_1)/2s,$$

this becomes

$$A=I_0s\int_{-\frac{\nu_2+\nu_1}{2s}}^\infty[1-\exp-xa\{e^{-(y+r)^2}+be^{-(y-r)^2}\})]dy.$$

If the absorption is very weak this can be simplified and integrated directly.

$$A=I_0sax\sqrt{\pi}(1+b).$$

By means of the doublet separation of 0.037A for line 28 given by Birge[13] and the intensity

[13] R. T. Birge, Astrophys. J. **55**, 280 (1922).

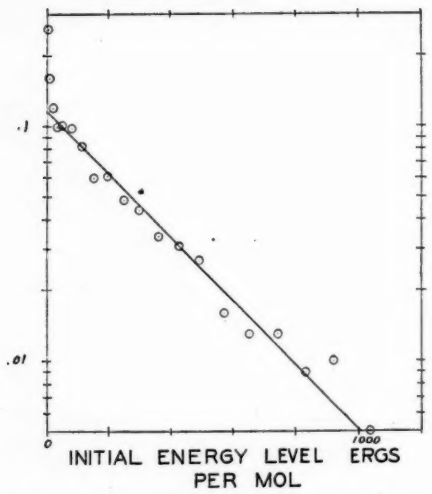

FIG. 6. Absorption coefficient against initial energy level.

formulas from Jevons[14] the values of, s, r, and b were calculated for the first eighteen lines of the R branch of the 0,0 band in the $^2\Sigma \rightarrow {}^2\Sigma$ transition.

$$s=0.0395, \quad r=0.115(K+\tfrac{1}{2}), \quad b=\frac{2K+1}{2K-1}\frac{K-1}{K+1},$$

where K is the rotational quantum number of the higher level of the transition. The integral was evaluated numerically for values of $ax=0.5$, 1, 2, 3, 4, and 6 for each of the lines $K=2$, 4.7, 10, and 20.5. Curves of A/I_0s were plotted against ax for these lines, and those for the intermediate ones were interpolated between them. The correction to the integral for temperatures other than 300°K was calculated to be less than 1 percent for every 12°. It was neglected. The curves are shown in Fig. 5 as functions of A/I_0s, and of the observed maxima of absorption.

Calculation of relative concentrations

Under the conditions of very weak absorption, the amount of light absorbed is directly proportional to the number of absorbing molecules. For stronger absorption the linear relation with concentration holds only for the integrated absorption coefficient, B, rather than for the amount of light removed. The absorption coefficients found above were integrated over all frequencies and summed over all the lines of the R branch of the band. The first 18 lines were measured directly; the others were predicted by the Boltzmann distribution at the observed rotational temperature. The final quantity, $\sum_K B$, is a direct measure of the amount of CN present in the tube. Fig. 6 shows the logarithm of each absorption coefficient divided by its i factor plotted against the energy of the initial level of the line. The slope of this curve equals $-1/T$. The rotational temperatures found in this way varied from 350°K at the end of the discharge down to 320°K after a hundredth of a second.

[14] W. Jevons, *Report on Band Spectra*, p. 137.

RESULTS

Reaction kinetics

The mechanism of the disappearance of the CN radicals after their formation in the discharge has been studied in detail. Concentrations were measured as functions of time over a large range of pressure and dilution. In all cases the reaction was found to be first order, i.e., the rate of disappearance was proportional only to the concentration of CN present. Fig. 7 shows a graph of the averages of the points from several plates plotted against time on semi-log paper to find out if there is any departure from the first-order rate law. The unit of concentration is the partial pressure of CN as found below. There

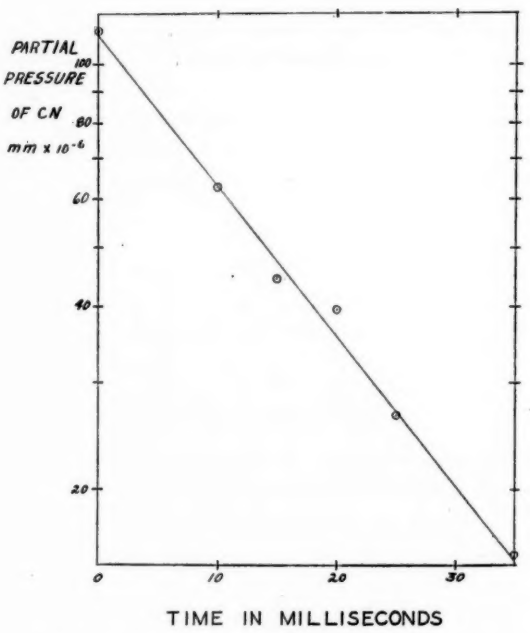

FIG. 7. Mean disappearance of CN concentration.

was no dependence on total pressure or on partial pressure of cyanogen. There was a qualitative relationship with the intensity of the discharge forming the CN; the more vigorous the discharge, the more rapid the disappearance. The longest observed lifetime was 1/15 second, the mean half-life 11 milliseconds. The half-life as a function of total pressure and dilution with argon is shown in Table I. The probable errors in the table are of the order of one millisecond. The intervals of pressure and dilution were so chosen that the partial pressure of cyanogen remains constant on moving diagonally down to the right in the table. In the cases where two discharge intensities were used, both half-lives are given, the one corresponding to the more intense discharge coming first.

The conceivable reactions by which a radical might disappear are: (1) direct recombination to cyanogen; (2) addition to cyanogen; (3) reaction on the walls limited by the rate of diffusion to them; (4) reaction on the walls limited by the wall area; (5) ionization by loss or addition of an electron; (6) reaction with some product formed during the discharge. The first four of these are each impossible, because: (1) the reaction is not second order in CN; (2) the reaction is invariant to the partial pressure of cyanogen; (3) the reaction is invariant to the total pressure; (4) the reaction chamber is so large that the diffusion coefficient would have to be about 50 times that of nitrogen to account for the observed half-life on this basis.

TABLE II. *Appearance potentials, excitation potentials, and relative abundances of particles present in the discharge.*

PARTICLE	APPEARANCE POTENTIAL IN VOLTS	RELATIVE ABUNDANCE	EXCITATION POTENTIAL IN VOLTS
$C_2N_2^+$	14.1	3.4	
CN^+	21.3	0.7	
C_2^+	18.6	0.2	
CN^+	19.8	0.1	
CN	6.0		3.2, 1.3
A^+	15.5		
A			11.5

Number (5) does not disagree with any of the observed evidence. As the CN radical resembles a halogen atom electronically, it is practically certain not to lose an electron outside of a discharge. It might, however, pick up a free electron or even remove one from some other neutral molecule. The presence of enough free electrons to account for the disappearance for more than 0.001 second is impossible. If electrons are being removed from some molecule, the observed rate should be pressure dependent, and the molecule must be present in equal quantities in the cyanogen and in commercial argon. Thus the last mechanism is the only one remaining.

Number (6) is in agreement with the observed increase in rate with discharge intensity and with the findings of the two preliminary experiments described above. It explains the more rapid rate found in the first experiment using a direct-current discharge instead of radiofrequency to produce the dissociation. It can be further limited by the results of the second, when the gas in the discharge tube was only changed every 500 flashes. As the rate of disappearance was then about the same, the only conclusion is that the reaction involved an ion that subsequently was neutralized between flashes. Any reasonable mechanism must give the proper end product, paracyanogen, when all the reactions are completed. A mechanism that meets all these requirements can be built on a theory of the condensation of the radicals on active centers of complex ions formed in the discharge. The ions known to occur in a discharge through cyanogen,[15] along with their ionization potentials, relative abundances, and other useful data, are given in Table II. The first step is the formation during the discharge of a complex ion by the addition of a CN radical to one of those in Table II. As the most abundant of these is the only one that will give a polymer of cyanogen on neutralization of the addition product, the

TABLE III. *Ratio of intensities of 0,0 to 1,1 Band for different pressures and dilutions.*

PRESSURE MM	PURE	9 : 1	99 : 1	999 : 1	9999 : 1
0.15	0.088		0.49		
0.475	Trace	0.18			0.42
1.5	Trace	0.081			0.26
4.75			0.24	0.22	

[15] J. T. Tate, P. T. Smith, and A. L. Vaughan, Phys. Rev. **48**, 525 (1935).

indicated first step is

$$CN+C_2N_2^+ \rightarrow C_3N_3^+.$$

The amount of $C_2N_2^+$ formed in a weak discharge through cyanogen is independent of the pressure for the same applied voltage. The failure to observe any emission spectrum of argon indicates that even at considerable dilution most of the positive current was being carried by cyanogen ions. Therefore down to the limit of observation of strong absorption by CN radicals one should expect about the same number of $C_2N_2^+$ ions to be formed.

The density of ions needed to carry the current is very much less than the concentration of cyanogen put in the tube, even at the greatest dilutions where rate measurements could be made. If each of the ions formed adds a CN by the equation above, at the end of the discharge there is always about the same number of complex ions left in the tube. They are so large that they do not diffuse rapidly to the walls, but stay in the gas. The observed disappearance of the CN radicals after the discharge is by a chain of successive additions to these complexes:

$$C_3N_3^+ + CN \rightarrow C_4N_4^+$$
$$C_4N_4^+ + CN \rightarrow C_5N_5^+, \text{ etc.}$$

The complexes formed should have enough vibrational and rotational energy levels to absorb the excess energy in the collisions in the absence of any third bodies. This mechanism is in complete harmony with the work of Hogness and Liu-Sheng T'sai[16] on the photopolymerization of cyanogen. From the quantum yield in the absence of ions they postulated an addition of CN to a cyanogen molecule. The failure to observe this reaction in the present work only indicates that it is very slow compared to the addition to the ion.

Persistence of vibration

The distribution of the CN radicals in the rotation levels of the ground state is about what is predicted by the Boltzmann theory. There is a small temperature inhomogeneity in the lowest levels, but it is not large enough to be very significant. The case of vibration is entirely different. In equilibrium at 330°K, 1/8000 of the radicals should be in the first vibration level. Actually at the end of the discharge an appreciable fraction has been observed in this state in all cases. The fraction is larger at low pressures and large dilutions. In one case the band still remained with measurable intensity 5 milliseconds after the discharge. From this observation the half-life of the vibrating state was calculated to be 3 milliseconds, or one-fourth that of the ground state. The pressure dependence shown in Table III indicates that some of the excited radicals are being reduced to the ground state by collisions, as well as being destroyed completely. During a half-life the radicals suffer about 10,000 collisions with argon atoms. This confirms predictions of the persistence of vibration from the increase of the velocity of sound at high frequencies and the work of Dwyer[17] on iodine vapor. The persistence of the vibrations is naturally dependent on the nature of the gas present. In commercial argon they last about ten times as long as in pure cyanogen.

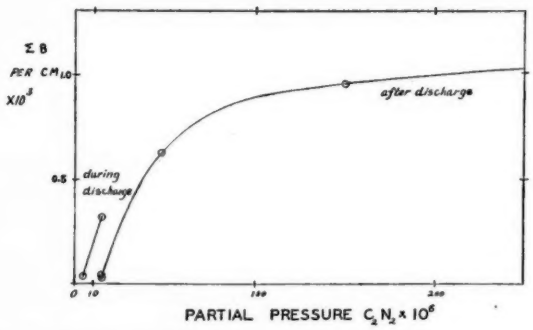

FIG. 8. CN absorption against partial pressure of cyanogen.

Absolute concentrations and *f* values

When the cyanogen in the discharge tube was diluted with argon, the intensity of the CN spectrum remained about constant for a while, then fell off slowly, and finally disappeared quite suddenly. A series of measurements of the absorption intensity near the point of disappearance were taken, some during the discharge and some immediately after it. The relative concentrations, $\sum B$, calculated from them are shown in Fig. 8 as functions of the partial pressure of

[16] T. R. Hogness and Liu-Sheng T'sai, J. Am. Chem. Soc. **54**, 123 (1932).

[17] R. J. Dwyer, J. Chem. Phys. **7**, 40 (1939).

cyanogen present. The graph of those after the discharge against the partial pressure of cyanogen remains about level until the dilution is 10,000 : 1, when it falls off sharply but does not pass through the origin. The graph of those during the discharge is parallel to the other but displaced to lower concentrations. The final slope of the two curves is taken as a limiting relation between the partial pressures of cyanogen and CN. The latter must be less than or equal to what would be obtained if all the cyanogen present were dissociated to CN. If the dissociation had been caused by a much shorter and more intense discharge, the points could be corrected back to zero time, when they should lie on a line through the origin. Although this correction could not be made completely, the graph during the discharge shows a large improvement over the other. If it could be made the fraction dissociated would be found to increase regularly with dilution until it approached and flattened out at a limiting value. If we take the final slope of the two graphs as the best value and remember that a molecule of cyanogen dissociates to two CN radicals, the partial pressure of CN in millimeters is $(0.0075/x)\sum_K B$ for room temperatures, where, if the absorption is weak, $\sum_K B/I_0 x$ is the total amount of light absorbed per centimeter by the R branch of the band. This must be corrected for the number of molecules in higher vibrational levels. At these pressures and dilutions the ratio of the intensities of the 0,0 and 1,1 bands, obtained from Table III, was 0.45. Dividing by 0.87, the ratio of the relative probabilities of these transitions,[18] the ratio of the populations of these levels is 0.52. If the vibrational levels are populated according to an exponential distribution with 0.52 as the ratio of the second to the first, the total population is 2.1 times that of the ground level. Dividing by this, the partial pressure of CN in millimeters is

$$P_{CN}=\frac{0.0035}{x}\sum_K B.$$

All the absolute concentrations have been calculated with this limiting figure. The question of how close to the limit the dissociation actually is will be discussed in a later paper, where it will be shown that the dissociation is almost complete.

For very weak absorption the total light removed by a single line in cm^{-1} is

$$A=I_0 sax\sqrt{\pi}=B.$$

In terms of the total absorption per cm of the R branch of the band,

$$A=0.0081\frac{I_0 i e^{-\epsilon/kT}}{x}\sum_K B,$$

where ϵ is the energy of the initial level of the particular line considered. The total absorption can also be expressed in the form given by dispersion theory. Korff and Breit[19] give as the formula for the same quantity,

$$A=\frac{\pi F_s e^2}{mc^2}I_0,$$

where e is the charge on the electron, M its mass, and F_s the number of dispersion electrons per cubic centimeter. If we eliminate A, the density of dispersion electrons for each line is

$$F_0=9.2\times10^9\frac{i e^{-\epsilon/kT}}{I_0 x}\sum_K B.$$

The density of molecules causing this line is the total density present times the fraction in the proper state to absorb it. The density under standard conditions is 2.70×10^{19} molecules/cc, which corresponds to 2.94×10^{16} at 330°K and 1 millimeter pressure. The number in any state is

$$N=2.94\times10^{16}p\frac{(K+1)e^{-\epsilon/kT}}{\sum_K(2K+1)e^{-\epsilon/kT}},$$

where p is in millimeters.

$$N=8.4\times10^{11}\frac{\sum_K B}{x}(K+1)e^{-\epsilon/kT}.$$

The absolute f value is defined as the number of dispersion electrons per molecule for a particular line.

$$f=\frac{F_s}{N}=0.012\frac{K+1}{K+\frac{1}{2}}$$

$$=0.012(\pm0.003)$$

[18] L. S. Ornstein and H. Brinkman, Proc. Amsterdam Acad. **34**, 1 (1931).

[19] A. Korff and G. Breit, Rev. Mod. Phys. **4**, 471 (1932).

for large values of K. The f value for the whole band including the P branch is twice this. $f=0.022$. For the whole $^2\Sigma\rightarrow{}^2\Sigma$ transition including the 0,1 band with a relative probability of 0.16[15], $f=0.026$ (± 0.006). As this is based on the upper limit for the concentration of CN, it is only a lower limit for the f value. This value should be compared with 0.00013 found by Oldenberg[20] for OH. It agrees quite well with Mulliken's[21] prediction based on absorption in the sun that transition probability of the violet CN band system is about a thousand times greater than that of the OH system. The value may also be compared with that for the D lines of sodium, $f=99.7$ percent.

Application to carbon arc

The absolute absorption coefficient can also be expressed in terms of a mean collision cross section. Thus light of the proper frequency passing through a cloud of CN radicals at room temperature is half-absorbed if each photon passes within 25A of a radical in the proper state to absorb it. Considering only one molecule and light of the proper frequency with respect to its motion the radius of absorption is of the order of ten times this.

In the ordinary carbon arc the CN bands are observed to have a different rotational temperature in the core and the outer part. If much CN were present, the radiation from the core would all be absorbed in the outer part. Lochte-Holtgreven and Maecker[22] have found a bend in the temperature curves for the cores corresponding to this effect. If the light in their case is assumed to be half-absorbed by a layer three millimeters thick, allowing a factor of five for the difference in line widths, there must be 8×10^{13} radicals per cc absorbing the most intense lines. Adding for all the rotation and vibration levels there must be a total of about two hundred times this, or 2×10^{16} radicals per cc in the arc. This corresponds to a partial pressure of about $\frac{1}{2}$ millimeter at room temperatures or 10 millimeters at the temperature of the arc.

In conclusion I should like to mention the possible errors in this work. All parts of the apparatus were carefully designed and constructed, and whenever an improvement was thought possible, they were rebuilt. By stroboscopic tests the timing was found to be correct to better than a thousandth of a second. The probable photometric errors were of the order of ten percent. While undetected variations in the discharge through cyanogen may have introduced small numerical errors, they cannot have been large enough to affect the nature of the conclusions. The greatest uncertainty, which lies in the assumption of complete dissociation of the cyanogen to CN at very great dilution, will be considered in detail in a later paper.

[20] O. Oldenberg and F. H. Rieke, J. Chem. Phys. **6**, 439 (1938).
[21] R. S. Mulliken, Astrophys. J. **89**, 283 (1939).
[22] W. Lochte-Holtgreven and H. Maecker, Zeits. f. Physik **105**, 1 (1937).

The Calculation of Force Constants in Some Methyl Compounds

J. W. LINNETT
St. Johns College, Oxford, England

(Received October 17, 1939)

In this paper are described force constant calculations on ethane, the methyl halides, methyl cyanide and isocyanide. The potential function used is based on a valency type force field with the introduction of one cross term rendered likely by physical considerations. The applicability of this function to the molecules under consideration is tested with the ethane molecule. The carbon-carbon bond force constant in methyl cyanide is found to be considerably greater than in ethane, indicating that the bond has some double-bond character in the cyanide, as has been suggested by Pauling, Springall and Palmer. It is found that the bending constant of the HCH angle remains very constant in the four methyl halides, there being changes, however, on passing to the other compounds. Other variations in the force constants of corresponding links, similar to these, are studied and their significance discussed.

THE determination of bond force constants has been shown to be a valuable aid in the elucidation of molecular structure. In addition to obtaining information regarding the nature of chemical linkages, the value of the force constants may be used to obtain bond lengths, the results obtained being comparable in accuracy and reliability with those obtained by more direct methods.[1] In the present paper are described calculations of stretching and deformation force constants in ethane, the methyl halides, methyl cyanide and isocyanide. A comparison is made between the constants obtained for similar links in this series of methyl compounds.

For the comparison of force constants in the examination of the structure of molecules it is necessary both that a satisfactory potential function shall be used in all cases and also that the function shall be of similar form for all the molecules concerned. One test of the applicability of a given potential function is that it should, for a particular molecule, reproduce the magnitudes of the observed fundamental frequencies when the number of constants is less than the number of fundamental frequencies observed. In the present case the form of the potential function has been tested by application to ethane, in which case ten of the fundamental frequencies are reproduced using a function involving only five constants.

Various forms of potential function have been used in the calculation of the fundamental frequencies of polyatomic molecules, the most important types being those based on central force field and valency force field. It appears that the greatest success has been obtained with a function of the second type which includes, in addition to the squared-terms required by the simple valency force field, those cross terms which are rendered likely by physical considerations.[2, 3]

ETHANE

Howard[4] applied a simple valency force field type potential function to ethane and obtained fairly satisfactory results. More recently Stitt has determined the fundamental frequencies of hexadeuteroethane and has considered the application of functions which involve cross terms in addition to the simple squared-terms. With nine constants Stitt[3] has reproduced the twenty-two fundamental frequencies of the two isotopic molecules. In the present case no attempt has been made to use such a complete function as that employed by Stitt since it would be impossible to use one containing so many constants with the other methyl compounds under consideration. Also since the fundamental frequencies of the trideuteromethyl molecules are not known for the other compounds under consideration the present function has not been applied to the deutero-compound in this case.

[1] Badger, J. Chem. Phys. **2**, 128 (1934); Douglas-Clark, Phil. Mag. **18**, 459 (1934).

[2] Thompson and Linnett, J. Chem. Soc. 1376 (1937).
[3] Stitt, J. Chem. Phys. **7**, 297 (1939).
[4] Howard, J. Chem. Phys. **5**, 442 (1937).

Sutherland and Dennison,[5] using a special potential function, obtained expressions for the nondegenerate vibration frequencies of ethane. One of the frequencies they employed was, however, incorrect.

Observed frequencies

The values given by Stitt for the fundamental frequencies of ethane are used here. These do not differ greatly from the values given by Crawford, Avery and Linnett.[6] The evidence for the magnitude 1170 cm^{-1} for the $\bar{E}$ frequency is still obtained by indirect reasoning, but this value is probably the best that can be obtained at the present time. Barker[7] has suggested a rather different assignment. Objections to his assignment have been discussed by Stitt.

Dimensions of the molecule

It has been presumed that the arrangement of valency bonds round each carbon atom is tetrahedral. There is no direct evidence for this, but it is most unlikely that the angles depart from the tetrahedral values by more than a degree or two. The carbon-hydrogen bond length has been taken to be 1.093A, the value found by Barker and Ginsberg in methane.[8] The carbon-carbon distance, 1.54A, has been determined by electron diffraction.[9]

Potential function

A potential function of the simple valency force type consists of four terms involving four constants. There are the carbon-hydrogen and carbon-carbon bond force constants and the HCH and HCC bending force constants. In addition to these four terms, a cross term between the carbon-carbon bond and the HCH angles has been introduced. A cross-term constant of this type was found by Thompson and Linnett[10] to be important in the corresponding methylene compounds ethylene, formaldehyde, and ketene. Physically the introduction of this cross term means that changes in the carbon-carbon bond length lead to a distortion of the tetrahedral arrangement of the methyl group. Such a state of affairs is rather to be expected.

The potential function that is used is therefore:

$$V=\tfrac{1}{2}k_{CC}(\Delta CC)^2+\tfrac{1}{2}\Sigma k_{CH}(\Delta CH)^2 +\tfrac{1}{2}\Sigma k_{HCH}(\Delta HCH)^2+\tfrac{1}{2}\Sigma k_{HCC}(\Delta HCC)^2 +\tfrac{1}{2}\Sigma k'(\Delta CC)(\Delta HCH).$$

This function leads to the expressions for the vibration frequencies.

Calculations

Using the molecular dimensions given above and the following values for the constants: $k_{CH}=4.81\times10^5$ and $k_{CC}=4.53\times10^5$ dynes per cm, $k_{HCH}=0.561\times10^{-11}$ and $k_{HCC}=0.545\times10^{-11}$ dyne cm per radian, and $k'=-0.38\times10^{-5}$, the values calculated for the frequencies are those given in Table I. It will be seen that ten of the eleven observed frequencies are satisfactorily reproduced. The difference between the observed and calculated values of the eleventh frequency arises because no account has been taken of the interaction between the methyl groups. This was shown by Stitt. In the other compounds of this series only one methyl group is involved so that the above results for ethane indicate that a potential function of this form would be completely satisfactory for use with the methyl halides, cyanide and isocyanide. It is important to notice that the values for the carbon-hydrogen and carbon-carbon bond force constants obtained here do not differ appreciably from the values given by Stitt for these constants. Therefore the values obtained for these bond constants may be compared with complete safety with values obtained for similar bonds in the other methyl compounds.

TABLE I. *Comparison of the calculated and observed frequencies for ethane (in cm^{-1}).*

A_1		A_2		E		$\bar{E}$	
Calc.	Obs.	Calc.	Obs.	Calc.	Obs.	Calc.	Obs.
2901	2925	2895	2925	3025	2980	3031	2970
1375	1375	1380	1380	1484	1465	1463	1460
993	993			835	827	1006	1170

[5] Sutherland and Dennison, Proc. Roy. Soc. **A148**, 250 (1935).
[6] Crawford, Avery and Linnett, J. Chem. Phys. **6**, 682 (1938).
[7] Barker, J. Chem. Phys. **7**, 277 (1939).
[8] Barker and Ginsberg, J. Chem. Phys. **3**, 668 (1935).
[9] Brockway and Pauling, J. Am. Chem. Soc. **59**, 1223 (1937).
[10] Linnett and Thompson, J. Chem. Soc. 1384 (1937).

Methyl Halides

Force constant calculations have been made on the methyl halides by Sutherland and Dennison[5] who used a potential function which could be applied to the nondegenerate vibrations only. This means that they had only three frequencies with which to calculate the four constants of their potential function. Nevertheless the values obtained by them for the stretching force constants of the carbon-halogen links agree closely with those calculated in the present work. Voge and Rosenthal[11] made frequency calculations on the chlorine substituted compounds of methane, including methyl chloride, using a more general potential function, different in type from the one employed here. Recently Slawsky and Dennison[12] have applied to the methyl halides the same potential function that is used here. However, they have fixed two of the constants required by applying a similar function to methane and then using the same values for the corresponding constants in the methyl halides. Because of this the constants given by them are different from the values obtained in the present calculations.

Methyl fluoride

The values of the observed frequencies are taken from Sponer's *Molekülspektren*. They are, for the nondegenerate vibrations: *ca.* 2862, *ca.* 1460, and 1048, and for the degenerate vibrations: 2987, 1476, and 1200 cm^{-1}. The value *ca.* 2862 is the smaller of the two members of a resonance doublet, the greater having the value 2965 cm^{-1}. Resonance occurs with the first overtone of the 1476 cm^{-1} fundamental. Since $2\times1476=2952$ is close to 2965 cm^{-1} the smaller value has been taken for the fundamental frequency.

Molecular dimensions.—The shape of the methyl group in the methyl halides is not known with any degree of certainty. However, the experimental evidence does seem to indicate that the methyl group in these compounds is not radically different from the methyl group in methane, in which case, of course, there must be a tetrahedral arrangement of valencies.[13]

[11] Voge and Rosenthal, J. Chem. Phys. **4**, 137 (1935).
[12] Slawsky and Dennison, J. Chem. Phys. **7**, 522 (1939).
[13] Johnston and Dennison, Phys. Rev. **48**, 868 (1935).

TABLE II. *Comparison of the calculated and observed frequencies for methyl fluoride (in cm^{-1}).*

Nondegenerate		Degenerate	
Calc.	Obs.	Calc.	Obs.
2859	*ca.* 2862	2988	2987
1468	*ca.* 1460	1476	1476
1048	1048	1200	1200

Penney has, from theoretical considerations, concluded that in methyl chloride the angles do not differ greatly from the tetrahedral value.[14] He has also concluded that the dipole moment requires that the carbon-chlorine link shall take on something of a polar character and estimates that the polar contribution is about a sixth of the total. The methyl ion would be expected to be planar, so that the ionic character will tend to decrease the magnitude of the HCX angle in CH_3X. Let β be the angle $180-HCX$. If the arrangement of the valencies is tetrahedral β is 70.5, but if the methyl group is planar β equals 90°. The angle β, which must be very much closer to 70.5° than to 90°, has been taken to be 72.5° in all the methyl halides. This cannot be far from the correct value.

No unambiguous measurement of the carbon-hydrogen distance in the methyl halides has been made. It has been taken to be the same as that in methane, *viz.* 1.093A, in all cases. The carbon-fluorine bond length has been taken to be 1.40A which is the mean of the spectroscopic and electron diffraction values.[15] Actually changes in the bond length would have little effect on the results of the calculations.

Potential function.—The potential function is quite analogous to that used for the ethane molecule. It is:

$$V=\tfrac{1}{2}\Sigma k_{CH}(\Delta CH)^2+\tfrac{1}{2}k_{CF}(\Delta CF)^2$$
$$+\tfrac{1}{2}\Sigma k_{HCH}(\Delta HCH)^2+\tfrac{1}{2}\Sigma k_{HCF}(\Delta HCF)^2$$
$$+\tfrac{1}{2}\Sigma k'(\Delta CF)(\Delta HCH).$$

The force field is of the valency type, but it is supposed that changes in the carbon-fluorine distance cause changes in the configuration of the

[14] Penney, Trans. Faraday Soc. **31**, 734 (1935).
[15] Sutherland, Trans. Faraday Soc. **34**, 325 (1938).

TABLE III. *Comparison of the calculated and observed frequencies for methyl chloride (in cm^{-1}).*

NONDEGENERATE		DEGENERATE	
Calc.	Obs.	Calc.	Obs.
2915	*ca.* 2920	3045	3045
1356	1356	1460	1460
731	732	1020	1020

methyl group. This explains the introduction of the particular cross term.

Calculations.—By using the molecular dimensions given above and the following values of the constants: $k_{CH}=4.71\times10^5$ and $k_{CF}=5.64\times10^5$ dynes per cm, $k_{HCH}=0.517\times10^{-11}$ and $k_{HCF}=0.946\times10^{-11}$ dyne cm per radian and $k'=-1.3\times10^{-3}$, the frequencies calculated are those given in Table II. It will be seen that there is extremely close agreement between the calculated and observed values.

Methyl chloride

The values of the observed frequencies are taken from Sponer's *Molekülspektren.* They are, for the nondegenerate vibrations: *ca.* 2920, 1355 and 732 cm^{-1}, and for the degenerate vibrations: 3047, 1460 and 1020 cm^{-1}. As in methyl fluoride the largest fundamental of the first class resonates with the first overtone of the 1460 cm^{-1} vibration. Since the members of the resonance doublet are at 2880 and 2967 cm^{-1} and since $2\times1460=2920$, which is almost halfway between them, we might expect the frequency of the undisturbed fundamental to be *ca.* 2920 cm^{-1}.

Molecular dimensions.—The magnitude of β and of the carbon-hydrogen bond length are taken to have the same values as were assumed in methyl fluoride. The carbon-chlorine bond length has been assumed to be 1.71A which is the mean of the spectroscopic and electron diffraction values given by Sutherland.[15] Again small variations in the values for the bond lengths would not have a large effect on the calculations.

Potential function.—The potential function is precisely similar to that given for methyl fluoride. With the following constants: $k_{CH}=4.90\times10^5$ and $k_{CCl}=3.35\times10^5$ dynes per cm, $k_{HCH}=0.523\times10^{-11}$ and $k_{HCCl}=0.701\times10^{-11}$ dyne cm per radian, and $k'=-0.71\times10^{-3}$, the calculated values for the frequencies are those given in Table III.

Methyl bromide

The observed frequencies are taken to be, for the nondegenerate class: *ca.* 2930, 1305 and 610 cm^{-1}, and for the degenerate class: 3061, 1450 and 957 cm^{-1}. In this case the members of the resonance doublet are at 2860 and 2972 cm^{-1}. Since $2\times1450=2900$ cm^{-1} and this is 40 cm^{-1} larger than the smaller component, it might be expected that the nondegenerate fundamental had an undisturbed frequency not far from 2930 cm^{-1}.

Molecular dimensions.—The angle β and the carbon-hydrogen bond length have been presumed to be the same as in methyl fluoride. The carbon-bromine bond length has been taken to be 1.90A. The electron diffraction value is 1.91A and the spectroscopic value given by Sutherland[15] 1.88A.

Potential function and calculations.—The potential function is precisely the same as that given for methyl fluoride. With $k_{CH}=4.95\times10^5$ and $k_{CBr}=2.83\times10^5$ dynes per cm, $k_{HCH}=0.516\times10^{-11}$ and $k_{HCBr}=0.632\times10^{-11}$ dyne cm per radian, and $k'=-0.71\times10^{-3}$, the calculated frequencies have the values given in Table IV.

Methyl iodide

The observed fundamental vibration frequencies of the methyl iodide molecule are, for the nondegenerate class: *ca.* 2940, 1252 and 532 cm^{-1}, and for the degenerate class: 3074, 1445 and 885 cm^{-1}. For methyl iodide the members of the resonance doublet have frequencies: 2971 and 2860 cm^{-1}. Since $2\times1445=2890$ and this is 20 cm^{-1} larger than the smaller component it might be expected that the nondegenerate vibration had an undisturbed frequency not far from 2840 cm^{-1}.

Molecular dimensions.—The angle β and the carbon-hydrogen bond length have been given

TABLE IV. *Comparison of the calculated and observed frequencies for methyl bromide (in cm^{-1}).*

NONDEGENERATE		DEGENERATE	
Calc.	Obs.	Calc.	Obs.
2928	*ca.* 2930	3060	3061
1305	1305	1450	1450
610	610	958	957

the same values as in the other methyl halides. The carbon-iodine bond length has been taken to be 2.2A. The electron diffraction value is 2.28 ± 0.05A[16] and the spectroscopic value of Sutherland 2.07 ± 0.16A.[15]

Potential function and calculations.—The potential function and frequency expressions are the same as for methyl fluoride. With $k_{CH}=5.00\times10^5$ and $k_{CCl}=2.32\times10^5$ dynes per cm, $k_{HCH}=0.516\times10^{-11}$ and $k_{HCl}=0.550\times10^{-11}$ dyne cm per radian, and $k'=-0.64\times10^{-3}$, the frequencies calculated are those given in Table V.

Discussion.—In all cases the observed frequencies are reproduced with great precision. Since in the above cases k_{CH} is mainly concerned in the fixing of the values of the frequencies about 3000 cm^{-1} and the other four constants fix the values of the other four frequencies the methyl halides do not provide a test of the potential function employed. However the function has been tested by application to ethane and in the methyl halides the number of frequencies is sufficient for a unique determination of the constants.

It is interesting to compare the values of the corresponding constants in the four cases. For this purpose the values of the constants are listed in Table VI. It is immediately apparent that the bending constants of the HCH angle remain very constant throughout this series of compounds. This is very interesting since previous work has tended to indicate that bending constants were susceptible to great variation on passing from one compound to another. It should be noted that the value of the HCH bending constant here is about 10 percent lower than in ethane.

The variation in the carbon-hydrogen force constant indicates that it is not correct to regard the carbon-hydrogen bond as having an absolutely constant length in these compounds. However, the extreme variation to be expected from the changes in force constant is only about 1 percent. If it is presumed that the carbon-hydrogen bond length in ethane is really 1.093A, and that $k\cdot r^6=$constant, the carbon-hydrogen bond lengths in the methyl halides will have the following values: Fluoride, 1.097; chloride, 1.089; bromide, 1.088; iodide, 1.086A. These small changes from the value 1.093A would not affect the calculations appreciably.

TABLE V. *Comparison of the calculated and observed frequencies for methyl iodide (in cm^{-1}).*

NONDEGENERATE		DEGENERATE	
Calc.	Obs.	Calc.	Obs.
2944	*ca.* 2940	3074	3074
1252	1252	1445	1445
532	532	885	885

TABLE VI. *Comparison of the stretching and bending force constants in the four methyl halides,* CH_3X.

MOLECULE	$k_{CH}\times10^{-5}$	$k_{CX}\times10^{-5}$	$k_{HCH}\times10^{11}$	$k_{HCX}\times10^{11}$	$k'\times10^3$
CH_3F	4.71	5.64	0.517	0.946	−1.30
CH_3Cl	4.90	3.35	0.523	0.701	−0.71
CH_3Br	4.95	2.83	0.516	0.632	−0.71
CH_3I	5.00	2.32	0.516	0.550	−0.64

It is interesting to note that k_{HCX} and k_{CX} vary in much the same way, the change from the iodide to the bromide being much the same as that from the bromide to the chloride, but only a third or a quarter of the change from the chloride to the fluoride. It is found that $(k_{HCX}\times10^{11}-0.272)/(k_{CX}\times10^{-5})$ is equal to 1.20 for methyl fluoride, 1.28 for the chloride, 1.27 for the bromide, and 1.20 for the iodide. A similar type of change is to be seen in k', the value for the fluoride being very different from the values for the chloride, bromide and iodide.

The negative sign of the cross term indicates that a lengthening of the CX link tends to cause an increase in the HCH angle, that is to make the methyl group more planar. From this we should conclude that this arises because the CX link has become more polar. This would be expected because the sum of the ionic radii of the two atoms must be greater than the normal length of the link. It would therefore be expected that a lengthening of the link would cause an increase in the polar contribution.

Before concluding the remarks on the methyl halides it is of interest to compare the values of the force constants of the carbon-halogen links obtained here with those given by Sutherland and Dennison[5] and by Slawsky and Dennison.[12] The average difference between the figures given

[16] Brockway, Rev. Mod. Phys. **8**, 231 (1936).

here and those given by Sutherland and Dennison amounts to only 2 percent. This agreement is as good as can be expected. On the other hand the force constants given by Slawsky and Dennison differ by an average of about 30 percent from those listed above. This would seem to indicate that the method used by Slawsky and Dennison for fixing their constants is unsatisfactory.

Methyl cyanide

The earlier work on the Raman spectrum of methyl cyanide is summarized in Kohlrausch's *Smekal Raman Effekt*. A more recent examination has been carried out by Reitz and Skrabal.[17] The infra-red absorption spectrum has been studied by Coblentz,[18] by Bell,[19] and by Gordy and Williams.[20] A comparison of the results obtained seems to indicate that there are quite definite absorption bands at 3.25μ, 4.38μ, 7.08μ, 9.6 to 9.65μ, and 10.9μ. The frequencies corresponding to these wave-lengths are 3077, 2283, 1412, 1040, and 917 cm^{-1}.

The symmetry of the methyl cyanide molecule corresponds to the group C_{3v}. It has four non-degenerate and four doubly degenerate fundamental vibration frequencies. All these vibrations may appear in both the Raman and infra-red spectra. The more intense Raman lines have the frequency shifts: 2942, 2250, 1370, and 917 cm^{-1}. It is presumed that these correspond to the non-degenerate vibrations. It is to be noted that the second and fourth also appear in the infra-red spectrum at 2283 and 917 cm^{-1}. A guide as to the magnitudes of these four frequencies is, of course, obtained if the form of the vibrations in this class is considered. The first is primarily the carbon-hydrogen valency vibration, the second the carbon-nitrogen valency vibration, the third the symmetrical deformation vibration of the methyl group, and the fourth the carbon-carbon valency vibration. For the frequency of the carbon-hydrogen valency vibration of the second class we have to choose between the Raman line at 2996 cm^{-1} and the infra-red band at 3077 cm^{-1}. It has been presumed that the latter is the correct value, the Raman line arising from a combination level brought into prominence by resonance with the fundamental at 2942 cm^{-1}. For the remaining frequencies in this class we have *ca.* 1415 (Raman, 1417; infra-red, 1412), 1040 (infra-red) and 376 cm^{-1} (Raman). Again the form of the vibrations assists in the fixing of the probable approximate magnitudes.

TABLE VII. *Comparison of the calculated and observed frequencies for methyl cyanide (in cm^{-1}).*

NONDEGENERATE		DEGENERATE	
Calc.	Obs.	Calc.	Obs.
2949	2942	3076	3077
2259	*ca.* 2265	1417	1415
1370	1370	1040	1040
918	917	376	376

Molecular dimensions.—As in the methyl halides there is no evidence for the size of the angle β or for the carbon-hydrogen distance. The values assumed for these are the same as in the halides. Brockway,[21] from electron diffraction measurements, gave the carbon-carbon bond length in methyl cyanide as 1.54±0.03 and the carbon-nitrogen bond length as 1.16±0.02A. More recent measurements have been made by Pauling, Springall and Palmer[22] who give the figures 1.49±0.03 and 1.16±0.03A for these two lengths. These values have been used here.

Potential function.—The potential function used here is:

$$V=\tfrac{1}{2}\Sigma k_{CH}(\Delta CH)^2+\tfrac{1}{2}k_{CC}(\Delta CC)^2+\tfrac{1}{2}k_{CN}(\Delta CN)^2+\tfrac{1}{2}\Sigma k_{HCH}(\Delta HCH)^2+\tfrac{1}{2}\Sigma k_{HCC}(\Delta HCC)^2+\tfrac{1}{2}k_{CCN}(\Delta CCN)^2+\tfrac{1}{2}\Sigma k'(\Delta CC)(\Delta HCH).$$

This is analogous to those used for ethane and the methyl halides.

Calculations.—With the constants having the following values: $k_{CH}=5.0\times10^5$, $k_{C-C}=5.3\times10^5$ and $k_{C\equiv N}=17.5\times10^5$ dynes per cm, $k_{HCH}=0.487\times10^{-11}$, $k_{HCC}=0.685\times10^{-11}$ and $k_{CCN}=0.320\times10^{-11}$ dyne cm per radian, and $k'=-0.51\times10^{-3}$, the calculated values of the frequencies are those given in Table VII. Since six of the frequencies

[17] Reitz, Wien Ber. **146**, 398 (1937).
[18] Coblentz, Carnegie Inst. Publ. (1905), Vol. 35.
[19] Bell, J. Am. Chem. Soc. **57**, 1023 (1935).
[20] Gordy and Williams, J. Chem. Phys. **3**, 664 (1935); **4**, 85 (1936).
[21] Brockway, J. Am. Chem. Soc. **58**, 2516 (1936).
[22] Pauling, Springall and Palmer, J. Am. Chem. Soc. **61**, 927 (1939).

are below 2900 cm^{-1} and six of the constants are mainly concerned in fixing their calculated values, this case can provide no test of the potential function employed. A unique determination of the constants is, however, possible.

Methyl isocyanide

The Raman spectrum of this compound has been examined by Dadieu.[23] The infra-red absorption spectrum of the liquid has been studied by Gordy and Williams.[20] By employing similar arguments to those used for methyl cyanide and by comparing the frequencies obtained for the cyanide with those obtained in this case, it seems that the vibration frequencies may be assigned in the following way: Nondegenerate class: 2951, *ca.* 2170 (Raman 2161; infra-red, 2183), 1444, and 928; Degenerate class: 3077, 1456, 1041, and 290 cm^{-1}.

Molecular dimensions.—Brockway[21] has shown that there is a linear arrangement of the two carbon and one nitrogen atoms in this compound. As for the cyanide the value of β and the length of the carbon-hydrogen bond have been assumed to be the same as in the halides. The lengths of the other two bonds have been determined by Brockway using electron diffraction. He gives the lengths 1.48 ± 0.03 and 1.17 ± 0.02A for the carbon-nitrogen single and triple bonds, respectively.

Potential function and calculations.—The potential function and frequency expressions are similar to those used for the cyanide. By using the following values for the constants: $k_{CH}=5.0\times10^5$, $k_{C-N}=5.45\times10^5$, and $k_{N\equiv C}=16.3\times10^5$ dynes per cm, $k_{HCH}=0.522\times10^{-11}$, $k_{HCN}=0.681\times10^{-11}$, and $k_{CNC}=0.205\times10^{-11}$ dyne cm per radian, and $k'=-0.34\times10^{-3}$, the frequencies calculated have the values given in Table VIII. As for methyl cyanide the isocyanide provides no test of the potential function, but a unique determination of the constants is possible.

Discussion.—The most striking fact that emerges from the above calculations is the considerable increase of the carbon-carbon force constant in methyl cyanide, where it has the value 5.3×10^5, over the constant for the same bond in ethane, where it has the value 4.53×10^5 dynes per cm. If it is presumed that the force constant varies inversely as the sixth power of the bond length, we should expect the carbon-carbon bond length in methyl cyanide to be 1.50A, assuming 1.54A for the length in ethane. If, however, it varies inversely as the fifth power, as has been suggested more recently by Fox and Martin,[24] we should expect the length to be 1.49A. Either of these is in satisfactory agreement with the electron diffraction value of 1.49 ± 0.03A. This effect of the triple bond on the force constant of the adjacent single bond is similar to that already found in hydrogen cyanide, in acetylene, and in dimethylacetylene.[25] Pauling, Springall and Palmer[22] have explained the corresponding effect on the bond length by suggesting that there is some change in the hybridization of the carbon atomic orbitals and that there is resonance between the normal single-triple bond structure and a double-double bond structure by which the single bond takes on some double bond character. This suggestion is in agreement with the force constant results. Before leaving this topic it is interesting to note that the carbon-carbon frequency in ethane, 993 cm^{-1}, is greater than the carbon-carbon frequency in methyl cyanide, 917, a fact that would lead to a conclusion, on preliminary consideration, very different from that obtained when detailed force constant calculations are made.

Comparing methyl cyanide and isocyanide it is found that the CCN bending constant in methyl cyanide is much bigger than the CNC bending constant in the isocyanide. The value of the carbon-nitrogen stretching force constant in methyl cyanide is 17.5×10^5 compared with 18.1×10^5 in hydrogen cyanide and 17.5×10^5 in

TABLE VIII. *Comparison of the calculated and observed frequencies for methyl isocyanide (in cm^{-1}).*

NONDEGENERATE		DEGENERATE	
Calc.	Obs.	Calc.	Obs.
2948	2951	3077	3077
2167	*ca.* 2170	1455	1456
1413	1414	1042	1041
928	928	292	290

[23] Dadieu, Monatsheft **57**, 437 (1931).

[24] Fox and Martin, J. Chem. Soc. 884 (1939).

[25] Crawford, J. Chem. Phys. **7**, 555 (1939).

the cyanogen halides.[26] In the cyanogen halides it was necessary to assume that there was some resonance with a double-double bond structure, so that the value of this force constant in methyl cyanide confirms that there is resonance with a double-double bond structure in this case also. The force constant of the corresponding bond in the isocyanide is smaller still, being 16.3×10^5. This might mean that there is some contribution from the structure $CH_3-N=C$, though this is unlikely since the molecule would be nonlinear in this case and would not therefore be expected to resonate with the linear structure. An alternative explanation is that this decrease may occur because of the "lone pair" of electrons on the carbon atom in the isocyanide molecule.

The value of 5.0×10^5 for the carbon-hydrogen stretching force constant in methyl cyanide and isocyanide suggests that the length of this bond is 1.086A, as in methyl iodide.

In conclusion I wish to thank Dr. B. L. Crawford who, because of the present situation in Europe, has been kind enough to carry through the publication of this paper.

[26] Thompson and Linnett, J. Chem. Soc. 1399 (1937).

JANUARY, 1940 JOURNAL OF CHEMICAL PHYSICS VOLUME 8

Investigations on the High Temperature Photolysis of Acetaldehyde

DAVID C. GRAHAME* AND GERHARD K. ROLLEFSON
Department of Chemistry, University of California, Berkeley, California

(Received October 25, 1939)

A detailed investigation of the high temperature photolysis of acetaldehyde vapor has given results differing in certain details from those of previous investigators. The heat of activation found for the over-all reaction (8.6±0.3 kcal.) leads with one assumption to a value of 75 kcal. for the energy of the C–C bond in acetaldehyde. The reaction between methyl radicals is rather accurately bimolecular. Values are given for the relative quantum efficiencies for the production of free radicals in acetone and acetaldehyde at elevated temperatures at two wave-lengths.

IN a previous paper[1] the authors had occasion to repeat some of the experiments of Leermakers[2] on the high temperature photodecomposition of acetaldehyde vapor and found, in the course of this work, several discrepancies which could not at the time be explained satisfactorily. In view of the interest and importance which attaches to this photochemical process, it was thought desirable to extend the investigations in an effort to reveal the cause of the discrepancies and in order to settle any doubts concerning the rate law followed by the process. In addition special experiments have been carried out to test specific points of interest concerning the mechanism of the decomposition and the origin of the fluorescence of acetaldehyde.

EXPERIMENTAL METHOD

The experimental methods employed were essentially the same as those used previously. Monochromatic light, obtained by the use of a quartz mercury arc and fused quartz prism monochromator, was measured with the aid of two barrier-layer photronic cells as previously described. The calibration of the apparatus for the determination of absolute quantum yields has been carried out by a more elaborate method than we have used before and is described below.

Much care has been taken in all experiments to exclude the last traces of air. For this purpose the system was always evacuated to a very low pressure (10^{-5} mm or better) and the reaction vessel then flushed out briefly with degassed acetaldehyde. When for any reason air had been admitted into the reaction vessel, this was removed by pumping and heating to a temperature

* Present address, Department of Chemistry, Amherst College, Amherst, Massachusetts.

[1] G. K. Rollefson and D. C. Grahame, J. Chem. Phys. **7**, 775 (1939).

[2] J. Leermakers, J. Am. Chem. Soc. **56**, 1537 (1934).

higher than that subsequently to be employed. The acetaldehyde used was distilled twice in vacuum and was further degassed by alternately boiling it and pumping off the vapors. As before, the acetaldehyde was stored in contact with hydroquinone and anhydrous calcium sulfate. In all experiments with pure acetaldehyde vapor, stopcocks and stopcock grease were entirely absent. This is not known to be necessary, but since it introduced no great inconvenience, it was thought to be desirable. In the experiments with mixtures of acetone and acetaldehyde vapors, however, the acetone was confined in a reservoir closed with an ordinary glass stopcock greased with Apiezon L stopcock lubricant. There is no reason to believe that this circumstance introduced any error into the measurements since acetone vapor is relatively inert and since acetaldehyde vapor did not come into contact with this stopcock at any time.

Temperatures were measured with a copper-constantan thermocouple in conjunction with a high grade Leeds and Northrup potentiometer. The thermocouple was calibrated in the usual manner from cooling curves of several pure metals. The thermocouple wires were wound around the reaction vessel in a manner which insured good contact with the cell. Since the reaction vessel was relatively short (5.4 cm) and the electric furnace housing it was much larger, there is little reason to doubt that the tempera- of the cell was fairly uniform. A few experiments were carried out with a stirrer operated inside the furnace to circulate the air and to insure a more uniform temperature throughout. These experiments agreed well with identical experiments performed without such stirring. Every effort was made to obtain correct temperature measurements in these experiments, since it seemed possible that the discrepancy between our results and those of Leermakers might be explained by an error either in his temperature measurements or in ours.

Analyses were carried out as before by the method of Blacet, MacDonald and Leighton,[3, 4] except that in a few cases the amount of volatile gases produced in the reaction was too small to be analyzed accurately even by these micro-methods. In these cases it was assumed that the product gases contained 48.5 percent of CO, this being the average of the analyses of many other samples obtained under similar conditions. We note also that this value agrees satisfactorily with the $CO/(CO+CH_4+H_2)$ ratios obtained by Blacet and Volman[5] at 30°.

TABLE I. *Absorption coefficients of acetaldehyde vapor.*

T	3130A ϵ, LITERS MOLES^{-1} CM^{-1}	2652A ϵ, LITERS MOLES^{-1} CM^{-1}
300°C	18.9	16.9
200	17.6	17.1
100	15.7	16.7
60	14.9	—
30	14.9	17.9

In order to limit possible side reactions with the products of the photolysis, only a small fraction of the acetaldehyde present was decomposed in an experiment. The fraction of the incident light absorbed was calculated from the absorption coefficients given in Table I, taking into account the slight change in concentration of the acetaldehyde occurring during the photolysis.

Prolonged irradiation of hot acetaldehyde vapor finally results in an approximate doubling of the initial pressure. However, after a short irradiation the pressure increases less than one calculates from a measurement of the amount of carbon monoxide and methane formed. This evidently means that at elevated temperatures, as at 30°, polymer formation and decomposition both occur during the irradiation and that the polymer decomposes photochemically in a prolonged irradiation. No detailed study of the kinetics of the polymerization process has been carried out, but the existence of such a process casts doubt upon the results of those investigators who have used pressure measurements to follow the course of the reaction.[6]

CALIBRATION OF THE OPTICAL SYSTEM

The calibration of the optical system for the determination of absolute quantum yields has

[3] F. E. Blacet, G. D. MacDonald and P. A. Leighton, Ind. Eng. Chem. Anal. Ed. **5**, 272 (1933).
[4] F. E. Blacet and G. D. MacDonald, Ind. Eng. Chem. Anal. Ed. **6**, 334 (1934).
[5] F. E. Blacet and D. Volman, J. Am. Chem. Soc. **60**, 1243 (1938).
[6] J. W. Mitchell and C. N. Hinshelwood, Proc. Roy. Soc. **A159**, 32 (1937).

the cyanogen halides.[26] In the cyanogen halides it was necessary to assume that there was some resonance with a double-double bond structure, so that the value of this force constant in methyl cyanide confirms that there is resonance with a double-double bond structure in this case also. The force constant of the corresponding bond in the isocyanide is smaller still, being 16.3×10^5. This might mean that there is some contribution from the structure $CH_3-N=C$, though this is unlikely since the molecule would be nonlinear in this case and would not therefore be expected to resonate with the linear structure. An alternative explanation is that this decrease may occur because of the "lone pair" of electrons on the carbon atom in the isocyanide molecule.

The value of 5.0×10^5 for the carbon-hydrogen stretching force constant in methyl cyanide and isocyanide suggests that the length of this bond is 1.086A, as in methyl iodide.

In conclusion I wish to thank Dr. B. L. Crawford who, because of the present situation in Europe, has been kind enough to carry through the publication of this paper.

[26] Thompson and Linnett, J. Chem. Soc. 1399 (1937).

JANUARY, 1940 JOURNAL OF CHEMICAL PHYSICS VOLUME 8

Investigations on the High Temperature Photolysis of Acetaldehyde

DAVID C. GRAHAME* AND GERHARD K. ROLLEFSON
Department of Chemistry, University of California, Berkeley, California
(Received October 25, 1939)

A detailed investigation of the high temperature photolysis of acetaldehyde vapor has given results differing in certain details from those of previous investigators. The heat of activation found for the over-all reaction (8.6 ± 0.3 kcal.) leads with one assumption to a value of 75 kcal. for the energy of the C—C bond in acetaldehyde. The reaction between methyl radicals is rather accurately bimolecular. Values are given for the relative quantum efficiencies for the production of free radicals in acetone and acetaldehyde at elevated temperatures at two wave-lengths.

IN a previous paper[1] the authors had occasion to repeat some of the experiments of Leermakers[2] on the high temperature photodecomposition of acetaldehyde vapor and found, in the course of this work, several discrepancies which could not at the time be explained satisfactorily. In view of the interest and importance which attaches to this photochemical process, it was thought desirable to extend the investigations in an effort to reveal the cause of the discrepancies and in order to settle any doubts concerning the rate law followed by the process. In addition special experiments have been carried out to test specific points of interest concerning the mechanism of the decomposition and the origin of the fluorescence of acetaldehyde.

EXPERIMENTAL METHOD

The experimental methods employed were essentially the same as those used previously. Monochromatic light, obtained by the use of a quartz mercury arc and fused quartz prism monochromator, was measured with the aid of two barrier-layer photronic cells as previously described. The calibration of the apparatus for the determination of absolute quantum yields has been carried out by a more elaborate method than we have used before and is described below.

Much care has been taken in all experiments to exclude the last traces of air. For this purpose the system was always evacuated to a very low pressure (10^{-5} mm or better) and the reaction vessel then flushed out briefly with degassed acetaldehyde. When for any reason air had been admitted into the reaction vessel, this was removed by pumping and heating to a temperature

* Present address, Department of Chemistry, Amherst College, Amherst, Massachusetts.
[1] G. K. Rollefson and D. C. Grahame, J. Chem. Phys. **7**, 775 (1939).
[2] J. Leermakers, J. Am. Chem. Soc. **56**, 1537 (1934).

higher than that subsequently to be employed. The acetaldehyde used was distilled twice in vacuum and was further degassed by alternately boiling it and pumping off the vapors. As before, the acetaldehyde was stored in contact with hydroquinone and anhydrous calcium sulfate. In all experiments with pure acetaldehyde vapor, stopcocks and stopcock grease were entirely absent. This is not known to be necessary, but since it introduced no great inconvenience, it was thought to be desirable. In the experiments with mixtures of acetone and acetaldehyde vapors, however, the acetone was confined in a reservoir closed with an ordinary glass stopcock greased with Apiezon L stopcock lubricant. There is no reason to believe that this circumstance introduced any error into the measurements since acetone vapor is relatively inert and since acetaldehyde vapor did not come into contact with this stopcock at any time.

Temperatures were measured with a copper-constantan thermocouple in conjunction with a high grade Leeds and Northrup potentiometer. The thermocouple was calibrated in the usual manner from cooling curves of several pure metals. The thermocouple wires were wound around the reaction vessel in a manner which insured good contact with the cell. Since the reaction vessel was relatively short (5.4 cm) and the electric furnace housing it was much larger, there is little reason to doubt that the tempera- of the cell was fairly uniform. A few experiments were carried out with a stirrer operated inside the furnace to circulate the air and to insure a more uniform temperature throughout. These experiments agreed well with identical experiments performed without such stirring. Every effort was made to obtain correct temperature measurements in these experiments, since it seemed possible that the discrepancy between our results and those of Leermakers might be explained by an error either in his temperature measurements or in ours.

Analyses were carried out as before by the method of Blacet, MacDonald and Leighton,[3, 4] except that in a few cases the amount of volatile gases produced in the reaction was too small to be analyzed accurately even by these micro-methods. In these cases it was assumed that the product gases contained 48.5 percent of CO, this being the average of the analyses of many other samples obtained under similar conditions. We note also that this value agrees satisfactorily with the $CO/(CO+CH_4+H_2)$ ratios obtained by Blacet and Volman[5] at 30°.

TABLE I. *Absorption coefficients of acetaldehyde vapor.*

T	3130A ϵ, LITERS MOLES^{-1} CM^{-1}	2652A ϵ, LITERS MOLES^{-1} CM^{-1}
300°C	18.9	16.9
200	17.6	17.1
100	15.7	16.7
60	14.9	—
30	14.9	17.9

In order to limit possible side reactions with the products of the photolysis, only a small fraction of the acetaldehyde present was decomposed in an experiment. The fraction of the incident light absorbed was calculated from the absorption coefficients given in Table I, taking into account the slight change in concentration of the acetaldehyde occurring during the photolysis.

Prolonged irradiation of hot acetaldehyde vapor finally results in an approximate doubling of the initial pressure. However, after a short irradiation the pressure increases less than one calculates from a measurement of the amount of carbon monoxide and methane formed. This evidently means that at elevated temperatures, as at 30°, polymer formation and decomposition both occur during the irradiation and that the polymer decomposes photochemically in a prolonged irradiation. No detailed study of the kinetics of the polymerization process has been carried out, but the existence of such a process casts doubt upon the results of those investigators who have used pressure measurements to follow the course of the reaction.[6]

CALIBRATION OF THE OPTICAL SYSTEM

The calibration of the optical system for the determination of absolute quantum yields has

[3] F. E. Blacet, G. D. MacDonald and P. A. Leighton, Ind. Eng. Chem. Anal. Ed. **5**, 272 (1933).
[4] F. E. Blacet and G. D. MacDonald, Ind. Eng. Chem. Anal. Ed. **6**, 334 (1934).
[5] F. E. Blacet and D. Volman, J. Am. Chem. Soc. **60**, 1243 (1938).
[6] J. W. Mitchell and C. N. Hinshelwood, Proc. Roy. Soc. **A159**, 32 (1937).

been done by a comparison of our results at 30°C with the absolute quantum yields of decomposition of acetaldehyde given by Leighton and Blacet.[7] At $\lambda=3130$A, these authors have given values for the decomposition quantum yield under conditions which could be closely reproduced in our apparatus except that our reaction vessel was short (5.4 cm) compared to theirs. Inasmuch as the quantum yield of decomposition is a function of the light intensity, a small correction was necessary before the comparison could be made. From the plot of γ_d *vs.* $1/(I_{abs})^{\frac{1}{2}}$ given by Blacet and Volman[5] for the decomposition quantum yield of acetaldehyde at 30°C, 200 mm pressure, and using light of wave-length 3130A, we obtain the equation:

$$\gamma_d^{30°,\ 3130\text{A},\ 200\ \text{mm}}=0.17+0.250\times10^{-6}I_{abs}^{-\frac{1}{2}}.$$

This equation gives the quantum yield of formation of carbon monoxide in a short reaction vessel as a function of the intensity of light absorbed, where the latter is expressed in the units, Einsteins cc^{-1} $sec.^{-1}$.[8] We have used it directly to set all of our quantum yield determinations at $\lambda=3130$A on an absolute basis.

At the wave-length $\lambda=2652$A, data were not available for writing an empirical equation of the same sort. Accordingly we have carried out a series of experiments to determine the form of the equation required and have used Leighton and Blacet's data at 2652A, together with our own, to fix the absolute magnitude of the constants. The equation so derived is:

$$\gamma_d^{30°,\ 2652\text{A}}=0.63+0.445\times10^{-6}I_{abs}^{-\frac{1}{2}}+0.016(CH_3CHO)I_{abs}^{-\frac{1}{2}}$$

where $\gamma_d^{30°,\ 2652\text{A}}$ is the quantum yield of carbon monoxide formation in a short reaction vessel at 2652A from acetaldehyde at 30°, (CH_3CHO) is the concentration of acetaldehyde vapor in moles per cc, and I_{abs} is the intensity of light absorbed in Einsteins cc^{-1} $sec.^{-1}$. It will be noted that the last term in this expression, which has the form of the important part of the high temperature equation, (*vide infra*) makes only a small contribution to the total quantum yield at ordinary concentrations of acetaldehyde. This contribution, moreover, is much less than that expected from an extrapolation of the high temperature results to 30°. This falling off of the high temperature term is undoubtedly to be attributed to the increased stability of acetyl and formyl radicals at temperatures below 100°.

It is of interest that an equation similar to the one above can be derived from the following set of reactions:

(1) $CH_3CHO+h\nu\rightarrow CH_4+CO$, (k_1)

(2) $CH_3CHO+h\nu\rightarrow CH_3+CHO$, (k_2)

(3) $CH_3+CH_3CHO\rightarrow CH_4+CH_3CO$, (k_3)

(4) $CH_3CO\rightarrow CH_3+CO$, (k_4)

(5) $CH_3CO+HCO\rightarrow CH_3CHO+CO$. (k_5)

Corresponding to this set of reactions the expression for the quantum yield of CO formation is:[9]

$$\gamma_d=k_1+k_2+k_4k_2^{\frac{1}{2}}k_5^{-\frac{1}{2}}I_{abs}^{-\frac{1}{2}},$$

which has the form of the empirical expression except that it omits the small high temperature term. The important feature of the above reaction scheme is that it makes the unimolecular decomposition of the acetyl radical the rate-determining step. A more complicated mechanism in which this feature was retained, but in which several alternative chain-terminating steps were included, would probably result in a rate equation almost equivalent to the one here de-

TABLE II. *Quantum yield of decomposition of acetaldehyde at 30°C with light of wave-length 2652A.*

(CH_3CHO) moles/cc $\times10^6$	I_0 ergs/sec.	I_{ABS} ergs/sec.	γ_{OBS} molecules/quantum	γ_{CALC} molecules/quantum
16.92	1820	1455	0.87	0.87
16.13	1820	1425	.86	.87
15.87	1415	1100	.89	.90
10.68	1415	904	.89	.90
10.65	1415	900	.90	.90
10.50	1420	900	.92	.90
10.60	523	332	1.19	1.07
10.57	523	332	0.99	1.07
10.84	163	105	1.46	1.41
10.67	162	105	1.39	1.41
5.36	1415	566	0.91	0.92
2.78	1415	330	.99	.98

[7] P. A. Leighton and F. E. Blacet, J. Am. Chem. Soc. **55**, 1766 (1933).

[8] We are indebted to Professor P. A. Leighton for information which made it possible to restate his results in these units.

[9] In this derivation we have assumed that reaction 3 is rapid compared to reaction 4.

TABLE III. *Summary of data.*

EXP.	T, °C	I_0 ERGS/SEC.	I_{ABS} ERGS/SEC.	t SEC.	I_{ABS} QUANTA $\times 10^{-16}$	(CH_3CHO) MOLES/CC $\times 10^{-6}$	CO-PRODUCED MOLECULES $\times 10^{-18}$	γ MOLECULES / QUANTUM	k_2
				3130A					
1	350	976	280	600	2.67	3.44	21.30	799	324
2	300	1293	378	600	3.61	3.39	14.06	389	186.5
3	200	735	431	240	1.65	9.28	3.70	224.5	41.9
4	200	4465	1930	360	11.05	5.95	6.95	62.8	38.7
5	200	699	297	720	3.48	5.98	5.74	166	40.2
6	200	4465	1353	360	8.02	3.94	4.00	49.9	39.4
7	200	4465	544	900	7.94	1.39	2.41	30.4	42.8
8	200	4465	325	1800	9.30	0.794	2.22	20.4	45.8
9	100	985	226	9000	32.3	3.04	2.48	7.7	3.1
				2562A					
10	350	1147	302	600	2.45	3.36	15.40	628	248
11	300	1435	542	360	2.64	5.25	9.76	370	127
12	300	1435	346	361	1.69	2.92	4.48	265	131
13	300	1420	165	1080	2.41	1.36	3.96	164	111
14	300	1435	81	2700	2.96	0.64	2.80	95	102
15	300	1560	363	495	2.43	2.92	6.32	260	131
16	300	555	128	810	1.40	2.89	5.97	425	129
17	300	223	52	1440	1.01	2.91	5.80	574	110
18	252	1425	313	900	3.80	2.74	5.63	148	73.4
19	212	1425	322	1200	5.23	2.89	4.23	81	39.2
20	200	1135	291	2400	9.43	3.26	6.89	73	30.0
21	100	1140	288	7200	28.0	3.19	2.08	7.4	2.7
22	96	1420	544	3600	26.4	5.25	1.79	6.8	2.1
23	96	1420	324	4200	18.4	2.85	1.05	5.7	2.5
24	96	1420	51	25800	17.7	0.40	0.52	2.9	3.2
				3303A					
25	300	43.4	5.8	1200	0.117	5.61	4.43	3775	142
26	200	44.2	5.9	2400	.239	5.62	1.88	788	30
27	100	46.3	6.2	7200	.750	5.61	0.39	52	2.0
28	60	~84.0	11.2	30420	5.73	5.58	0.42	~7.4	

rived. Unfortunately, such a calculation cannot be carried out because of the nature of the mathematical difficulties encountered. Reaction 5 in the above scheme is the simplest, but not the most probable, chain-terminating step in a mechanism embodying the desired features. It was adopted because it rendered possible the mathematical solution of the problem.

Regardless of the reaction mechanism assumed, the dependence of the quantum yield upon the light intensity proves that free radicals play a part in the reactions at room temperature at 2652A and at 3130A.

The experimental data obtained at 30° and $\lambda = 2652$A are given in Table II. The generally good agreement between γ_{obs} and γ_{calc} shows, merely, that the empirical equation fits the data from which it was originally obtained.

It has frequently been assumed that the absorption coefficient of acetaldehyde vapor does not vary appreciably with a change of temperature.[2, 6, 10] The results of our measurements, contained in Table I, show that this assumption is not fully justified for light of wave-lengths 3130 or 2652A. At any one temperature, however, we find that Beer's law is obeyed.

Using filtered light from a mercury arc Leermakers[2] found much less light absorbed by acetaldehyde vapor than one would calculate from Table I for monochromatic light. This means, of course, that light of longer wave-length than $\lambda = 3130$A was present, since light of longer wave-lengths would be absorbed much less or not at all. At temperatures above 200°, Leermakers

[10] E. I. Akeroyd and R. G. W. Norrish, J. Chem. Soc. 890 (1936).

calculated the fraction of light absorbed from these "averaged" absorption coefficients, a procedure which is unsatisfactory where the concentration of acetaldehyde differs appreciably from that at which the absorption coefficient was measured.

Akeroyd and Norrish[10] repeated and extended Leermakers' investigation of the photolysis of acetaldehyde at elevated temperatures, but their optical arrangements were not suitable for precise measurements of photochemical reaction rates.

Results and Discussion

The results of our experiments on the photolysis of acetaldehyde vapor at elevated temperatures are presented in Table III. The second column gives the temperature, the third, the light energy incident upon the acetaldehyde vapor, the fourth, the light energy absorbed by the vapor, the fifth, the time of irradiation, the sixth, the total number of light quanta absorbed, the seventh, the average concentration of acetaldehyde vapor in the quartz reaction vessel during the run, the eighth, the yield of CO obtained, the ninth, the observed quantum yield, the tenth, the observed value of the rate constant k_2 evaluated from Eq. (II) below, and given in the units Einsteins$^{-\frac{1}{2}}$ cc$^{\frac{1}{2}}$ sec.$^{-\frac{1}{2}}$.

Most experiments have been run in duplicate or triplicate, in which case data are given for one typical run. Duplicate runs ordinarily agreed within about three percent.

From the data in Table III we may test the validity of the rate law given by Leermakers:

$$\frac{d(\mathrm{CO})}{dt}=k_1 I_{\mathrm{abs}}+k_2(\mathrm{CH_3CHO})(I_{\mathrm{abs}})^{\frac{1}{2}} \qquad \text{(I)}$$

or its equivalent form:

$$\gamma_d=k_1+k_2(\mathrm{CH_3CHO})(I_{\mathrm{abs}})^{-\frac{1}{2}}. \qquad \text{(II)}$$

The quantity k_1 is negligible in all experiments except No. 21–24, where a value of 0.63, given by the experiments at room temperature, has been used in the calculations.

The experiments performed at 3130A show a satisfactory agreement with Eqs. (I) and (II), as is indicated by the approximate constancy of k_2 at any one temperature.[11] A plot of log k_2 *vs.* $1/T$ gives a linear relation with a slope corresponding to an activation energy of 8.6 kcal. Leermakers also found agreement with Eqs. (I) and (II), but his values of k_2 are considerably lower than ours and his over-all activation energy is considerably higher. Part of the discrepancy may be due to causes already discussed (erroneous absorption coefficients, etc.) but the differences are too large to be accounted for in this way entirely. Since many cross checks have been made to verify the accuracy of our experimental procedures, we feel considerable confidence in the present values. As usual in such experiments, the relative values of the rate constants may be expected to be more reliable than the absolute values.

It appears likely from data to be presented below that both methyl and formyl radicals are capable of inducing a chain decomposition in acetaldehyde at elevated temperatures. These effects may be attributed either to a catalytic action of the radicals or to definite reactions of the sort usually adopted to explain chain reactions. In view of the high reactivity of free radicals in general, it seems safe to assume that definite chemical reactions (apart from catalytic effects) occur at least part of the time in long reaction chains such as we have to deal with in the high temperature photolysis of acetaldehyde. Such an assumption leads to the conclusion that formyl radicals formed in the primary photochemical dissociation process will be short lived under the experimental conditions, either because of a decomposition into hydrogen atoms and carbon monoxide or because of a reaction with acetaldehyde to give, for example, formaldehyde and acetyl radicals. Any such scheme ultimately results in the formation from formyl radicals of methyl radicals equal in numbers to the formyl radicals destroyed. Thus we conclude that the chain-terminating step in the high temperature photolysis of acetaldehyde involves a reaction between methyl radicals, since these are the only radicals present in appreciable concentrations.

Experiments 3 to 8 (Table III) were carried out under conditions especially favorable to a study of the kinetics of the chain-terminating step. If this reaction is bimolecular, the rate law

[11] Data already published (reference 1) show that k_2 is sensibly constant over a fivefold range of light intensities. At very low light intensities k_2 falls off markedly, as discussed later.

derivable from any of the usual reaction schemes for the high temperature photolysis of acetaldehyde requires the rate of decomposition to be proportional to the first power of the concentration of acetaldehyde, which is the relationship actually found. On the other hand, if the reaction requires the presence of a third body, the third body would have to be acetaldehyde under the conditions of our experiments. Under such circumstances, the rate should be proportional to the square root of the acetaldehyde concentration, a requirement definitely excluded by the experimental facts. We conclude, therefore, that the reaction of two methyl radicals is rather accurately bimolecular. Although theoretical considerations make it appear improbable that two methyl radicals could combine to form a stable ethane molecule, the results of Cunningham and Taylor[12] on the photolysis of dimethyl mercury are difficult to explain without the use of such a reaction. The reactions:

$$CH_3+CH_3\rightarrow CH_4+CH_2$$

and

$$CH_3+CH_3\rightarrow C_2H_4+H_2$$

would produce methane or hydrogen, neither of which was obtained by Cunningham and Taylor in appreciable amounts.

In accordance with these ideas we write for the high temperature photolysis of acetaldehyde reactions 1, 2, 3 and 4 above, together with the following:

$$(6)\qquad CHO\rightarrow CO+H, \qquad (k_6)$$

$$(7)\qquad H+CH_3CHO\rightarrow H_2+CH_3CO, \qquad (k_7)$$

$$(8)\qquad CH_3+CH_3\rightarrow C_2H_6. \qquad (k_8)$$

This set of reactions is almost identical with the scheme proposed by Rice and Herzfeld[13] for the thermal decomposition of acetaldehyde.

It may be that reactions (2) and (6) occur in a single step as may also reactions (3) and (4). Reaction (8) has been selected for the reasons stated above. Its exact nature does not affect the rate law nor our considerations.

The above system of reactions leads to the rate law:

$$d(CO)/dt=k_1I_{abs}+2k_2I_{abs}+\sqrt{2}k_3k_2^{\frac{1}{2}}k_8^{-\frac{1}{2}}(CH_3CHO)I_{abs}^{\frac{1}{2}}$$

for which the over-all heat of activation at elevated temperatures will be:

$$E_{photochem}=E_3-\tfrac{1}{2}E_8=8.6\pm0.3 \text{ kcal.} \quad (III)$$

It is still uncertain whether or not the *thermal* decomposition of acetaldehyde proceeds through a free radical mechanism, but some recent evidence lends support to the assumption that it does so in the range of temperatures and pressures ordinarily employed.[14] If we assume that the first step in the thermal reaction is chiefly:

$$(9)\quad CH_3CHO\rightarrow CH_3+CHO, \quad (k_9)$$

the rate of decomposition will be given by

$$d(CH_3CHO)/dt=2k_9(CH_3CHO)+\sqrt{2}k_3k_9^{\frac{1}{2}}k_8^{-\frac{1}{2}}(CH_3CHO)^{\frac{3}{2}} \quad (IV)$$

and for the over-all heat of activation of the reaction (given by Letort[14] as 46±0.5 kcal.)

$$E_{thermal}=E_3-\tfrac{1}{2}E_8+\tfrac{1}{2}E_9=46.0\pm0.5 \text{ kcal.} \quad (V)$$

Regardless of the particular chain mechanism assumed, the coefficients of E_3 and E_8 in Eqs. (III) and (V) will be the same, hence one can subtract one from the other to get an equation independent of the chain mechanism and independent of any assumptions regarding the magnitudes of E_3 and E_8. Thus one obtains:

$$2(E_{thermal}-E_{photochem})=E_9=2(46-8.6)=74.8\pm1.6 \text{ kcal.}$$

This result is to be compared with that of Rice and Johnston[15] who, by a direct method, obtain $E_9=69.4\pm3$ kcal. The disagreement may be attributed to error in one or more of the three measurements involved or to error in the assumption made above regarding the mechanism of the first step in the thermal decomposition.

A study of the heat of activation of the thermal decomposition of azomethane-acetaldehyde mixtures by Allen and Sickman[16] taken together with data on the heat of activation of the thermal

[12] J. P. Cunningham and H. S. Taylor, J. Chem. Phys. **6**, 359 (1938).
[13] F. O. Rice and K. F. Herzfeld, J. Am. Chem. Soc. **56**, 284 (1934).
[14] M. Letort, J. chim. phys. **34**, 265, 355, 428 (1937).
[15] F. O. Rice and W. R. Johnston, J. Am. Chem. Soc. **56**, 214 (1934).
[16] A. O. Allen and D. V. Sickman, J. Am. Chem. Soc. **56**, 2031 (1934).

decomposition of azomethane alone, leads to a value of $E_3-\frac{1}{2}E_8=13.8\pm2$ kcal. This is much higher than the value 8.6 ± 0.3 kcal. obtained in the present investigation directly from the heat of activation of the photolysis of acetaldehyde. The disagreement in this case is possibly due to an erroneous assumption regarding the mechanism of the pyrolysis of azomethane.[17] A combination of the value of $E_3-\frac{1}{2}E_8$ given by the azomethane-acetaldehyde method with the heat of activation of the thermal decomposition of acetaldehyde gives a value of $E_9=64.4\pm5$ kcal. This agrees with Rice and Johnston's value (69.4 ± 3), but the agreement would appear to result from the large limits of error assigned to the two values.

Our experiments on the high temperature photolysis of acetaldehyde at 2652A lead to a heat of activation for the over-all reaction of 8.3 ± 0.5 kcal. This is equal, within the limits of error, to that observed at 3130A.

The experiments carried out at elevated temperatures with light of wave-length 2652A gave only an approximate agreement with Eqs. (I) and (II) (Table III). At 300° the effects of varying the pressure and light intensity appear to indicate that some recombination occurs at the walls. That this effect was not observed at 3130A is probably to be attributed to the higher light intensities available at that wave-length which gave rise, therefore, to a shorter mean life for the radicals. In other experiments, not listed in Table III, similar deviations were noted when light of wave-length ~3130A was used at very low incident intensities.

TABLE IV. *Rates of decomposition of acetone-acetaldehyde mixtures.*

λ, A	T°C	(CH_3CHO) MOLES/CC $\times10^6$	(CH_3COCH_3) MOLES/CC $\times10^6$	γ MOLECULES/QUANTUM	I_{ABS} EINST. CC^{-1} SEC.$^{-1}$ $\times10^{12}$	k_2
3130	200	3.33	0	41.9	9.4	38.6
	200	3.39	0	42.2	9.6	38.6
	200	2.72	3.82	26.6	13.7	36.2
	200	3.08	3.88	28.5	14.4	35.1
	200	3.36	2.76	33.4	13.5	36.5
2652	300	3.67	0	441	1.16	129
	300	3.06	0	405	0.99	132
	300	2.90	2.88	316	2.08	157.5
	300	2.85	2.84	315	1.90	152.5

[17] T. W. Davis, F. P. Jahn and M. Burton, J. Am. Chem. Soc. **60**, 10 (1938).

At 96° the reaction deviates considerably from the high temperature rate law but in the opposite direction from the above-mentioned deviations. Too few experiments were performed to characterize the rate law completely, but the sign and magnitude of the deviations showed clearly that the low temperature mechanism was becoming important at that temperature.

Several experiments were carried out with light of wave-length 3303A from a sodium vapor lamp. Although the light intensity was inconstant and exceedingly small one can estimate that the heat of activation for the over-all reaction (between 200 and 300°) was again about 8.3 kcal. The values of k_2 were smaller than those observed at 3130A, but in view of the very low light intensities used, this result should be attributed to recombination of methyl radicals at the walls. The high quantum yield observed at 60° demonstrates the existence of a pronounced chain reaction even at a temperature where the acetyl and formyl radicals may be long lived or stable. A similar result was obtained by Leighton and Blacet[7] at 3342A and 30°C, where high quantum yields were observed at very low light intensities.

A few experiments have been carried out on the photolysis of mixtures of acetone and acetaldehyde vapors in an effort to measure the relative yields of free radicals per quantum of light abosrbed in the two substances. The experimental conditions were such that the fraction of the incident light absorbed by each substance was accurately known. The results are presented in Table IV. k_2 is the rate constant calculated from the relation, $k_2=\gamma(I_{abs})^{\frac{1}{2}}(CH_3CHO)^{-1}$. Other things being equal, it may be thought of as a quantity proportional to the quantum yield of decomposition of the acetaldehyde. Since acetone does not suffer a chain decomposition under these conditions, the acetone contributes free radicals but does not otherwise alter the quantum yield appreciably.[18]

[18] Methyl radicals react slightly with acetone at elevated temperatures to yield methane and, presumably, CH_2COCH_3 (J. Leermakers, J. Am. Chem. Soc. **56**, 1899 (1934); Taylor and Rosenblum, J. Chem. Phys. **6**, 119 (1938)). Since the radical CH_2COCH_3 is undoubtedly very reactive chemically (or else unstable to yield reactive fragments) we assume that its reactions are analogous to those of methyl radicals in the system. If such is the case, the presence of acetone will have no significant effect on the quantum yield of disintegration, even at temperatures such that methyl radicals react readily with acetone.

Qualitatively the results show (1) that at 3130A the yield of free radicals is slightly greater in acetaldehyde than in acetone, (2) that at 2652A the reverse is true, and (3) that both methyl and formyl radicals are capable of inducing decomposition in acetaldehyde. This last statement is derived from the fact presented by Gorin[19] that the efficiency of the primary process for the production of free radicals from acetone at 3130A is about 0.8. Since, then, on the average about 1.6 radicals are formed in acetone per quantum of light absorbed, and since we find slightly more than that number in acetaldehyde (statement 1 above), it follows that both methyl and formyl radicals participate in the chain decomposition of acetaldehyde.

The participation of formyl radicals is probably via reactions 6 and 7 above. Alternatively, if it should later be found that formyl radicals are stable at 200°C (in the absence of acetaldehyde vapor, of course), one could suppose that formyl radicals react with acetaldehyde directly to form, perhaps, formaldehyde and CH_3CO. In either case, each formyl radical is replaced ultimately by a methyl or acetyl radical and its efficiency in promoting the decomposition of acetaldehyde will be that of the methyl and acetyl radicals formed from it.

One can calculate from the data in Tables III and IV the relative yields of free radicals per quantum of light absorbed in acetone and acetaldehyde at 3130 and 2652A. The figures so obtained are presented in Table V. Because of the high sensitivity of the calculations to small experimental errors and because of uncertainties regarding the exact role of the acetonyl radical discussed above, the results are of semi-quantitative significance only. By setting the highest of these relative values in Table V equal to unity, our value for acetone at 3130A is roughly in agreement with the absolute determination of the same quantity by Gorin. The figures in Table V therefore, can be considered as approximately correct on an absolute basis.

TABLE V. *Relative quantum efficiencies for the primary photochemical processes in the dissociation of acetone and acetaldehyde into free radicals at elevated temperatures.*

λ, A	ACETALDEHYDE	ACETONE
3130	1.00	0.70
2652	0.55	0.92

OBSERVATIONS ON THE FLUORESCENCE OF ACETALDEHYDE

It has already been reported that the fluorescence of acetaldehyde vapor decreases in intensity with increasing temperature,[1] and we have interpreted this result to mean that the predissociation process is favored by the increased vibrational energy of the activated molecules. Such an interpretation would not necessarily be valid if, as it has been suggested,[20, 21] the fluorescence of acetaldehyde were due to a combination of acetyl radicals to form activated biacetyl. This would require that the fluorescence should persist for a time comparable to the lifetime of the acetyl radicals themselves. Observations made through a pair of rotating sectors so arranged that the reaction vessel was viewed 1/400 second after illumination with light of wave-length 3130A revealed no afterglow in acetone or acetaldehyde vapor. We conclude either that the fluorescence of these substances is not due to the recombination of acetyl radicals or that the lifetime of these radicals is short compared to the interval between illumination and observation. There are no data available for an independent estimate of the lifetime of acetyl radicals under these conditions.

It has been reported that no fluorescence is observed in acetaldehyde irradiated with light of wave-length 2652A.[1, 7] A re-examination of this observation by a more sensitive method than we have used heretofore reveals a very slight fluorescence in acetaldehyde at this wave-length. If fluorescence had been found to be entirely absent, it would have been difficult or impossible to reconcile this observation with the "biacetyl" theory of the origin of the fluorescence in view of the fact established above that acetaldehyde decomposes in part via a free radical mechanism under the same conditions. The very low intensity of the fluorescence observed, however, still presents a considerable difficulty in the way of accepting the biacetyl theory of fluorescence as applied to acetaldehyde.

[19] E. Gorin, J. Chem. Phys. **7**, 256 (1939).

[20] W. A. Noyes and F. C. Henriques, J. Chem. Phys. **7**, 767 (1939).

[21] M. S. Matheson and J. W. Zabor, J. Chem. Phys. **7**, 536 (1939).

Supersonic Effects of Water Vapor in CO_2 and Their Relation to Molecular Vibrations

W. H. Pielemeier, H. L. Saxton and D. Telfair
Department of Physics, The Pennsylvania State College, State College, Pennsylvania

(Received July 25, 1939)

Acoustic interferometer measurements at approximately 28°C and atmospheric pressure were made from which the velocity and the absorption in CO_2 were computed. Various H_2O-concentrations were used with each frequency, covering the range 284 to 1595 kc/sec. At each frequency, μ (the absorption per wave-length) rises with increasing humidity to a maximum of about 0.28 and then drops slowly, but with the lower frequencies it also passes through a shelf or minor peak before saturation is reached. As the first absorption peak is approached the *velocity* drops about 10 m/sec. and a 1-m/sec. drop occurs near the minor peak. As the frequency is increased the critical H_2O-concentration h_m is increased also but at different rates for the two peaks. For the major peak $f_m=[60+8(10)^4h]$ kc/sec. for the minor peak $f_m'=[50+2(10)^4h']$ kc/sec. Thus the average lifetime of a quantum of vibrational energy is decreased rapidly with humidity. These facts are presented as graphs. They are also correlated with results by other investigators, none of whom has observed a *minor* absorption peak and dispersion region.

Most of these facts are represented quite accurately by theory, the results of which are included.

Experimental Procedure

THE experimental[1–6] and theoretical[7] work reported in this article is a continuation of a general investigation of sound velocity and absorption in gases. The *velocity* of sound is determined by measuring the "resonance" positions of the reflector in an acoustic interferometer. The frequency is obtained by beating it or one of its higher harmonics with the carrier frequency of one or more radio broadcasting stations. The absorption is determined from the changes in plate current in the driving circuit as the acoustic path is increased.

The readings used in calculating the sound velocity and the sound absorption were taken simultaneously so the two calculated values are for the same conditions. The temperature was approximately 28°C in each case. (Extremes 26° and 30°C.) The pressure was the existing barometric pressure (72–75 cm). The CO_2 was obtained from a tank of commercial grade CO_2 or by vaporizing solid CO_2 (dry ice) and passing it through dryers or humidifiers and thence through the sound chamber. In order to obtain vapor pressures between zero and 4.57 mm, two calibrated flow meters were used in parallel. One of these carried CO_2 that then passed through a drying tube containing phosphorus pentoxide (P_2O_5), and the other carried CO_2 that then passed through two humidifiers in series which were immersed in an ice bath. Then the mixed stream passed through the interferometer while the necessary plate currents and reflector positions were observed. For higher humidities only the two humidifiers in series in the proper temperature bath were used. It was found, after taking many discordant readings, that the inner wall surface of one of the interferometers was highly hygroscopic so its equilibrium humidity was adjusted to the desired value and then the CO_2 was humidified to this same value. Thus this property served as a stabilizer of vapor pressure and a bane was converted into a blessing. Unfortunately this interferometer is not adapted to the desired temperature control. Our new one has its gas chamber made of copper and it is fitted with a water jacket which is heat insulated. (See Fig. 1.)

It is fitted with a thermometer graduated to 0.1°C and with several thermocouples so that temperature gradients within the gas can be detected. It can also be fitted with a pressure gauge.

In determining the velocity the first few resonance positions were discarded because they are irregularly spaced due to interference and diffraction effects.[8, 9] For the cases of maximum

[1] W. H. Pielemeier, Phys. Rev. **34**, 1184 (1929).
[2] W. H. Pielemeier, Phys. Rev. **36**, 1005 (1930).
[3] W. H. Pielemeier, Phys. Rev. **38**, 1236 (1931).
[4] W. H. Pielemeier, Phys. Rev. **41**, 833 (1932).
[5] W. H. Pielemeier, J. Acous. Soc. Am. **7**, 37 (1935).
[6] W. H. Pielemeier, J. Acous. Soc. Am. **9**, 212 (1937).
[7] H. L. Saxton, J. Chem. Phys. **6**, 30 (1938).
[8] M. Grabau, J. Acous. Soc. Am. **5**, 1 (1933).
[9] E. Grossmann, Physik. Zeits. **35**, 83 (1934).

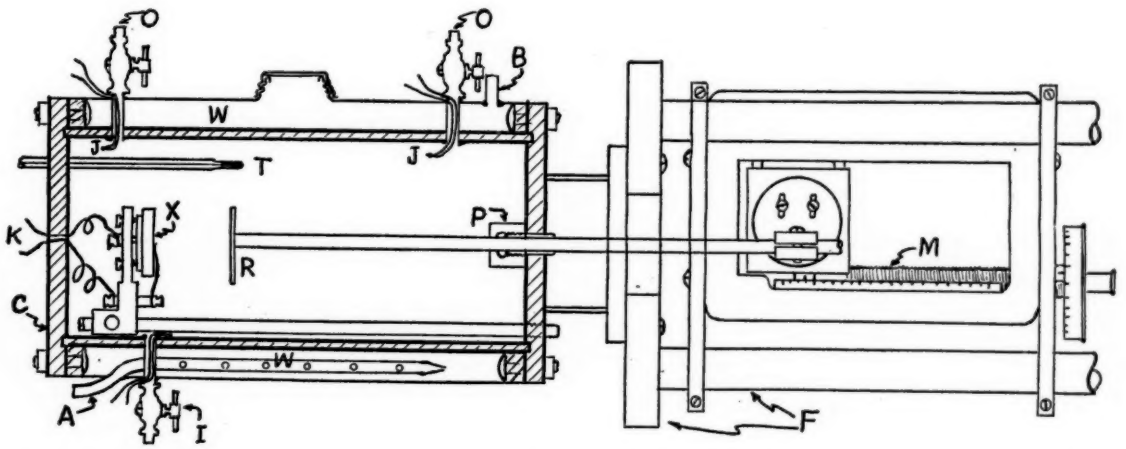

FIG. 1. Cross section of new acoustic interferometer. *A*, water inlet; *B*, water outlet; *W*, water chamber; *C*, end plate; *X*, supersonic source; *R*, reflector; *P*, packing nut; *T*, thermometer; *J*, thermocouple; *K*, electrical connections to supersonic source; *O*, *I*, stopcocks communicating with gas chamber; *F*, screw frame; *M*, precision screw.

absorption the uncertainty in the velocity is larger because the observable path length is small (30 to 40 half-wave-lengths).

To observe the frequency of the quartz plate serving as sound source the signal from the driving circuit is fed into a radio receiver which is tuned to a broadcasting station having a frequency near one of the harmonics of the quartz plate. The audible "beat note" is made to produce resonance in a telescoping tube held to the ear or it is matched with a calibrated audio oscillator. Some quartz plates vibrate in several modes simultaneously and emit supersonic waves of slightly different frequency than that observed electrically. In such cases it is best to calibrate the quartz plates with air or some other gas in the interferometer for which the sound velocity is known accurately.[10]

Two methods were used to calculate the absorption. The first method is that of computing twice the logarithmic decrement in the height of two adjacent peaks of the plate current. This method involves assumptions as to the relationship between the "amplitude" of the plate current in the driving circuit and the pressure amplitude at the crystal surface. This is recognized as an objection so the second method which does not involve these assumptions was devised. Plane waves and Alleman's[11] reflection coefficient were assumed and the fraction of a wave-length beyond the tenth peak was calculated for which the plate current should be the same as it is at the twentieth peak. This was done for several assumed absorption values. These were plotted as a μ *versus* $\Delta x/\lambda$ diagram. (See Fig. 2.) In practice the twentieth current peak was read. Then the

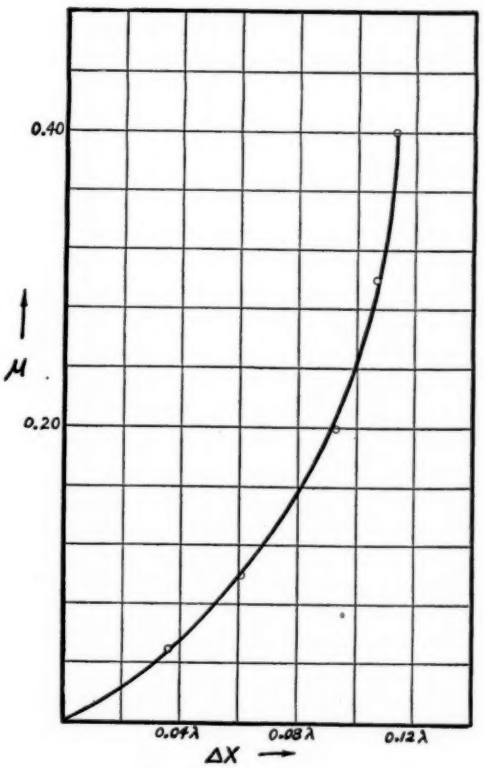

FIG. 2. μ *vs.* Δx curve.

[10] W. H. Pielemeier, J. Acous. Soc. Am. **10**, 313 (1939).
[11] R. S. Alleman, Phys. Rev. **55**, 87 (1939).

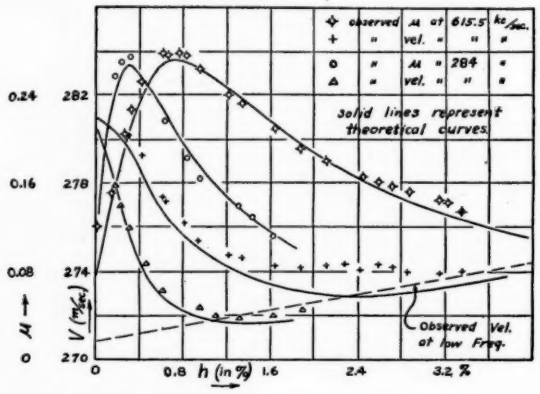

FIG. 3. Velocity and absorption curves for CO_2 as functions of water vapor concentration.

reflector was set for the same current immediately preceding and following the tenth peak. Half of the distance between these adjacent reflector positions is the half peak width Δx and the corresponding μ value is read from the curve. Since the two methods agreed quite well for those quartz plates which yielded good wave forms it was concluded that the assumption involved in the first method was essentially correct for the apparatus in question. The maximum value of μ thus obtained also agreed with the greatest value of μ obtained with a pressure vane in 1932.

EXPERIMENTAL RESULTS

The various velocities and μ values at 284 kc/sec. and 615 kc/sec. are shown as a function of h, the H_2O concentration, in Fig. 3. Similar sets of readings for other frequencies were obtained. At higher frequencies the μ peaks become more blunt or spread out and they are shifted toward larger h values. The dispersion region along the velocity curves is shifted in a similar manner. The *minor* μ peaks and the corresponding dispersion regions are shifted more rapidly. These facts are shown in Fig. 4 in which the supersonic frequencies f_m and f_m' are plotted as functions of h, the concentration producing maximum absorption per wave-length. The primed symbols refer to minor peaks.

The observed absorption at peak value is so great that a layer of CO_2 in the resonance column 12 wave-lengths thick absorbs about 99 percent of the wave energy. At the highest frequency (1595 kc/sec.) such a CO_2 layer is less than 2.1 mm thick. This is roughly comparable with the best sound absorbing materials for audible sound or black glass for visible light, or lead for x-rays.

EXPLANATION OF RESULTS

In a gas at equilibrium, the number of molecules per unit volume in any excited state is determined by the classical quantum statistics together with a knowledge of the value of the quantum of energy associated with that state as determined spectroscopically. There is then a certain probability that any molecule at collision may undergo a transition in which kinetic energy of translation is changed into internal energy or vice versa. Thus there is an average flow of energy into any internal state and, at equilibrium, an equal average flow out of that state.

If equilibrium is disturbed so that a number of molecules greater than the equilibrium number is in an excited state, there are more molecules eligible for transition out of this state and fewer molecules eligible for transition into this state than at equilibrium. Accordingly the rate out exceeds the rate in until equilibrium is restored.

In this connection the relaxation time, so often used, may be defined. In the case of a two-state gas (ground state and one excited state, other states so sparsely populated as to contribute a negligible amount to the specific heat) let us suppose that the number of molecules in the

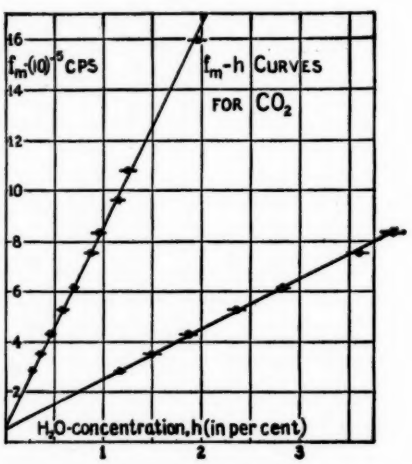

FIG. 4. The line of greater slope locates the H_2O-concentration and the corresponding sound frequency producing maximum absorption per wave-length. The other line locates the corresponding concentration and frequency for the minor absorption peak. Maximum dispersion (in wave velocity) occurs just below critical H_2O-concentration.

excited state exceeds the equilibrium number by δN_0 at a particular instant. Then if the temperature and pressure of the gas are held constant the gas will approach equilibrium by the law,

$$\delta N = \delta N_0 e^{-t/\tau}, \tag{1}$$

where the number δN is the deviation from equilibrium at any instant, t is the time and τ is a constant having the dimensions of time and called the relaxation time. The relaxation time is thus the time required for the deviation from equilibrium to reach $1/e$ of its original value under the above stated conditions. For the two-state gas this constant is related to the collision transition parameter S_{10} by the relation

$$\tau = \frac{1}{\rho S_{10}(1+N_1/N_0)}. \tag{2}$$

Dwyer's[12] work in which the persistence of molecular vibrations in iodine vapor were observed optically, illustrates the existence of a relaxation time.

In more complicated cases, where other states are involved, the relaxation time is not so readily defined. Another element of time which we prefer to use is the mean lifetime of a quantum (hereafter called mean lifetime) which is the ratio of the number of molecules in an excited state to the rate at which they undergo transitions out of the state, at equilibrium. This constant β is related to the collision transition parameters by the relation

$$\beta = 1/\rho S_{10}$$

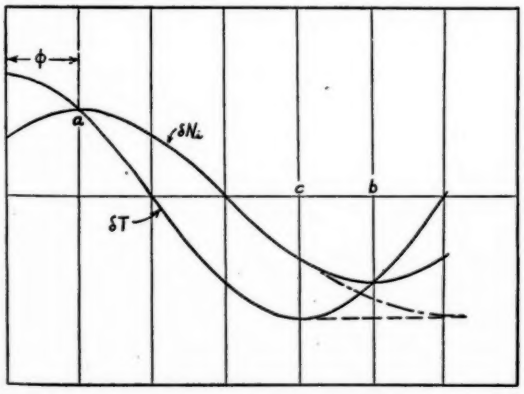

FIG. 5. Relation between δN_i and δT during propagation of sound wave, as functions of time.

[12] R. J. Dwyer, J. Chem. Phys. 7, 40 (1939).

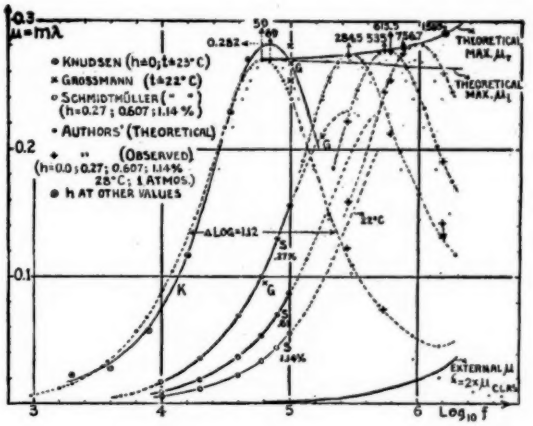

FIG. 6. The dotted bell-shaped curves are theoretical ones for $h=0$, 0.27, 0.61 and 1.14 percent. The three that approach a peak near $\mu=0.23$ are for approximately 20°C and do not include external absorption. The other dotted curves are for 28°C and twice the classical absorption is included. The solid line K is drawn through Knudsen's observed points and is extended beyond them to Grossmann's highest frequency. The other three solid lines are drawn through Schmidtmüller's observed points. Most of the authors' observed points fit the curves.

for the two-state gas and in general by

$$\beta_i = 1/\rho \sum_k S_{ik}. \tag{3}$$

The mean lifetime depends upon the collision rate and the efficiency of collisions in bringing about transitions. In pure carbon dioxide the mean lifetime for the first excited state of the deformation mode of vibration is about 4.5×10^{-6} sec. at 28°C and 730 mm pressure as determined from our data and this is in good agreement with the average of other observations. Under these conditions, an efficiency of only about 1 in 50,000 is indicated for CO_2 molecules colliding with other CO_2 molecules.

When a sound wave is passed through a gas, there result sinusoidal variations in temperature, δT, as illustrated in Fig. 5. δN_i, the variation of number of molecules in the ith internal state attempts to follow δT but the mechanism, by which δN_i is produced, introduces a phase lag ϕ of δN_i behind δT. This phase lag is small at low frequency because the mechanism has time to maintain δN_i nearly at equilibrium. If the frequency is raised, or if the mean lifetime is increased (mechanism slowed down), the phase lag increases.

The relation between phase lag and response of the excited state is graphically illustrated in Fig.

CO_2 Vibrations			Wave No., ν' ($\nu = c\nu'$)		Spectrum Type & λ	Char. Energy, E	Char. Temp., $\theta = E/R$	Fraction Excited, F, $x(10)^4$ ($F = N_i/N$)	Internal Molar Ht. Capacity, C_i
Model	Mode	State	Obs.	Calc.					
			(cm^{-1})			(cal/mole)	(°K)	For 28°C	(cal/mole/°)
O–C–O	$^2\delta_u\perp$	1st	667.5	—	Infra-red 15 μ	1898	955	400.	0.774 (x 2)
"	"	2nd	1388.4	1336	(Raman)	3948	1987	13.2	0.111 (x 2)
"	"	3rd	— (rs)	2003	—	5704	2865	0.68	0.024 (x 2)
O–O–O	$\upsilon_t\parallel$	1st	1285.5	1336	Raman	3656	1840	22.2	0.160
"	"	2nd	—	2672	—	7312	3680	0.0047	0.0014
O–O–O	$\upsilon_u\parallel$	1st	2350.1	—	Infra-red 4.3 μ	6684	3362	0.14	0.0034

(R = 1.9864 cal/mole/degree) For T = 301°K, Total C_i = 1.9495

Characteristic Energy $= E = \frac{h\nu N_0}{J} = \frac{6.547(10)^{-27}\, 2.998(10)^{10}(\nu')\, 6.064(10)^{23}}{4.185(10)^7}$

$$F = N_i/N = e^{-\theta_i/T} / 1 + \sum_j e^{-\theta_j/T}$$

$$C_i = R\,(N_i/N)(\theta_i/T)\left[(\theta_i/T) - \sum_j (N_j/N)(\theta_j/T)\right]$$

$$\mu_m = \pi R C_i / \left[C_0(C_0+R)\, C_\infty(C_\infty+R)\right]^{1/2} = \text{Max. Internal Absorption Per Wave-Length} = 0.265$$

FIG. 7. Most of the data in columns 1–6 are taken from H. Sponer.* In two cases there is a shift from nearly equal undisturbed values to the observed wave number, ν'. These are cases of "resonance splitting." They are marked (*rs*). The states of the deformation mode are doubly degenerate (two degrees of freedom); hence the factors, 2, in the last column.

5. The scales for δN_i and δT are so chosen that the curves coincide at equilibrium. In the region a to b the number of molecules in the excited state is greater than the equilibrium number and hence is decreasing. If the value of the temperature T at c could be held stationary for some time, as indicated by the dashed line, the value of δN_i would fall to equilibrium value for this δT, as indicated by dots and dashes, but since the value of δT quickly rises, δN_i never reaches this equilibrium value but instead reaches equilibrium at b. It is then apparent that an increase in phase lag decreases the amplitude of δN_i.

The observable effects of continuously increasing phase lag are first, an increasing velocity because the smaller excitation of the excited state makes the effective specific heat less, or makes the gas "stiffer";[13] second, a variation in intramolecular absorption, increasing at first because of the increasing phase lag but decreasing later because of the smaller excitation of the excited state. If the phase lag is increased by increasing the frequency of the sound wave, this latter effect gives rise to the bell-shaped absorption curves of Fig. 6.

A change in the phase lag of an excited state may be effected at constant frequency by changing the mean lifetime as given by (3). It is apparent that the mean lifetime may be shortened by increasing the density so as to bring about more collisions per molecule per second. Also, the value of S_{ik} may be changed by changing the collision efficiency which depends on temperature and on the nature of the colliding molecules. For instance, water vapor molecules possess relatively high efficiency in bringing about transitions in the CO_2 molecule at collision. The addition of 0.1 percent of H_2O molecules to carbon dioxide gas approximately doubles the average efficiency of all collisions, doubles the parameter S, and halves the mean lifetime. The authors have used principally this dependence of S on h to control the mean lifetime in CO_2.

* H. Sponer, *Molekülspektren* (Springer, 1935) Vol. I, p. 75.

[13] H. L. Saxton J. Acous. Soc. Am. **10**, 318 (1939).

Richardson[14] has found an increased supersonic absorption in CO_2 when this gas is irradiated with infra-red rays of its own natural frequency. This indicates a change in β.

The data of Fig. 3 are explained as follows. At zero h, the mean lifetime of some group A of internal states is 4.5×10^{-6} sec. This is long in comparison to the acoustic period divided by 2π which is 5.6×10^{-7} sec. at 284 kilocycles, and 2.6×10^{-7} sec. at 615.5 kc. Consequently the internal state or states involved scarcely follow the temperature changes at all with a consequent "freezing out" of their contribution to the specific heat resulting in high velocity and low absorption. As h, the H_2O concentration, is increased, the mean lifetime decreases becoming equal to first the longer acoustic period, then the shorter, and finally less than either. This increases the effectiveness of the internal specific heat bringing the velocity curves down and carrying the absorption curves through their maxima. The most obvious explanation of the observed absorption shelf and minor velocity dip is a mean lifetime for some other group B of internal states which decreases less rapidly with increasing h than does the mean lifetime for group A. There is evidence that group A is the deformation mode of vibration (see Fig. 7) and group B the symmetrical valence mode.

The pertinent mathematical formulas taken mostly from Saxton's[7] paper, with some modifications, are:

$$v'^2=(RTg/M)(1+Rd/C), \tag{4}$$

$$v^2=\text{real part of } v'^2, \tag{5}$$

$$\mu=\frac{2\pi\times\text{imaginary part of } v'^2}{\text{real part of } v'^2}+\mu_c, \tag{6}$$

$$\mu_c=\frac{2\pi\omega C_\infty}{\rho(R+C_\infty)}\left(\frac{4\eta M}{3RT}+\frac{MLR}{v^2C_\infty{}^2}\right), \tag{7}$$

$$C=C_\infty+\frac{C_vS_v}{S_v+\dfrac{j\omega}{\rho}}+\alpha\left[\frac{(C_1+C_2)S_{10}S_{21}+\dfrac{j\omega R}{\rho Nk^2T^2}\{N_1\epsilon_1{}^2S_{10}+N_2(\epsilon_2-\epsilon_1)^2S_{21}\}}{S_{10}S_{21}-\dfrac{N_0\omega^2}{N\rho^2}+\dfrac{j\omega}{\rho}\left\{\left(1-\dfrac{N_2}{N}\right)S_{10}+\dfrac{N_0}{N}\left(\dfrac{N-N_0}{N_1}\right)S_{21}\right\}}\right], \tag{8}$$

$$\beta=\frac{1}{\omega_m}\left(\frac{C_0(R+C_0)}{C_\infty(R+C_\infty)}\right)^{\frac{1}{2}}, \tag{9}$$

in which the symbols have the following significance:

v' = complex velocity of sound
v = actual velocity of sound
μ = wave-length absorption constant
μ_c = classical wave-length absorption constant
C = complex molar heat capacity
β = mean lifetime of a quantum
T = absolute temperature
R = molar gas constant
M = effective molecular weight of the mixture of gases
ρ = density of the mixture of gases.

g and d are factors resulting from the van der Waals correction (using the second virial coefficient) and given by $g=1+2b\rho/M-2a\rho/RTM$ and $d=1+a\rho/RTM$, in which a and b are van der Waals' constants.

C_∞ = effective molar heat capacity at very high frequency (vibrational modes "frozen out").

C_0 = effective molar heat capacity at very low frequency (vibrational modes wholly effective).

C_v = molar heat capacity associated with the symmetrical valence mode.

C_1 = molar heat capacity associated with the first state of one δ-mode.

C_2 = molar heat capacity associated with the second state of one δ-mode.

S_v = collision transition parameter for the symmetrical valence mode.

S_{10} = collision transition parameter for the transition from the first excited state to the ground state of the deformation mode.

S_{21} = collision transition parameter for the transition from the second excited state to the first excited state of the deformation mode.

N = total number of molecules per unit volume.

N_0, N_1, N_2 are number of molecules per unit volume in the ground, first excited, and second excited states, respectively, in one δ-mode.

ϵ_1 and ϵ_2 are the energy per molecule associated with the first and the energy per molecule associated with the second excited state of the δ-mode.

α = numerical factor (approximately 2 to take into account the degeneracy of the deformation mode) discussed later.

[14] E. G. Richardson, Nature **143**, 638 (1939).

$\omega = 2\pi$ times the acoustic frequency.
ω_m = value of ω at maximum absorption.
$j = (-1)^{\frac{1}{2}}$.

Equation (4) does not contain the classical contributions of heat conduction and viscosity. These have a negligible influence on (5) and are introduced into (6) through (7).

The complex nature of C is the mathematical formulation of its dependence on frequency and mean lifetimes with the introduction of a phase lag behind the temperature changes. This makes V'^2 in (4) complex, indicating absorption.

In (8) C_∞ includes the contribution of the rotational degrees of freedom because the temperature dependence of absorption, together with the magnitude of the absorption peak definitely indicates that the rotational states are not involved and that they have a very short mean lifetime so as essentially to maintain energy equilibrium with the external degrees of freedom. The second term on the right is the contribution of the symmetrical valence mode of vibrational (hereafter the v mode) and the last is the contribution of the perpendicular or deformation mode of vibration (hereafter δ-mode). Reference to Fig. 7 will show that the first excited state of the v mode and the first three excited states of the δ-mode contribute appreciable amounts to the molar heat capacity. The simplest method of treating a mode in which higher states than the first excited state are of importance is to treat the mode as two-state obtaining a contribution to C of $C_i S/(S+j\omega/\rho)$ and then to increase C_i to include in it the C's of the higher states. This procedure is not deemed accurate enough for the δ-mode which contributes the major portion of the absorption. Accordingly the δ-mode is considered as three-state leading to the last term of (8). α multiplies the whole term by 2 to take into account the degeneracy of this mode and also includes a factor of 1.0135 to approximate the contribution of the third excited state.

In the last term of (8) the possibility of transitions directly from the second excited state to the ground state has been ignored principally because one probably cannot discern experimentally the exact mechanism by which the second excited state receives its excitation and the $1 \rightleftarrows 2$ transition seems most likely. There are three collision transition parameters to be determined experimentally. Since S_{10} plays a major role in locating the absorption peak it is not difficult to obtain its value with considerable accuracy. The other parameters S_{21} and S_v must be of the same order of magnitude in order to afford sufficient stacking of the various contributions to C to account for the high absorption peak and the large velocity change. They may, however, exhibit a somewhat different dependence on h, the water vapor concentration.

When the parameters are assigned the following values,

$$S_{10} = S_{21}/2 = S_v = 1.5\times 10^8 + 2.1\times 10^{11} h,$$

the theoretical curves for velocity and absorption (at 284 and 615.5 kc/sec.) become those of Figs. 3 and 6. This selection is made to afford a fair over-all fit with the velocity data at 615.5 kc. insofar as the shape of the curve is concerned. The other curves then appear to fit as well, or better. These simple relations between the parameters are chosen deliberately with no attempt to produce the observed minor effects which are consequently entirely absent. μ_c is given twice its value in (7) as explained later.

The data of Figs. 3, 4 and 7, seem to indicate that the minor effects are caused by the v mode. One obtains some indication of an absorption shelf and a minor velocity dip in the theoretical calculations by making $S_v = 1.2\times 10^8 + 5.0\times 10^{10} h$ as suggested by a comparison of the slopes and intercepts of Fig. 4 and value of S_{10} previously assigned. In the plotted theoretical curve, however, no minor effects are discernible, because they are too much spread out. It will be observed in Fig. 3 that the absorption peak is more spread out when it occurs at $h = 0.68$ percent than when it occurs at $h = 0.26$ percent. Any peak above 1 percent would be very much more spread out according to the theory. An objection to this alternative choice of S_v is that it decreases the height of the theoretical absorption curve at the major peak where it is already a bit too low.

There is some indication that the form of the last term of (8) may give rise to "minor" effects with some choices of S_{21}, for instance with an S_{21} which changes its ratio to S_{10} as h changes. Indeed we have found combinations of S_{10} and S_{21} which appear to give minor effects in about the right positions, but the checks afforded have

not been conclusive. It should be remarked that we have considered and have had to reject several other mechanisms which might conceivably offer an explanation of these minor effects, for example, variation of classical absorption with the effective value of C, and dependence of S_v on h^2.

In Fig. 6, the wave-length absorption constant μ is plotted as a function of $\log f$ for fixed values of h, the H_2O concentration, of T, the temperature, and of the total pressure (one atmos.). The dotted curve peaking at 59 kc/sec. is the theoretical curve for dry CO_2 at 28°C computed from the approximate formula:

$$\mu=\frac{2\pi\omega}{\rho}\frac{RC_iS}{C_0(R+C_0)S^2+C_\infty(R+C_\infty)(\omega^2/\rho^2)}+\mu_e.$$

It includes both μ_i, the intramolecular absorption, and μ_e, the external absorption, the latter including the μ_c of (7) caused by viscosity and heat conduction. Up to nearly 100 kc/sec. μ_e is negligibly small compared to μ_i. The μ_i *vs.* $\log f$ curve for dry CO_2 is a symmetrical bell-shaped curve which at half-maximum has a width equivalent to about 3.7 octaves ($\Delta \log = 1.12$). For higher h values this μ_i curve is merely shifted to the right an amount that makes its peak frequency agree with the proper value of h_m in Fig. 4.

If the stacking of the major and minor μ-peaks changes with increasing h, as suggested by Fig. 4, the resultant maxima should fall on the line marked "theoretical max. μ_i" in Fig. 6. We find that the observed maxima fall on the line marked "observed max. μ_i." The $\Delta\mu$ between these lines is considered as the external absorption μ_e and when plotted against f appears to be a linear function of the frequency as in (7) but of about twice the value predicted by this equation. This is not unexpected. Herzfeld[15] discusses other contributions to μ_e and a discrepancy between μ_c and μ_e has been noted by several observers.

Correlation with Other Investigations

The frequency f_m for maximum absorption in "dry" CO_2 has been explicitly or implicitly reported by various investigators all the way from 54 to 220 kc/sec.* The work reported in this article shows that this wide range may be due to f_m's extreme sensitivity to water vapor. A minute trace (less than 1.5 mm) of this impurity would shift f_m from 54 to 220 kc/sec.

Pielemeier[1] reported the discovery of the marked effect of water vapor on the absorption of supersonic waves in CO_2 in 1928. In 1932 an increase in velocity at 300 kc/sec. was observed by him when freshly dried CO_2 was mixed with that which had stood for a while. Rogers[16] investigated the effect of humidity on absorption in different concentrations of CO_2 in air at a frequency of 416 kc/sec. It seems probable now that the peak he found corresponds to the minor peak in Fig. 3. (Also see point R, Fig. 4.) Rogers' hygrometer was later found to read too low and his K values should be multiplied by $\log_e 10$. These corrections place point R approximately as shown and give the expected values of m and μ for the *minor* peak. Kneser's[17] early work on velocity and Pielemeier's[4] early work on velocity and absorption in CO_2 indicate that nearly 1.5 mm of water vapor were present ($f_m = 220$ kc/sec.). Grossmann's[18] work on absorption seems to indicate that h was nearer zero but that it did not have the *same* value for the several measurements which he made. (See points G, Fig. 6.) His value (0.27) for μ_m at 100 kc/sec. is in good agreement with the writers'. His μ value for 63.6 kc/sec. and possibly that for 177.8 kc/sec. appear to be measured at $h \doteq 0.003$. (See Fig. 5.)

For a total pressure of 745 mm, $f_m \doteq 67$ kc/sec. as derived from Wallmann's[19] velocity values at 600 mm, indicating that the vapor content was nearly zero. This f_m value is in good agreement with that obtained from the velocity measurements of Railston and Richardson.[20] According to a statement by the latter that they obtained maximum dispersion at $n/p = 100$ we have $f_w = n = 74.5$ kc/sec. at 745 mm and $f_m \doteq 71.8$ kc/sec. Their curve for 42.3 kc/sec. gives $f_m \doteq 68$ kc/sec. Wallmann states, in effect, that $f_m \leqq 67$ kc/sec. for the symmetrical valence vi-

[15] K. F. Herzfeld, Ann. d. Physik **23**, 465 (1935).

* Some recent work in the laboratory of Dr. Knudsen indicates that this peak may come as low as 30 kc/sec.

[16] H. H. Rogers, Phys. Rev. **45**, 208 (1934).

[17] H. O. Kneser, Ann. d. Physik **11**, 777 (1931).

[18] E. Grossmann, Ann. d. Physik **13**, 681 (1932).

[19] v. M-H. Wallmann, Ann. d. Physik **21**, 671 (1934).

[20] W. Railston and E. G. Richardson, Proc. Phys. Soc. **47**, 533 (1935).

bration. This is in agreement with our results and others that will be mentioned later. (See Fig. 4.)

The approximate value of f_m derived from Richards and Reid's[21] measurements is 50 kc/sec. and indicates that the CO_2 was quite dry.

The work on *absorption* in "dry" CO_2 by Knudsen and Fricke[22] yields points (μ values) which they combine with points obtained by Curtis[23] in order to compare with Kneser's[24] bell-shaped absorption curve. For dry CO_2 this theoretical curve agrees approximately with Bourgin's[25] and Saxton's[7] curves. (See Fig. 6.) The points obtained by Curtis[23] are somewhat scattered. This scattering was probably due in part to small variations in H_2O content and in part to the very short sound path that he used. If his points are omitted and the characteristic bell-shaped curve of maximum ordinate 0.282 at 69 kc/sec. is fitted to Knudsen's and Fricke's points it is found that the curve fits these points very well. (See Fig. 5.) However even a maximum of 0.282 is somewhat in excess of that obtained by Saxton's[7] equation for 28°C with all possible modes and states of vibration included and stacked. Knudsen's data were obtained at 22 to 23°C. The two highest points were obtained by extrapolating to 100 percent from less than ten percent concentration of CO_2 in O_2. Possibly this accounts for the seemingly high values of μ_m.

Schmidtmüller's[26] observations stop at 100 kc/sec. but his μ-values fit the appropriate bell-shaped curves exceedingly well. We have extended these curves through our own observed values of μ_m which are not independent of frequency because they include the "classical" absorption due to viscosity and heat conduction. (See Fig. 6.) In general agreement with Schmidtmüller's observations on O_2 we find the "classical" absorption in CO_2 approximately twice its theoretical value. According to Kneser's[27] picture, this would be the start of a characteristic bell-shaped curve for classical absorption having a very high peak at very high frequency.

Eucken and Nümann[28] using a single frequency of 203.5 kc/sec. measured the *relative* absorption and the wave velocity at a number of total pressure values in dry CO_2 and in CO_2 with a concentration of about $\frac{1}{2}$ percent water vapor. This process was repeated at various temperatures ranging from approximately 20°C to 400°C. If the absorption and velocity are plotted as a function of f/p or of $\log f/p$ an absorption peak and the characteristic S curve of dispersion are obtained. The value of β for the equivalent frequency f_m at one atmosphere may be calculated from such curves for dry CO_2 for each temperature. In a similar manner β may be obtained for $CO_2+0.005$ H_2O at each temperature. Their published β-values show a continual drop with rising temperature for dry CO_2 but for CO_2+H_2O there is a small drop to a minimum value near 100°C beyond which the β-values increase slowly. They failed to find two β-values at each temperature of the CO_2+H_2O as we would expect.

A plausible explanation of these results may be given on the basis of the theory which we have suggested of different mean lifetimes for the δ and v modes. In Fig. 4, their method corresponds to a vertical trace since an increase in pressure is equivalent in its effect to a decrease in frequency. In coming down the frequency axis ($h=0$ for dry CO_2) they encounter the two peaks practically superimposed on each other. Their data indicate that increasing the temperature shifts both curves of Fig. 4 upward.

With $CO_2+0.005$ H_2O, their method corresponds to following a vertical trace in Fig. 4 at $h=0.5$ percent. In this case they should encounter two peaks but the minor peak could be easily overlooked considering the large steps in pressure variation which they took. At low temperature the peak corresponding to the upper line would predominate, and if this were raised by increasing the temperature, the mean lifetime would become shorter. Simultaneously, the v mode peak would increase in weight and in some temperature range the resultant of the two peaks would have its center of weight shifted down toward the lower curve giving an increase in mean lifetime. We should expect the resultant (or apparent) ab-

[21] W. T. Richards and J. A. Reid, J. Chem. Phys. **2**, 193 (1934).
[22] V. O. Knudsen and E. F. Fricke, J. Acous. Soc. Am. **10**, 89 (1938).
[23] R. W. Curtis, Phys. Rev. **46**, 811 (1934).
[24] H. O. Kneser, Ann. d. Physik **21**, 682 (1935).
[25] D. G. Bourgin, Phys. Rev. **50**, 355 (1936).
[26] N. Schmidtmüller, Akustische Zeits. **3**, 8 (1938).
[27] H. O. Kneser, Physik. Zeits. **39**, 806 (1938).
[28] A. Eucken and E. Nümann, Zeits. f. physik. Chemie **B36**, 163 (1937).

sorption peak, found by Eucken and Nümann[28] in dry CO_2 at 20°, to appear near 50 kc/sec. for a pressure of one atmosphere (near the common Y intercept, Fig. 4). For CO_2+0.005 H_2O at 20°C we should expect their resultant peak conditions to be $h=0.5$ percent, $f_m=400$ kc/sec., $p=1$ atmos. The two frequencies calculated from their observations are $f_m=480$ kc/sec. and $f_m'=160$ kc/sec.

At high temperature f_m and f_m' might be separated enough to make the *two* peaks detectable even by Eucken's method of changing the pressure by large steps. This would be in harmony with the excellent Figs. 2 and 3 recently published by Eucken and Küchler.[29] Their chart for CO_2+H_2O shows a large uncertainty in Z^* for the highest temperature. Probably the approaching condition for *two* detectable peaks is responsible for the large uncertainty in the location of the *resultant* absorption peak from which Z^* is computed. Except for this effect we would expect their Z^* values to decrease again at still higher temperatures as they *do* when He or H_2 are used as impurities. The slope of the Z^* curves is least (most negative) where the slope of the resultant f_m curve is greatest. Their diagrams of chemical and van der Waals potential valleys deserve attention. The same may be said of Kneser's[27] diagrams on relaxation times, etc. These and a noteworthy paper on CO_2 by L. Küchler[30] are too recent to be included in the excellent treatment of "Supersonic Phenomena" by Richards;[31] likewise a paper by Itterbeek and Mariens.[32]

Probably Eucken and Küchler's Z^*_{293}/Z^*_{673} ratio for Cl_2+CO is larger than they expected because a diatomic gas would probably not exhibit *two* β-values for a single concentration of the impurity. Only the symmetrical valence vibration is possible in the Cl_2 molecule; therefore we would expect a single f_m curve for Cl_2. We would expect the slope of this curve to be small (similar to our f_m'-curve for CO_2+H_2O partly because the probability for the proper endwise blow for the v_t vibration is less than the probability for the proper sidewise blow to start the δ-vibration). Then Cl_2+CO should have a Z^* curve of the same general shape as the corresponding curve for pure Cl_2 which however should have larger ordinates. Using the Z values published by Eucken and Becker[33] and by Schultze,[34] we plotted the curves and found them to have the shape and relative height that we expected. Conversely we might say that the absence of kinks in the Z^* curve and the value 3 or 4 for Z^*_{293}/Z^*_{673} for Cl_2+CO suggests that *our* f_m' curve for CO_2+H_2O involves the valence vibration, the only kind possible with Cl_2 molecules.

Warner's[35] results do not clash with general observations on the temperature effect although most of his values for velocity and for velocity decrements seem too great. This opinion is upheld by the recent measurements of Overbeck and Wiler.[36]

Jatkar[37] states that anomalous velocity results are due to experimental methods. If he includes dispersion in his statement we must differ with him in view of the fact that our individual $\lambda/2$-spaces agree to 0.01 mm and that we have duplicated our results many times (even in different interferometers). Such regularity as that represented in Fig. 4 would be uncanny if produced by diffraction effects. In our apparatus the walls of the gas chamber are so far from the sound beam that wall reflections can be ignored for CO_2. If Jatkar's[38] recently published value for the velocity in CO_2 at 49.4 kc/sec. had been obtained with thoroughly *dry* CO_2 we believe that the result would have been about 5 m/sec. higher. A trace of water vapor evidently shifted the maximum absorption region to the next frequency that he tried (94 kc/sec.) for which he states that the absorption was so great that he could not make measurements.

[29] A. Eucken and L. Küchler, Physik. Zeits. **39**, 835 (1938).
[30] L. Küchler, Zeits. f. physik. Chemie **B41**, 199 (1938).
[31] W. T. Richards, Rev. Mod. Phys. **11**, 36 (1939).
[32] A van Itterbeek and P. Mariens, Physica **5**, 153 (1938).
[33] A. Eucken and R. Becker, Zeits. f. physik. Chemie **27B**, 235 (1934).
[34] R. Schultze, Ann. d. Physik **34**, 41 (1939).
[35] G. W. Warner, J. Acous. Soc. Am. **9**, 30 (1937).
[36] C. J. Overbeck and E. Wiler, Paper No. 85, Washington Meeting of Am. Phys. Soc., April 27–29, 1939.
[37] S. K. K. Jatkar, J. Ind. Inst. Sci. **21A**, 455 (1938).
[38] S. K. K. Jatkar, J. Ind. Inst. Sci. **22A**, 93 (1939).

Statistical Mechanics of Condensation Phenomena in Mobile Monolayers

WILLIAM BAND
Department of Physics, Yenching University, Peiping, China
(Received September 22, 1939)

The dissociation method developed previously is modified to cover the condensation phenomena observed in mobile monolayers. The saturated tension equations are found to depend only on the number of bonds with nearest neighbors, and the mean energy per bond per molecule in the condensed phase. Assuming six bonds with mean energy per bond 3.7×10^{-14} erg per molecule, good agreement is obtained with the curves published by Adam and Jessop for the fatty acids.

INTRODUCTION

THE dissociation treatment of condensing systems has given a perfect-gas analog for the equation of the saturated vapor pressure curves of ordinary vapors,[1] and has also been extended to give a more precise equation which takes into account the finite sizes of the clusters.[2] The treatment does not require a detailed knowledge of the force-field around molecules, and is easily applied to two-dimensional vapors, monolayers, formed by large molecules at the interface of two fluids.[3]

For molecules as complex as those for which this phenomenon has been observed, it would in any case be quite impossible to represent the molecular potential field by a simple point function of the radius. The dissociation clustering method is for this reason specially suitable, since comparison of its results with experimental data gives only mean values for the interaction energy between molecules in a cluster.

The imperfect gas analog will first be developed; the resulting equations will then be simplified by neglecting the molecular sizes. While this neglect at first appears rather serious, it is found that the equations so obtained do give a fairly accurate representation of observed results with reasonable choice of bond number and energy. The reliability of such results must, however, be confined to temperatures well below the critical point.

[1] W. Band, "Dissociation Treatment of Condensing Systems," J. Chem. Phys. **7**, 324–326 (1939).
[2] W. Band, "Dissociation Treatment of Condensing Systems. II," J. Chem. Phys. **7**, 927 (1939).
[3] Adam, *Physics and Chemistry of Surfaces* (Oxford, 1938), Chapter II, § 13.

THE PARTITION FUNCTIONS

The partition function for a cluster of s molecules each of mass m, free to move only in a plane, may be written:

$$f_s(T)=A(1-\beta_s)(2\pi mskT)h^{-2}\times\exp(-W_s/kT)\cdot R_s(T). \quad (1)$$

Here A is the total area available to the film, W_s is the mean energy per cluster, $R_s(T)$ the rotational partition function, β_s is the correction for cluster size. Assuming the clusters to occupy an approximately circular area, the classical form of $R_s(T)$ will be $(2\pi/h)(2\pi C_s kT)^{\frac{1}{2}}$ where C_s is the moment of inertia about a central axis normal to the plane of A. If each molecule occupies an area a, the cluster having a circular area sa, then $C_s=ms^2a/2\pi$, and hence

$$R_s(T)=(2\pi s/h)(makT)^{\frac{1}{2}}. \quad (2)$$

To consider W_s, picture a cluster as consisting of interior molecules and of periphery molecules, the interior molecules each having on the average g bonds with nearest neighbors. For large clusters each periphery molecule will have $(\frac{1}{2}g+1)$ bonds with nearest neighbors. Suppose the potential energy of a molecule in such a cluster consists only of the interaction bonds with nearest neighbors, and the energy of attachment to the surface upon which the film is formed.

Let ϵ represent the mean energy per molecule per bond: the total energy per bond being 2ϵ. Let χ be the mean energy of attachment of a molecule with the surface. Let $\tilde{\omega}_s$ be the number of periphery molecules in a large cluster of type s. The total potential energy for the cluster will now be:

$$W_s=s\chi+(s-\tilde{\omega}_s)g\epsilon+\tilde{\omega}_s(\tfrac{1}{2}g+1)\epsilon$$
$$=s\chi+[sg-\tilde{\omega}_s(\tfrac{1}{2}g-1)]\epsilon. \quad (3)$$

For very large clusters an approximate value of $\tilde{\omega}_s$ can be derived by assuming that the area occupied by the periphery molecules is equal to the periphery of the cluster times the square root of the area per molecule. This gives at once

$$\tilde{\omega}_s = 2(\pi s)^{\frac{1}{2}}, \quad \text{large } s. \tag{4}$$

For smaller clusters, on the other hand, when, for instance, $s < g+1$, the number of periphery molecules has no definite meaning. Each molecule will be bound to every other molecule in the cluster. The total energy will then be

$$W_s = s\chi + s(s-1)\epsilon, \quad 1 < s < g+1. \tag{5}$$

When $s=1$, for a single unclustered molecule, it will be assumed, for simplicity, that

$$W_1 = \chi, \tag{6}$$

although in fact a single molecule may not be lying on the surface in the same way as a clustered molecule. There does not appear to be any data available on the difference between the energy of attachment to the surface of a single and a clustered molecule; to include it in the theory would merely add an indeterminate parameter.

For convenience a smoothed function of s will be chosen that fits approximately with both forms (3) and (5). This can be done by choosing a slightly different value of $\tilde{\omega}_s$ instead of (4), namely:

$$\tilde{\omega}_s = 2(\pi s)^{\frac{1}{2}} - 1, \tag{7}$$

and using the form (3) throughout the range from $s=2$ and up.

In this way it follows that, for all values of s,

$$W_s = sW - \phi_s, \tag{8}$$

where

$$W = \chi + g\epsilon \tag{9}$$

and for

$$s \geqslant 2, \quad \phi_s = \epsilon(g-2)[(\pi s)^{\frac{1}{2}} - \tfrac{1}{2}], \tag{10}$$

while

$$\phi_1 = g\epsilon. \tag{11}$$

Here W is the base of that part of W_s which is proportional to the cluster size, and ϕ_s is the part that increases less rapidly than s.

Finally the correction for cluster size may be written:

$$\beta_s = (1/A)\textstyle\sum_r N_r a_{rs}, \tag{12}$$

where N_r is the mean number of clusters of type r, and where a_{rs} is the effective interaction area between two clusters of types r and s. If a is the area per molecule in the cluster, assumed independent of cluster size, as before, then:

$$a_{rs} = a(r^{\frac{1}{2}} + s^{\frac{1}{2}})^2, \tag{13}$$

so that (12) may be written:

$$\beta_s = (a/A)\textstyle\sum_r N_r (r^{\frac{1}{2}} + s^{\frac{1}{2}})^2. \tag{14}$$

Using Eqs. (2), (8), (14), the partition functions (1) are expressible in terms of physical quantities.

Saturated State Equations

The equations to be assumed in this section are (a) the pressure equation, which in two dimensions becomes the surface tension equation:

$$FA = kT\textstyle\sum_s N_s/(1-\beta_s): \tag{15}$$

and (b), the law of mass action which remains in the form:

$$N_s/(N_1)^s = f_s(T)/[(f_1(T)]^s. \tag{16}$$

Introduce the familiar notation

$$\left.\begin{aligned} \mu_s &= N_s/N \\ \lambda &= \textstyle\sum_s' s\mu_s \quad \text{from} \quad s=2 \end{aligned}\right\}, \tag{17}$$

where N is the total number of molecules in the film. Then making use of the expression for $f_s(T)$ developed in the last section, the law of mass action can be written:

$$\frac{\mu_s}{1-\lambda} = s^2 e^{(\phi_s - \phi_1)/kT}\left\{\frac{1-\beta_s}{1-\beta_1}\right\} \times \left[\frac{h^3(1-\lambda)e^{-\phi_1/kT}}{4\pi^2 a^{\frac{1}{2}}(mkT)^{\frac{1}{2}}A(1-\beta_1)/N}\right]^{(s-1)}. \tag{18}$$

Writing

$$\rho = \left[\frac{h^3 e^{-\phi_1/kT}}{4\pi^2 a^{\frac{1}{2}}(mkT)^{\frac{1}{2}}}\right], \tag{19}$$

the discontinuity in μ_s occurs when

$$A(1-\beta_1)/N = \rho(1-\lambda), \tag{20}$$

at which point

$$\frac{\mu_c}{1-\lambda} = \left\{\frac{1-\beta_s}{1-\beta_1}\right\} s^2 \exp{(\phi_s - \phi_1)kT}. \tag{21}$$

TABLE I.

ACTUAL ACID	TEMPERATURE	EQUIVALENT	TEMPERATURE	FA/NkT
Lauric	14.5°C	Myristic	34.5°C	Above T_c
Tridecylic	14.5	Myristic	24.5	0.41
Myristic	14.5	Myristic	14.5	0.44
Pentadecylic	14.5	Myristic	4.5	0.75
Palmitic	12.0	Myristic	−8.0	0.56

Again from (17) applied at the point given by (20) it follows that at saturation

$$(1-\lambda)=1/(1+\sigma^*), \tag{22}$$

where

$$\sigma^*=\sum_s' s^3 \exp(\phi_s-\phi_1)/kT \cdot\{(1-\beta_s)/(1-\beta_1)\}. \tag{23}$$

With (21), (22), and (17) in (15) it easily follows that

$$FA(1-\beta_1)/NkT=(1+\nu)/(1+\sigma^*), \tag{24}$$

where

$$\nu=\sum_s' s^2 \exp(\phi_s-\phi_1)/kT. \tag{25}$$

The Eq. (24) gives the relation between the film tension F and its area per molecule A/N at the saturation or transition point between the expanded and the condensed phases. This result is accurate, and methods of approximation can be applied similar to those outlined previously.[2] In the present paper only the roughest approximation will be used, namely that in which the β_s are all neglected.

In this case Eq. (24) becomes simply

$$FA/NkT=(1+\nu)/(1+\sigma), \tag{26}$$

where

$$\sigma=\sum_s' s^3 \exp(\phi_s-\phi_1)/kT. \tag{27}$$

Referring to (10) and (11), it is seen that the two sums ν and σ, are given explicitly by

$$\left.\begin{aligned}\nu&=\exp\{-(3g-2)\epsilon/2kT\}\sum_s' s^2 \times\exp\{(g-2)(\pi s)^{\frac{1}{2}}\epsilon/kT\}\\ \sigma&=\exp\{-(3g-2)\epsilon/2kT\}\sum_s' s^3 \times\exp\{(g-2)(\pi s)^{\frac{1}{2}}\epsilon/kT\}\end{aligned}\right\}. \tag{28}$$

METHOD OF ANALYSIS

Write

$$B=\exp\{-(3g-2)\epsilon/2kT\} \tag{29}$$

and

$$\alpha=-(g-2)\pi^{\frac{1}{2}}\epsilon/kT, \tag{30}$$

$$S_1=\sum_s' s^2 \exp-\alpha s^{\frac{1}{2}}, \tag{31}$$

$$S_2=\sum_s' s^3 \exp-\alpha s^{\frac{1}{2}}. \tag{32}$$

Then

$$\nu=BS_1, \tag{33}$$

$$\sigma=BS_2. \tag{34}$$

So long as α is not less than about 5, these series both converge fairly rapidly, six or seven terms of S_1 and nine or ten terms of S_2 being enough for present purposes. If α is less than about 5, direct summation becomes tedious and it seems better to transform the sums to integrals:

$$S_1 \text{ becomes } I_1=\int_2^\infty s^2 \exp(-\alpha s^{\frac{1}{2}})ds \tag{35}$$

and

$$S_2 \text{ becomes } I_2=\int_2^\infty s^3 \exp(-\alpha s^{\frac{1}{2}})ds. \tag{36}$$

These can be evaluated by elementary methods in finite terms:

$$\left.\begin{aligned}I_1&=2C\exp(-\alpha 2^{\frac{1}{2}})\\ I_2&=2D\exp(-\alpha 2^{\frac{1}{2}})\end{aligned}\right\}, \tag{37}$$

where

$$C=4\times 2^{\frac{1}{2}}/\alpha+20/\alpha^2+40\times 2^{\frac{1}{2}}/\alpha^3 +120/\alpha^4+120\times 2^{\frac{1}{2}}/\alpha^5+120/\alpha^6, \tag{38}$$

and

$$D=8\times 2^{\frac{1}{2}}/\alpha+56/\alpha^2+168\times 2^{\frac{1}{2}}/\alpha^3 +840/\alpha^4+1680\times 2^{\frac{1}{2}}/\alpha^5+5040/\alpha^6 +5040\times 2^{\frac{1}{2}}/\alpha^7+5040/\alpha^8. \tag{39}$$

Let

$$G=2B\exp(-\alpha 2^{\frac{1}{2}}), \tag{40}$$

then

$$\nu=G\cdot C, \tag{41}$$

$$\sigma=G\cdot D. \tag{42}$$

From (29) and (30) B can be written as a function of α and g:

$$B=\exp\{\alpha(3g-2)/(g-2)2\pi^{\frac{1}{2}}\}, \tag{43}$$

TABLE II.

$g\epsilon=22\times10^{-14}$ erg,		$g=6$,		$\alpha T=1829.$
t°C	24.5	14.5	4.5	−8.0
α	6.145	6.360	6.589	6.900
$S_1\cdot10^4$	10.03	7.172	5.051	3.137
$S_2\cdot10^4$	25.11	17.62	12.21	7.412
$B\cdot10^{-3}$	1.026	1.309	1.694	2.404
$1+\nu$	2.028	1.940	1.855	1.765
$1+\sigma$	3.576	3.307	3.070	2.782
$\frac{1+\nu}{1+\sigma}$	0.567	0.587	0. 604	0.631

and by (40), G also can be expressed in terms of α and g.

In cases where there is no information available concerning either the number of bonds, g, or the energy of interaction 2ϵ, it is possible to use the above equations to obtain curves of $(1+\nu)/(1+\sigma)$ against α for several possible values of g. Fitting these curves to the data of FA/NkT will then determine both g and ϵ; g by the slope of the curve, and ϵ through the relation between α and T from Eq. (30). Whether summation or integration methods should be used would have to be determined by a preliminary rough check on what range of α-values was going to be significant.

The results derivable from this analysis of the saturated state curves are therefore the mean number of bonds per clustered molecule, and the mean energy of interaction between clustered molecules. Since, from (8), (9) and (10), the latent heat of formation of the condensed phase from the expanded phase, per molecule, is asymptotically $g\epsilon$, this physical quantity is also derivable from the analysis.

Application to the Fatty Acids

The only set of data available in sufficient details is that on the fatty acids.[4] Fortunately the latent heat can be estimated from the tension changes during condensation. According to Adam[5] this is 22×10^{-14} erg per molecule in the case of myristic acid. Langmuir[6] has given evidence that the number of bonds is six, $g=6$. These values determine the quantity αT in Eq. (30), and the significant values of α are thus known in advance, simplifying the preliminary analysis.

Table III.

α	5.90	6.00	6.10	6.25	6.50
G	0.3702	0.3608	0.3496	0.3360	0.3120
C	1.934	1.878	1.823	1.759	1.634
D	5.857	5.630	5.422	5.117	4.665
$1+\nu$	1.716	1.678	1.637	1.589	1.510
$1+\sigma$	3.168	3.032	2.895	2.719	2.455
$\frac{1+\nu}{1+\sigma}$	0.542	0.554	0.565	0.585	0.615

[4] Adam and Jessop, Proc. Roy. Soc. **A110**, 423 (1926), Fig. 1.
[5] Reference 4, p. 431.
[6] Langmuir, J. Chem. Phys. **1**, 769 (1933), Fig. 7.

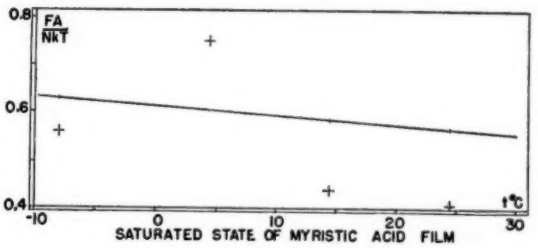

Fig. 1. Experimental points, crosses: Curve, theoretical.

Unfortunately the tension data on different acids are available for only one temperature each; they have to be reduced to equivalent data on a single substance at different temperatures before they can be used. To do this Adam's statement[5] may be accepted, that the addition of one carbon atom to the molecule is equivalent to reducing the state of the original molecule by about ten degrees C. The Table I is then derived for the saturated state of myristic acid films from the data of Adam and Jessop.[4] For these temperatures, with $g=6$, and with $g\epsilon=22\times10^{-14}$ erg, the significant range of α-values is from 5.0 to 8.0. The direct summation method was therefore employed. The results are summarized in Table II. These results are shown in Fig. 1, for comparison with the values of FA/NkT in Table I. The agreement is about as good as the precision of the data. The experimental curves of F against A are so flat that the exact point where condensation begins cannot be determined with any high degree of precision.

The integration method was also carried out, with results summarized in Table III; they agree finally with the summation results to within a few percent. This method would thus be sufficiently reliable in cases where direct summation was too tedious.

Rough calculations have been made for $g=3$ and $g=4$; the results set the curve considerably higher than that for $g=6$, and give it a much steeper gradient. Thus $g=6$ gives definitely better agreement with the data. The curve could be brought lower if desired, by choosing a slightly smaller value for $g\epsilon$ than that given by the latent heat data.

Statistical Fluctuations in Autocatalytic Reactions

MAX DELBRÜCK[1]
William G. Kerckhoff Laboratories of the Biological Sciences, California Institute of Technology, Pasadena, California
(Received August 29, 1939)

The differential equations describing the statistical fluctuations of a simple autocatalytic reaction mechanism are set up and solved completely. The fluctuations are found to approach a constant limiting value when the amount of reaction product is large compared to the amount which initiates the reaction. The relative fluctuations which arise from the reaction mechanism are then equal to the reciprocal of the square root of the initial number of particles. Conversely the fluctuation in the time required to attain a threshold amount of reaction product also approaches a limiting value for high thresholds. This limiting value is greater than one time unit if the reaction is initiated by one particle, and becomes equal to one divided by the square root of the number of initiating particles if this number is large.

RECENT work by Kunitz and Northrop, and by Herriott[2] on the proteolytic enzymes, trypsin and pepsin, has shown that these substances can be produced from precursors by an autocatalytic process, the rate of production of the enzyme being proportional both to the concentration of precursor and to the concentration of the enzyme itself. Such a type of reaction can function like an amplifier, inasmuch as a very small amount of enzyme is sufficient to initiate the reaction and to let the amount of enzyme grow exponentially to macroscopic size. In fact one molecule of pepsin should be sufficient under favorable conditions to convert in a few hours any weighable amount of pepsin-precursor. In experiments designed to test this one must be prepared to encounter very large statistical fluctuations in the amount of reaction taking place in a given time, or vice versa in the time required to effect a given amount of reaction. Since in all other cases of chemical kinetics the statistical fluctuations are negligibly small, these reactions offer a unique opportunity for the study of such fluctuations.[3] A closer theoretical study of their finer details seems therefore desirable as an aid for the design of experiments and to prepare the way for a discussion of the possible importance of such fluctuations for cell physiology. From such an aim we are however still far removed, because for none of the biological S curves, in which enthusiastic biological speculators have seen the manifestation of autocatalytic reactions has such a mechanism ever been established.

For the sake of simplicity of calculation it will be assumed that the amount of precursor throughout the course of the reaction is large compared to the amount of enzyme and that the change in concentration of precursor is negligible, i.e., we will only consider the initial stages of the reaction.

We further assume that the rate of the reaction is always strictly proportional to the concentration of enzyme. Since we want to consider the case of few molecules we have to explain a little further what we mean by "rate." Let us consider an experiment where we set up at time zero a very large number of samples containing each one molecule of enzyme and a large amount of precursor. We want to assume then that the fraction of samples which form their second

[1] International Fellow of the Rockefeller Foundation.

[2] For a summary see J. H. Northrop, *Crystalline Enzymes, The Chemistry of Pepsin, Trypsin and Bacteriophage* (Columbia University Press, New York, 1939).

[3] While we do not feel qualified to review adequately the chemical literature on autocatalysis it should be pointed out that none of the well-known autocatalytic reactions lend themselves to a study of these fluctuations. Those reactions where the catalyst is the H^+ ion are unsuitable, because the H^+ ion concentration cannot be made small enough. The photochemical decomposition of N_2O_5 into NO_2 and O_2 is autocatalyzed by the light-absorbing NO_2

$$NO_2+h\nu\rightarrow NO+\tfrac{1}{2}O_2$$
$$NO+N_2O_5\rightarrow 3NO_2$$
$$NO_2+h\nu+N_2O_5\rightarrow 3NO_2+\tfrac{1}{2}O_2.$$

But here the spontaneous thermal decomposition of N_2O_5 is too fast even at 0°, so that this reaction initially will furnish more NO_2 than the autocatalytic reaction.

enzyme-molecule in a given time-element is always proportional to the fraction of samples which have not yet done this at the beginning of the time-element, and independent of the time which has elapsed since the samples were set up. This means that we rule out a reaction mechanism in which the reaction consists of separable steps each requiring the completion of its forerunner before it can occur, and each requiring a finite average time for its completion. In actual fact it is quite probable that most autocatalytic reactions will be separable into such steps, but our simplified model will still apply to such cases if one step of the reaction is much slower than all the others, for instance if the average time between collisions of an enzyme-molecule with any precursor-molecule is sufficiently long, and this can always be secured by working at low concentrations.

1. The Fundamental Equation

In ordinary reaction-kinetics we are only concerned with the average number of molecules of each reactant as function of time, since the deviations from these average values in individual cases are negligibly small. For our model we would then have

$$dn/dt = kn, \quad n = n_0 e^{kt}, \tag{1}$$

where n is the number of enzyme-molecules present at time t, and n_0 is the number of enzyme molecules present at time zero. k is the reaction rate constant, which will depend on the concentration of precursor, but will be constant during the course of the reaction according to our assumption. This equation will hold also for our case if we substitute for n the *average* number of molecules $\bar{n}$, averaged over a very large number of samples starting from the same initial conditions. We must therefore write

$$d\bar{n}/dt = k\bar{n}, \quad \bar{n} = \bar{n}_0 e^{kt}. \tag{2}$$

However we want to inquire beyond this information about the average number $\bar{n}$, into the statistical fluctuations of n as function of time and of n_0. We therefore do not deal with n as function of time but with the probability of having n particles at time t. This probability, i.e., the fraction of a very large number of similar samples, which contains n particles, we will call $p_n(t)$. Instead of the one function $\bar{n}(t)$ we therefore will have to handle the infinite series of functions $p_n(t)$.

Let us find the differential equation determining p_n as function of time. The probability that of n particles any one will double in the small interval dt is equal to $nkdt$. The samples in which this happens will leave the class p_n and enter the class p_{n+1}. The probability that more than one particle will double in this interval is small of a higher order in dt and can therefore be neglected. The quantity p_n will change in the time interval dt for two reasons. Firstly it will increase by $(n-1)kp_{n-1}dt$ because so many of the samples containing $n-1$ particles will produce one additional particle and will thereby be promoted to the class p_n. Secondly it will decrease by $nkp_n dt$ because so many of the samples containing n particles will advance to the class p_{n+1}.

We therefore have as our differential equation

$$dp_n/dt = (n-1)kp_{n-1} - nkp_n. \tag{3}$$

These equations, together with the initial conditions $p_n(0)$ will determine all the functions p_n for all times.

2. The Standard Deviations

Before we go on to establish and to discuss the general solutions of these equations we will consider what we can derive about the fluctuations without explicit knowledge of the p_n. It will be found that we can follow the change in the mean square deviation of the number of particles from their mean value without knowing the actual distribution of the samples over the classes p_n at any time.

The standard or root mean square deviation s is defined by

$$s^2 = \langle (n-\bar{n})^2 \rangle_{Av} = \langle n^2 \rangle_{Av} - \bar{n}^2.$$

Let us consider the change in time of the mean square $\langle n^2 \rangle_{Av}$.

We have, by definition,

$$\frac{d}{dt}\langle n^2 \rangle_{Av} = \frac{d}{dt}\sum_{n=0}^{n=\infty} n^2 p_n.$$

The right-hand side we are now going to differentiate term by term and to substitute for the

derivative of p_n its value from the fundamental Eq. (3)

$$=\sum n^2[(n-1)kp_{n-1}-nkp_n].$$

Now, since we have to sum over all values of n, we can always combine the $(n+1)$ term of the first member with the n term of the second member, and obtain in this way

$$\begin{aligned}&=\sum[(n+1)^2n-n^3]kp_n\\&=\sum(2n^2+n)kp_n\\&=2k\langle n^2\rangle_{Av}+k\bar{n}.\end{aligned}$$

Now we know already $\bar{n}$ as a function of time, Eq. (2); therefore this is a differential-equation for $\langle n^2\rangle_{Av}$ alone. Its solution is

$$\langle n^2\rangle_{Av}=Ae^{2kt}-\bar{n}_0e^{kt}=A(n/\bar{n}_0)^2-n. \tag{4}$$

The mean square deviation is obtained from this by simply subtracting $\bar{n}^2$. The constant A will be determined by the standard deviation at time zero, which we will call s_0^2. Thus we obtain for the relative standard deviation at an arbitrary time

$$s^2/\bar{n}^2=s_0^2/\bar{n}_0^2+1/\bar{n}_0-1/\bar{n}. \tag{5}$$

Here the last term is negligible compared to $1/n_0$ at any late time when $\bar{n}\gg n_0$. The relative standard deviation is then the sum of its initial value and the constant $1/n_0$. If the initiating amount is obtained by sampling from a large reservoir, the first term will also be $1/\bar{n}_0$ and the total relative standard deviation will be twice this value.

3. A Complete Solution of the Fundamental Equations for the Case, in Which the Initial Number of Particles is Known

So far we have derived information about the average number of particles and about the standard deviation from this average as functions of time. This would be sufficient for all practical purposes if we could be assured that the probability distribution was always normal. However, since we have already seen that in cases where the initial number of particles is very small the standard deviation is of the same order of magnitude as the mean, the distribution is not likely to be normal and we must try to obtain the complete distribution. This is fortunately possible.

The Eqs. (3) are linear. The general solution consists therefore of the linear combinations of any linearly independent complete set of solutions. As such we can choose those for which we have at time zero a definite number, say n_0, particles, i.e.,

$$p_{n_0}=1 \tag{6}$$

and $p_s=0$ for all values of s unequal to n_0. This particular set of solutions, which conforms to the initial conditions just mentioned we will designate by $p_n^{(n_0)}$. We find

$$p_n^{(n_0)}=\frac{(n-1)!}{(n_0-1)!(n-n_0)!}\frac{{n_0}^{n_0}}{\bar{n}^{n_0}}\left(1-\frac{n_0}{\bar{n}}\right)^{n-n_0}. \tag{7}$$

These are functions of the initial number of particles, n_0, of the time (through $\bar{n}$, which is a function of n_0 and of the time, see Eq. (2)), and of n, the index number of the function, designating the class of samples the frequency of which is given by the formula. It is easily verified that these functions satisfy both the initial conditions and the differential-equations. To prove that the initial conditions are satisfied, one simply has to put $\bar{n}=n_0$. To prove, that the differential equations are satisfied one has to substitute our solution in both sides of these equations. It is then found that both sides are equal to

$$kn_0\cdot p_n^{(n_0)}\cdot(n-\bar{n})/(\bar{n}-n_0). \tag{8}$$

4. Reactions Initiated by One Particle

We will use the solution (7) first to consider the case where we start with one particle at time zero, $n_0=1$. We then have

$$p_n^{(1)}=\frac{1}{\bar{n}}\left(1-\frac{1}{\bar{n}}\right)^{n-1}. \tag{9}$$

We are mainly interested in the probability distribution at a late time, when $\bar{n}$ represents a chemically or enzymatically measurable amount, i.e., when $\bar{n}$ is large compared to one. We can then replace the second factor by an exponential function and obtain a very simple expression for our distribution, *viz.*

$$p_n^{(1)}=\frac{1}{\bar{n}}e^{-n/\bar{n}}. \tag{10}$$

We see then that the distribution is by no means normal. At all times the probability of finding one particle is greater than the probability of finding any other specified number of particles. In particular, the probability of finding the average number of particles is $1/e$ times the probability of finding one particle. As function of n the probability falls off with a "decay-constant" $1/\bar{n}$. It is easily verified, that the standard deviation is in this case equal to the mean in agreement with the general formula (5).*

5. Reactions Initiated by n_0 Particles

Returning to the general solution (7) we will also here restrict our discussion to a phase of the reaction when the number of particles is already large compared to the initial number n_0.

We will first find out for which value of n the distribution has its maximum. To do this we observe that p_{n+1} and p_n stand in the simple relation

$$p_{n+1}=\frac{n}{n+1-n_0}(1-n_0/n)\cdot p_n. \tag{11}$$

p_{n+1} arises from p_n by multiplication with a factor which is at first greater than one and continuously decreases. p_n will have its maximum where this factor is equal to one. This occurs for

$$n=\bar{n}(1-1/n_0). \tag{12}$$

At this point the distribution has therefore its maximum. It is interesting to note that the maximum does not occur at the average value $\bar{n}$, but a definite distance towards smaller values of n away from it.

We now want to know what the distribution looks like in the neighborhood of this maximum. We introduce a new variable f to replace n. f shall measure the distance from the maximum on the n axis and its unit shall be this $n_{\max}$. We define f by the equation

$$\begin{aligned} n&=n_{\max}(1+f)\\ &=\bar{n}(1-1/n_0)(1+f). \end{aligned} \tag{13}$$

Substituting this value for n into our solution (7) we obtain (for n large compared to n_0)

$$p_n=C\left[(1+f)(1-n_0/\bar{n})^{f\bar{n}/n_0}\right]^{n_0-1}, \tag{14}$$

where C is independent on f. Here we can replace

$$(1-n_0/\bar{n})^{f\bar{n}/n_0} \quad \text{by} \quad e^{-f}.$$

If $\log p_n$ is then developed into a power series of f it is found that the first-order term vanishes, the second-order term has the coefficient $-\frac{1}{2}(n_0-1)$ and the terms of higher order in t are small in the region where p_n is appreciable. We obtain therefore

$$p_n=C\cdot e^{-\frac{1}{2}(n_0-1)f^2}. \tag{16}$$

This is indeed a normal distribution with a relative standard deviation equal to one divided by the square root of the initial number of particles, as given in (5). Under ordinary experimental conditions already the initiating sample n_0 would exhibit a standard deviation from n_0 by this amount. The square of the total final relative standard deviation of n would then be the sum of these two (5), i.e. it would be $2/\bar{n}_0$.

6. The Distribution of the Time at Which a Given Number of Particles is Attained

Up till now we have been concerned with the probability distribution of the number of particles at a given time. This corresponds to a type of experiment, where we set up at time zero a large number of samples with each containing the same number of initiating particles, and where we test at a certain later time the number of particles produced in the interval in each sample. We can, however, look at the problem of the fluctuations from a different standpoint. Suppose that a certain threshold-value n is required to produce a given effect. We must then expect great fluctuations in the time required by different samples starting with the same number of particles to attain this threshold-value. Let us call the fraction of samples which

* In general experimental conditions will be such that also initially we will have a statistical distribution rather than having precisely one particle in each sample. We can however approximate the above condition by making the *average* initial number of particles, $\bar{r}$, small compared to unity. Then $e^{-\bar{r}}$ samples will have no particles, $\bar{r}e^{-\bar{r}}$ will have one particle and a much smaller fraction $(\bar{r}^2/2)e^{-\bar{r}}$ will have two particles. These will cause an alteration in the final distribution, which works out to be

$$f(n)=Cp_n^{(1)}\left[1+\frac{\bar{r}}{2}\frac{n-1}{\bar{n}}\right]. \tag{10'}$$

The change becomes large for $n/\bar{n}>1/\bar{r}$.

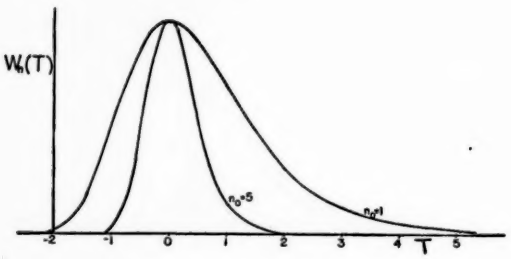

FIG. 1. The distribution in time of the arrival at a high threshold value of samples, starting from one or five particles.

attain this threshold-value in the time interval between t and $t+dt$ $w_n(t)dt$. This fraction is given by

$$w_n(t)dt=(n-1)kp_{n-1}dt, \tag{17}$$

because this is the rate at which the class $n-1$ goes over into the class n, multiplied by the abundance of the class $n-1$. By virtue of Eq. (3) it follows from this that

$$-w_n(t)=\frac{d}{dt}(p_1+p_2+\cdots p_{n-1}). \tag{18}$$

That means that the flux into the class n is equal to the net loss of all the lower classes.

Substituting our general solution (7) into (17) we obtain

$$w_n(t)=C\frac{1}{\bar{n}^{n_0}}\left(1-\frac{n_0}{\bar{n}}\right)^{n-1-n_0}. \tag{19}$$

For late times, when $\bar{n}$ is large compared to n_0, this can again be approximated by

$$w_n(t)=C\frac{1}{\bar{n}^{n_0}}\cdot e^{-(n/\bar{n})n_0}, \quad \bar{n}=n_0\cdot e^{kt}. \tag{20}$$

Here C stands for all the factors which are not dependent on the time, and $\bar{n}$ is given by (2) as a function of t and of n_0.

Let us now take a closer look at these functions $w_n(t)$, which give the rate at which samples starting with an equal number of particles reach their threshold-value of n particles. For n greater than n_0+1 they all start with zero at time zero (when $n=n_0$), then rise to a maximum and fall again to zero for large times. The maximum is easily found to occur at

$$t_{\max}=\frac{1}{k}\log\frac{n-1}{n_0} \quad \text{when} \quad \bar{n}=n-1. \tag{21}$$

We will introduce a new time-variable T, taking $t_{\max}$ as the origin and $1/k$ as the time unit. This time unit is the span in which the average number of particles increases by a factor e,

$$\bar{n}=(n-1)e^T. \tag{22}$$

Substituting this in (20) we obtain

$$w_n(T)=C\exp\left[-n_0(T+e^{-T})\right]. \tag{23}$$

This function we have plotted for $n_0=1$ and for $n_0=5$ in Fig. 1. It will be seen that the curve for $n_0=1$ is rather asymmetrical, it rises in two time units from 0.005 to its maximum and takes five time units to fall back to the same value. The spread in time naturally is smaller when we start with more than one particle. For large values of n_0 we obtain a very sharp maximum, we can then expand the second term in the exponent on the right-hand side of (23) and obtain a simple normal distribution curve

$$w_n(T)=C\exp\left(-\frac{n_0}{2}T^2\right). \tag{24}$$

The standard deviation of this distribution is again equal to one divided by the square root of the initial number of particles:

$$\langle\Delta T^2\rangle_{Av}=1/n_0. \tag{24a}$$

LETTERS TO THE EDITOR

This section will accept reports of new work, provided these are terse and contain few figures, and especially few halftone cuts. The Editorial Board will not hold itself responsible for opinions expressed by the correspondents. Contributions to this section should not exceed 600 words in length and must reach the office of the Managing Editor not later than the 15th of the month preceding that of the issue in which the letter is to appear. No proof will be sent to the authors. The usual publication charge ($3.00 per page) will not be made and no reprints will be furnished free.

Raman Effect of Fluorochlorobromomethane

We have observed eleven Raman lines for fluorochlorobromomethane, using our usual equipment.[1] The compound was cooled during exposures by means of a stream of air at room temperature. Illumination was by means of eight concentric neon-mercury lamps. No filters were used, but there was no evidence of photochemical decomposition during the exposures. The Steinheil 3-prism type GH spectrograph employed was thermostatted at 35±0.1 degrees. Eastman Spectroscopic plates type 1-J were used. Results obtained are shown in Table I.

TABLE I. *Raman lines of fluorochlorobromomethane.*

$\Delta\bar{\nu}$ cm^{-1}	% Mean Deviation	Exciting Lines*	No. of Readings	Relative Intensities
225.0	0.36	*a b c d*	10	10
313.0	.35	*a b c d*	13	9
425.0	.31	*a b c*	10	9
648.9	.19	*a c*	6	6
658.7	.18	*a b c d*	10	10
735.1	.10	*c*	2	2
773.4	.23	*a c*	3	5 (broad)
1062.6	.24	*a c*	3	3 (diffuse)
1204.6	.17	*a c*	4	4
1301.7	.11	*a c*	4	5
3017.8	.05	*a b c*	10	7 (broad)

* a=4046, b=4077, c=4358, d=4347.

About 6 cc of fluorochlorobromomethane was used for this study. It was prepared according to the procedure of Swarts from dibromochloromethane.[2] The latter substance was made from chloroacetal and contained bromoform as an impurity. Dibromofluoromethane was expected to be present in small amounts in the fluorochlorobromomethane, and actually 3 faint lines were observed in the Raman spectrum of the latter substance which can be attributed to this impurity. ($\Delta\bar{\nu}$=169.7, 359.6, 622.2 as Stokes lines from 4358.) Two additional faint lines were observed at $\Delta\bar{\nu}$=278.7 and 458.2 as Stokes lines from 4358 which are probably due to some other impurity. The density at 16°C of the fluorochlorobromomethane was 1.994. Its boiling point was 38–39° at 734 mm. Further consideration of these results will appear in a later publication.

GEO. GLOCKLER
G. R. LEADER

University of Minnesota,
Minneapolis, Minnesota,
December 5, 1939.

[1] Glockler and Bachmann, Phys. Rev. **54**, 970 (1938).
[2] Swarts, Bull. Acad. Royale de Belgique [3] **26**, 102–106 (1893).

On the Induction Period in Thermal Explosions

In connection with a recent paper by Rice and Campbell[1] it may be noted that the calculation of the induction period cannot be regarded as an appropriate method for comparing the theory of thermal explosions with experiment and, in particular, for computing the thermal effect of explosive reactions, and this for the following reasons.

(1) In close vicinity to the explosion limit such calculations inevitably become very inexact because of the marked dependence of the induction period on the distance of the experimental point from the explosion limit, which distance cannot be exactly determined, and also because of the mathematical difficulties involved.

(2) The length of the induction period is usually of the same order of magnitude as the time required for the admission of the reacting mixture into the explosion vessel and for its attaining the temperature of the latter.

(3) It is difficult to determine accurately the time required for this heating; indeed, if, as it is the common practice, the reacting mixture is admitted into the explosion vessel through a narrow tubing placed partly inside the furnace, the mixture becomes heated in passing this tubing where the heat transfer is very intense owing to forced convection.

(4) The heating of the first portion of the gaseous mixture entering the reaction vessel may be due to hydraulic impact and to adiabatic compression, and this may shorten the induction period below the theoretical value. The above phenomena are not easily accounted for.

(5) In the case of an autocatalytic reaction, or if the evolution of heat is mainly connected, not with the primary step, but with secondary reactions, the induction period may, on the contrary, prove longer than that calculated by the simple theory.

The method of calculation adopted by Todes[2] avoids successfully the difficulties stated in (1) and (3), since he calculates the adiabatic induction period comparing it with the limiting value which the induction period attains with the increase of pressure at constant temperature, and also since he neglects entirely the time required for the heating of the mixture, and this, under the usual experimental conditions, seems quite justifiable. In the case of methyl nitrate such calculations are in fairly good agreement with experiment.

An examination of the calculations of Rice and Campbell[1] shows that, sufficiently far from the explosion limit,

the calculated heating time is three times greater than the calculated induction period. These calculations are based on the assumption that the gas enters the vessel when cold, heating up in the vessel itself. As shown by the calculation of Todes, it would be far more reasonable to assume that the gas enters the vessel already at furnace temperature. For this reason alone the heat of reaction calculated by Rice and Campbell must work out four times greater than the actual value. Calculations based on the values of the induction period near the explosion limit are, as already mentioned, rather inaccurate.

In a previous paper[3] I expressed the opinion that the value of the heat of reaction given by Allen, Campbell and Rice[4] for ethyl azide is probably too high. This supposition is strongly supported by the results obtained by Campbell and Rice for methyl nitrate.

It seems probable that the heat of reaction calculated by Rice and his collaborators for ethyl azide is not less erroneous than their value for methyl nitrate. This would explain quite satisfactorily the discrepancy obtained by the present author[3] in calculating the thermal explosion limit for ethyl azide. The true heat of reaction should not be higher than 10 kcal. I leave open the question whether this value can be brought into agreement with the possible energy content of ethyl azide and with the mechanism suggested by Leermakers for its decomposition.

The only accurate method for comparing the theory of thermal explosions with the experimental data available is the calculation of the thermal explosion limit using the well-known laws of thermal transfer.[3] This method shows quite definitely that the explosion of methyl nitrate is truly a thermal explosion.

D. A. Frank-Kamenetzky

Institute of Chemical Physics,
Leningrad, U. S. S. R.,
November 12, 1939.

[1] Rice and Campbell, J. Chem. Phys. **7**, 700 (1939).
[2] Appin, Todes and Chariton, Acta physicochim. URSS **5**, 655 (1936).
[3] Frank-Kamenetzky, Acta physicochim. URSS **10**, 366 (1939).
[4] Rice, Allen and Campbell, J. Am. Chem. Soc. **57**, 2212 (1935).

Interpretation of the Raman Spectra and Infra-Red Spectra of the Halogen Derivatives of Methane

In a previous article[1] we determined the diffusion and absorption spectra of the chlorobromo derivatives of methane, and we indicated the correspondence between the modes of vibration of these molecules and the frequencies observed. In a recent article in this Journal, Glockler and Leader[2] gave the measurements of the Raman spectrum of fluorotrichloromethane. We would point out that the results obtained by these authors confirm our own interpretation. Only one line of CF_2Cl_2 — 320 cm^{-1} assumed as resulting from the triplication of δ_{345} should be attributed to the duplication of δ_{12}. It will be seen from the results of Table I that the frequencies observed by Glockler and Leader for $CFCl_3$ occur exactly between those of CCl_4 and CF_2Cl_2. The spectrum of CF_2Cl_2 was determined by Bradley.[3]

It will be remarked that in assuming for $CFCl_2$ the symmetry C_{3v}, as we have done for $CClBr_3$ and CCl_3Br, there must be six distinct fundamental frequencies: three simple δ_3, ν_1, ν_4, and three double δ_{12}, δ_{45}, ν_{23}. This is entirely in accordance with the results of Glockler and Leader. Moreover, as was to be expected, the line 535.3 cm^{-1} corresponding to the symmetrical vibration ν_1 is indeed the strongest of the Raman spectrum and the line 1067.2 cm^{-1} attributed to the antisymmetrical vibration ν_4 remains very weak.

H. Volkringer
J. Lecomte
A. Tchakirian

Laboratoire Chemie C à la Sorbonne,
Laboratoire des Recherches Physiques à la Sorbonne (J. L.),
Paris, France,
December 1, 1939.

[1] J. of Phys. **9**, 105 (1938); Comptes rendus **204**, 1927 (1937).
[2] G. Glockler and G. R. Leader, J. Chem. Phys. **7**, 278 (1939).
[3] C. A. Bradley, Phys. Rev. **40**, 908 (1932).

Table I.

		δ_{12}	δ_{345}	ν_1	ν_{234}
CF_2Cl_2	R.	260 320	? 433 455	664	877 919 1082 cm^{-1}
$CFCl_3$	R.	243.7	349.5 397.5	535.3	833.2 1067.2
CCl_4	R.	217	313	459	791
	I.R.	inac.	—	inac.	797
CCl_3Br	R.	187	243 289	418	710 765
	I.R.	—	— —	—	717 764
CCl_2Br_2	R.	141 164	230 252 318	370	672 720 759
	I.R.	— —	— — —	—	680 727 764
$CClBr_3$	R.	139	210 266	326	674 734
	I.R.	—	— —	—	667 740
CBr_4	R.	123	183	265	667
	I.R.	inac.	—	inac.	667

R = Raman, I.R. = infra-red. The sign, —, indicates that the measurements were not made in the corresponding region.

The Lattice of Rubber

The lattice of rubber has already been the subject of a number of investigations.[1] All the unit cells suggested in these papers give an x-ray density which is far higher than the measured one (8–10 percent). Furthermore, in all Weissenberg pictures published it is striking that the equator reflection A_2 is much longer than A_1 and A_3. We believe therefore that A_2 is not a single reflection and that the angle between A_1 and A_2 is not 90° or nearly 90°. While we investigated this question experimentally, Morss[2] published a paper also assuming that A_2 is a double reflection and making the assumption of double orientation. He calculated the unit cell for a number of angles and found an agreement with the observations at the angle of 70.5°. The cell contains 8 chains.

By simultaneously stretching and squeezing a piece of latex film we got a sample with rather good higher orientation. A Weissenberg picture shows the splitting of A_2 into two reflections of equal intensity and shape (see Fig. 1).

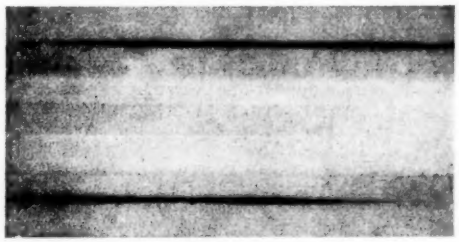

FIG. 1. Weissenberg picture of A_2.

The angle between the two maxima is 39.2°. The splitting is shown by all reflections but those of two zones perpendicular to each other, one of them containing A_1 and A_3. Therefore there are two directions perpendicular to each other which are crystallographic directions. Because—as it is known—the best orientated rubber samples give sharp diatrops, there is a third crystallographic direction perpendicular to the two others. For that reason the rubber lattice can be described as pseudorhombic. The smallest cell consistent with the diffraction data is: $a=8.97$A, $b=8.20$A and $c=25.2$A. The same cell described in monoclinic parameters: $a=8.97$A, $b=8.20$A, $c=26.7$A and $\beta=70.4°$ which is about the same cell as given by Morss. A smaller monoclinic cell would not be consistent with the reflections observed. The cell contains 16 isopren units (8 chains). The calculated density is 0.97 in agreement with 0.965, the highest measured value for stretched rubber.

The determination of this unit cell is unequivocal but it is not completely satisfactory. The cell seems too large and the number of missing spectra is about 90 percent; the equator alone could be explained by a cell of $\frac{1}{8}$ of the large cell, containing one chain only. But a smaller unit cell can only exist if there are several structures present simultaneously (dimorphism). One of the cells has to be monoclinic because of the diatrops, the other one may be triclinic, because the double orientation would give in any case the monoclinic symmetry observed in the Weissenberg patterns of the layer lines. All reflections would be explained by two unit cells: M_2, monoclinic, $a=8.97$A, $b=8.20$A, $c=6.68$A, $\beta=70.4°$, containing 2 chains and T_1, triclinic, $a=6.12$A, $b=8.20$A, $c=6.99$A, $\alpha=73.2°$, $\beta=64.1°$, $\gamma=47.3°$, containing 1 chain. Whether or not this assumption is justified has to be determined by further experiments.

This investigation was carried out in 1938 in Geneva. The authors wish to thank K. H. Meyer for his constant interest in the progress of this work. The details of the investigation will be published elsewhere.

LORE C. MISCH
Eastman Laboratory,
Massachusetts Institute of Technology,
Cambridge, Massachusetts,

A. J. A. VAN DER WYK
École de Chimie,
University of Geneva,
Geneva, Switzerland,
December 2, 1939.

[1] H. Mark and G. von Susich, Kolloid. Zeits. **46**, 11 (1928); W. Lotmar and K. H. Meyer, Monatsh. **69**, 115 (1936); C. J. B. Clews, Proc. Rubber Tech. Conf. London, 955 (1938).
[2] H. A. Morss, J. Am. Chem. Soc. **60**, 232 (1938).

Comment on Born's Thermodynamic Theory of Melting[1]

Introduction.—Born refers to previous theories of the melting process and then indicates that such a theory should properly concern itself with investigating the stability of a lattice under shearing stress. This he proceeds to do by means of the methods of classical statistics and thermodynamics for a lattice subjected to finite strains. Born finds that a regular lattice will become mechanically unstable whenever one of the following conditions is fulfilled:

$$C_{11}+2C_{12}\leqq 0; \qquad C_{11}-C_{12}\leqq 0; \qquad C_{44}\leqq 0.$$

If the first condition is satisfied first, as the temperature is raised sublimation will occur. If the second occurs first, transition to a "gel" state ensues, and the last condition is the condition for melting.

Experimental evidence.—First of all I wish to call attention to the work of Durand,[2] who has measured the elastic moduli of NaCl, KCl and MgO over a fairly wide range of temperature with very good precision. Among other things he finds that the isothermal modulus C_{12} is independent of temperature to within the precision of his measurements and furthermore he finds that extrapolation of his values of C_{11} to the temperature at which $C_{11}=C_{12}$ yields the melting points of the three substances mentioned above rather well. However, at this temperature his extrapolated values of C_{44} are still far from being zero.

In the second place Born refers to Brillouin[3] as the only author he knows who has applied the above-mentioned natural condition for melting. Brillouin reproduces Sutherland's curve as support for his point of view. Sutherland's curve exhibits the variation of the isothermal rigidity modulus of a number of polycrystalline metals with temperature. The form of the curve requires that the rigidity modulus vanish at the melting temperature. Now Quimby and Siegel[4] have measured the temperature variation of the elastic moduli of single crystal sodium from 90°K to 210°K, and a simple calculation reveals that their values of the

rigidity modulus are in definite disagreement with Sutherland's curve.

Therefore, the most accurate data yet obtained for the thermal variation of the elastic moduli of single crystals does not appear to bear out the contentions of either Brillouin or Born. However, Brillouin points out that the methods for measuring elastic moduli developed by Quimby, Rose, Durand and myself should prove fruitful in settling the theoretical questions herein raised. These methods would be difficult to apply in the neighborhood of the melting point and I feel that a combination of calorimetric studies and the more recent supersonic diffraction method of Ludloff and Seitz would be more satisfactory for such an investigation.

Comment on the theory.—Born's theory combines the assumption of long range order with the usual type of lattice dynamics, in which the elastic constants are computed from more or less rapidly converging sums. This, it seems to me, argues the effectiveness of small domains in determining the elastic behavior of a system. The implicit use of long range order in setting up the partition function for the solid ignores the effect of significant energy fluctuations arising with increasing temperature and the consequent departure from long range order within the solid phase contemplated for example by Lennard-Jones and Devonshire[5] and Frenkel[6] in their theories. Brillouin indirectly indicates the need for considerations along this line when he emphasizes the fact that a liquid has a finite microscopic rigidity even though unable to react on a macroscopic scale to a shear.

Furthermore Born suggests in his paper that his method when properly improved would probably represent the macroscopic properties of a liquid and its parent solid by means of a single analytic function, i.e., "the liquid state would be represented by the continuation of the curve, exactly as in van der Waals theory of condensation." Now it is precisely in this respect that Mayer[7] has shown van der Waals theory to be incorrect. Mayer shows that the van der Waals theory of the critical point differs essentially both from experiment and from Mayer's theoretical results.

In conclusion then I would like to reiterate that the chief criticism of Born's theory of melting is that he ignores what I believe to be the chief factor in determining the macroscopic properties of a solid in the neighborhood of melting; namely, the departure of the lattice from long range order before melting occurs. And it is for this reason that I feel that any thermodynamic theory of a lattice under finite strain cannot be safely extrapolated to the melting point.

LEWIS BALAMUTH

Department of Physics,
College of the City of New York,
New York, New York,
December 11, 1939.

[1] M. Born, J. Chem. Phys. **7**, 591 (1939).
[2] M. Durand, Phys. Rev. **50**, 449 (1936).
[3] L. Brillouin, Phys. Rev. **54**, 916 (1938).
[4] S. L. Quimby and S. Siegel, Phys. Rev. **54**, 76 (1938).
[5] J. E. Lennard-Jones and A. F. Devonshire, Proc. Roy. Soc. **A169**, 317 (1939).
[6] J. Frenkel, J. Chem. Phys. **7**, 200 (1939); **7**, 538 (1939).
[7] J. Mayer, J. Chem. Phys. I, **5**, 67; II, **5**, 74 (1937); III, **6**, 87; IV, **6**, 101 (1938).

Evidence of Krypton in Iodyrite

Evidence of krypton in iodyrite was found. Heretofore, the presence of this gas in minerals has been reported only in helium from clevite and in fergusonite.[1] In the present experiment after slightly fusing a several gram, natural, massive sample of iodyrite (Ag I), which was enclosed in a side limb of a vacuum tube, the more loosely occluded air in the sample thus freed was drawn off with a vacuum pump in order to minimize the danger of atmospheric gases masking the spectrum, and the tube sealed. Then the sample was thoroughly fused to free possible gases more deeply imprisoned, and a discharge of approximately 12,000 volts from an a.c. transformer passed through the tube. When the resulting spectrum was viewed in comparison with the spectrum from a tube of krypton simultaneously excited by the same discharge, it was observed that a line (of estimated 3 intensity in a scale from 1–10) of the iodyrite spectrum in the upper half of the band appeared to coincide unquestionably with 5870.9 in the krypton spectrum below, that is, with one of the two persistent lines of krypton. The other persistent line of krypton, 5570.2, could not be identified in the iodyrite spectrum since a band obscured this region. Interference by lines of other elements in the iodyrite spectrum likewise prevented the identification of any other krypton lines.

In view of other evidence, however, this one persistent line seems sufficient to identify krypton. Adjacent lines did not interfere, and the line could not be assigned to any other element. Approximate wave-lengths 5860 and 5888 were the closest observable on each side of 5870.9, so that the coincident line could clearly be seen; and when the krypton spectrum was reduced to the same intensity as that of iodyrite, the concurrence of the known persistent line with the unknown line above seemed certain. Further, lines tabulated for other elements in this region are for neon or are 1 or less intensity lines for heavy metals, mostly rare earths, that do not generally vaporize and thus are rare in vacuum tubes especially in a sufficient quantity that their weakest lines are visible. Cerium has a 3 intensity line, 5871, but it is for arc not spark. No neon was detected in the iodyrite spectrum when this spectrum was compared with the spectrum from a tube of neon. The most intense lines in the latter did not concur with those in the former; in fact, there were no lines at all in the former from about 6150 to 6563 although there were many intense ones in the latter. Also, as observed by Mr. McReynolds alone, the 9 intensity, 5872.8, of neon (very faint in the neon tube) did not coincide with the suspected krypton line in the iodyrite; and, moreover, when the pure krypton spectrum was blended below with the neon spectrum, 5870.9 in the former was distinguishable from 5872.8 in the latter showing that they could not be mistaken as coincident. Lines from the electrodes, which were Al alloyed with 2 percent Cu and some Mg, are not in the region. Thus krypton in iodyrite was indicated by a line that could reasonably be identified only as a persistent krypton line.

The experiment was by Mr. McReynolds and Mr. Hillis; the theory and report by Miss Feiring.

Acknowledgments are due Mr. M. S. Allen, Long Beach Junior College; the John Herman Laboratory, Los Angeles; and Mr. Hassler, of the Applied Research Laboratory, for consultation; Dallons Neon Laboratory, Los Angeles; the Electrical Products Corporation; and Carl Frye, sign painter, Long Beach, for vacuum tubes; Mrs. Ida Stoner, Mr. and Mrs. W. R. Feiring, and others.

F. W. HILLIS

Braun Corporation,
Los Angeles, California,

R. C. MCREYNOLDS

Halliburton Oil Well Cementing Company,
Laboratory Department,
Duncan, Oklahoma,

EVELYN B. FEIRING

Long Beach, California,
October 10, 1939.

[1] J. W. Mellor, *Comprehensive Treatise on Inorganic and Theoretical Chemistry* (Longmans, Green and Co., Ltd., 1922), Vol. 7, pp. 898–9.

A New Uviol Glass of the Binary System CaF_2—SiO_2

On melting fluorite in an oxy-coal-gas flame, it was found that the size of the small fused quartz rod to which the molten bead was attached became smaller and smaller. This shows that quartz is quite soluble in molten fluorite. This solution generally solidifies to an opaque grayish-white enamel, like in the case of pure fluorite; but under favorable heating conditions, a transparent solid solution is obtainable. A score of glassy beads of the CaF_2—SiO_2 system have been prepared by this method. Two kinds of fluorite have been used in the preparation, one of which was precipitated and the other a clear natural crystal, and the fused quartz used was prepared from clear crystalline quartz. The densities of these beads were found to lie within the narrow interval between 2.80 and 2.91. It seems quite unlikely that a clear solid with its density lying beyond the indicated interval can be formed. Assuming the volume of the glass and of its constituents to be additive in the process of glass formation, it is inferred from the density data that the new glass contains about 70 to 79 percent of fluorite and about 30 to 21 percent of silica. A determination using a Pt-PtRh thermocouple indicated that this glass begins to melt at about 1460°C, which is some 50°C above the melting point of the fluorite and some 150°C below that of the fused quartz.

The transparency of the new glass in the ultraviolet region has been investigated and compared with that of fused quartz using a fluorite spectrograph. The plates used for comparison were all 2 mm in thickness. The limit of transparency was found to vary in an irregular manner with the density of the glass. In the case of the variety containing natural fluorite, this variation was small, usually not exceeding 20A but in the variety containing precipitated fluorite, the variation was several times greater. The first and second spectrograms of Fig. 1 were taken from the most transparent pieces of the two varieties of new glass. It may be seen from the figure that the one containing precipitated fluorite is somewhat less transparent than the other variety, owing perhaps to the effect of impurity, and that pure fused quartz is by far more transparent than both of them. The result is somewhat unexpected, since according to its composition, the limit of transparency of the glass would be expected to lie between those of quartz and fluorite, that is to say, beyond λ1795 instead of being in the vicinity of λ2044. The abnormality in transparency of the new glass thus furnishes us a new example of the futility of regarding physical properties as direct additive functions of the constituents of the glass.

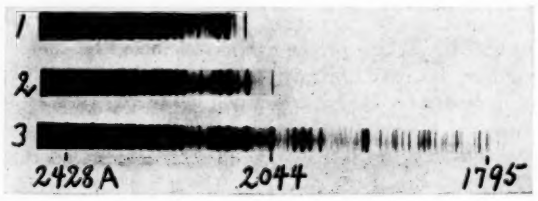

FIG. 1. Spark spectra of gold showing the transparent limits of the new glass and of quartz: (1) glass containing precipitated fluorite, (2) glass containing clear natural fluorite, (3) pure fused quartz.

CHOONG SHIN-PIAW

Institute of Radium,
National Academy of Peiping,
Shanghai, China,
November 20, 1939.

States of Monolayers on an Aqueous Subphase

A monolayer is not a Gibbs phase, but part of an interficial region. It may be considered to consist of phases in two dimensions analogous to Gibbs in three. The transitions in a general case along an isotherm as the pressure is increased are (Fig. 1):

$$\text{Gas} \xrightarrow{\text{1st order}} \text{Liquid I (expanded)} \rightarrow \text{Intermediate} \xrightarrow{\text{2nd order}} \text{Solid.}$$

The intermediate phase may be considered to consist of two or more parts, which may later be proved to be phases:

(1) Transition, with great compressibility; exhibits hysteresis, but not as yet demonstrated as heterogeneous, which changes more or less gradually to

(2) Liquid II (condensed), compressibility relatively low.

Dervichian considers the intermediate phase as mesomorphous, or an array of two-dimensional crystals, because this phase lies between a solid and a liquid. This implies that helium II is a liquid crystal. With this designation we cannot agree without evidence. Thus he considers liquid I as the only true liquid.

The analogy to a three-dimensional liquid is closer in:

(*a*) *L* I (expanded) in that it is formed by a first-order change from a gaseous film.

(*b*) *L* II (condensed), with respect to coefficient of expansion and compressibility.

Thus for *L* I at *low* pressures the coefficient of expansion (α) is of the order of ten times that of a three-dimensional liquid, while for compressibility the factor is of the general order of 100.

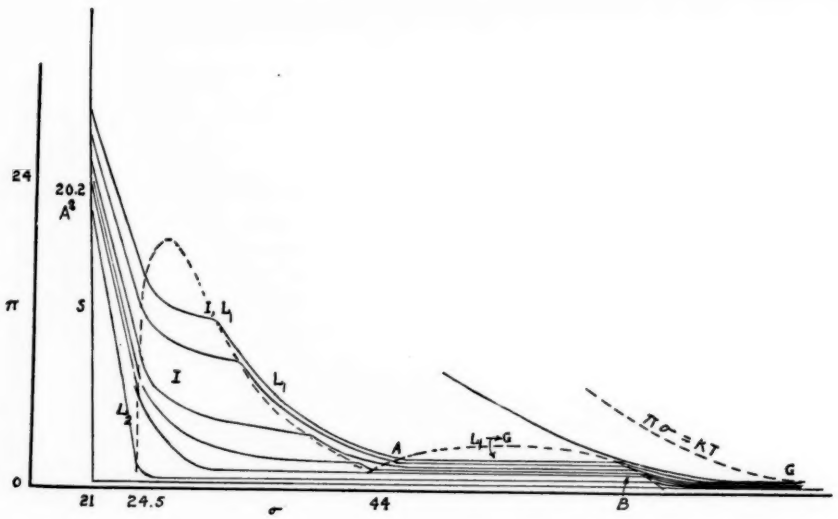

FIG. 1. Pressure (π), area (σ in A^2) diagram for monolayers. Region of L_{II} to left and of L_I to right of the area enclosed by dotted lines (areas 24.5 and 44).

Also $\alpha_{L_I}(L_I,G)C_{15}$ acid$\sim 750\times10^{-5}$,

$\alpha_{L_{II}}(1\text{ dyne})C_{16}$ acid$\sim 350\times10^{-5}$,

$\alpha_{\text{Bulk}}\ C_7$ acid$=100\times10^{-5}$.

The general magnitudes of some compressibilities (k) and energies of expansion (q) are given in Table I.

If a film of pentadecylic acid, or a similar compound, is compressed isothermally, islands of liquid I appear at point B, while on further compression to L I, the vapor disappears. Here D. assumes the liquid film to be isotropic, with a mean thickness $V^{\frac{1}{3}}$, and area $V^{\frac{2}{3}}$. His Table I (p. 940) indicates close agreement with the area $V^{\frac{2}{3}}$, but our columns 1 and 2 for acids, Table II, show that commonly the largest area for liquid I is only about two-thirds of this, while at the point $I\ L_I$ this decreases to the order of one-half. Thus liquid I is not isotropic but exhibits a considerable degree of molecular orientation, which increases with pressure.

He considers that the exact molecular areas in solid crystals (19.5, 20.5, 23.5 for the paraffin chain acids) reappear in monolayers as the areas at which transitions of the first, second, or third order occur. Thus he tacitly assumes that these molecular areas in films are determined entirely by molecular tilt. In addition he considers that the film collapses at 18.5A², the area of the cross section of the molecules in a plane perpendicular to the long axis.

TABLE I.

FILM	AREA SQ. A	$K\times10^{12}$ ABSOLUTE UNITS	q(ERGS/CM²) APPROXIMATE
Liquid I Pentadecylic acid	44	5800	50
Liquid I	34	3200	
Transition region		very great	350
Liquid II Stearic acid	21	2000	
Octadecyl alcohol	21	1200	
Solid Stearic acid	20.2	240	
Octadecyl alcohol	20.2	170	
Liquid in bulk Palmitic acid		100 (100°C)	
		150 (185°C)	

TABLE II. *Characteristic areas in A².**

	ACIDS				ALCOHOLS		
No. C ATOMS	1 $L(I)_A$	2 $V^{\frac{2}{3}}$	3 $L(II)_0$	4 S_k	1 $L(II)_0$	2 S_0	3 S_k
14	45	57			22.0	21.1	20.5
15	45	60		20.5	21.9	21.0	20.7
16	45	62			21.9	20.9	20.6
17			24.6	20.2	21.8	20.6	20.4
18			24.4		21.8	20.6	20.4
19			24.0	20.1			
20			23.6				
20+14	38	64					

* Sub-zero =extrapolated to zero pressure. Sub k =at kink

The values of our laboratory do not correspond with just these specific areas (acids 3, 4, and alcohols 1, 2, 3), though, since these are condensed states, they must be closely related to molecular size. Thus they do not seem to support the idea that at each transition point the molecules have just the angle of tilt found in the three-dimensional crystal. They seem rather to indicate that the nature of the transitions in condensed states depends upon the closeness of packing of the cylindrical molecules (elliptic cylinders) but that for any particular type of transition the hydrocarbon chains are drawn closer together as an increase of the length of the chains increases the van der Waals forces between them.

WILLIAM D. HARKINS
EDWARD BOYD

Kent Chemical Laboratory,
University of Chicago,
Chicago, Illinois,
December 14, 1939.

The Entropy of Dimethyl Acetylene from Low Temperature Calorimetric Measurements. Free Rotation in the Dimethyl Acetylene Molecule

The separation of the methyl groups in the dimethyl acetylene molecule, $H_3C-C\equiv C-CH_3$, is much greater than it is in ethane, and if the potential barrier[1] of about 3000 cal./mole restricting internal rotation in the latter is due to interactions between the methyl groups, then this barrier should be much smaller in dimethyl acetylene. If, on the other hand, the restricting potential in ethane is largely due to resonance with double bonded structures as proposed by Gorin, Walter and Eyring,[2] the fact that the length of the C−C single bonds in dimethyl acetylene[3] is such as to indicate considerable double bond character might lead one to expect a barrier about as large as in ethane. In order to determine the magnitude of this barrier we have calculated the entropy of dimethyl acetylene from low temperature calorimetric measurements and have compared this experimental value with that computed from molecular data.

The heat capacities, heat of fusion, and heat of vaporization were determined in an adiabatic calorimeter in the temperature range 15 to 291°K. The amount of material in the calorimeter was 0.8671 mole, and there was an impurity of 0.23 mole percent, as estimated from the change in melting point with proportion melted. Temperatures were measured with a platinum resistance thermometer which was compared with a National Bureau of Standards platinum thermometer down to 90°K and with a helium gas thermometer between 14 and 90°K. It is believed that our temperature scale agrees with that adopted at the National Bureau of Standards[4] to about 0.01°. Measurements of energy and resistance were made with an autocalibrated White double potentiometer and standards recently calibrated at the National Bureau of Standards. A detailed account of the apparatus and results will be published later.

In Table I are presented in itemized form the entropy changes calculated from our calorimetric data. The correction for gas imperfection was made under the assumptions that the gas follows a Berthelot equation of state, that the critical temperature is 489°K, as estimated by Morehouse and Maas,[5] and that the pressure of 41 atmos. obtained by extrapolation of the vapor pressure equation[6] to 489°K is the critical pressure.

TABLE I. *Molal entropy of dimethyl acetylene from calorimetric data.*

0–14.70°K, Extrapolation	0.25
14.70–240.93°K, Graphical	31.01
Fusion, 2206.7/240.93	9.16
240.93–291.00°K, Graphical	5.45
Vaporization at 291.00°K and 536 mm, 6440/291.00	22.13
Entropy of actual gas at 291.00°K and 536 mm	68.00±0.1
Correction for gas imperfection	0.14
Entropy of ideal gas at 291.00°K and 536 mm	68.14 cal./deg. mole

A summary of the calculation of the entropy from molecular data by the methods of statistical mechanics is given in Table II. For the vibrational entropy the frequencies used were those given by Crawford.[7] In the calculation of the rotational entropy it was assumed that the configuration of the methyl groups is the same as in methane and that the methyl groups are entirely free to rotate. The interatomic distances used, C−H=1.09A, C−C=1.47A, and C≡C=1.20A, are due to Pauling, Springall and Palmer.[3]

The deviation of the calorimetric from the statistical entropy, namely 0.32 cal./deg. mole, is greater than our estimated experimental error, ±0.1 cal./deg. mole, and is possibly to be ascribed to an error of a few cm^{-1} in the lowest frequency, 213 cm^{-1}, to neglect of any anharmonicity in the vibrations, and to uncertainty in the correction for gas imperfection.

TABLE II. *Molal entropy of gaseous dimethyl acetylene from molecular data, for 291.00°K and 536 mm.*

S_{trans}	38.47
S_{vib} (harmonic)	6.72
S_{rot} (with free internal rotation)	22.63
Total entropy	67.82 cal./deg. mole

It appears from the agreement between the calorimetric entropy, 68.14 cal./deg. mole, and that calculated from the existing molecular data on the assumption of free internal rotation, 67.82 cal./deg. mole, that within the limits of experimental error there is no appreciable barrier restricting the rotation of the methyl groups with respect to each other. Indeed, the assumption of any barrier would result in a decrease in the value of the statistical entropy, and this in turn would make the deviation from the experimental value still greater. Crawford and Rice[8] have reached essentially the same conclusion from the results of their gas heat capacity measurements. The results presented above, however, are less dependent on the correction for gas imperfection and on the vibrational frequencies above 1000 cm^{-1}.

We wish to express our indebtedness to Professor Alexander Goetz for supplying us with liquid hydrogen, and to Mr. Thurston Skei and Mr. Russell Doescher for preparing and purifying the dimethyl acetylene.

DARRELL W. OSBORNE*
CLIFFORD S. GARNER**
DON M. YOST

Gates Chemical Laboratory,
California Institute of Technology,
Pasadena, California,
December 10, 1939.

[1] J. D. Kemp and K. S. Pitzer, J. Am. Chem. Soc. **59**, 276 (1937).
[2] E. Gorin, J. Walter and H. Eyring, J. Am. Chem. Soc. **61**, 1876 (1939).
[3] L. Pauling, H. D. Springall and K. J. Palmer, J. Am. Chem. Soc. **61**, 927 (1939).
[4] H. J. Hoge and F. G. Brickwedde, Nat. Bur. Stand. J. Research **22**, 351 (1939).
[5] F. R. Morehouse and O. Maas, Can. J. Research **11**, 637 (1934).
[6] G. B. Heisig and H. M. Davis, J. Am. Chem. Soc. **57**, 339 (1935).
[7] B. L. Crawford, Jr., J. Chem. Phys. **7**, 555 (1939).
[8] B. L. Crawford, Jr. and W. W. Rice, J. Chem. Phys. **7**, 437 (1939).
* A. A. Noyes Fellow in Chemistry.
** A. A. Noyes Fellow in Chemistry. Present address: Chemistry Department, University of Texas, Austin, Texas.